

This item was submitted to Loughborough University as a PhD thesis by the author and is made available in the Institutional Repository (<https://dspace.lboro.ac.uk/>) under the following Creative Commons Licence conditions.



For the full text of this licence, please go to:  
<http://creativecommons.org/licenses/by-nc-nd/2.5/>

**BOILOVER  
IN  
LIQUID HYDROCARBON TANK FIRES**

by

Azizul Buang

A Doctoral Thesis submitted in partial fulfilment of the requirements for the award of the degree of Doctor of Philosophy in Chemical Engineering

© by Azizul Buang (2014)

## Abstract

Boilover is a violent ejection of certain liquid hydrocarbons due to prolonged burning during a storage tank fire. It happens due to vaporization of the water sub-layer that commonly resides at the base of a storage tank, resulting in the ejection of hot fuel from the tank, enormous fire enlargement, formation of a fireball and an extensive ground fire. Boilover is a very dangerous accidental phenomenon, which can lead to serious injuries especially to emergency responders. The boilover can occur several hours after the fuel in a storage tank caught fire. The delayed boilover occurrence is an unknown strong parameter when managing the emergency response operations. Modelling and simulation of the boilover phenomenon will allow the prediction of the important characteristics features of such an event and enable corresponding safety measures to be prepared. Of particular importance is the time from ignition to the occurrence of boilover.

In order to establish a tool for the prediction of the boilover events, it is essential to understand what happens within the fuel during a fire. Such understanding is important in order to recognize and determine the mechanisms for the hot zone formation and growth which are essentials, especially for predicting the onset time of boilover. Accordingly, boilover experiments and tests were planned and carried out at field scale by the Large Atmospheric Storage Tank FIRE (LASTFIRE) project with the intentions to evaluate the nature and consequences of a boilover, and to establish a common mechanism that would explain the boilover occurrence. Undertaking field scale experiments, however, is difficult to carry out so often due to high costs and high safety concerns. In order to obtain more detailed measurements and visual records of the behaviour of the liquids in the pool, a novel laboratory scale rig has been designed, built and commissioned at Loughborough University. The vessels used in the field scale tests and the laboratory scale rig were instrumented with a network of thermocouples, in order to monitor the distribution in temperature throughout the liquid and its variation with time. The temperature distribution variation as a function of time enabled the recognition of the phases of the

evolution of the hot zone and hence the mechanism of boilover. The rig has allowed well defined and repeatable experiments to be performed and hence enable to study and assess boilover in a reproducible manner. In addition, visualisation of the fuel behaviour during the experiments could be obtained to better understand the formation and growth of hot zone, the boiling of water layer and hence the boilover occurrence.

A number of small and larger scale experiments had been completed to obtain a wide spectrum of results, evaluating the effect of tank diameters, fuel depth, and water depth on the rate and extent of the boilover. The analysis of the results had elucidated further the processes of the hot zone formation and its growth, and hence mechanisms involved in the boilover occurrence. The important observation was that there are three stages observed in the mechanism of boilover incidence. At the start of the fire there is a stage when the hot zone is formed. This is followed by a period when the bottom of the hot zone moves downwards at a pseudo constant rate in which the distillation process (vaporisation of the fuel's lighter ends) is taking place. The final stage involved the heating up of the lowest fuel layer consisting of components with very high boiling points and occurrence of boilover.

Based on the observations of the mechanisms involved in the hot zone formation and its growth, predictive calculations were developed which focus on the provision of an estimate on the time to boilover upon the establishment of a full surface fire and an estimate of the amount of fuel remaining in the tank prior to the occurrence of the boilover. A predictive tool was developed in order to provide predictions on the important parameters associated with a boilover event i.e. the time to boilover, the amount of fuel remaining in the tank prior to boilover and hence the quantity of fuel that would be ejected during boilover and the consequences of a boilover i.e. fire enlargement, fireball effects and the ground area affected by the expulsion of oil during a boilover event. The predictive tool developed is capable of providing good estimates of onset time to boilover and predicts consequences of the boilover. The tool predicting the time to boilover of the LASTFIRE field scale test and the laboratory scales tests

was shown to produce predictions that correlated with the observed time to boilover. Apart from the time to boilover, the predictive calculation is also able to provide an estimate of fuel amount remained in the tank at the instance of boilover occurrence. Consequently, the tool is capable of predicting the quantity of burning fuel being ejected and hence the area affected by the extensive ground fire surrounding the tank. The predictive results are conservatives but yet show good agreement with observed time to boilover in real boilover incidents.

Certain considerations in the development of safe and effective fire fighting strategies in handling fire scenario with a potential of boilover occurrence, can be assessed using the predictive tool developed.

*Keywords:* storage tank fire, hot zone, boilover, liquid hydrocarbon, time to boilover, affected area

## Acknowledgments

I would like to thank my supervisor, Professor Geoffrey Hankinson, for the expert guidance, considerate support and continual encouragement that were readily provided throughout the course of this research project. The enlightening suggestions and earnest comments provided were invaluable to the development of this thesis. I would also like to thank all staff members within the Chemical Engineering Department of Loughborough University especially Mr. Jim Muddimer, Mr. Steve Bowler and Mr. Mark Barron for their help with the fabrication of the laboratory scale rig; and Mr. Tony Eyre and Mr. Graham Moody for their assistance with the laboratory experimental work.

Furthermore, I express my deepest gratitude to Resource Protection International for the support I received when undertaking the field experimental work.

I am also grateful to Universiti Teknologi PETRONAS for the financial support provided for the duration of this work.

Much love and thanks to my parents, my wife Roziah Mohamad and my children Athirah, Afiq, Aneesa and Adrina, who are the source of my happiness: it is the unfailing support of my family that has enabled me to complete this Ph.D. project.

*Thank you.*

# Table of Contents

List of Figures.....	vii
List of Tables.....	xii
1 INTRODUCTION.....	1
1.1 BOILOVER.....	1
1.1.1 Hot Zone Boilover .....	2
1.1.2 Thin Layer Boilover.....	5
1.2 MOTIVATION.....	6
1.2.1 Boilover Accidents .....	6
1.2.2 Modelling and Simulation.....	8
1.3 OBJECTIVES.....	9
1.4 THESIS STRUCTURE .....	10
2 LITERATURE REVIEW.....	13
2.1 HOT ZONE BOILOVER PHENOMENON.....	14
2.1.1 Layering Effect within Burning Fuels .....	15
2.1.2 Hot zone due to Bulk Circulation of Fuels .....	16
2.1.3 Hot Zone Propagation by Heat Conduction.....	17
2.1.4 Tank Dimensions on Hot Zone Progression.....	18
2.1.5 Depth of Fuel on Boilover Onset.....	20
2.1.6 Heat Transfer in Hot Zone Formation.....	21
2.1.7 Boilover Premonitory Noise: Micro-explosion.....	23
2.1.8 Heat transfer mechanisms in burning oil-water systems .....	26
2.1.9 Large Scale Tests and the Influence of Water Content on Boilover .....	31
2.2 LIQUID HYDROCARBON TANK FIRES .....	33
2.2.1 Definition of a Pool Fire.....	33
2.2.2 Burning Modes and Fuel Consumption Rate.....	34
2.2.3 Experimental Values of Burning Rate .....	42
2.3 EXISTING MODELS FOR ONSET OF HOT ZONE BOILOVER.....	44
2.3.1 Model for Hot Zone Boilover Onset .....	45
2.3.2 Physical-thermodynamic Laws Model for Boilover Onset.....	45
2.3.3 Model of Boilover Consequences .....	49
2.3.4 Conclusion.....	53
3 BOILOVER FIELD SCALE TESTS.....	55
3.1 LASTFIRE BOILOVER STUDY.....	55
3.1.1 Details of Preliminary Tests .....	57

---

3.1.2	Details of Field Scale Instrumented Tests Series .....	60
3.1.3	Details of Abu Dhabi Field Scale Tests .....	66
3.1.4	Details of Asturias Field Scale Tests .....	68
3.2	<b>PRESENTATION OF THE OBSERVATIONS AND TEMPERATURE MEASUREMENTS</b> .....	<b>69</b>
3.2.1	Presentation of the Observed Time to Boilover .....	69
3.2.1.1	Preliminary Tests .....	69
3.2.1.2	Field Scale Instrumented Tests .....	70
3.2.1.3	Abu Dhabi Field Scale Tests .....	71
3.2.1.4	Asturias Field Scale Tests .....	71
3.2.2	Fire Spread during Boilover .....	73
3.2.3	Indicators of the Onset of Boilover .....	74
3.2.4	Temperature Measurements within the Fuel and Water Layers .....	76
3.2.4.1	Crude Oil Tests .....	78
3.2.4.2	Diesel-Gasoline Tests .....	82
3.2.4.3	Gasoline Test .....	85
3.2.4.4	Diesel Tests .....	87
3.3	<b>ANALYSIS OF THE TEST RESULTS</b> .....	<b>89</b>
3.3.1	Can a Boilover Occur? .....	89
3.3.2	If a Boilover Occurs, When Will It Occur? (Time to Boilover) .....	90
3.3.2.1	Depth of Water Layer at Base of Tank .....	95
3.3.2.2	Distribution of Temperature in the Fuel Layer .....	96
3.3.2.3	Speed of the Base of the Hot Zone .....	104
3.3.2.4	Average Surface Regression Rate vs. Speed of Base of Hot Zone .....	109
3.3.3	When a Boilover Occurs, What Will Be the Consequences? (Consequences of Boilover) .....	110
3.3.3.1	Fuel Surface Regression Rate .....	111
3.4	<b>EFFECT OF REDUCING THE HEAT FLUX FROM THE FLAME TO THE FUEL SURFACE</b> .....	<b>116</b>
4	<b>LABORATORY SCALE BOILOVER EXPERIMENT</b> .....	<b>122</b>
4.1	<b>CONSIDERATION FOR DEVELOPMENT OF LABORATORY RIG</b> .....	<b>123</b>
4.1.1	Design of Heating Mechanism .....	124
4.1.2	Inerting of Boilover Tank .....	126
4.1.3	Observational Window .....	127
4.1.3.1	Maximum Pressure during Confined Combustion .....	128
4.1.3.2	Maximum Pressure during Boilover .....	129
4.1.3.3	Limiting Pressure for Glass Window .....	130
4.2	<b>BOILOVER LABORATORY SCALE RIG</b> .....	<b>131</b>
4.2.1	Heating System .....	133



---

4.2.1.1	Cartridge Heater .....	133
4.2.1.2	Temperature Controller.....	134
4.2.2	Temperature Measurement .....	135
4.2.3	Data Acquisition System .....	136
4.2.3.1	Programming Software .....	136
4.2.3.2	Communication Network/Module .....	136
4.2.4	Safety System .....	138
4.2.4.1	Inert Gas .....	138
4.2.4.2	Gas Detector.....	138
4.2.4.3	High Temperature Glass Panel .....	140
4.2.5	Video Recording .....	140
4.3	LABORATORY SCALE (LS) EXPERIMENTAL SERIES .....	140
4.3.1	Fuels Used .....	141
4.3.2	Number of Test.....	142
4.3.3	Test Routine .....	143
5	MAIN CHARACTERISTICS OF BOILOVER IN THE LABORATORY SCALE EXPERIMENTS WORKS .....	146
5.1	Conditions Necessary for Boilover .....	146
5.1.1	Preliminary Test Observations .....	147
5.1.1.1	LS Prelim 1 .....	147
5.1.1.2	LS Prelim 2 .....	148
5.1.2	Observations on Tests with Boilover .....	153
5.1.2.1	Temperature Profiles of Temperature-Time Curve.....	154
5.1.2.2	Photographs of Hot Zone Formation and Boilover .....	157
5.1.3	Observations on Tests with No Boilover .....	159
5.1.3.1	Temperature Profiles of Temperature-Time Curve.....	159
5.1.3.2	Photographs of Gasoline Test .....	164
5.2	IDENTIFICATION OF BOILOVER PHENOMENON IN THE LABORATORY SCALE EXPERIMENT .....	166
5.2.1	Temperature Profiles of Temperature-Time Curve.....	166
5.2.2	Violent Boiling of Fuel-Water Interface.....	168
5.3	CHARACTERISTIC PARAMETER AND OBSERVATION .....	168
5.3.1	Time to Boilover.....	169
5.3.2	Initial Fuel Layer Thickness on Boilover Onset .....	170
5.3.3	Fuel Surface Regression Rate.....	172
5.3.4	Speed of the Base of the Hot Zone.....	179
5.3.5	Influence of Initial Fuel Temperature.....	183
5.3.6	Heating Temperature vs. Boilover Onset .....	184

---

5.4	TEMPERATURE PROFILES WITHIN THE LIQUID LAYER – EVOLUTION OF TEMPERATURE WITH TIME .....	185
5.4.1	Crude Oil Tests.....	186
5.4.2	Diesel-Gasoline Test .....	190
5.4.3	Gasoline Test .....	193
5.4.4	Biodiesel Test.....	196
5.4.4.1	Photographs of Biodiesel Test.....	199
5.5	VALIDITY OF LABORATORY SCALE RIG RESULTS .....	201
6	PREDICTIVE TOOL FOR BOILOVER PHENOMENON.....	203
6.1	BEHAVIOUR WITHIN THE BURNING LIQUID .....	206
6.1.1	Boilover Fire .....	206
6.1.2	Non-boilover Fire .....	209
6.2	TEMPERATURE PROFILES OF BURNING LIQUID.....	212
6.3	PREDICTION OF TIME TO BOILOVER AND HOT ZONE TEMPERATURE .....	217
6.3.1	Heat Balance Equation .....	217
6.3.2	Prediction of Boilover Onset .....	220
6.3.3	Estimates of Specific Heat, Latent Heat of Vaporisation, Heat Flux Radiated (from flame to fuel) and Heat of Combustion.....	222
6.3.3.1	Specific Heat.....	223
6.3.3.2	Heat of Vaporization .....	226
6.3.3.3	Radiant Heat Flux (from flame to fuel).....	228
6.3.3.4	Mass Burning Flux .....	230
6.3.3.5	Heat of Combustion .....	231
6.3.3.6	Fraction of Radiative Heat Feedback for Hot Zone .....	232
6.3.4	Fraction of Fuel Vaporised.....	233
6.3.5	Hot Zone Temperature prior to Boilover.....	234
6.3.6	Analysis of the Predictive Parameter .....	235
6.3.6.1	Influence of Radiation Heat Flux on Boilover Onset.....	235
6.3.6.2	Influence of Fuel Storage Temperature .....	237
6.3.6.3	Impact of Fuel Density and Effect of Fuel Boiling Points.....	238
6.4	CONSEQUENCES OF BOILOVER PHENOMENON .....	241
6.4.1	Mass of Liquid Fuel Remaining Prior to Boilover.....	241
6.4.2	Consumption of Vaporised Fuel in a Fireball-Like Flame during Boilover .....	241
6.4.3	Thermal Effects of Fireball .....	244
6.4.3.1	Fireball Diameter, Duration and Elevation .....	245
6.4.3.2	Surface Emissive Power .....	247
6.4.4	Area Affected by the Spread of Burning Fuel.....	250
6.5	CONCLUSIONS.....	254

---

7	COMPARISON OF PREDICTIVE TOOL AND EXPERIMENTAL DATA.....	256
7.1	REQUIRED INPUT FOR PREDICTIVE TOOL .....	256
7.1.1	Initial Direct Input Parameters.....	257
7.1.2	Interim Parameters for Boilover Onset.....	257
7.1.2.1	Specific Heat.....	258
7.1.2.2	Latent Heat of Vaporisation .....	258
7.1.2.3	Mass Burning Rate .....	259
7.1.2.4	Heat Flux Radiant to Fuel Surface.....	259
7.2	CALCULATION PROCEDURE OF PREDICTIVE TOOL.....	260
7.2.1	Input for Predictive Tool.....	260
7.2.2	Interim Parameters Estimated.....	261
7.2.3	Calculation of the Time to Boilover, Fraction of Fuel Vaporised and Temperature of Hot Zone.....	262
7.2.4	Calculation of Mass of Liquid Fuel Remaining Prior to Boilover ...	263
7.2.5	Consumption of Vaporised Fuel in Fireball-Like Flame during Boilover .....	263
7.2.6	Thermal Effects of Fireball .....	265
7.2.7	Determination of the Area Affected by the Spread of Burning Fuel .....	267
7.3	COMPARISON OF EMPIRICAL MODEL AND PREDICTIVE TOOL: FIELD AND LABORATORY SCALE TESTS .....	268
7.3.1	Field Scale Tests .....	269
7.3.1.1	Crude Oil.....	269
7.3.1.2	Fire Spread due to Boilover .....	272
7.3.1.3	Diesel and Gasoline Mixture.....	273
7.3.2	Comparison with Laboratory Field Test.....	274
7.3.2.1	Crude Oil.....	274
7.3.2.2	Diesel and Gasoline Mixture .....	275
7.4	COMPARISON OF EMPIRICAL MODEL AND PREDICTIVE TOOL: BOILOVER STUDIES .....	276
7.4.1	Experimental Study of Boilover in Crude Oil Fires (Koseki, Kokkala and Mulholland, 1991).....	276
7.4.2	Large-scale Boilover Experiments using Crude Oil (Koseki <i>et al.</i> , 2006).....	277
7.5	COMPARISON OF EMPIRICAL MODEL AND PREDICTIVE TOOL: BOILOVER INCIDENTS.....	279
7.5.1	Czechowice-Dziedzice Refinery, Poland.....	279
7.5.2	Tacoa Power Plant, Venezuela.....	284
7.5.3	Amoco Refinery, Milford Haven, United Kingdom .....	288
7.6	CHARACTERISTICS OF PREDICTIVE TOOL.....	293
7.6.1	Limitation of Predictive Tool.....	295

---

7.6.2	Application of Predictive Tool.....	296
7.6.2.1	Safer and More Effective Fire Fighting Strategies.....	296
7.6.2.2	Safety Distances .....	297
7.7	CONCLUSION .....	298
8	HIGHLIGHTS OF WORK AND CONCLUSION .....	300
8.1	Highlights of Work.....	300
8.2	Conclusion .....	303
8.3	Future Recommendations.....	308
	REFERENCES.....	310

## List of Figures

Figure 1-1:	Fuel temperature profiles that (a) generates and (b) does not generate a hot zone. ....	3
Figure 2-1:	Schematic illustration of boilover. Three Stages in the formation and propagation of a hot zone during a fire (Time: $t_1 < t_2 < t_3$ / Surface temperature: $T_{s1} < T_{s2} < T_{s3}$ ).....	21
Figure 2-2:	Dependence of burning velocity and hot zone propagation velocity on the diameter of the tank [Data extracted from Koseki (1999)]......	22
Figure 2-3:	Evolution of the sound intensity with time in a tank fire (Fan <i>et al.</i> , 1995). ....	24
Figure 2-4:	The temperature of the fuel-water layer and the micro-explosion noise level in the premonitory period as a function of the burning time (Fan <i>et al.</i> , 1995). ....	24
Figure 2-5:	The temperature profile within the fuel-water layer prior to boilover .....	25
Figure 2-6:	Temperature profile under the surface of non-hot-zone fuel in the 2 m tank: comparison of measured and calculated results .....	28
Figure 2-7:	Temperature profile in relation to the distance to the tank bottom for a crude oil (Arabian light, tank diameter = 1 m, height = 0.5 m, initial filling height = 151 mm).....	29
Figure 2-8:	Fuel surface regression rate data against pool diameter (crude oil). ....	37
Figure 2-9:	Effect of $[\Delta h_c / (\Delta h_{th} + \Delta h_{heat})]$ on burning rate. Circles stand for alcohols, a triangle stands for acetone, and squares stand for hydrocarbon. C denotes carbon number of fuel compounds. That is, C <sub>1</sub> is methanol, C <sub>2</sub> is ethanol, C <sub>3</sub> is acetone, C <sub>4</sub> is butanol, C <sub>5</sub> is pentane, C <sub>6</sub> is hexane, C <sub>7</sub> is heptane, and C <sub>8</sub> is octane. The data were extracted from Koseki (1989) for 1 m diameter fires. The data for the dotted line were extracted from Zabetakis <i>et al.</i> (1961). ....	38
Figure 2-10:	Relation between mass burning rate and fuel thermochemical properties. Data extracted from Mudan (1984) .....	40
Figure 2-11:	Position of fireball and target. ....	51
Figure 3-1:	Test set-up for Preliminary Tests (RPI, 2004). ....	58
Figure 3-2:	Schematic of thermocouples location in the 1.2 m diameter tank (RPI, 2004).....	62
Figure 3-3:	Location of thermocouples in the 2.44 m diameter tank (RPI, 2005).....	64
Figure 3-4:	Spread of the fire estimated due to the boilover in FS Test 2, 3, 4, 5, 6, 9, 10 and 11 .....	74
Figure 3-5:	Photo of FS Test 3 – Difference flame size (a) during steady burning and (b) during the boilover occurrence.....	75
Figure 3-6:	Temperature profiles within liquid in the storage tank in the course of experiment for FS Test 6: (a) A sharp change in the temperature profiles is observed as boilover starts and b) Thermocouples within fuel show a large decrease in the temperature .....	76
Figure 3-7:	Tank wall temperature measurement for FS Prelim 9 (RPI, 2004). ....	77
Figure 3-8:	Temperature profiles within the crude oil for the FS Test 41 .....	79
Figure 3-9:	Evolution of temperature in diesel-gasoline fuel mixture for boilover study of FS Test 42.....	83
Figure 3-10:	Evolution of temperature in gasoline for the FS Test 31 .....	85
Figure 3-11:	Evolution of temperature in diesel for the FS Test 29 .....	88

Figure 3-12:	Time to boilover against initial fuel depth for field scale tests for crude oil.....	91
Figure 3-13:	Vertical temperature profile for FS Test 41.....	94
Figure 3-14:	Time to boilover against depth of water at the tank base for field scale tests involving crude oil.....	95
Figure 3-15:	Temperature distribution in the liquid at time (b) 1500 s and (c) 2000 s for FS Test 22 .....	97
Figure 3-16:	Temperature distribution in the fuel at time of boilover (a) 3000 s, (b) 4000 s, (c) 4500 s and (d) 4530 s.....	98
Figure 3-17:	Temperature distribution in the liquid at time of (a) 4600 s, (b) 4700 s, (c) 4800 s and (d) 5375 s for the FS Test 22.....	100
Figure 3-18:	Temperature distribution in the liquid at time of 3500 s for FS Test 31 .....	102
Figure 3-19:	Temperature distribution in the liquid at time of (a) 4800 s, (b) 5222 s, (c) 5400 s, (d) 5500 s, (e) 5800 s and (f) the end of experiment – 6355 s; for the FS Test 31 .....	104
Figure 3-20:	Time at which the base of hot zone with temperature of 110°C for FS Test 23 involving 500 mm crude oil .....	105
Figure 3-21:	Observed against predicted time to boilover for crude oil .....	108
Figure 3-22:	Temperature profiles of fuel in field scale tests in which hot zone was not formed - FS Test 37 (light fuel oil) .....	110
Figure 3-23:	Time histories of temperatures for diesel-gasoline mixture test FS Test 47.....	114
Figure 3-24:	Relations of the depth of the non conducting material with the ratio of depth of fuel-time to boilover for FS Test 43, 44 and 45 .....	118
Figure 3-25:	Vertical temperature profile FS Test 44 (crude oil with 50 mm depth of non conducting material).....	120
Figure 4-1:	Schematic of the proposed laboratory scale boilover tank with the heating source.....	124
Figure 4-2:	Plan view of ceramic radiant heaters (Godfrey C., CMG Thermal, personal communication, Dec. 1, 2008) .....	125
Figure 4-3:	Schematic of cartridge heater assembly (a) Side view and (b) Plan view. ....	126
Figure 4-4:	Boilover Experimental Rig: (a) Main Tank, (b) Condenser & (c) Secondary Expansion Container.....	131
Figure 4-5:	Schematic of Boilover Experimental Rig .....	132
Figure 4-6:	Cartridge heater assembly with ten cartridge heater elements.....	134
Figure 4-7:	Temperature Setting on the Heater System Control Panel.....	135
Figure 4-8:	K-type thermocouples of 1.5 mm probe diameter placed at 10 mm height intervals from the tank base for detailed and fast measurements within the liquid .....	136
Figure 4-9:	Nitrogen (N <sub>2</sub> ) Gas System – N <sub>2</sub> cylinder is connected by the green tubing to the main tank.....	138
Figure 4-10:	Gas/Oxygen Detecting System (a) Control Setting + Alarm Module and (b) Sensor/Transmitter Module.....	139
Figure 5-1:	Temperature profiles within fuel in the tank in the course of test LS Prelim 1.....	147
Figure 5-2:	Vertical temperature profiles during heating of water for test LS Prelim 1.....	148
Figure 5-3:	Temperature profiles within fuel in the tank in the course of test LS Prelim 2.....	150

---

Figure 5-4:	Vertical temperature profiles during heating of water for test LS Prelim 2.....	150
Figure 5-5:	Formation of hot zone: Hot zone has grown further downwards of the tank after about 2100 s to 2200 s of heating.....	153
Figure 5-6:	Temperature profiles within liquid in the tank in the course of LS Test 3. The sharp drops in the temperature indicate vaporisation of water layer at the tank base.....	155
Figure 5-7:	Vertical temperature profiles during heating of mineral oil and n-butyl acetate mixture for LS Test 3.....	156
Figure 5-8:	Formation of hot zone and boilover occurrence for LS Test 3.....	158
Figure 5-9:	Temperature profiles within liquid in the tank in the course of experiment for LS Test 13.....	160
Figure 5-10:	Vertical temperature profiles according to height of fuel in which hot zone were not formed for laboratory scale boilover studies.....	161
Figure 5-11:	Photographs of fuel surface regression and vertical temperature profiles during heating of gasoline for LS Test 13: At the end of the test at which the surface has regressed to 50 mm from the base. ....	163
Figure 5-12:	Photo of Laboratory Boilover Test LS Test 13 involving gasoline.....	165
Figure 5-13:	Temperature profiles within liquid in the tank in the course of experiment for LS Test 11. ....	167
Figure 5-14:	Photo of Laboratory Boilover Test LS Test 7 (a) During the start of heating – bubbling is observed near the heaters and (b) During the start of boilover – boiling of water occurred where vigorous bubbling (mixing of fuel and water) was observed. ....	168
Figure 5-15:	Boilover Onset Time vs. Initial Thickness of Fuel Layer for Laboratory Scale Tests involving mixture of mineral oil + n-butyl acetate, mixture of diesel + gasoline and crude oil.....	171
Figure 5-16:	Time histories of temperatures for LS Test 5 involving mineral oil + n-butyl acetate.....	173
Figure 5-17:	Photos taken during the progression of LS Test 5: (a) Left: Photo taken at the beginning of the test and (b) Right: Photo taken after 8100 s of heating. ....	174
Figure 5-18:	Time histories of temperatures for LS Test 12.....	175
Figure 5-19:	Photos taken during the progression of LS Test 12: (a) Left: Photo taken at 180 s after the heating started and (b) Right: Photo taken after 4080 s. ....	175
Figure 5-20:	Time histories of temperatures for LS Test 20.....	176
Figure 5-21:	Photos taken during the progression of LS Test 20: (a) Left: Photo taken at the beginning of the test and (b) Right: Photo taken after 4500 s.....	177
Figure 5-22:	Vertical temperature profiles during heating of fuel for LS Test 22: Crude oil. ....	181
Figure 5-23:	Effect of heating temperature on the time to boilover.....	185
Figure 5-24:	Evolution of temperature in the crude oil for Laboratory Boilover Study for LS Test 23.....	188
Figure 5-25:	Evolution of temperature in diesel-gasoline fuel mixture for laboratory scale boilover study LS Test 12.....	192
Figure 5-26:	Evolution of temperature in gasoline for LS Test 13.....	194
Figure 5-27:	Evolution of temperature in biodiesel for LS Test 15.....	196

---

Figure 5-28:	Temperature profiles within fuel in the tank in the course of test LS Test 15 .....	198
Figure 5-29:	Photo of Laboratory Boilover Test LS Test 15 involving biodiesel .....	200
Figure 6-1:	Temperature profiles within crude oil for test FS Test 22 .....	207
Figure 6-2:	Temperature profiles within diesel and gasoline mixture for test FS Test 39 .....	209
Figure 6-3:	Temperature profiles within gasoline for test FS Test 31 .....	210
Figure 6-4:	Temperature profiles within diesel for test FS Test 29 .....	212
Figure 6-5:	Plot of height against temperature for the field scale testing and laboratory scale experimental work during the initial stage of burning when heat transfer is assumed to be conduction. Note the exponential temperature profile measured by the top thermocouples .....	213
Figure 6-6:	Plot of height against temperature for field scale testing and laboratory scale experimental work during the subsequent stage of burning when the hot zone is forming. Note the similar temperature readings by two or more of the top thermocouples .....	214
Figure 6-7:	Plot of height against temperature during the period when the base of the hot zone is moving downwards towards the fuel/water interface. Note the horizontal section of the temperature profile regresses gradually towards the tank base. The temperature of the hot zone is also increasing gradually. ....	214
Figure 6-8:	Plot of height against temperature when the base of the hot zone has reached the fuel/water interface. The red line indicates the boilover occurrence. Note that the boilover did not occur immediately though the hot zone base reached the interface at the vaporisation point of water .....	215
Figure 6-9:	The temperature profile of the overall mechanism observed during a fire prior to the boilover occurrence. ....	216
Figure 6-10:	Simplified temperature profile within burning liquid as a basis for boilover onset predictive tool development .....	218
Figure 6-11:	Time required to boilover based on the different fraction of radiation heat flux returned to fuel. The experimental results are from the field scale tests in 1.2 m diameter tank involving crude oil .....	237
Figure 6-12:	Influence of initial storage temperature on the time to boilover. The experimental results are from the field scale tests in 1.2 m diameter tank involving crude oil .....	238
Figure 6-13:	Prediction of time to boilover based on the different fuel's densities. The experimental results are from the field scale tests in 1.2 m diameter tank involving crude oil .....	239
Figure 6-14:	Prediction of time to boilover based on the fuel's average boiling point. The experimental results are from the field scale tests in 1.2 m diameter tank involving crude oil .....	240
Figure 6-15:	Position of fireball and target .....	249
Figure 6-16:	Simple basis to determine height of the fuel-steam mixture .....	251
Figure 7-1:	Photographs taken during progression of steady burning (left) and the boilover occurrence (right) of FS Test 5. Take note on the difference of the size (height) of the fireball-like flame during the occurrence of the boilover .....	265
Figure 7-2 :	Comparison of area affected due to spillage of hot burning fuel due to boilover between the experimental results and predictive calculation. ....	268

---



---

Figure 7-3:	Experimental results versus predicted time to boilover by Empirical Model 1 for field scale tests involving crude oil .....	271
Figure 7-4:	Observed time to boilover against predicted time to boilover by Empirical Model 2 for field scale tests involving crude oil .....	271
Figure 7-5:	Observed time to boilover against predicted time to boilover by Predictive Tool for field scale tests involving crude oil .....	272
Figure 7-6:	Observed versus predicted area affected due to fire spread during boilover for test FS Test 2, 3, 4, 9, 10 and 11 .....	272
Figure 7-7:	Observed time to boilover against predicted time to boilover by Predictive Tool for laboratory scale tests involving crude oil.....	275
Figure 7-8:	Observed time to boilover against predicted time to boilover by Predictive Tool for laboratory scale tests involving mixture of diesel and gasoline.....	276
Figure 7-9:	Tank specification for experiment.....	278
Figure 7-10:	Position of thermocouples along with the pan axis .....	278
Figure 7-11:	Comparison between real incident time to boilover with the predicted values from the empirical models and the predictive tool developed for Czechowice-Dziedzice incident .....	282
Figure 7-12:	Comparison between real incident time to boilover with the predicted values from the empirical models and the predictive tool developed for Tocoa incident.....	287
Figure 7-13:	Comparison between real incident time to boilover with the predicted values from the empirical models and the predictive tool developed for Milford Haven incident .....	292

## List of Tables

Table 2-1:	Comparison of calculated and experimental hot-zone growth rates for a Forties crude oil (1 m tank, heat flux = 34 kW m <sup>-2</sup> ).....	31
Table 2-2:	Burning modes as a function of pool fire diameter (Babrauskas, 1983) .....	34
Table 2-3:	Compilation of experimental values of burning rate (surface regression rate) for tanks with diameter of 1.0 m and above .....	43
Table 3-1:	Details of the Preliminary Tests .....	58
Table 3-2:	Details of the arrangements of the thermocouples.....	61
Table 3-3:	Summary of boilover tests conducted in the LASTFIRE Field Scale Tests.....	65
Table 3-4:	Summary of boilover tests conducted in the Abu Dhabi Boilover Study .....	67
Table 3-5:	Summary of boilover tests conducted in the Asturias Boilover Study.....	68
Table 3-6:	Observed Time to Boilover for the Preliminary Tests.....	69
Table 3-7:	LASTFIRE Field Scale Tests Results – Time to Boilover .....	70
Table 3-8:	LASTFIRE Abu Dhabi Field Scale Tests Results – Time to Boilover .....	71
Table 3-9:	LASTFIRE Asturias Field Scale Tests Results – Time to Boilover .....	72
Table 3-10:	Temperatures for each thermocouple at various stages of the crude oil fire in the FS Test 41. ....	81
Table 3-11:	Temperatures for each thermocouple at various stages of the diesel-gasoline fuel mixture experiments .....	84
Table 3-12:	Temperatures for each thermocouple at various stages of the gasoline experiments .....	87
Table 3-13:	Temperature reached by each thermocouple throughout the experiments on diesel .....	88
Table 3-14:	Comparison between time required for the fuel-water interface to reach boiling point of water and time of boilover start for the field scale tests involving crude oil tests .....	99
Table 3-15:	Temperature of crude oil at specific depth from the tank base at specific time for FS Test 23. ....	105
Table 3-16:	Speed of the base of the hot zone of the field scale tests.....	106
Table 3-17:	Average surface regression rate for the field scale tests .....	115
Table 3-18:	Effects of depth of the non conducting material towards time to boilover.....	118
Table 4-1:	Properties of Quartz Glass Panel (Gilmore, S., personal communication, June 2009).....	128
Table 4-2:	Characteristics of the PID500 Temperature Controller .....	135
Table 4-3:	Characteristics and Specifications of Module cFP-2120, cFP-TC-120 and cFP-CB-3 .....	137
Table 4-4:	Summary of properties of fuels used in the boilover experiments .....	142
Table 4-5:	Summary of experimental programme .....	142
Table 4-6:	Volume based on the Thickness of Fuel Layer .....	144
Table 5-1:	Laboratory Scale Boilover Study Experimental Results .....	169
Table 5-2:	Constant of proportionality for the fuels of Figure 5-15 .....	171
Table 5-3:	Average Fuel Surface Regression Rates for the Laboratory Scale Boilover Study .....	177
Table 5-4:	Experimental values of burning rate (surface regression rate) for tanks with diameter below than 1.0 m).....	179

Table 5-5:	Data of Speed of the Base of the Hot Zone for Laboratory Scale Boilover Study.....	182
Table 5-6:	Temperatures for each thermocouple at various stage of LS Test 23.....	189
Table 5-7:	Temperatures for each thermocouple at various stages of the LS Test 12.....	193
Table 5-8:	Temperatures for each thermocouple at various stages of the gasoline experiments.....	195
Table 5-9:	Temperature reached by each thermocouple throughout the experiments on diesel in LS Test 19.....	197
Table 6-1:	Numerical constants for Equation 6-18.....	227
Table 6-2:	Constants for Equation 5-17 (Riazi & Daubert, 1987).....	235
Table 6-3:	Data for constant parameters $a$ , $b$ , $c$ , and $d$ of the empirical relationships for fireball diameter and duration from literature.....	245
Table 6-4:	Measured and predicted fireball diameter and duration - Comparison based on data from Roberts <i>et al.</i> (2000).....	246
Table 6-5:	Empirical relationships for spillage affected area and data for parameters in the relationship $a$ and $b$ .....	253
Table 7-1:	Input Data for Predictive Tool for FS Test 5 and 6.....	260
Table 7-2:	Interim Parameters estimated for the prediction of time to boilover for FS Test 5 and 6.....	261
Table 7-3:	The predicted time to boilover, the fraction of fuel that vaporised and hot zone temperature prior to boilover for FS Test 5 and 6.....	262
Table 7-4:	Predictions on the mass of liquid remaining in tank prior to boilover and the mass that consumed in fireball and the calculations on the diameter, duration and elevation of the fireball-like flame formed during the boilover.....	264
Table 7-5:	Estimations on the power flux received by a target/receptor at a distance away from the fireball in FS Test 5 and 6.....	266
Table 7-6:	Determination of the area affected due to the expulsion of hot burning fuel due to boilover occurrence for FS Test 5 and 6.....	267
Table 7-7:	Predictive results on the time to boilover for field scale tests involving crude oil by the empirical models and predictive tool proposed.....	269
Table 7-8:	Prediction on time to boilover using the empirical models deduced from Chapter 3.....	270
Table 7-9:	Predictive results on the time to boilover for field scale tests involving mixture of diesel and gasoline by the empirical model and predictive tool proposed.....	273
Table 7-10:	Predictive results on the time to boilover for laboratory scale tests involving crude oil by the predictive tool proposed.....	274
Table 7-11:	Predictive results on the time to boilover for laboratory scale tests involving mixture of diesel and gasoline by the predictive tool proposed.....	275
Table 7-12:	Summary of selected test details, the results on the time to boilover observed in the test and the predicted time to boilover.....	277
Table 7-13:	Summary of Koseki <i>et al.</i> (2006) Experimental Results.....	278
Table 7-14:	Predicted time to boilover determined using the empirical models for the Japanese large-scale boilover experiments using crude oil.....	279
Table 7-15:	Key information on the tank specifications, time to boilover and post boilover effects for Czechowice-Dziedzice boilover incident.....	280

---

Table 7-16:	Input parameters for predictive calculation for boilover incident at Czechowice-Dziedzice, Poland .....	281
Table 7-17:	Results of predictive tool calculation on boilover onset time.....	281
Table 7-18:	Results of predictive tool calculation on boilover onset time and area affected for Czechowice-Dziedzice incident.....	283
Table 7-19:	Key information on the tank specifications, time to boilover and post boilover effects for Tocoa boilover incident .....	284
Table 7-20:	Input parameters and interim parameters calculated for predictive calculation of boilover incident at Tocoa, Venezuela .....	285
Table 7-21:	Results of predictive tool calculation on boilover onset time for Tocoa boilover incident.....	286
Table 7-22:	Results of predictive tool calculation on boilover onset time and area affected for Tocoa boilover incident.....	287
Table 7-23:	Key information on the tank specifications, time to boilover and post boilover effects for Milford Haven boilover incident.....	289
Table 7-24:	Input parameters and interim parameters calculated for predictive calculation of boilover incident at Milford Haven, United Kingdom .....	290
Table 7-25:	Results of predictive tool calculation on boilover onset time for Milford Haven incident. ....	291
Table 7-26:	Results of predictive tool calculation on boilover onset time and area affected for Milford Haven incident. ....	293
Table 7-27:	Fraction of heat radiated to the fuel that contributes to the hot zone formation used in the comparison study.....	294

# 1 INTRODUCTION

There is an abundance of storage tank facilities built and being built in many countries. Hence to make a study of the burning of the contents of a large storage tank is of significant interest to fire safety science, fire fighting and the regulation of liquid hydrocarbon storage facilities.

Fires involving storage tanks containing liquid hydrocarbons are unlikely to occur nowadays due to improved safety systems and maintenance procedures implemented by the industries. Even though storage tank fires are rare, the importance of fire control and loss prevention measures must not be ignored. Fires in storage tanks pose a high threat and may result in fatalities, capital losses and environmental destruction. Fires involving tanks containing liquid hydrocarbons, if left to burn over a prolonged period, may lead to fuel eruptions. The fuel eruptions occur in three main forms: slop over, froth over and boilover (Broeckmann & Schecker, 1995 and API-2021, 2001). Slop over is the least serious form of fuel eruption. It is a discontinuous frothing release of fuel over a section of a tank's wall. Froth over is a continuous low intensity fuel frothing release from a tank over its wall. The most dangerous form of fuel eruption is boilover.

## 1.1 BOILOVER

A boilover is a violent ejection of certain liquid hydrocarbons and occurs after a prolonged duration during a storage tank fire. It happens due to vaporization of the water sub-layer that commonly resides at the base of a storage tank, resulting in the ejection of hot fuel from the tank, enormous fire enlargement, formation of a fireball and an extensive ground fire (Hall, 1925, Koseki, 1991 and Broeckmann & Schecker, 1995). The water sub-layer exists at the base of a tank as a consequence of water being present in the fuel, the tank being open to atmosphere and hence subject to rain ingress and the introduction of water during fire fighting.

The phenomenon of boilover, as described in many relevant publications, may occur as:

- i. Hot zone boilover – when the fuel layer is very large at the time boilover occurs.
- ii. Thin layer boilover – when the fuel layer is very thin at the time boilover occurs.

The following is a brief description of the two types of boilover.

### **1.1.1 Hot Zone Boilover**

This type of boilover may occur during a storage tank fire, and is characterized by a great thickness of fuel with a wide boiling range burning above an aqueous substrate i.e. a water layer residing at the bottom of the tank at the time of the fire.

In the event of a full surface fire in a storage tank, the surface of the liquid receives heat from the flame and very quickly approaches the temperature at which the heavier components of the fuel mixture boil. Heat is conducted down into the pool and a distillation process commences in the liquid immediately below the surface (Hasegawa, 1989 and Broeckmann & Schecker, 1995). The liquid in this region assumes the boiling temperature of the components being vaporised. The liquid is enriched progressively as the most volatile components are depleted and heavier components are vaporized. The rise in vapour bubbles causes thorough mixing of the liquid in this region creating a layer of uniform temperature and composition called the hot zone. The temperature of the hot zone increases as the distillation process proceeds and its depth grows as heat is conducted into the cold liquid below thus introducing more fuel into the hot zone. When the bottom of the hot zone reaches the water sub-layer and, providing the temperature of the hot zone is sufficiently above 100°C, the water is superheated and hence vaporizes explosively, pushing large quantities of hot oil out of the tank (Hasegawa, 1989). The consequences of the projection of the

burning hot oil out of the tank are severe thermal effects due to the fire enlargement and fireball formation, the spread of a ground fire around the tank, and the possibility of escalation of the incident by ignition of the contents of adjacent storage tanks. In addition a boilover event can endanger the lives of fire fighters and/or emergency responders attending the incident. Figure 1-1 shows the potential temperature profiles within the fluid during a storage tank fire containing a fuel that: (a) generates a hot zone and (b) does not cause a hot zone to be formed.

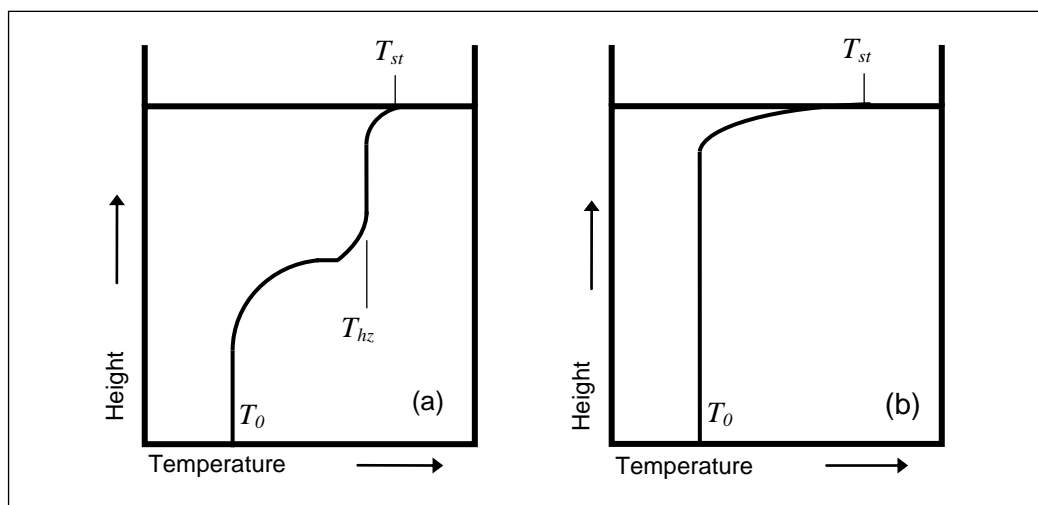


**Figure 1-1: Fuel temperature profiles that (a) generates and (b) does not generate a hot zone.**

It has been observed in the first case (a) that the temperatures within the fuel reach values higher than the initial temperature ( $T_0$ ) at greater depths than in case (b) due to the formation and growth of a hot zone. The profile represents a homogenization of composition and temperature within the hot zone. By contrast, in the second case (b), the temperature rises only in the vicinity of the surface. At greater depths, the temperature is equal to  $T_0$ .

Given that a hot zone is formed, then a boilover will occur if:

- i. the temperature of the hot zone is higher than the boiling point of water by an amount sufficient to superheat the water to a temperature at which it explosively vaporises; and

- ii. the rate of growth of the hot zone is greater than the regression rate of the fuel surface (Koseki, 1994);

when the hot zone reaches and mixes with the water layer at the base of the tank, the water is superheated and the change from liquid water to steam occurs explosively. The violent generation of steam bubbles pushes the fuel out of the tank. After leaving the tank, the fuel comes into contact with the flame and burns rapidly, forming a large fireball and generating a greatly enlarged fire.

Following a theoretical interpretation of experiments by Hall (1925), it has been established that the formation of a hot zone is possible only for a fuel with a wide range of boiling points, e.g. crude oil. The formation mechanism is likely to involve a selective evaporation of lighter fractions. Hall suggested that the hot zone is generated by continuous vaporisation of the light components. Burgoyne and Katan (1947) suggested that the volatile light fractions at the interface of hot and cold fuel rise in succession up to the surface. In a review paper, Koseki (1994) identified that the formation of a hot zone is a necessary requirement for boilover and commented that multi-component fuels have a stronger tendency of forming a hot zone.

The most important findings on hot zone boilover are the identification of conditions which must exist in order for a boilover to occur: (1) presence of water; and (2) occurrence of a hot zone. In addition, Hall (1925) had also observed that boilover occurrence did not take a violent form unless (3) the oil was viscous in nature. As reviewed in the literature, for a boilover to occur, the hot zone must achieve an appropriate thickness and temperature in the burning oil (Burgoyne & Katan, 1947; Hasegawa, 1989; and Robertson, 2000). When the lower boundary of the hot zone reaches a layer of water at the bottom tank, the water will become superheated, and rapidly vaporise to steam up to 1700 times its original volume. This sudden vaporization of water pushes the fuel out of the tank.



### 1.1.2 Thin Layer Boilover

Relatively thin layers of fuel floating over a water layer, as happens in a hydrocarbon spill onto water (e.g. the sea), also present a risk of boilover when ignited. Such boilover is known in the technical literature as thin layer boilover (Evans *et al.*, 1991; Koseki & Mulholland, 1991). This type of boilover is less violent and destructive than hot zone boilover due to the shallow depth of fuel. However, the change from steady burning to boilover is very fast.

Similarly to hot zone boilover, the thin layer boilover is marked by a significant increase in the size and radiation of the flame due to the generation and expulsion of steam bubbles from the water covered by the fuel. Though it has been reported that there is no clear borderline between hot zone boilover and the thin-layer boilover (Koseki, 1994), they are somewhat different in nature. The main differences are that in thin layer boilover, a hot zone is not formed (Broeckmann & Schecker, 1992, 1995) and the heat transfer from the fuel surface to the liquid phase appears to be limited by conduction (Garo *et al.*, 2006).

In the case where a hot zone is not formed, the fire heats only a thin layer of fuel which gradually descends to the bottom of the tank at the same speed as the regression rate of the fuel surface (Broeckmann & Schecker, 1992, 1995). For this reason, when the water boils, only a very small layer of fuel remains, hence the consequential effects of boilover in a large storage tank are greatly reduced. It was further suggested by Broeckmann and Schecker that a fuel that does not form a hot zone, whatever the initial thickness, can only lead to thin layer boilover because when the water is brought to its boiling point, there will always only be a small amount of fuel remaining.

The studies of thin layer boilover are relatively recent (Koseki *et al.*, 1991; Koseki, 1994; Garo *et al.*, 1994, 1996, 1999, 2006, 2007; Garo & Vantelon, 1999; Chatris *et al.*, 2001; Torero *et al.*, 2003; Hristov *et al.*, 2004; Ferrero *et al.*, 2006, 2007; Kozanoglu *et al.*, 2007). Most of these studies of thin layer boilover have been made using small diameter pools. The studies were undertaken,

principally to study the rate at which the fuel was consumed and the heat transfer mechanisms involved, and to predict the time of boilover in order to evaluate combustion as a way of mitigating spills of fuels onto water.

Overall, the boilover phenomenon is well accepted to be complex and that there are a variety of aspects involved in the process. Understanding further the conditions in a liquid hydrocarbon storage tank during a fire affecting the onset of hot zone boilover is one of the main aspects of this study. In this sense, this thesis aims to expand knowledge of the phenomenon and add to current understanding of the phenomenon, through the analysis of recently conducted field scale experiments and through the design, construction and use of a laboratory scale facility for the study of boilover.

## **1.2 MOTIVATION**

### **1.2.1 Boilover Accidents**

*'Had the observers better understood a devastating phenomenon known as boilover, the eruption of steam and hot oil that followed would not have claimed more than 150 lives (including 53 fire fighters)'*  
- *Inferno at TACO*A ([http://www.fireworld.com/ifw\\_articles/boilover\\_0409.php](http://www.fireworld.com/ifw_articles/boilover_0409.php))

Although accidents involving storage tanks can be considered infrequent, they still happened and pose a threat to life, cause severe damage and high losses. A study of storage tank accidents over the last 40 years (Chang & Lin, 2006) revealed that out of 242 cases reviewed, tank fires were the most frequent with 145 cases, followed by tank explosions with 61 cases. Oil spill and toxic release were the third and the fourth most frequent, with 18 and 13 cases respectively. The study also stated that 80 accidents were caused by lightning and 72 were due to poor operation and maintenance errors. The study also pointed out that the design of tank most frequently involved in the accidents was the atmospheric external floating roof type and the second most frequent was the atmospheric fixed cone roof type.

A number of boilovers associated with fires in large storage tanks that occurred in the last century have also been reported (Persson & Lonnermark, 2004).

Some of these accidents resulted in high loss of life and significant property damage due to the consequences of the expulsion of hot burning oil. The following summaries of three of the accidents illustrate the severity of a boilover event.

In 1971, lightning hit a 33 m diameter tank at Czechowice-Dziedzice Refinery, Poland that contained crude oil, causing its cone roof to collapse and causing a full surface fire (Persson & Lonnermark, 2004). Five hours after the fire started, a rapid boilover occurred, throwing burning oil in all directions up to 250 m away. It was reported that 33 people died as a consequence of the boilover.

Another case of a similar nature was reported in 1982 at a power plant in Tocoa, Venezuela. A three-person crew went to measure the amount of fuel in a tank which contained No. 6 fuel oil. Moments later, a huge explosion ripped off the tank roof (Garrison, 1984). By the time the fire brigade had arrived, a fire involving the contents of the tank was well established. About 8 hours after the fire had started, there was a violent boilover. The oil expulsion and resulting fireball killed over 150 people because the ejected burning liquid raced down the hillside toward the plant and local population.

In 1983, another boilover occurred at the Amoco Refinery tank farm in Milford Haven, United Kingdom. A fire started in a 78 m diameter floating-roof crude oil storage tank, which had a volume capacity of 94000 m<sup>3</sup>. Unfortunately, hours later, the floating roof lost its structural integrity and sank. After a short period of time, loud crackling noises with increasing flame intensity forced the fire fighters to evacuate the scene. The rare phenomenon of multiple boilovers occurred in this incident. During each boilover, steam pushed the oil out of the tank to a height of almost 900 m (3000 ft). Although the incident did not jeopardize life or production, the value of the estimated loss of crude oil was £4 million (1983 prices) (Robertson, 2000 and Persson & Lonnermark, 2004).

### 1.2.2 Modelling and Simulation

Boilover is a dangerous accidental phenomenon. A boilover can occur several hours after ignition. Consequently, the time from the start of the fire to boilover is an unknown parameter which is of great importance when managing the emergency response operations in oil tank farms storing fuels with the potential to boilover.

Modelling and simulation of boilover allows the desired characteristics of a storage facility to be determined and enables corresponding safety measures to be prepared.

Much of the existing research focuses on the heat transfer processes from the flame to the burning fuel. A number of mathematical models for hot zone formation, internal temperature profiles and convection mechanisms inside the fuel have been created and made available from these researches. Few works have actually focussed on the practical application of theory to the problems associated with fighting tank fires with boilover potential. Although undeniably useful, the mathematical models are idealised and it is unlikely that the complex expressions that have been developed will prove to be helpful at the time of an incident.

In addition, the approaches used in developing the models are very scientific and less accessible for personnel involved in handling emergencies at storage sites. Different heat transfer models have been proposed to predict the temperature evolution in the fuel and water layers, and the time for boilover to occur. Usually, unsteady, turbulent, free convective motion of fluid contained in a cylindrical enclosure is modelled using the Boussinesq approximation of the Navier-Stokes equations. The governing equations are mass continuity, conservation of momentum and heat/energy equations. With a limited set of initial and boundary conditions, the governing equations are solved numerically using computational fluid dynamics. The model simulates and predicts the temperature histories in the burning fuel and water layers. The time to reach the

vaporisation temperature of water at the oil-water interface is determined which gives the boilover time.

These models, although providing reasonably accurate estimates of the occurrence of a boilover, are not designed to be run during a crisis. These models which require significant computer capacity and time to achieve a solution are more suited to the planning or research stages (Cornwell, 1999).

### **1.3 OBJECTIVES**

As indicated in the first paragraph of this chapter, the objective of this work is to study an accident scenario involving the ignition and burning of the contents of a large storage tank. In particular the purpose of this work is to study the phenomenon of boilover, which, in this context, is defined as the ejection of hot burning fuel out of the tank in sufficient quantities to endanger the lives of fire fighters and possibly cause escalation of the incident by igniting the contents of adjacent tanks.

From the descriptions of hot zone boilover and thin layer boilover presented in Sections 1.1.1 and 1.1.2, it is clear that hot zone boilover is the type that is of relevance to the objectives of this research. Consequently, it is hot zone boilover that will be addressed, primarily, during the remainder of this thesis.

The main objectives of this research are to develop a greater understanding of boilover pertaining to fires involving the contents of large storage tanks and to produce predictive tools capable of predicting the important parameters associated with a boilover event. The predictive tools must be capable of estimating:

- i. The potential of a fuel to boilover
- ii. The time to boilover
- iii. The temperature of the hot zone
- iv. The amount of fuel remaining in the tank prior to boilover and hence the quantity of fuel that would be ejected during boilover

- v. The consequences of a boilover i.e. fire enlargement and fireball effects and the ground area affected by the expulsion of oil during a boilover event

The main criterion of the predictive tools is that they should produce readily accessible results to guide a wide range of emergency response personnel on handling the boilover phenomenon. In order for the predictive tools to be useful during a crisis, they should be easy to use, capable of modelling the situation at hand and produce a conservative, easy to understand representation of the incident in a very short period of time (Cornwell, 1999).

An additional objective which was realised during the course of the work was the design and construction of a laboratory scale experimental facility to enable well controlled boilover experiments to be undertaken more cheaply and easily than in the field.

## 1.4 THESIS STRUCTURE

In **Chapter 2** a review of the literature on hot zone boilover is presented. This includes the heat transfer mechanisms between the flame and the fuel surface and within the liquid. The development of the temperature profile within the liquid during a fire involving the contents of a storage tank is examined for the case when a hot zone is formed and when a hot zone is not formed. This information is particularly important in identifying those fuels that will boilover and those that will not.

The research described in this thesis has been supported by the LASTFIRE project. The LASTFIRE stands for Large Atmospheric Storage Tank Fires and is a collaborative project funded and guided by the following oil and gas companies: ADCO (Abu Dhabi), BP (Britain), IDEMITSU (Japan), MERO (Czech Republic), MOL (Hungary), NESTE OIL (Finland), PETRONAS (Malaysia), QATAR PETROLEUM (Qatar), SAUDI ARAMCO (Saudi Arabia), SINOPEC (China), SHELL (Netherland-Britain), TAKREER (Abu Dhabi),

TOTAL (France) and ZADCO (Abu Dhabi). The LASTFIRE project is managed by Resource Protection International.

The LASTFIRE project has provided access to the results of many field scale experiments carried out over a number years on 0.61 m, 1.22 m, 2.44 m and 4.5 m diameter tanks. Much of the more recent data on 1.22 m, 2.44 m and 4.5 m diameter tanks were obtained by Loughborough University whilst providing assistance to Resource Protection International. The field scale experiments are described in **Chapter 3** together with an analysis of the data obtained and the use of the data to develop empirical predictive tools to achieve the objectives of the project.

Undertaking field scale experiments is very expensive, gathering detailed data is difficult and the experiments are subject to the vagaries of weather. In order to allow well defined and repeatable experiments to be performed and to obtain more detailed measurements and visual records of the behaviour of the liquids in the tank, a novel laboratory scale rig has been designed, built and commissioned at Loughborough University. This is described in **Chapter 4**.

In **Chapter 5** the programmes of experiments undertaken in the laboratory scale rig are described. The data and visual records obtained from these experiments are presented together with an analysis of the data.

In **Chapter 6** the development of a model of hot zone boilover is described. The model is based on the theory that the hot zone is formed as a result of a distillation process taking place within the upper region of the multi-component fuel. Mixing is induced by the rise of bubbles following the vaporisation of the lighter components of the liquid below its surface. This causes a downward flow of the heavier components with the result that a layer known as a hot zone is formed towards the top of the liquid of both uniform composition and temperature. The temperature of the hot zone is determined by the boiling point of the lightest component within the zone and this temperature can change with time as the hot zone develops and its composition changes.

In **Chapter 7** the predictions from empirical model developed in Chapter 3 and the model described in Chapter 6 are compared with the laboratory and field scale data and with information obtained from boilover incidents.

**Chapter 8** presents a discussion of the work presented in this thesis together with suggestions for future research into the topic of boilover. The chapter also highlights the main conclusions of the research.



## 2 LITERATURE REVIEW

The purpose of this chapter is to provide a review of the major work done to date to characterize the boilover phenomenon. The review presents information for improving the level of knowledge about the phenomenon and gathers data that can be used to plan new experiments, to compare results obtained from different experimental programmes and for model development and validation. In this chapter, a review on burning oils is presented to technically evaluate prior experimental and theoretical boilover scenario studies. The review acts as a basic introduction for further investigation focusing specifically on hot zone boilover phenomena.

This chapter is divided into several sections. In the first section, the review focuses on the studies conducted towards understanding the hot zone boilover problem. It discusses, based on the studies of many researches, the conditions necessary for the phenomenon to occur.

In the second section, the review focuses on storage tank fires, which can be considered as pool fires. The main variables of pool fires such as burning rate, total heat release rate, radiation fraction and liquid oil temperature, will be discussed. The review of these variables will act as the foundation in developing predictive tools for boilover onset; which was mentioned in Chapter 1. The subsequent part of this section defines the thermal and physical properties of liquid hydrocarbon fuels, based on different factors such as specific gravity.

The third section reviews the literature dealing with the mathematical modelling of pool fires. It presents a number of models which can be utilised to estimate temperature profiles in the bulk of a burning liquid. The section discusses the pros and cons of the models. In the last part of this section, the review discusses the use of models or tools in emergency situations.

The final section of this chapter focuses on the consequences of boilover. Literature is reviewed on the characteristics and consequences of fires and fireballs and their potential to cause injury and escalation is discussed.

## **2.1 HOT ZONE BOILOVER PHENOMENON**

As described in Chapter 1, a hot zone boilover that is of concern with regard to large atmospheric storage tanks is defined as a sudden and violent expulsion of hot oil from a burning tank. It occurs, generally, in fuel tanks where a full surface fire has been burning for a significant period of time.

During burning, components of the oil with a low boiling point are vaporised first and the vapour bubbles ascend to the surface. The ascent of these bubbles causes rising and sinking flows within the bulk liquid which results in continual and strong convection currents (Hasegawa, 1989). This mechanism homogenizes the fuel and produces a hot isothermal layer which is termed the hot zone.

Boilover happens when the hot zone, formed within the burning fuel, reached a water sub-layer at the base of the tank. The water vaporizes and pushes the hot fuel out from the tank, resulting in enlargement of the fire, formation of fireball and an extensive pool fire on the ground. Hot zone boilover results from the onset of boiling at the fuel/water interface when a significant depth of fuel exists above the interface. Therefore, the time from ignition to the onset of boilover correlates well with the time needed for the thermal wave to reach the water (Garo *et al.*, 1994).

In this section, the historical progression of boilover theory is outlined and organized chronologically. From the first observations of boilover, it was clear that the phenomenon is connected to heat transfer from the flame to the liquid surface and within the liquid fuel, which affects the temperature profile within the fuel. Therefore, the review will focus on this aspect.

### 2.1.1 Layering Effect within Burning Fuels

The first attempt towards understanding the boilover phenomenon was a series of large-scale pool fire experiments carried out in 1920s (Hall, 1925). Using varying tank sizes and numerous types of oils, it was discovered that a layering effect formed in those tests in which boilover occurred. A general explanation of temperature changes beneath the surface of the oil was deduced by Hall based on the findings of the experiments. There was a very hot surface layer where the flames existed and under that there was an isothermal hot layer, sitting above a somewhat colder layer. This layering effect was due to a distillation process taking place. The very hot surface layer consisted of the heaviest components at their boiling point. The isothermal layer consisted of uniform composition and temperature in which the most volatile components were vaporized. This layer was then progressively enriched since the proportion of higher boiling point components increased and consequently its temperature also increased. This high temperature isothermal layer was called the hot zone. There were sharp discontinuities between the temperatures of the surface and the hot zone and between the hot zone and the colder oil. It was also observed that the hot zone grew as the fire burned. A boilover occurred when the bottom of the hot zone layer reached the water at the bottom of the tank which was then vaporised. One of the most important findings of Hall's study was the identification of three physical conditions which must exist in order for a boilover to occur. These conditions are: (1) presence of water, (2) occurrence of a hot zone, and (3) viscous liquid fuels (Hall, 1925).

The presence of water in a storage tank is the significant condition for boilover to occur. The energy generated from the conversion of water to steam is the source of the force behind the ejection of fuel out of the tank. The forces developed by the formation of steam are sufficient to overcome the fuel surface tension and head force developed from the bulk fuel weight. The water sub-layer exists in the lower parts of tanks for different reasons. Naturally, mineral water is present in fuel tanks in a separate layer at the base. Water can also be found in an emulsified form within the fuel due to process requirements (contamination) e.g. water being introduced during the desalting stage in crude

oil processing. In addition, fuels are usually stored in tanks for various processing requirements over a long period of time, and during these long intervals, water due to its larger specific gravity settles down to the bottom of the tanks. The tanks are often open to the atmosphere allowing ingress of rain and in the event of a fire, fire fighting water can enter the tank.

### **2.1.2 Hot zone due to Bulk Circulation of Fuels**

Based on the theoretical interpretation of Hall's (1925) experiments, it was established that the formation of the hot zone is possible for compound fuels consisting of components having a wide range of boiling points.

Burgoyne & Katan (1947) extended the work of Hall and similarly reported that boilover occurred when the hot zone reached a water layer at the bottom of the tank. Experiments were conducted in the open air using two tanks; a 0.56 m (22 inches) diameter tank and a 2.75 m (9 feet) diameter tank. Temperatures at various fixed points in the tank were observed through horizontally oriented thermocouples. The rate at which fuel was lost was measured by means of a manometer located at the bottom of the tank.

The work showed that for many refined fuels, the surface fire burned almost all the fractions very close to the surface and the bulk of the fuel was not affected. Hence, these were categorized as non-hot-zone-forming fuels for which a hot zone boilover does not occur. Diesel was used in the most detailed experiment in which a hot zone was not formed. For these experiments, the manometer results showed a constant reduction in the weight of the fuel column within the burning period of about 60 minutes. This could be translated into a steady mass burning rate of the oil and hence a linear drop of the surface with time during the fire. The thermocouple records showed that when the steady conditions of burning had been achieved, significant heating of the fuel did not penetrate more than 50 mm below the surface. At the instant when the thermocouples intersected the fuel surface, the mean temperature recorded was 354°C, which appeared to be close to the final boiling point of 375°C. This, according to Burgoyne and Katan, showed that the complete range of fractions of the fuel

was burned as the surface fell during the fire, implying that a distillation process resulting in the formation of a hot zone did not occur.

Experiments involving crude and fuel oils showed that the most volatiles components were removed first and those hot, less volatile components accumulated. These oils were classified as hot-zone-forming fuels and the experimental work focused on fuel oils. From the thermocouple recordings, it was observed that the heating of fuel penetrated significantly below the surface. For example, thermocouples located at about 76 mm (3 inches) and 127 mm (5 inches) from the surface respectively, registered similar temperatures of 250°C after approximately 50 minutes of burning. This showed the presence of a hot zone that was steadily increasing in depth beneath the surface. In the experiments, samples of oil were collected from various levels in the tank. Based on the analysis conducted, the samples taken from the hot zone were found to be the residue that formed when lighter fractions from the original fuel had been removed.

Burgoyne and Katan also put forward a theory that the hot zone is formed due to bulk circulation of the fluid. As the fuel burns, some energy is used to vaporise light ends at the hot-cold interface which supply the fire, and some heat is retained to drive the mass circulation of the hot zone. As the hot zone grows, the vaporised light ends add to the stirring effect of the mass circulation within the hot zone. Hence it was suggested that the temperature and composition of the hot zone are determined by the heat transfer coefficients at the bottom of the hot zone and at the surface of the fuel and the thermal properties of the fuel rather than by mass transfer effects as proposed by Hall (1925).

### **2.1.3 Hot Zone Propagation by Heat Conduction**

In 1961, experiments undertaken by Russian researchers on boilover at the laboratory scale revealed that the water under the burning fuel became superheated without boiling and the subsequent explosive phase change lead to boilover (Blinov & Khudyakov, 1961). When water is heated to its boiling

point, nucleation points are required for boiling to occur and form vapour bubbles. If suitable nucleation points are not available then the water becomes superheated. In the case of a tank fire, the wall usually provides adequate nucleation sites.

The laboratory tests by Blinov and Khudyakov were performed using small vessels heated externally through the wall. The tests ended up with explosive fuel ejection or boilovers. Consequently, and different to the mechanisms proposed earlier (Hall, 1925 and Burgoyne & Katan, 1947), it was proposed, somewhat radically, that the hot zone growth could be propagated by conduction through the wall of the tank. The authors indicated that heat transfer through the wall affected the hot zone formation and that the onset of boilover occurred around the wall at the height of the fuel-water interface.

#### **2.1.4 Tank Dimensions on Hot Zone Progression**

In 1988, boilover tests were conducted by the National Research Institute of Fire and Disaster (NRIFD), Japan, using a range of open top cylindrical tanks to burn diesel, gasoline and mixture of diesel and gasoline (Hasegawa, 1989). Detailed observations of temperature changes below the surface, density of the fuel and thermal radiation were measured and analysed. In the tests, the vaporisation of light components of a fuel mixture at the base of the hot zone was observed. The vapour bubbles of the light components formed at the interface enhanced the mixing and stirring of fuels within the hot zone. Through this observation, it was shown that the hot zone was uniform in composition and temperature both horizontally and vertically, supporting the bulk circulation mechanism proposed by Burgoyne & Katan (1947).

In the tests involving diesel, a hot zone was not formed. The hot zone was formed when the mixture of diesel and gasoline was used. Hot zone formation and boilover occurred in compounds ranging from 50-90% diesel when the temperature of the hot zone rose above 130°C and the speed with which the base of the hot zone penetrated down into the cold liquid was greater than the

regression rate of the fuel surface. From this observation, it was further confirmed that hot zone formation was due to the effect of the boiling range of the fuel.

In this experimental campaign, investigations were also carried out to determine the effect of tank size and tank material on hot zone formation. It was concluded that hot zone formation was very much dependent on the size and material of the tank. For a tank diameter of less than 800 mm, the appearance of the hot zone was strongly dependent on the material of construction of the wall, because this influenced the surface temperature of the fuel. Hot zone formation was found to be a complex function between thermal interaction between the wall and the fuel at the location of the fuel surface and the location of the hot-cold interface. However, for tanks greater than 900 mm diameter, the formation of the hot zone depended only on the properties of the oil. Since the research described in this thesis is concerned with boilover in large atmospheric storage tanks, the wall effects described above for tank diameter of less than 800 mm need not be taken into account.

The experiments also revealed that there was an oscillating interface between the hot and cold layers. Observation showed a curved interface between the two layers which moved down and oscillated continuously. The interface was initially at rest, then began moving slowly up and down and continued to increase gradually to reach maximum amplitude. The interface then disappeared and its motion ceased. After a while, the interface was formed again and again started to oscillate. This cycle of motions was repeated intermittently and resulted in an increase in the rate of conversion of cold fuel to hot fuel thereby increasing the thickness of the hot zone. The fuel above the interface waved and shimmered with heat. The fresh cold fuel was entrained into the hot zone due to the oscillation and to the heat exchange through the interface. This finding showed a relationship exists between the cold fuel-hot fuel conversion rate and the heat and mass transfer at the interface.

### 2.1.5 Depth of Fuel on Boilover Onset

A study by Koseki *et al.* (1991a) showed the importance of the initial thickness of the fuel towards onset of boilover and its intensity. Regression rate of the fuel surface, the speed at which the base of the hot zone progressed towards the bottom of the tank, external radiation and the time to boilover were measured for Arabian light crude oil burning in tanks with diameters ranging from 0.3 to 2.0 m.

When reporting the results from burning a 30 mm deep layer of crude oil in a 1 m diameter tank, the authors described that the regression rate of the fuel reached a plateau at an average value of  $0.033 \text{ mm s}^{-1}$  at about two minutes after ignition and was maintained until boilover occurred. The intensity of boilover as indicated by the splashing of water and fuel and a measurable increase in the radiative heat flux was found to increase with increasing initial fuel layer thickness. Such a conclusion is not surprising since the deeper the fuel layer the deeper will be the fuel above the fuel-water interface at the time boilover occurs given that the speed with which the base of the hot zone progresses towards the bottom of the tank is greater than the regression rate of the fuel surface.

The speed with which the hot zone progressed towards the bottom of the tank was obtained through the relationship between the initial fuel layer thickness and the time to boilover. After analysing the results, the authors cautioned that the formation of the hot zone could be the key mechanism for the occurrence of boilover.

The time to boilover and its intensity were found to be directly proportional to the initial thickness of the fuel layer. It was also found that a hot zone of at least 5 to 10 mm thickness was necessary for the appearance of boilover.



### 2.1.6 Heat Transfer in Hot Zone Formation

Koseki (1994) published further work on boilovers in which he delved further into the theory of hot zone formation with respect to heat transfer mechanisms.

The observations from the study recognized that:

- i. The uniformity of the hot zone is due to strong convection currents induced by fuel vapour bubbles as they ascend through it.
- ii. The sharp discontinuity in the temperature profile (Hall, 1925) at the hot-cold interface is because heat is only being transferred by conduction, from the hot zone to the cold liquid below. The fuel temperature below the hot zone decreased with depth exponentially (refer to Figure 1-1 in Chapter 1).
- iii. Only in the case where the base of the hot zone propagates at a velocity,  $v_{hz}$  towards the fuel-water interface which is greater than the regression rate of the fuel surface,  $v_a$  will boilover occur. Figure 2-1 explains this behaviour.

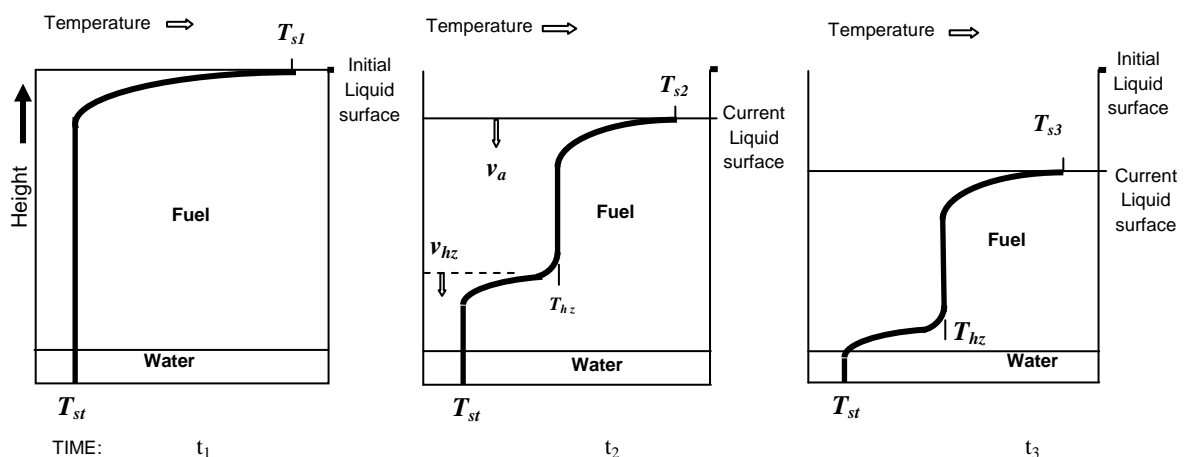


**Figure 2-1: Schematic illustration of boilover. Three Stages in the formation and propagation of a hot zone during a fire (Time:  $t_1 < t_2 < t_3$  / Surface temperature:  $T_{s1} < T_{s2} < T_{s3}$ )**

Note:  $v_a$  is the regression rate of fuel surface,  $v_{hz}$  is the speed of base of hot zone,  $T_{st}$  is the initial storage temperature and  $T_{hz}$  is the hot zone temperature.

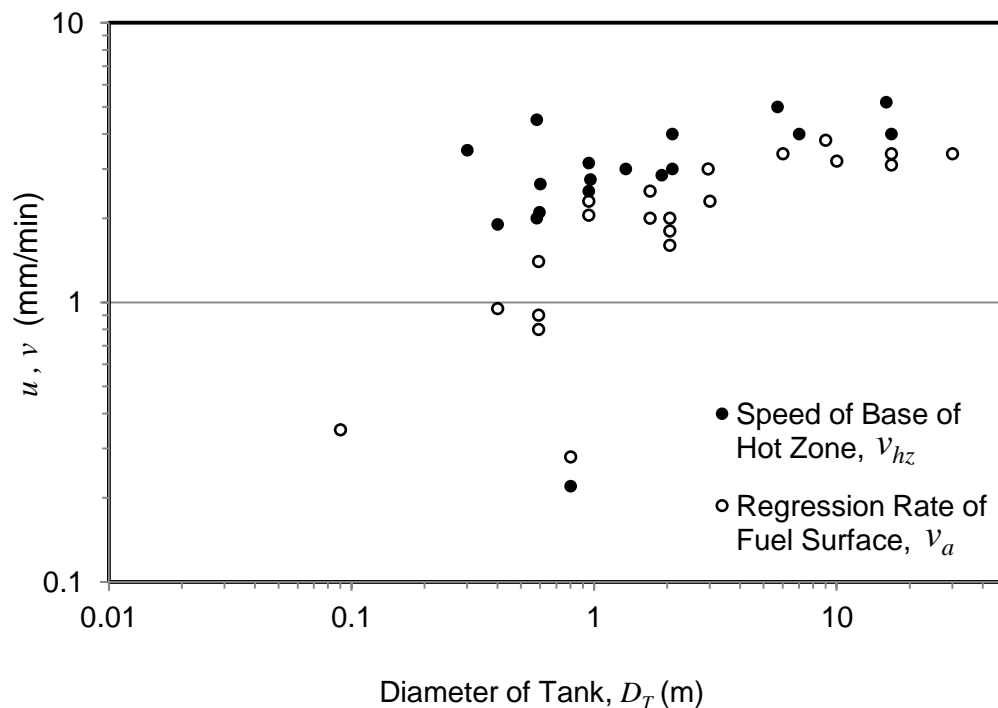


**Figure 2-2: Dependence of burning velocity and hot zone propagation velocity on the diameter of the tank [Data extracted from Koseki (1999)].**

The data in Figure 2-2 are presented in a review of works on pool fires (Koseki, 1999), and compares the regression rate of the fuel surface and the speed with which the base of the hot zone progresses towards the fuel-water interface as the tank diameter is increased (Koseki, 1994). It can be seen that both parameters increase with tank diameter. However, the regression rate of the fuel surface increases at a rate greater than the speed that the hot zone increases up to a diameter of about 5 m. For greater diameters, they remain approximately constant.

The heat balance within the hot zone was analyzed in order to further understand the formation mechanism. The conclusion from the study was that the energy for the hot zone formation comes directly from radiant heat from the flame, but only about 5% of the total heat release energy is transferred to the liquid fuel. Hence only a small amount of energy is used for hot zone formation. Subsequently, the findings instinctively support the idea proposed by Hasegawa (1989) that the heat contribution from conduction through the wall, that could affect the hot zone and boilover, was very small in a large tank fire. Since the

ratio of wall area to volume decreases with the radius, the heat transfer through the wall via conduction became less significant when compared to the volume of the tank. In addition, the amount of water present in the fuel layer does not influence the boilover. It was found that the bulk of the water remained at the same low initial temperature.

### **2.1.7 Boilover Premonitory Noise: Micro-explosion**

An experimental study of boilover in tanks containing oil above a layer of water was performed, not only to observe the basic features of boilover, but to record the micro-explosion noise emission and the seething process (violent agitation) at the oil-water interface (Fan *et al.*, 1995). A series of small-scale tests was conducted using different types of fuels such as gasoline, kerosene and machine oil. In these experiments, the structure of the flame was recorded and visualised through the use of camcorders, the temperature of the fuel and water were measured and the sound during the fire and boilover were recorded.

It was found that a typical process of liquid fuel burning on water consists of three basic stages which were characterized by distinctive sound levels, as seen in Figure 2-3:

- i. Quasi-steady state (AB) represents the initial phase of the fire, in which there is no boiling water and the sound spectrum is practically a line.
- ii. Premonitory period (BC): In this state, boiling of the water layer begins to occur, but not so intense boiling. Consequently, the bubbles are expelled immediately. The sound spectrum is not uniform, since there are some peaks attributable to the phenomenon called "micro-explosion noise", i.e., the explosion of vapour bubbles covered with fuel.
- iii. Boilover (CD): During this time, the boiling is very intensive, the bubbles cannot escape immediately, but must reach a certain size prior to expulsion. For this reason, an intense noise or "micro-explosion noise" is

observed. The noise is associated with the explosion of large vapour bubbles coated with fuel.

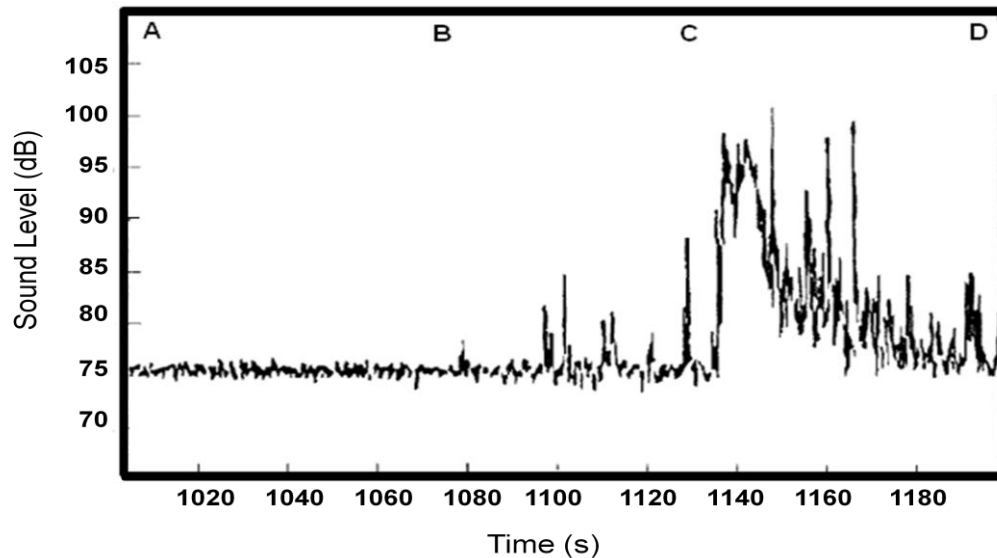


Figure 2-3: Evolution of the sound intensity with time in a tank fire (Fan *et al.*, 1995).

Figure 2-4 shows graphs of the temperature measured within the fluid and the micro-explosion noise level in the premonitory period, against time.

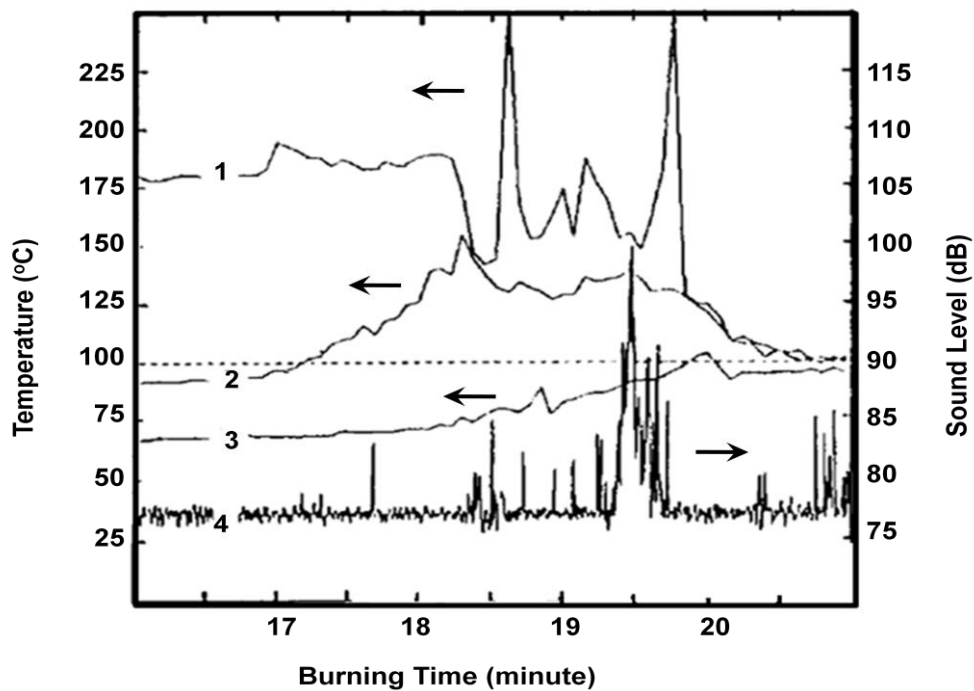


Figure 2-4: The temperature of the fuel-water layer and the micro-explosion noise level in the premonitory period as a function of the burning time (Fan *et al.*, 1995).

Note: Curves 1, 2 and 3 indicate the temperatures at the oil layer, on the interface and in the water layer, respectively. Curve 4 indicates the micro-explosion noise level.

When the temperature of the fuel-water interface is lower than  $100^{\circ}\text{C}$ , the fire is in the quasi-steady stage and there is no micro-explosion noise (constant decibels as shown by curve 4 in the Figure 2-4). Both temperature readings in the bulk fuel and the water layer show constant values as indicated by curves 1 and 3 respectively. When the interface reaches the boiling point of water, the interfacial temperature rises more quickly than that of the fuel layer or the water layer. The fuel layer temperature remains constant. However, the water layer temperature is slowly rising. The micro-explosion noise begins to show (indicated by the spike in the sound level).

When the interfacial temperature reaches its maximum value, a large quantity of bubbles is generated, creating a state of strong seething at the interface. As bubbles rise through the fuel layer, the relatively low temperature vapour causes the hot zone to cool and the interfacial temperature to reduce (indicated by a sharp drop in the temperature (curve 2) at the 18.5<sup>th</sup> minute of burning), leading to temperature fluctuations in the fuel layer (curve 1).

This observation is not surprising since at this time the base of the hot zone is located in the region of the interface where temperature gradients are high. Figure 2-5 summarizes the behaviour explained.

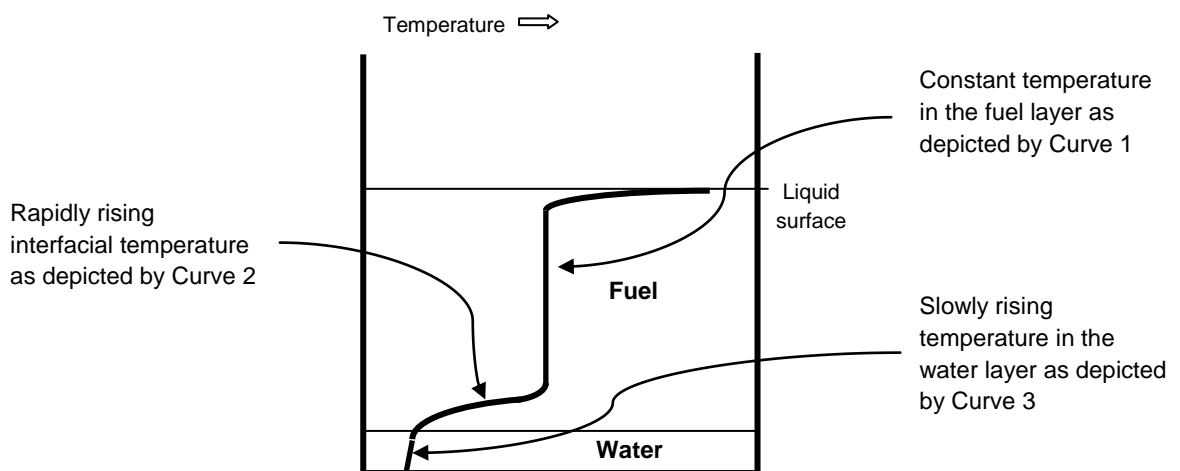


**Figure 2-5: The temperature profile within the fuel-water layer prior to boilover**

When strong seething occurs, more bubbles are being generated at the interface, micro-explosions occur more often and the noise level increases.

As a result of the strong increase in sound level due to water vaporisation at the fuel-water interface (followed by the occurrence of boilover), the authors proposed the possibility of using the micro-explosion noise as a tool to detect the onset of boilover from a remote location.

### **2.1.8 Heat transfer mechanisms in burning oil-water systems**

In the same year (1995), a study specifically focussed on the heat transfer mechanisms occurring in a storage tank fire was carried out for a wide range of fuels. The work was undertaken to determine which heat transfer mechanisms occurring in the liquid fuel leads to boilover (Broeckmann & Schecker, 1995). Experiments were conducted using cylindrical open steel tanks with diameters of 0.19 - 1.91 m. The temperatures in the fuels were measured using NiCr/Ni thermocouples with a diameter of 1.5 - 3.2 mm. The effects of water evaporation were recorded using a video camera, the temperature of the flames were observed through a thermal imager and the regression rate of the fuel surface was measured according to the time when the fuel surface was observed to reach the thermocouples.

Based on the analysis of the results, the authors stated that fuels could be classified into two broad categories:

- i. Non-hot-zone forming fuels: These are fuels such as solvents or compounds comprising of components with similar boiling points that do not give rise to the formation of a wave of heat (hot zone) and therefore cannot cause boilover.
- ii. Hot zone forming fuels: These fuels can produce a hot zone and, hence, can cause boilover when the hot zone reaches the water layer. This is the case of fuels made up of components with a wide range of boiling points.

For the case of non-hot-zone forming fuels, the change of temperature,  $T$  ( $^{\circ}\text{C}$ ) with time,  $t$  (s) at a certain vertical position,  $z$  (mm) can be derived from the equation below:

$$\frac{\partial T}{\partial t} = \frac{\partial}{\partial z} \left( a_{\varepsilon} \frac{\partial T}{\partial z} \right) + v_a \frac{\partial T}{\partial z} + \frac{\kappa}{\rho C_p} q \exp(-\kappa z) \quad \text{Equation 2-1}$$

where

$a_{\varepsilon}$  is the modified thermal conductivity,  $\text{mm}^2 \text{min}^{-1}$

$q$  is the radiant heat reflux from the flame to the liquid fuel,  $\text{W m}^{-2}$

$v_a$  is the speed that the liquid surface progresses downward towards the fuel/water interface,  $\text{m s}^{-1}$

$\kappa$  is the absorption-extinction coefficient of the liquid fuel,  $\text{m}^{-1}$

$\rho$  is the density of the liquid fuel,  $\text{kg m}^{-3}$

$C_p$  is the specific heat of the fuel,  $\text{J kg}^{-1} \text{K}^{-1}$

Equation 2-1 takes into consideration the fuel surface movement and the influence of convective motions. The heat flux,  $q$ , of the non-hot-zone-forming-fuel experiments was found to be about  $40 \text{ kW m}^{-2}$ . The absorption coefficient was set to  $100\text{-}150 \text{ m}^{-1}$  and the modified thermal conductivity,  $a_{\varepsilon}$  was assumed to be about  $30 \text{ mm}^2 \text{min}^{-1}$ . The calculated temperature profile showed good agreement with the experimentally derived results up to a depth of about 20 mm below the surface of the liquid fuel, as shown in Figure 2-6.

Based on Figure 2-6, deviations are observed in the deeper regions of the tank. On this observation, Broeckmann and Schecker stated that this was due to the influence of additional heat conducted from the tank wall and that these effects could not be explained by a one-dimensional approach. They also suggested that the observations indicate that a distillation process occurs within the layer near the surface. The authors termed this layer as the boiling zone in order to differentiate it from the hot zone.

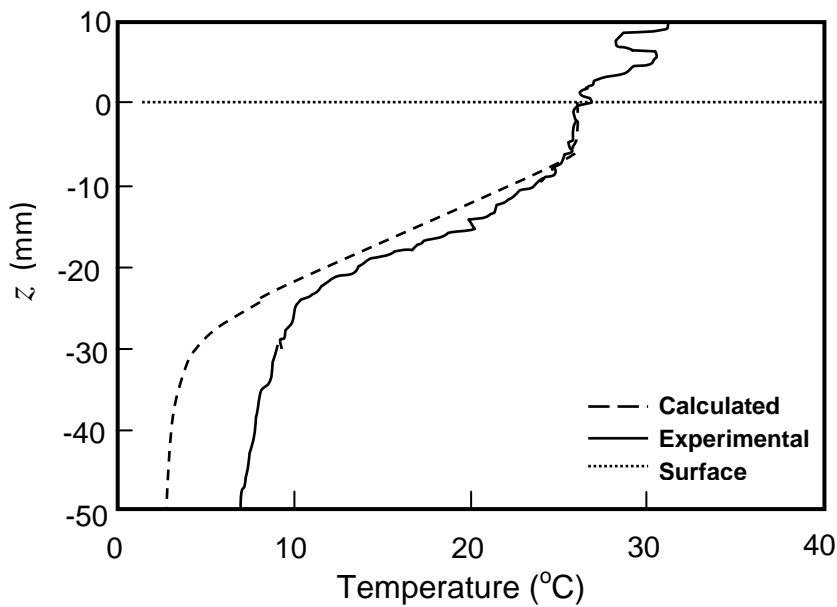


**Figure 2-6: Temperature profile under the surface of non-hot-zone fuel in the 2 m tank: comparison of measured and calculated results**  
[Data extracted from Broeckmann & Schecker (1995)]

In the case of fuels that cause a hot zone to be formed, the temperature evolution is different. The temperature profiles present a uniform temperature inside the hot zone layer within the fuel and not an exponential growth. There are two distinct heating phases influencing the temperature development in the hot-zone-forming-fuels.

The first phase is the heat-up phase where a steep rise in temperature occurs. An exponential temperature profile is observed just beneath the surface of the fuel. The second phase is the growth of the hot zone below the heat-up phase where stabilization of temperature within the fuels is achieved, as shown in Figure 2-7. The depth of the hot zone increases as the burning continues but the temperature remains constant.



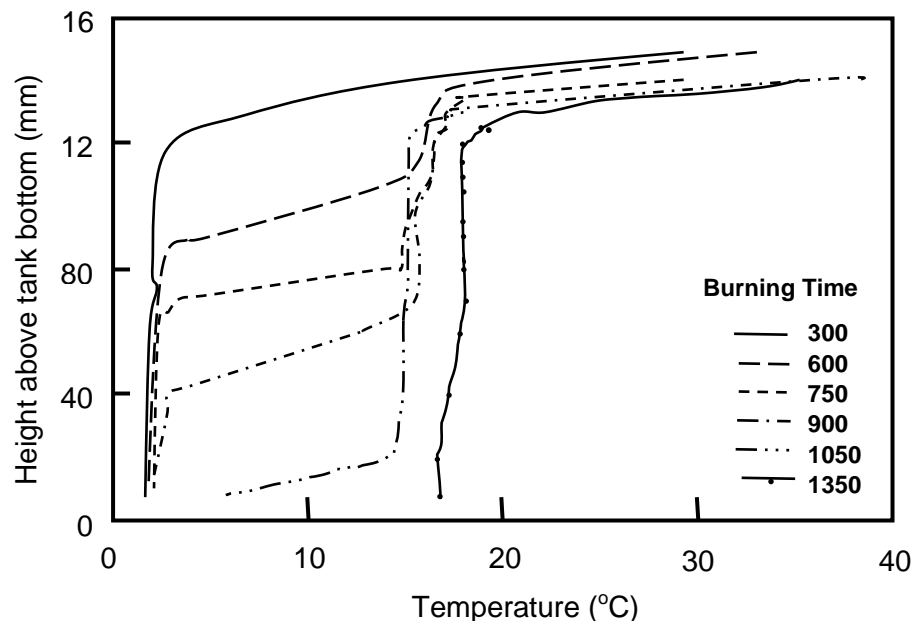


**Figure 2-7: Temperature profile in relation to the distance to the tank bottom for a crude oil (Arabian light, tank diameter = 1 m, height = 0.5 m, initial filling height = 151 mm)  
[Data extracted from Broeckmann & Schecker (1995)]**

It was further reported that an oscillation of the hot-cold fuel interface (at the base of the hot zone) were observed, right through the growth of the hot zone. This oscillating motion was linked to vapour formation and the resulting convective pulses (bubbles formed by the vaporisation of the most volatile components, moving upwards and entraining colder oil to replace them). Extensive mixing and homogenization of the fuel took place resulting in the formation of the hot zone (a layer of uniform temperature and composition). It was concluded that growth of the hot zone was due to this intense convective event caused by the vaporisation of the most volatile components at the hot-cold interface.

In addition, it was also concluded that the hot zone temperature was not a fixed value throughout an experiment and was not a specific constant for each fuel. The ambient conditions, tanks geometric factors and the fuel composition influenced the temperature. These were deduced from the experimental conditions and results. The hot zone temperature would then influence the hot zone growth rate,  $v_{hz}$  relative to the bottom of the tank. The hot zone growth rate

could be expressed in terms of molar fluxes of the vaporized and remaining fractions of the fuel:

$$v_{hz} = \frac{dz_{hz}}{dt} - \frac{dz_f}{dt} = \frac{M_0}{A_T \rho_0} (\dot{n}_L + \dot{n}_V) \quad \text{Equation 2-2}$$

where

- $\dot{n}_V$  is the fuel's molar flux of vaporized fraction, mol s<sup>-1</sup>
- $\dot{n}_L$  is the fuel's molar flux of fraction remaining in the liquid phase, mol s<sup>-1</sup>
- $A_T$  is the fuel surface area, m<sup>2</sup>
- $\rho_0$  is the fuel's initial density, kg m<sup>-3</sup>
- $M_0$  is the fuel's initial molecular weight, kg mol<sup>-1</sup>
- $z_f$  is the height/thickness of the fuel layer, m
- $z_{hz}$  is the height/thickness of the hot zone layer, m
- $t$  is the time, s

The rate of heat supplied from the fire that is required to raise the temperature of the cold fuel to the hot zone temperature and to vaporise the low boiling point fractions was calculated based on:

$$\Delta\dot{Q} = \dot{n}_V (\Delta h_{lh} + h(\bar{T}_{b,V}) - h(T_0)) + \dot{n}_L (h(T_{hz}) - h(T_0)) \quad \text{Equation 2-3}$$

where

- $\Delta\dot{Q}$  is the rate of heat received by the fuel from the fire, W
- $\Delta h_{lh}$  is the molar heat of vaporization of the vaporized fraction, J mol<sup>-1</sup>
- $h(\bar{T}_{b,V})$  is the fuel's molar enthalpy at the mean boiling temperature of the vaporized fraction, J mol<sup>-1</sup>
- $h(T_0)$  is the fuel's molar enthalpy at the initial/ambient temperature, J mol<sup>-1</sup>
- $h(T_{hz})$  is the fuel's molar enthalpy at the hot zone temperature, J mol<sup>-1</sup>

Equation 2-3 shows that the heat supply rate required to vaporise the vaporized fraction and to raise the temperature of the fraction remaining in the liquid phase can be equated to the rate of heat received from the fire. Broeckmann

and Schecker then accounted the hot zone growth rate,  $v_{hz}$  with the following equation:

$$v_{hz} = \frac{\Delta \dot{Q}}{A_T} \frac{M_0 / \rho_0}{\Phi [\Delta h_{lh} + h(\bar{T}_{b,v}) - h(T_0)] + (1 - \Phi)[h(T_{hz}) - h(T_0)]} \quad \text{Equation 2-4}$$

where  $\Phi$  is the fraction of fuel vaporized, which was expressed as:

$$\Phi = \frac{\dot{n}_V}{\dot{n}_L + \dot{n}_V}$$

Equation 2-4 was the earliest proposed model for hot zone growth. In the calculations, a vaporization temperature of 130°C was used as the hot zone temperature, and the heat flux rate from the fire was set at the same value as that obtained from the experiments with non-hot-zone-forming fuels. Table 2-1 shows a comparison between the calculated and measured hot-zone growth rate for a crude oil.

$T_{hz}$ (°C)	$T_0$ (°C)	$v_{hz,exp}$ (mm min <sup>-1</sup> )	$v_{hz,calc}$ (mm min <sup>-1</sup> )
88	3	22.9	14.2
110	5	17.0	10.6
111	20	18.5	11.9
117	-2	14.6	9.3
122	12	11.9	9.7
134	10	8.5	8.5

**Table 2-1: Comparison of calculated and experimental hot-zone growth rates for a Forties crude oil (1 m tank, heat flux = 34 kW m<sup>-2</sup>)**

The model presented was able to predict the hot zone growth rate within a factor of 2.

### 2.1.9 Large Scale Tests and the Influence of Water Content on Boilover

In Tomakomai, Japan (Koseki *et al.*, 2000, 2006), a large-scale experiment was conducted using a 5 m diameter tank filled with Arabian light crude oil. The

initial oil thickness was 0.45 m. A large boilover occurred at about 4200 s after ignition. Radiation outputs during boilover were noted to increase more than ten times that recorded during steady burning. The speed of the base of the hot zone was evaluated based on the measured temperature profile changes in the fuel. The rate of the speed of the base of the hot zone was 0.083 to 0.133 mm s<sup>-1</sup> until 1800 s after ignition, between 2400 and 3000 s after ignition it increased to more than 0.233 mm s<sup>-1</sup>. The speed then dropped to nearly 0 mm s<sup>-1</sup> during the period of 3600 – 4200 s after ignition.

In 2010, an experiment was conducted in Jebel Dhanna terminal area by the Abu Dhabi Company for Onshore Oil Operations (Shaluf & Abdullah, 2011). Two tanks with diameters of 2.4 m and 4.5 m were used to study the characteristics of large oil tank fires in order to gain more knowledge of boilover involving crude oil. These tests were carried out to determine: the speed of the base of the hot zone towards the base of the tank; the period from ignition to boilover and consequences of boilover. For the purpose of measuring the radiant heat during tests, radiometers were placed at the crosswind and downwind directions from the tank. In the 4.5 m diameter tank, the fire resulted in four large boilovers in quick succession followed by a major boilover at 9 hours 45 minutes after ignition. Based on the measured temperature profile changes in the fuel, the speed of the base of the hot zone was estimated to be about 0.1 mm s<sup>-1</sup>. After the fire had burned out, it was noted that the maximum distance realised by the ground fire was about ten tank diameters from the tank wall.

The large-scale tests conducted have elucidated further the process of hot zone formation and its growth, and hence the occurrence of boilover.

Some studies also focused on the influence of water content of the fuel on boilover. One of the significant studies was that by Koseki *et al.* (2003), which examined the effects of emulsified water on the onset of boilover using Sakurawa crude oil which contained about 0.3% (volume) water. Four experiments were carried out in a tank of 1.9 m diameter with fuel thicknesses of 100, 200, 300 and 400 mm. The most interesting result was the occurrence

of boilover at much shorter times than had been noted previously in similar studies in which no emulsified water was present. The speed of the base of the hot zone was recorded at about  $0.55 \text{ mm s}^{-1}$ , which was up to 10 times faster than had been obtained in the previous studies of Koseki *et al.* (1991a, 1991b).

## **2.2 LIQUID HYDROCARBON TANK FIRES**

Of all potential accidents in the process industry, fires are the most frequent (Persson & Lönnemark, 2004 and Chang & Lin, 2006).

A fire in a liquid hydrocarbon tank, which may lead to a boilover, can be considered as a form of a pool fire. Tank or pool fires are the most common (Planas-Cuchi *et al.*, 1997), and may be present in a large number of the accident scenarios that arise in the process industry.

### **2.2.1 Definition of a Pool Fire**

A pool fire is a fire involving a liquid fuel contained within an open topped vessel or bund or an unbounded pool formed following a spill of liquid onto the ground. The vessel could be a large atmospheric storage tank such that the base of the flame is located above ground at the top of the tank. The bund could either be a high walled bund in which case the flame would behave in a similar manner to a storage tank fire or a low walled bund when the base of the flame would be at ground level. For an unbounded spill, the base of the flame would be at the same level as the surface upon which the spill occurred. In all cases, a buoyancy-driven flame, due to highly exothermic reactions, exists (Lees, 1992).

One of the major motivations behind the work on pool fires is the necessity to understand the behaviour of large scale tank fires, because, in some situations, the fires can lead to a catastrophic boilover. Extinguishment of such fires is an extremely difficult and important practical task hence to understand the behaviour of a tank fire is important.

### 2.2.2 Burning Modes and Fuel Consumption Rate

Babrauskas (1983) divides the burning of pool fires based on pool diameter into four distinctive modes. Table 2-2 shows the existence of the two main modes of burning being classified as: a mode dominated by convection for pool fires with small diameters ( $D < 0.2$  m) and a mode dominated by radiation for larger diameter pool fires ( $D > 0.2$  m). There are two different categories of flow in the convective mode – laminar or turbulent, and in the radiation mode, there are two different kinds of flames – optically thin or optically thick.

Pool diameter (m)	Burning mode
< 0.05	Convective, laminar
0.05 to 0.2	Convective, turbulent
0.2 to 1.0	Radiative, optically thin
> 1.0	Radiative, optically thick

**Table 2-2: Burning modes as a function of pool fire diameter (Babrauskas, 1983)**

The classification of the burning modes is based on the analysis of Blinov and Khudiakov's work by Hoyt C.Hottel in 1959, as summarised and presented by Lees (2005). Hottel analysed the well-known work of Blinov and Khudiakov who conducted pool fire tests on several hydrocarbon blends contained in shallow trays. The analysis revealed that as the pan diameter increased the fire regime changed from laminar to turbulent.

Hottel's analysis also reported the link between pool diameter and the rate of fuel consumption. Mass burning rate or fuel surface regression rate is a key parameter that is commonly used in correlations that define the characteristics of pool fires. The analysis shows that the rate at which the fuel was burned decreased with increasing diameter within the convective laminar burning mode ( $D < 0.05$  m). In the transition mode (convective turbulent regime), the rate of burning first decreased and then increased with the pool diameter until it reached a fairly constant value. Within the turbulent radiative burning mode ( $D > 0.2$  m), the rate of burning was assumed to be constant with increasing pool diameter (Lees, 2005).

The analysis also suggested that for the large pools, the fuel consumption rate is determined by the rate of radiative feedback from the flame to the surface of the pool of liquid. Hottel pointed out that rate of heat transfer from the flame,  $\dot{Q}$  (W) to the fuel can be represented as sum of the rates of heat transferred by convection,  $\dot{Q}_c$ , radiation,  $\dot{Q}_r$  and through the tank rim,  $\dot{Q}_{rim}$ , as presented in Babrauskas (1983) and Lees (2005). Equation 2-5 defines the heat transfer mechanism proposed (with negligible  $\dot{Q}_{rim}$ ):

$$\dot{Q} = \dot{Q}_c + \dot{Q}_r = \frac{\pi D^2}{4} U (T_{flame} - T_b) + \frac{\pi D^2}{4} \sigma F (T_{flame}^4 - T_b^4) (1 - e^{-\kappa D}) \quad \text{Equation 2-5}$$

where

$D$  is the pool diameter, m

$F$  is the view factor of the flame

$\kappa$  is the absorption-extinction coefficient,  $m^{-1}$

$T_b$  is the absolute temperature of the liquid surface, K

$T_{flame}$  is the absolute temperature of the flame, K

$U$  is the heat transfer coefficient,  $W m^{-2} K^{-1}$

$\sigma$  is the Stefan-Boltzmann constant,  $5.6705 \times 10^{-8} W m^{-2} K^{-4}$

From the ratio of the average heat flow transferred per unit area (between the flame and the pool) and the fuel's latent heat of vaporization,  $\Delta h_{lh}$  ( $J kg^{-1}$ ), the mass burning rate,  $m_V''$  (rate of fuel mass loss per unit area:  $kg m^{-2} s^{-1}$ ) is obtained via:

$$m_V'' = \left( \frac{\dot{Q}}{\pi D^2 / 4} \right) / \Delta h_{lh} \quad \text{Equation 2-6}$$

The rate of burning in the mode of radiation dominated-optically thick burning (pools greater than 1 m diameter) has been studied in detail. For most liquid fuels, the radiative heat transfer and the rate of burning increase as the diameter increases. Based on Table 2-2 and Equation 2-6, for large pools

(diameters greater than about 1 m), the radiative heat transfer dominates the heat flux to the pool. If the flame's geometric view factor and flame temperature are assumed to be constant, then Equation 2-6 may be simplified to yield the following fuel surface regression rate correlation (Burgess *et al.*, 1961 and Mudan, 1984):

$$\dot{y} = \dot{y}_{max} (1 - e^{-\kappa D}) \quad \text{Equation 2-7}$$

Here,  $\dot{y}$  is the fuel surface regression rate of a finite diameter pool ( $\text{m s}^{-1}$ ) and  $\dot{y}_{max}$  is the fuel surface regression rate of an infinite (very large) diameter pool ( $\text{m s}^{-1}$ ).

For large diameter pools (i.e.  $D > 5$  or  $10$  m), a slight decrease in the burning rate is observed. For such cases of pool sizes, independence of the burning rate on  $D$  is assumed for this radiative regime. Qualitatively this is presumed to be due to poorer mixing, leading to a larger cool vapour zone, lower flame temperatures, and cooler smoke (which can act to shield a fire base from its flames) (Babrauskas, 1983 & 1986).

Figure 2-8 shows the fuel surface regression rate data against pool diameter,  $D$  for crude oil fires (Koseki and Mulholland, 1991a). The fuel surface regression rate increased with increasing pool size up to about 5 m diameter after which it remained constant. The maximum fuel surface regression rate was about  $0.075 \text{ mm s}^{-1}$  which can be taken as a value for  $\dot{y}_{max}$  in Equation 2-7 for crude oil.



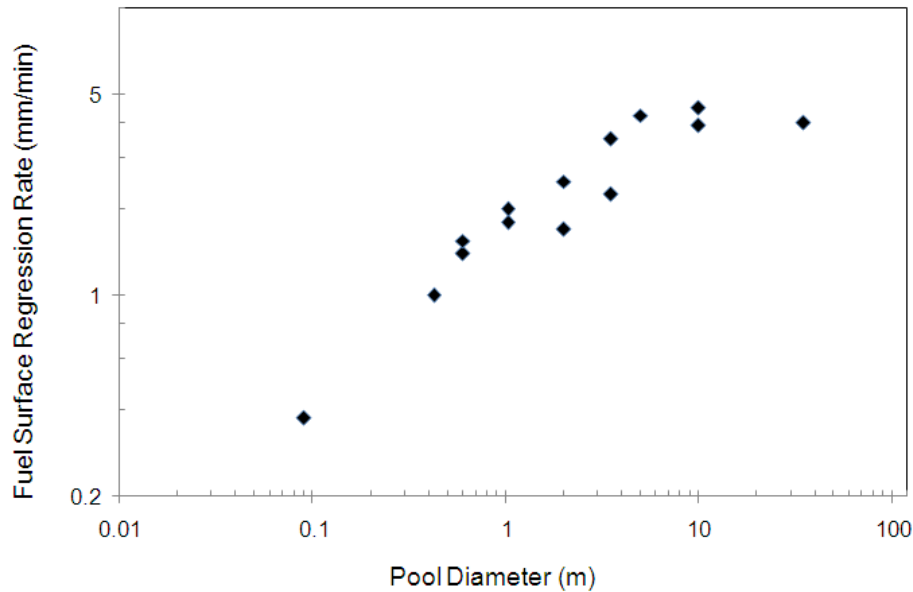


**Figure 2-8: Fuel surface regression rate data against pool diameter (crude oil).  
Data extracted from Koseki & Mulholland (1991a).**

Burgess *et al.* (1961) linked the fuel surface regression rate with the thermochemical properties of the fuel namely the heat of combustion and heat of vaporization. The authors showed that, for pool diameters of about one meter (radiation dominated-optically thick), the fuel surface regression rate of an infinite diameter pool ( $\dot{y}_{max}$ ) can be correlated with a fuel's thermochemical properties as shown by the following relationship:

$$\dot{y}_{max} = 1.27 \times 10^{-6} \frac{\Delta h_c}{\Delta h_{lh}} \quad \text{Equation 2-8}$$

where  $\Delta h_c$  (J kg<sup>-1</sup>) and  $\Delta h_{lh}$  (J kg<sup>-1</sup>) are the heat of combustion and the latent heat of vaporization at the boiling point of the liquid fuel, respectively.  $\dot{y}_{max}$  (unit of m s<sup>-1</sup>) is the fuel surface regression rate.

Zabetakis *et al.* (1961) suggested that the fuel surface regression rate in a large pool,  $\dot{y}_{max}$  (m s<sup>-1</sup>) can be expressed by the equation:

$$\dot{y}_{max} = \frac{k \Delta h_c}{\Delta h_{lh} + \Delta h_{heat}} \quad \text{Equation 2-9}$$

In Equation 2-9,  $\Delta h_c$  is the net heat of combustion in  $\text{J kg}^{-1}$ ,  $\Delta h_{lh}$  ( $\text{J kg}^{-1}$ ) is the latent heat of vaporization of fuel at the boiling temperature,  $\Delta h_{heat}$  ( $\text{J kg}^{-1}$ ) is the heat required to heat a fuel from the ambient temperature to the boiling temperature, and  $k$  is a constant (which will have the same units as  $\dot{y}_{max}$ ). **Figure 2-9** shows the effect of  $[\Delta h_c/(\Delta h_{lh} + \Delta h_{heat})]$  on the fuel surface regression rate for fires in a 1 m diameter tank (Koseki, 1989). The ratio of the heats governs the fuel consumption rate, and the larger the ratio, the greater the rate of burning. The dotted line was from Zabetakis *et al.* (1961).

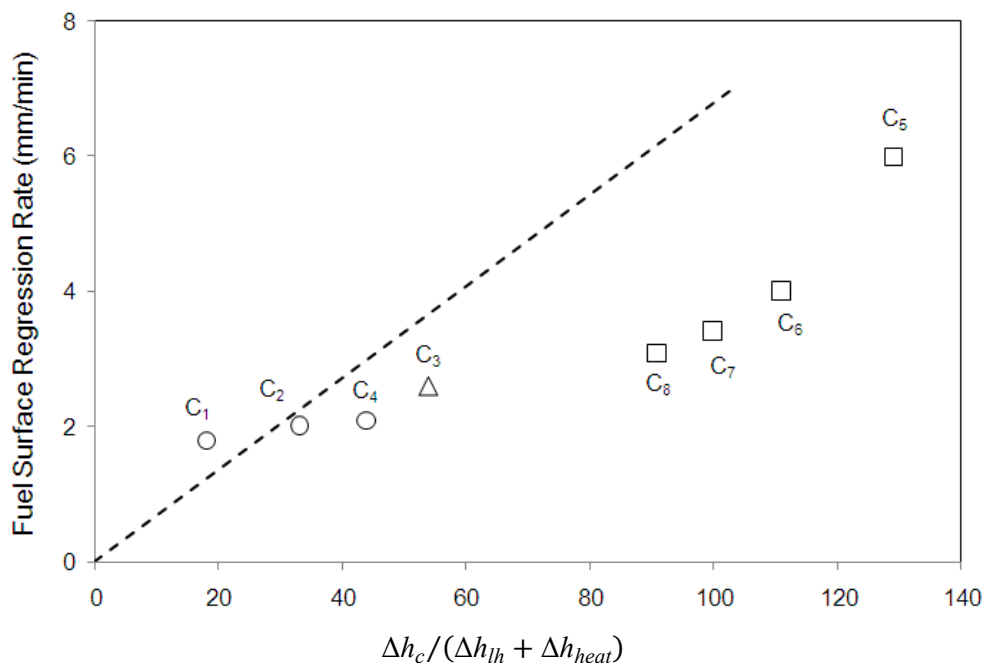


**Figure 2-9: Effect of  $[\Delta h_c/(\Delta h_{lh} + \Delta h_{heat})]$  on burning rate. Circles stand for alcohols, a triangle stands for acetone, and squares stand for hydrocarbon. C denotes carbon number of fuel compounds. That is, C<sub>1</sub> is methanol, C<sub>2</sub> is ethanol, C<sub>3</sub> is acetone, C<sub>4</sub> is butanol, C<sub>5</sub> is pentane, C<sub>6</sub> is hexane, C<sub>7</sub> is heptane, and C<sub>8</sub> is octane. The data were extracted from Koseki (1989) for 1 m diameter fires. The data for the dotted line were extracted from Zabetakis *et al.* (1961).**

A point that deserves particular attention is that fuel mixtures involved in liquid hydrocarbon storage tank fires may consist of several components and hence do not show a uniform rate of burning. Initially the rate of burning is due to evaporation of the more volatile components. As the fire progresses, the mixtures are enriched with less volatile components and the liquid temperature increases to values large enough to evaporate these less volatile components.

Consequently, in the final phase of the fire, the rate of burning will be controlled by components with higher boiling points.

The fuel surface regression rate,  $\dot{y}_{max}$  (m s<sup>-1</sup>) in a pool fire consisting of a liquid hydrocarbon mixture is given by (Grumer *et al.*, 1961):

$$\dot{y}_{max} = 1.27 \times 10^{-6} \frac{\sum_{i=1}^N n_{v,i} \Delta h_{c,i}}{\sum_{i=1}^N n_{v,i} \Delta h_{lh,i} + \sum_{i=1}^N n_{l,i} \int_{T_0}^{T_b} C_p(T) \cdot dT} \quad \text{Equation 2-10}$$

with empirical constants of  $1.27 \times 10^{-6}$  m s<sup>-1</sup> and where

$n_{v,i}, n_{l,i}$  is the mole fraction of component  $i$  in the vapour and liquid phases respectively

$\Delta h_{c,i}$  is the heat of combustion of component  $i$  of the fuel mixture, J kg<sup>-1</sup>

$\Delta h_{lh,i}$  is the latent heat of vaporisation of component  $i$  of the fuel mixture, J kg<sup>-1</sup>

$T_0, T_b$  is the initial and boiling temperatures, respectively, K

$C_p$  is the fuel's specific heat capacity, J kg<sup>-1</sup> K<sup>-1</sup>

The mass burning rate of the fuel per unit area of the fuel surface,  $m''_V$  (unit of kg m<sup>-2</sup> s<sup>-1</sup>) can be determined by multiplying the fuel surface regression rate,  $\dot{y}$  with the liquid fuel density. The correlation for the mass burning rate is given by (Mudan, 1984):

$$m''_V = 1.0 \times 10^{-3} \frac{\Delta h_c}{\Delta h_{lh}^*} \quad \text{Equation 2-11}$$

where  $\Delta h_{lh}^*$  is the modified heat of vaporization of the mixture, defined by the numerator of Equation 2-10.

Figure 2-10 shows the relationship between the mass burning rate and the thermochemistry of fuel i.e.  $\Delta h_c$  and  $\Delta h_{lh}^*$ .

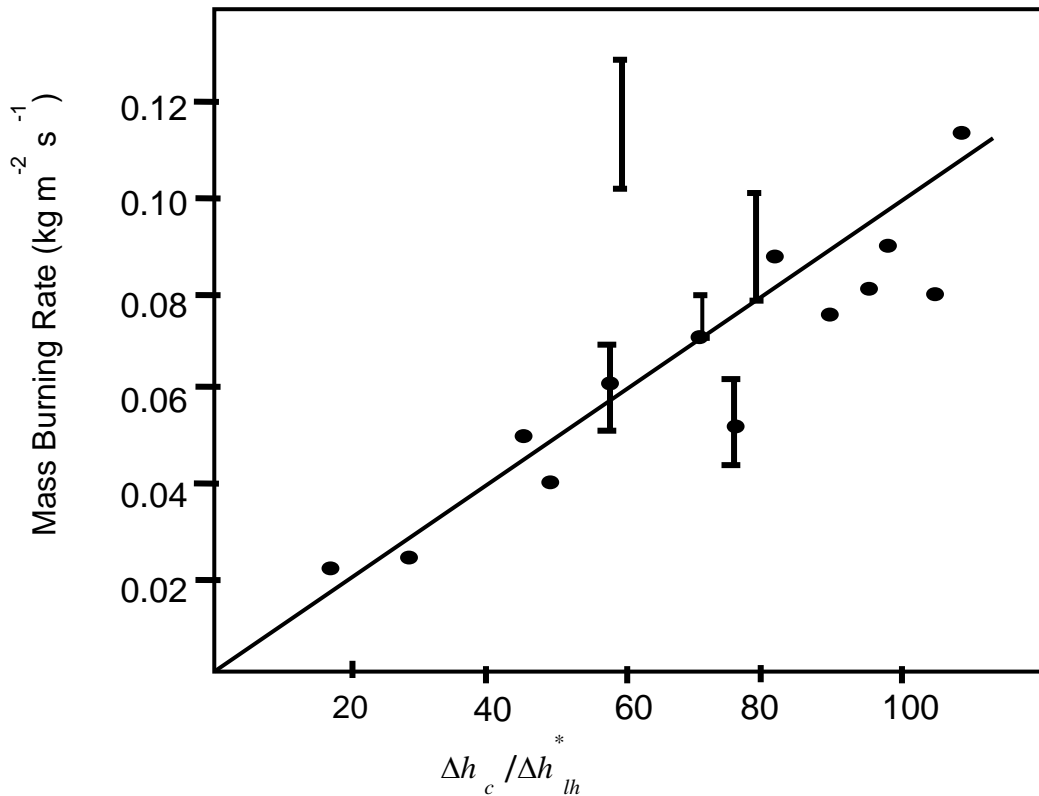


**Figure 2-10: Relation between mass burning rate and fuel thermochemical properties. Data extracted from Mudan (1984)**

The Yellow Book, edited by the Netherlands Organization for Applied Scientific Research (TNO), adopted the suggestion of Zabetakis *et al.* (1961) that the rate of burning could be correlated using the net heat of combustion ( $\text{J kg}^{-1}$ ) as the rate depends only on the consumption of the more volatile components of the fuel. The mass burning rate per unit area can be calculated using the empirical formula (TNO Yellow Book, 2005):

$$m_V'' = \frac{1.0 \times 10^{-3} \Delta h_c}{\Delta h_{lh} + C_p \Delta T} \quad \text{Equation 2-12}$$

in which  $\Delta h_c$  is the heat of combustion,  $\Delta h_{lh}$  is the latent heat of evaporation and  $C_p$  is the specific heat of the fuel;  $\Delta T$  is the difference between the boiling temperature and the ambient temperature. It is important to note that the mass flux vaporizing from a pool fire and the heat flux to the surface of the fuel are coupled in a positive feedback loop (Hamins *et al.*, 1996). The fuel evaporation rate (rate of burning) depends on the rate of heat feedback from the flame to the

fuel surface and the fuel evaporation rate drives the total heat release rate and hence the rate of heat feedback from the flame to the fuel surface.

The heat feedback occurs through radiative, convective and conductive heat transfer. These heat transfer modes are the main elements in quantifying the net heat feedback rate,  $\dot{Q}_{net}$  (W) for heat balance in a liquid fuel pool fire. The sum of the rate of convection,  $\dot{Q}_{conv}$  and rate of radiation,  $\dot{Q}_{rad}$  dominate  $\dot{Q}_{net}$ . The other less important thermal sources and sinks include the rate of heat gain by conduction,  $\dot{Q}_{cond}$  and the rate of heat loss due to reflection of a portion of the radiation incident upon the fuel surface,  $\dot{Q}_{ref}$ . The net heat feedback is balanced, primarily, with the rate at which heat must be provided to vaporise the fuel,  $\dot{Q}_{fuel}$  but also includes the rate of heat loss through radiation from the fuel surface to the surroundings,  $\dot{Q}_{rerad}$ , rate of heat loss from the sides and bottom of container,  $\dot{Q}_{loss}$  and the rate of heat required to grow the hot zone,  $\dot{Q}_{corr}$ . A heat balance for a control volume about the pool fire can be represented as (Drysdale, 1987; Koseki, 1994 and Hamins *et al.*, 1996):

$$\dot{Q}_{net} = \dot{Q}_{cond} + \dot{Q}_{conv} + \dot{Q}_{rad} + \dot{Q}_{reflect} \quad \text{Equation 2-13a}$$

$$\dot{Q}_{net} = \dot{Q}_{fuel} + \dot{Q}_{rerad} + \dot{Q}_{loss} + \dot{Q}_{corr} \quad \text{Equation 2-13b}$$

The rate of heat required to vaporise the fuel is given by (Hamins *et al.*, 1996):

$$\dot{Q}_{fuel} = m_V'' A (\Delta h_{lh} + C_p(T_b - T_{st})) \quad \text{Equation 2-14}$$

where  $A$  is the pool surface area.

The loss terms ( $\dot{Q}_{rerad}$ ,  $\dot{Q}_{loss}$  and  $\dot{Q}_{corr}$ ) in Equation 2-13b act as sinks to the rate of heat required for fuel vaporisation. However, they are very small compared to  $\dot{Q}_{fuel}$ .

Consequently, from Equation 2-13a and Equation 2-14, the burning rate (in  $\text{kg m}^{-2} \text{s}^{-1}$ ) is predicted as (Hamins *et al.*, 1999):

$$m_V'' = \frac{\dot{Q}_{cond} + \dot{Q}_{conv} + \dot{Q}_{rad} + \dot{Q}_{reflect}}{A (\Delta h_{lh} + C_p(T_b - T_{st}))} \quad \text{Equation 2-15}$$

Quantitatively, it has been pointed out the predominant heat flux,  $\dot{Q}_{rad}$ , which controls the rate of burning, is a function of the pool diameter. In the case of large diameter pool fires, radiation is recognised as the dominant mode of heat transfer from the flame to the pool surface controlling the rate at which the fuel is consumed (Drysdale, 1987). In storage tank fires, the rate at which the fuel burns as well as the increase in temperature throughout the pool is governed by radiative heat flux from the flame. The radiant heat depends on the characteristics of the fire such as: fuel type, efficiency of combustion, soot formation and heat lost to the entrained air (Lees, 2005).

In a study of crude oil fires in large scale storage tanks in 1998 in Japan (Koseki *et al.*, 2000, 2006), it was observed that the rate of fuel consumption increased as the ambient temperature (storage temperature) increased. In an experiment undertaken at a low ambient temperature, observation showed that the rate of consumption of crude oil was reduced. This was due to the fact that part of the energy from the flame was used to raise the temperature of the fuel to its boiling point before vaporisation could take place.

### 2.2.3 Experimental Values of Burning Rate

Subsection 2.2.2 discussed the rate of burning of liquid pool fires. The rate of burning of fuel is important in this work because of the inherent possibility of boilover. Factors that influence the rate of burning such as pool diameter and initial fuel temperature were studied based on the literature available. A survey was conducted to collect available data on the rate of fuel consumption for gasoline, diesel and crude oil pool fires. Table 2-3 summarizes the results of

experiments performed on pools above 1.0 m diameter and initial depth of fuel greater than 0.05 m that have been cited in previous works.

Author	Pool Diameter (m)	Initial Fuel Depth (m)	Fuels (Values in bracket showing fuel's density in kg m <sup>-3</sup> )	Average Fuel Surface Regression Rate	
				(mm s <sup>-1</sup> )	(mm min <sup>-1</sup> )
Petty (1983)	2.0		Crude oil (845)	0.050	3.0
Hasegawa (1988)	1.00	0.40	80% Diesel + 20% Gasoline	0.042*	2.5*
	1.00	0.40		0.053*	3.2*
	1.25	0.52		0.047*	2.8*
	1.25	0.52		0.052*	3.1*
Koseki (1989)	3.0		Gasoline	0.080	4.8
	5.4			0.077 - 0.108	4.6 - 6.5
	10.0			0.117	7.0
	22.3				3.5 - 6.3
	30.0		Kerosene	0.078	4.7
	50.0			0.078	4.7
	3.0		Crude oil	0.052	3.1
	6.5			0.058	3.5
	10.0			0.063	3.8
	11.0				3.4
	31.0				3.4
	6.0		Heptane	0.115	6.9
	10.0			0.143	8.6
	3.0		Hexane	0.118	7.1
	10.0			0.143	8.6
Koseki <i>et al.</i> (1991a)	1.0	0.06	Arabian light crude oil (850)	0.040	2.4
	1.0	0.10		0.037	2.2
Koseki <i>et al.</i> (1992)	6.0		Crude oil	0.058	3.5
Evans <i>et al.</i> (1991)	1.0		Murban crude oil	0.030	1.8
Broeckmann & Schecker (1995)	1.0	0.5	Crude oil	0.018	1.1
	1.0	0.5		0.030	1.8
	1.91	1.0		0.023 - 0.033	1.4 - 2.0
	1.91	1.0		0.042	2.5
	1.91	1.0		0.035	2.1
Koseki <i>et al.</i> (2000)	5.0	0.05	Crude oil equivalent to Arabian light (840)	0.038	2.3
	5.0	0.05		0.042	2.5
	10.0	0.05		0.048	2.9
	10.0	0.05		0.042	2.5
	20.0	0.05		0.057	3.4
	20.0	0.05		0.048	2.9

\* The surface regression rate (in mm/min) is predicted on the basis of the temperature history of fuel.

**Table 2-3: Compilation of experimental values of burning rate (surface regression rate) for tanks with diameter of 1.0 m and above**

Table 2-3 (continued)

Author	Pool Diameter (m)	Initial Fuel Depth (m)	Fuels (Values in bracket showing fuel's density in kg m <sup>-3</sup> )	Average Fuel Surface Regression Rate	
				(mm s <sup>-1</sup> )	(mm min <sup>-1</sup> )
Chatris <i>et al.</i> (2001)	1.5		Diesel (840)	0.042	2.5
	3.0			0.054	3.2
	4.0			0.068	4.1
	1.5		Gasoline (750)	0.087	5.2
	3.0			0.102	6.1
	4.0			0.102	6.1
Koseki <i>et al.</i> (2003)	1.9	0.1	Sakurawa crude oil (870)	0.063	3.8
	1.9	0.2		0.058 – 0.070	3.5 – 4.2
	1.9	0.3		0.053*	3.2*
	4.0	0.4		0.055*	3.3*
	4.0	0.4		0.062	3.7
Koseki <i>et al.</i> (2006)	5.0	0.45	Crude oil equivalent to Arabian light (840)	0.027	1.6
	5.0	0.45		0.033	2.0

\* The surface regression rate (in mm/min) is predicted on the basis of the temperature history of fuel.

## 2.3 EXISTING MODELS FOR ONSET OF HOT ZONE BOILOVER

The boilover phenomenon is interesting especially regarding its mechanism and the theoretical prediction of its onset. The efforts of researchers have concentrated on parameters such as depth of the fuel layer, type of fuel and temperature of the hot zone to define conditions for the occurrence of hot zone boilover and its intensity. In particular, the depth of the fuel layer was shown to have a great impact on the pre-boilover time. Investigations have been undertaken mainly through the conduct of experiments. Detailed analysis of the phenomenon involves two major groups of results (Hristov *et al.*, 2004):

- i. Experimental data concerning the time to hot zone boilover (mainly discussed in Section 2.1)
- ii. Models developed for the temperature distribution throughout the pool and hence for the prediction of the onset of hot zone boilover (These are discussed in Section 2.3.1 and 2.3.2)



### 2.3.1 Model for Hot Zone Boilover Onset

Broeckmann & Schecker (1995) proposed the only published model that addresses the formation of a hot zone. The model simulates the phenomenon through the mechanisms of heat conduction, radiation absorption and convection. The work introduced the concept of modified thermal conduction and used the vaporization temperature of the fuel involved in the hot zone as the temperature of the hot zone. The hot zone formation was described through distillation of the fuel. The details of the work of Broeckmann and Schecker were discussed in Section 2.1.8. In summary, the model presents a method to calculate the rate of descent of the base of the hot zone. The model predicts this velocity within a factor of 2. Based on the speed of descent of the base of the hot zone (Equation 2-4) and the initial depth of fuel in the tank, the moment at which boilover occurs can be estimated. For the modelling, a superheat water temperature of 130°C was used as the hot zone temperature. Also the heat flux from the flame to the fuel surface was considered to be the same value as that obtained during the experiments with non-hot-zone-forming fuels (Broeckmann & Schecker, 1995).

### 2.3.2 Physical-thermodynamic Laws Model for Boilover Onset

In 2005, Michaëlis, Dumas and Gautier from HSE Refining Division of TOTAL proposed a model to predict the time to boilover upon ignition and the consequences for receivers or targets (Michaëlis *et al.*, 2005). The model assumes that the thermal transfer towards the bottom of the tank is by the mechanism of mass transfer which agrees with Hall's theory (Hall, 1925). This assumption permits the use of simple equations based on the physical-thermodynamic laws and hence avoids modelling of the complex convective phenomena. The important aspects when modelling boilover and its consequences, as noted by the authors, are (Michaëlis *et al.*, 2005):

- i. The time to boilover
- ii. The heat wave temperature at boilover time

iii. The quantity of liquid fuel remaining in the tank at the time of boilover

The model considers a simple heat balance surrounding the pool fire in order to estimate the time to boilover.

Heat from the flame heats and vaporises the more volatile components; and also increases the temperature of the less volatile components up to the temperature of the hot zone. Hence, the time to achieve boilover is the time necessary to heat the more volatile fraction from the storage temperature to its boiling point and then to vaporise this fraction and to heat the less volatile fraction from the storage temperature to the hot zone temperature. The following heat balance was obtained (Michaëlis *et al.*, 2005):

$$\dot{Q}_f t_{bo} = z_{vap} \rho_L (T_{b,av} - T_{st}) + z_{vap} \rho_L \Delta h_{lh} + z_{bo} \rho_L C_p (T_{hz} - T_{st}) \quad \text{Equation 2-16}$$

where

$\dot{Q}_f$  is the rate at which heat from the flame enters the fuel through unit area of the surface,  $\text{W m}^{-2}$

$\rho_L$  is the density of fuel at ambient temperature,  $\text{kg m}^{-3}$

$t_{bo}$  is the time from ignition until the occurrence of boilover, s

$z_{vap}$  is the thickness of the fuel consumed by the fire (more volatile components) prior to boilover, m

$z_{bo}$  is the thickness of the remaining fuel (less volatile components) prior to boilover, m

$\Delta h_{lh}$  is the latent heat of vaporization of the liquid fuel,  $\text{J kg}^{-1}$

$C_p$  is the specific heat of the liquid fuel at  $T_{st}$ ,  $\text{J kg}^{-1} \text{K}^{-1}$

$T_{b,av}$  is the average boiling point of the liquid fuel, K

$T_{st}$  is the storage temperature of the liquid fuel, K

$T_{hz}$  is the temperature of the hot zone wave prior to boilover occurrence, K

The depth of fuel vaporised,  $z_{vap}$  is determined from the fuel surface regression rate,  $\dot{y}$  and the period until boilover occurs,  $t_{bo}$ .

Hence, the depth of the remaining fuel,  $z_{bo}$  could be determined via:

$$z_{bo} = z_f - z_{vap} = z_0 - \dot{y} t_{bo} \quad \text{Equation 2-17}$$

where  $z_f$  is the initial depth of fuel in the tank (m). Equation 2-17 is then substituted into Equation 2-16 to give:

$$t_{bo} = \frac{\rho_L z_f C_p (T_{hz} - T_{st}) + (0.001 \Delta h_c)}{\dot{Q}_f + \dot{y} \rho_L C_p (T_{hz} - T_{st})} \quad \text{Equation 2-18}$$

where the term  $0.001 \Delta h_c$  is the amount of heat required to raise the temperature and vaporise the more volatile fraction of the fuel – as stated in Equation 2-12 (TNO Yellow Book, 2005).

In order to solve Equation 2-18, the hot zone temperature was introduced via usage of the fuel distillation curve which expresses volume (or mass) percentage,  $x$  of fuel consumed where the fuel is at temperature,  $T$ ; or by establishing such a curve as a straight line passing through two known points in naperian logarithmic coordinates. The equation can be written as  $(\ln T = \alpha \ln x + \beta)$  where constants  $\alpha$  and  $\beta$  are defined using the initial distillation point ( $T_{in}$  and  $x_{in}$ ) and final distillation point ( $T_{fin}$  and  $x_{fin}$ ). The hot zone temperature is determined as follows:

$$\ln T_{hz} = \alpha \ln x_{bo} + \beta \quad \text{Equation 2-19}$$

$$\text{where } \alpha = \frac{\ln T_{fin} - \ln T_{in}}{\ln x_{fin} - \ln x_{in}} \text{ and } \beta = \ln T_{fin} - \alpha \ln x_{fin} .$$

In Equation 2-19,  $x_{bo}$  is the volume (or mass) of fuel consumed prior to boilover. In order to solve the equations, Michaëlis *et al.* (2005) assumed that at the initial distillation temperature, the fraction of fuel consumed,  $x_{in}$  was 0.15 and the final fraction of fuel consumed at the final distillation temperature,  $x_{fin}$  was 0.85.

Hence:

$$\beta = \ln T_{fin} + 0.1625 \alpha \quad \text{Equation 2-20}$$

The volume (or mass) fraction of fuel consumed prior to boilover is expressed as:

$$x_{bo} = \frac{\dot{y} t_{bo}}{z_f} + x_0 \quad \text{Equation 2-21}$$

where  $x_0$  is the fraction of fuel consumed at the storage temperature,  $T_{st}$ . It is the more volatile fraction of the fuel that vaporised during the storage period prior to the start of the fire.

The time to boilover is determined by assuming that the initial temperature of the hot zone is 130°C and then solving Equation 2-18. Consequently the fraction of fuel consumed prior to boilover can be estimated (Equation 2-21) and the new hot zone temperature predicted. The calculation is repeated until the difference between two successive hot zone temperatures is small (i.e. less than 1°C) (Michaëlis *et al.*, 2005).

A similar concept was used to predict the moment at which boilover occurs by Casal (2008). The maximum value of time to boilover,  $t_{bo}$  can be predicted from a heat balance of the fire i.e. the fuel surface is heated by the flame until all the fuel has reached the hot zone temperature,  $T_{hz}$  (Casal, 2008):

$$t_{bo} = \frac{\rho_L z_f C_p (T_{hz} - T_{st})}{\dot{Q}_f - \dot{m} (\Delta h_{lh} + C_p (T_{b,av} - T_{st}))} \quad \text{Equation 2-22}$$

The hot zone temperature was estimated from the distillation curve of the fuel by an iterative procedure. From Equation 2-22, a theoretical expression for the speed of the base of the hot zone towards the bottom of the pool,  $v_{hz}$  can be obtained via (Casal, 2008):

$$v_{hz} = \frac{z_f}{t_{bo}} = \frac{\dot{Q}_f - \dot{m} (\Delta h_{lh} + C_p (T_{b,av} - T_{st}))}{\rho_L C_p (T_{hz} - T_{st})} \quad \text{Equation 2-23}$$

### 2.3.3 Model of Boilover Consequences

The most serious effects of boilover are mainly the increase in size of the fire and the generation of a fireball. A boilover can also result in considerable rainout of burning hydrocarbon liquid over a wide area, posing an additional risk to people; and potentially, the ignition of neighbouring tanks.

Boilover starts when the hot zone within the fuel reaches the fuel-water interface at the bottom of the tank, resulting in the rapid vaporisation of water. Because of the rapid vaporisation of water, the pressure at the interface is significantly greater than atmospheric pressure plus the hydrostatic head of the fuel. Consequently, much of the hot fuel is expelled into the atmosphere. The force of the expulse breaks the liquid fuel into small droplets. They are quickly vaporised by the fire which expands as a consequence of the increased rates at which fuel is provided and air is entrained. The results are a greatly enlarged fire and the formation of a fireball. The large fire and the fireball emit large amounts of radiant energy which can cause injuries and damage over a wide area.

The mass of fuel contained within the fireball and the maximum diameter of the fireball are amongst the parameters assessed by physical and thermodynamic laws in the model proposed by the French researcher (Michaëlis, 2008), to quantify the thermal effects on the surroundings. The mass of fuel vapour,  $m_{vap}$  involved to the fireball formation (Michaëlis, 2008):

$$m_{vap} = (x' - x_{bo}) m_{liq} \quad \text{Equation 2-24}$$

where

- $m_{liq}$  is the initial mass of liquid fuel (at the instance when the fire started), kg
- $x'$  is the fraction of fuel consumed during stationary burning where the fuel is at temperature,  $T$  (determined using Equation 2-19)
- $x_{bo}$  is the fraction of fuel being vaporised during boilover

The mass of fuel vapour involved in the fireball is an important parameter in the equations for fireball radius and height that the fireball reaches above ground level. The radius of the fireball,  $r_{fb}$  is estimated via the volume of the fireball,  $V_{fb}$  (Michaëlis, 2008):

$$V_{fb} = \frac{4}{3} \pi r_{fb}^3 = \left( \frac{m_{vap}}{\rho_{vap}} \right) + \left( \frac{m_{air}}{\rho_{air}} \right) \quad \text{Equation 2-25}$$

where

$\rho_{vap}$  is the density of the fuel vaporized at temperature of flame during boilover ( $T_{flame}$ ),  $\text{kg m}^{-3}$

$\rho_{air}$  is the density of air at ambient temperature at the time boilover starts,  $\text{kg m}^{-3}$

$m_{air}$  is the mass of air introduced into the fireball, kg

The mass of air introduced into the fireball is estimated using the following equation:

$$m_{air} = \frac{(1 - UFL_f)}{UFL_f} \frac{m_{vap}}{\rho_{vap}} \rho_{air} \quad \text{Equation 2-26}$$

where  $UFL_f$  is the upper flammability limit of the fuel

The maximum height of the fireball above ground is predicted by the following equation (Michaëlis, 2008):

$$z_{fb} = \frac{68.571 t_{fb} T_{flame}^{9/3} m_{vap}^{1/3}}{(2.857 m_{vap}^{1/3} 10^{10}) + (t_{fb} T_{flame}^{10/3})} \quad \text{Equation 2-27}$$

where

$z_{fb}$  is the maximum lifting height of fireball above ground level, m

$t_{fb}$  is the duration of fireball existence, s

$T_{flame}$  is the temperature of flame during boilover, °C

The duration of the fireball is expressed as:

$$t_{fb} = \frac{r_{fb} - r_0}{v_{fla}} \quad \text{Equation 2-28}$$

where  $v_{fla}$  is the flame front velocity. The velocity is taken as  $5 \text{ m s}^{-1}$  since the fire is considered to be what is known as a flash fire rather than a vapour cloud explosion. Hence the velocity was assumed to be less than the slow deflagration limit (Michaëlis, 2008). The term  $r_0$  represents the initial radius of the fireball and it is estimated similar to Equation 2-25 but without the air.

As mentioned previously, the radius and the height that the fireball reaches above ground level are important factors in determining the thermal effects during a boilover.

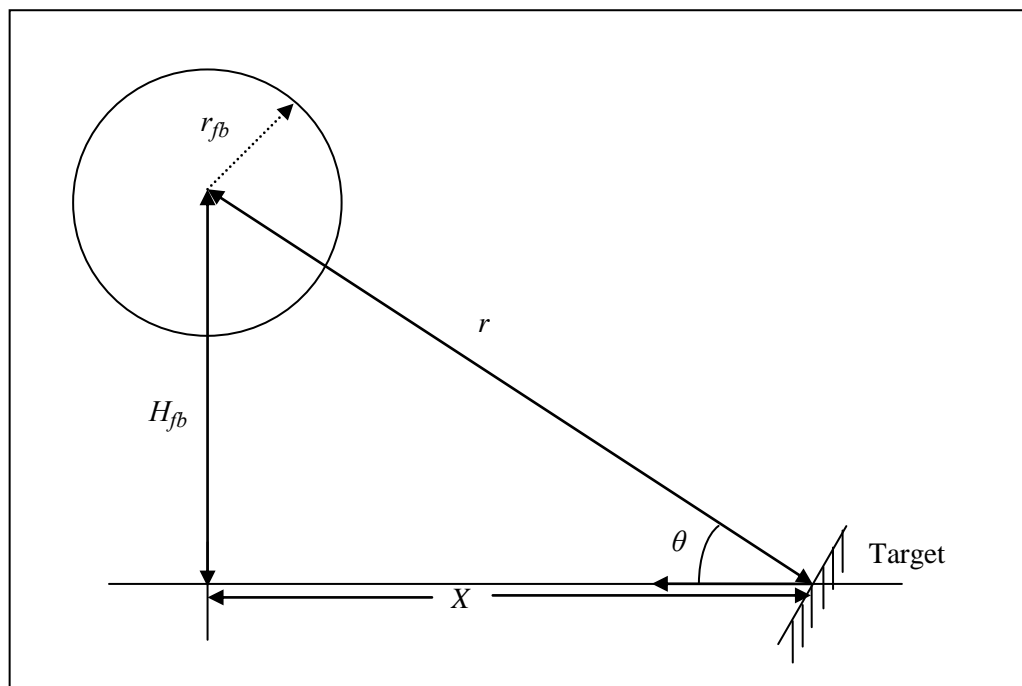


Figure 2-11: Position of fireball and target.

The incident radiation,  $\Phi_r$  ( $W m^{-2}$ ) received by a target at distance  $r$  from the centre of a fireball and orientated such that the normal to the surface of the target is parallel to the ground and towards the fireball as shown in Figure 2-11 is calculated by (Michaëlis, 2008):

$$\Phi_r = \Phi_{avg} F_v \tau \quad \text{Equation 2-29}$$

where  $\Phi_{avg}$  is the emissive power of the fireball ( $W m^{-2}$ ) and is obtained via:

$$\Phi_{avg} = \frac{\text{Average rate at which Energy is emitted by radiation}}{\text{Surface area of the fireball}}$$

$$\Phi_{avg} = \frac{(f_R M_{vap} \Delta h_c) / t_{fb}}{4 \pi r_{fb}^2} \quad \text{Equation 2-30}$$

where  $f_R$  is the fraction of heat radiated.

The view factor,  $F_v$  for a spherical fireball is determined using the following equation:

$$F_v = \left( \frac{r_{fb}^2}{r^2} \right) \cos \theta = \left[ \frac{r_{fb}^2}{(X^2 + z_{fb}^2)} \right] \cos \theta = \frac{r_{fb}^2}{(X^2 + z_{fb}^2)^{3/2}} \quad \text{Equation 2-31}$$

The atmospheric transmissivity,  $\tau$  is calculated using the TNO model (TNO Yellow Book, 2005):

$$\tau = 2.02 (P_w r)^{-0.09} \quad \text{Equation 2-32}$$

where

$r$  is the distance to the centre of the fireball, m

$P_w$  is the partial vapour pressure of water in the ambient air, Pa

$P_w = (\text{relative humidity}) \times (\text{vapour pressure of water at ambient temperature})$



Most of the relationships for the above fireball characteristics are available in the literature (Martinsen & Marx, 1999) for hydrocarbon fires and explosions. Though estimations of most of the characteristics are similar, none of them are specifically related to the boilover event.

Unfortunately, studies relating to the development of predictive techniques for the proportion of the fuel ejected from the tank that enters the fireball and the proportion that flows out of the tank and forms a pool fire on the ground or the proportion that rains out of the flame and fireball during a boilover are lacking.

### **2.3.4 Conclusion**

A review of the literature has provided information to aid the development of a boilover model. Mathematical expressions have been identified for modelling the hot zone formation, the heat transfer processes and the temperature profile within the liquid in the tank. The model by Broeckmann and Schecker (1995) was the earliest proposed model for the hot zone growth. In the calculations, however, a temperature of 130°C was used as the hot zone temperature, and the heat flux rate from the fire was assumed at the same value as that obtained from the experiments with non-hot-zone-forming fuels. Similarly, the model on the time to boilover by Michaëlis *et al.* (2005) required the assumption on the heat flux rate in order it to be solved. In addition, the authors assumed that the percentage of fuel consumed at the initial and final boiling temperatures,  $T_{in}$  and  $T_{fin}$ , are 15% and 95% respectively. These assumed values are then used to solve the temperature of the hot zone.

Apart from the physical-thermodynamics models to determine the boilover onset time, the mass continuity and energy balance governing equations can be solved numerically, with appropriate boundary conditions, through the application of computational fluid dynamics (CFD), enabling the temperature histories in the fuel and water layers to be predicted. Subsequently, the time to reach the vaporisation temperature of water at the fuel-water interface can be determined giving the time to boilover. The approaches used in developing and

using CFD models are complex, time consuming and not well suited to personnel involved in handling an emergency situation.

The majority of published work has addressed thin layer boilover and little has focussed on the practical application of theory to the problems associated with fighting tank fires with hot zone boilover potential. Previous research is able to provide guidance on the way forward to: identify those fuels that might boilover and those that might not; estimate the time to boilover; the consequences in the form of fire enlargement and the formation of a fireball.

### **3 BOILOVER FIELD SCALE TESTS**

Studies on large tank fires have become more and more important in order to understand the characteristics of large scale fuel burning. Boilovers have been known to occur when large storage tanks containing liquid fuels were on fire. It has been shown in Section 2.1.1 that a condition necessary for boilover is the formation of a hot zone within the burning fuel. The thickness of the hot zone increases with time after ignition, due to vaporisation of the light components of the fuel by the heat received from the flame at the burning surface. It is known that when the base of the hot zone reaches a water layer at the tank bottom, boilover might occur. However, the processes of the hot zone formation and its growth are complex, as well as the occurrence of boilover. In order to further clarify these processes, boilover experiments and tests were planned and carried out at field scale by the Large Atmospheric Storage Tank FIRE (LASTFIRE) project and by Loughborough University at laboratory scale. Analysis of the experimental data have been undertaken to further the knowledge of boilover events.

In this chapter, the description of the field scale test campaigns in which boilover studies were carried out is discussed. Details of the experiments carried out to obtain a wide range of results to study the effects on boilover of tank diameter, fuel type, fuel depth, and water depth are described. The chapter illustrates the series of boilover experiments that have been carried out by the LASTFIRE project. Brief descriptions are given of the tank design, the instrumentation employed and the properties of the fuel used. The results of the field scale tests are then presented and discussed.

#### **3.1 LASTFIRE BOILOVER STUDY**

LASTFIRE stands for Large Atmospheric Storage Tank Fires and is a collaborative project funded jointly by the following oil and gas companies: ADCO (Abu Dhabi), BP (Britain), IDEMITSU (Japan), MERO (Czech Republic), MOL (Hungary), NESTE OIL (Finland), PETRONAS (Malaysia), QATAR

PETROLEUM (Qatar), SAUDI ARAMCO (Saudi Arabia), SINOPEC (China), SHELL (Netherland-Britain), TAKREER (Abu Dhabi), TOTAL (France) and ZADCO (Abu Dhabi). The LASTFIRE project is managed by Resource Protection International.

The LASTFIRE project has provided Loughborough University with access to the results of the field scale experiments carried out over a number years on 1.22 m, 2.44 m and 4.5 m diameter tanks. Much of the more recent data on 1.22 m, 2.44 m and 4.5 m diameter tanks were obtained by Loughborough University whilst providing assistance to Resource Protection International. The main aims of the LASTFIRE Boilover Study were to evaluate the nature and consequences of a boilover and explain the boilover occurrence. Field scale experiments were completed to obtain a wide spectrum of results, evaluating the effect of tank diameters, fuel depth, and water depth on the boilover event. The key objectives were to provide accessible and meaningful data to assist a wide range of personnel and fire responders in evaluating the boilover phenomenon and thus to develop an effective fire fighting strategy for possible incidents. A programme of field-scale trials to investigate the boilover phenomenon was conducted consisting of four phases. The main objectives of the work were (RPI, 2007):

- i. To identify if boilover could occur during fires involving a range of fuels commonly stored in large atmospheric storage tanks
- ii. To identify when boilover could occur.
- iii. To identify and assess the consequences of a boilover event.

The conduct of a typical test carried out during the LASTFIRE boilover study campaign was as follows:

- i. Tank was installed in a bunded area in which markers were placed at 1m intervals around the tank for estimating the spread of fuel due to boilover.
- ii. Thermocouples were positioned at different levels inside the tank, and the thermocouple wiring was bundled and connected to the data acquisition unit (DAQ) to measure the liquid temperatures.

- iii. The tank was filled with water to the required level. Crude oil, refined fuel or a mixture of refined fuels was then added as required on top of the water.
- iv. The fuel was ignited and the fire was observed.
- v. Data (e.g. fuel temperatures) were observed and captured. Photographs and videos were also captured during the tests.

### **3.1.1 Details of Preliminary Tests**

The aim of these preliminary tests carried out by the LASTFIRE project was to observe the nature and consequences of boilover during relatively small and field scale experiments, so that a better understanding of the boilover phenomenon could be gained. The tests were carried out in order to establish a test methodology and identify the most important parameters to be measured in future tests. The tests were conducted using an un-instrumented 200-litre oil drum. The oil drum was 610 mm diameter and its height has been reduced to 610 mm. The set-up for the test is shown in Figure 3-1.

The main objectives of the preliminary tests were as follows:-

- i. Observe boilover phenomena
- ii. Establish key measurements of boilover event which includes time to boilover, spread of liquid outside of the tank as a result of boilover and potential 'indicators' on the onset of boilover(e.g. sound intensity)
- iii. Establish the 'after effects' of boilover to assist the undertaking of further tests (e.g. product residue, residual water, etc.)

Tests were carried out using three different types of crude oil, and involved different proportions of fuel and water as shown in Table 3-1. The crudes used were similar to Arabian-light but with different overall densities, sulphur content and water by volume (the number indicated in the table refers to a tank of origin). The tests used either 50 or 100 litres of crude oil, with the amounts of water ranging from 5 mm depth to 100 mm depth.

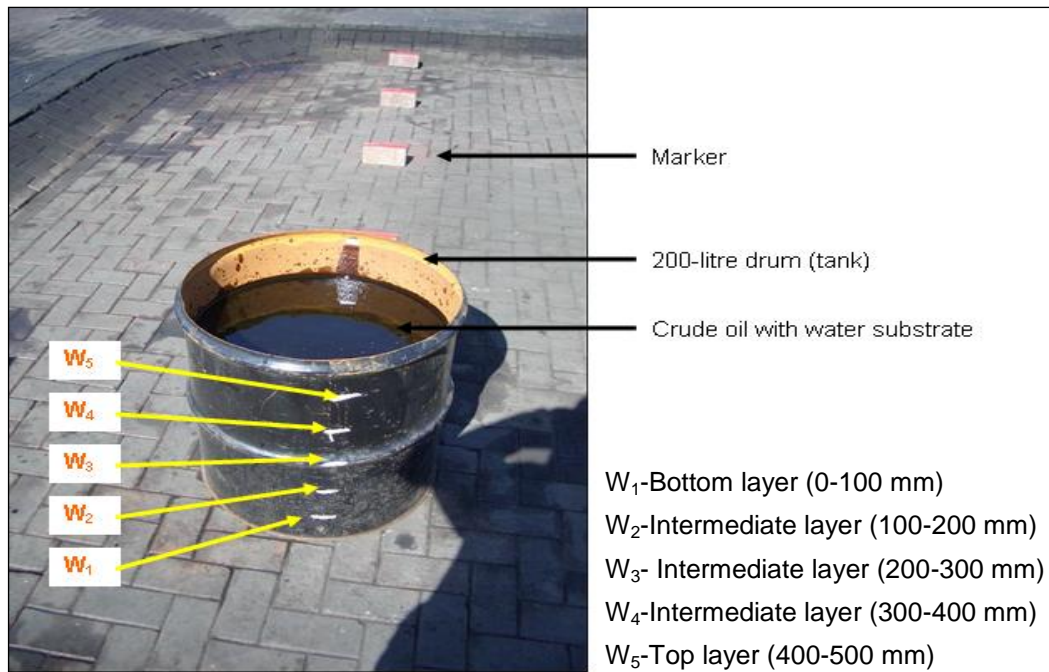


**Figure 3-1: Test set-up for Preliminary Tests (RPI, 2004).**

During the course of the tests, the fire was observed and tank wall temperature measurements were made. Ambient temperature was also noted. During these preliminary tests, the tank wall temperatures were measured using an infrared 'laser gun' type thermometer. Potential indicators of the onset of boilover such as steam ejection, intensity of boiling and audible indicators were noted. The tank was marked with 5 separate targets at different heights defining distinct 'layers' of liquid.

Test No.	LASTFIRE Study Phase 1	Crude Oil	Equivalent Fuel Depth (mm)	Water Depth (mm)
FS Prelim 1	Test 16	420x1	171	100
FS Prelim 2	Test 18	420x1	171	5
FS Prelim 3	Test 4	420x4	171	50
FS Prelim 4	Test 6	420x4	171	25
FS Prelim 5	Test 12	420x4	171	5
FS Prelim 6	Test 13	420x4	171	100
FS Prelim 7	Test 19	420x4	171	5
FS Prelim 8	Test 1	420x4	342	50
FS Prelim 9	Test 3	420x4	342	50
FS Prelim 10	Test 5	420x4	342	25
FS Prelim 11	Test 11	650x1	291	50

**Table 3-1: Details of the Preliminary Tests**

The results of the preliminary tests are presented in Section 3.2.1. The preliminary test enabled a good basis for future test work to be established. A number of important variables were identified which needed to be examined in greater detail, in the following series of tests.

- i. Differences in the time to boilover and the severity of the consequences were observed between different crude types, as well as between tests using the same crude. Crude specification may have some effects on the time to boilover and the consequences.
- ii. The preliminary tests managed to establish key measurement variables such as tank wall temperature, sound level and ambient conditions, etc. It was realized that future would require more instrumentation so that fuel and water temperatures could be monitored in greater detail. Thermocouples would be fixed within the tank to measure fuel and water temperatures throughout the test. Temperature data would be logged automatically to a PC and trends could be evaluated to assess the temperature profile and progress of any “hot zone” within the tank.
- iii. Based on the preliminary tests, fuel depth is a critical parameter that influences the boilover time.
- iv. Flaring, “steaming”, emission of water and crude droplets, as well as boiling noises were all observed in many of the preliminary tests and more work is needed to find out whether any of these could be accurate indicators that a boilover was about to occur.

### 3.1.2 Details of Field Scale Instrumented Tests Series

Following the preliminary tests of the boilover study, three further series of boilover tests were performed by the LASTFIRE project (RPI, 2004, 2005 and 2006) using larger tanks of 1.2 and 2.44 m diameter. These tests incorporated instrumentation to measure additional parameters such as fuel and water temperature.

The main objectives of the tests were similar to those in the preliminary trials with the addition of a more detailed study of:

- i. Time to boilover
- ii. Spread of boilover
- iii. Ambient conditions (wind, temperature etc.)
- iv. Effect of fuel depth
- v. Effect of water layer depth

The aim of these instrumented tests was to build on the knowledge obtained during the preliminary tests. The tests were performed to improve understanding of the boilovers and, if possible, establish parameters that will enable the onset of boilovers to be predicted so that safer fire fighting strategies can be deployed. The strong intention of carrying out this series of tests was to identify indicators that would help to identify when boilover will occur. Hence the objectives also include the following:

- i. To establish a means of estimating the time to boilover and the consequences.
- ii. To consider the escalation potential and the consequences of igniting additional tanks of crude oil.
- iii. To assess, in addition to crude oil, the boilover potential of refined fuels.



Two new tanks with diameters of 1.2 m and 2.44 m were designed, fabricated and used for the subsequent studies. A number of thermocouples were inserted into the tank and arranged as shown in Figure 3-2 and Figure 3-3. Table 3-2 shows the thermocouple arrangement. The thermocouples used were the K-type which composed of 1.5 mm probe diameter.

Tank	1.2 m Diameter	2.44 m Diameter
Thermocouple No.	Height from the Tank Base	
TC1	60 mm	390 mm
TC2	60 mm	390 mm
TC3	60 mm	390 mm
TC4	120 mm	390 mm
TC5	120 mm	290 mm
TC6	120 mm	290 mm
TC7	180 mm	290 mm
TC8	180 mm	290 mm
TC9	180 mm	20 mm
TC10	240 mm	150 mm
TC11	240 mm	20 mm
TC12	240 mm	150 mm
TC13	0 mm	0 mm
TC14	NA	0 mm
TC15		0 mm
TC16		0 mm
TC17		110 mm
TC18		0 mm
TC19		110 mm
TC20		0 mm

**Table 3-2: Details of the arrangements of the thermocouples**



Figure 3-2: (a) Photo of thermocouples placement in the 1.2 m diameter tank

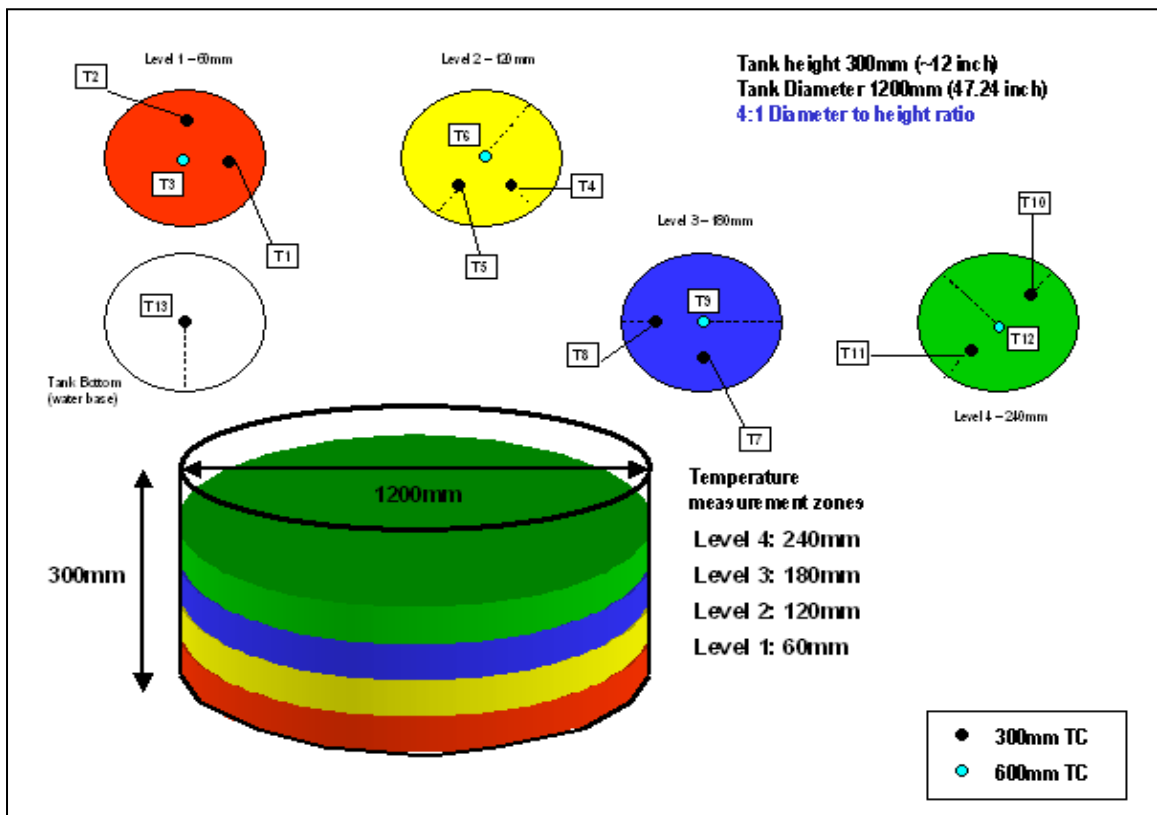


Figure 3-2: (b) Schematic of thermocouples location in the 1.2 m diameter tank (RPI, 2004)



Figure 3-3: (a) Photo of the 2.44 m diameter test pan with thermocouples placement



Figure 3-3: (b) Temperature probes connected to laptop / workstation in real time.

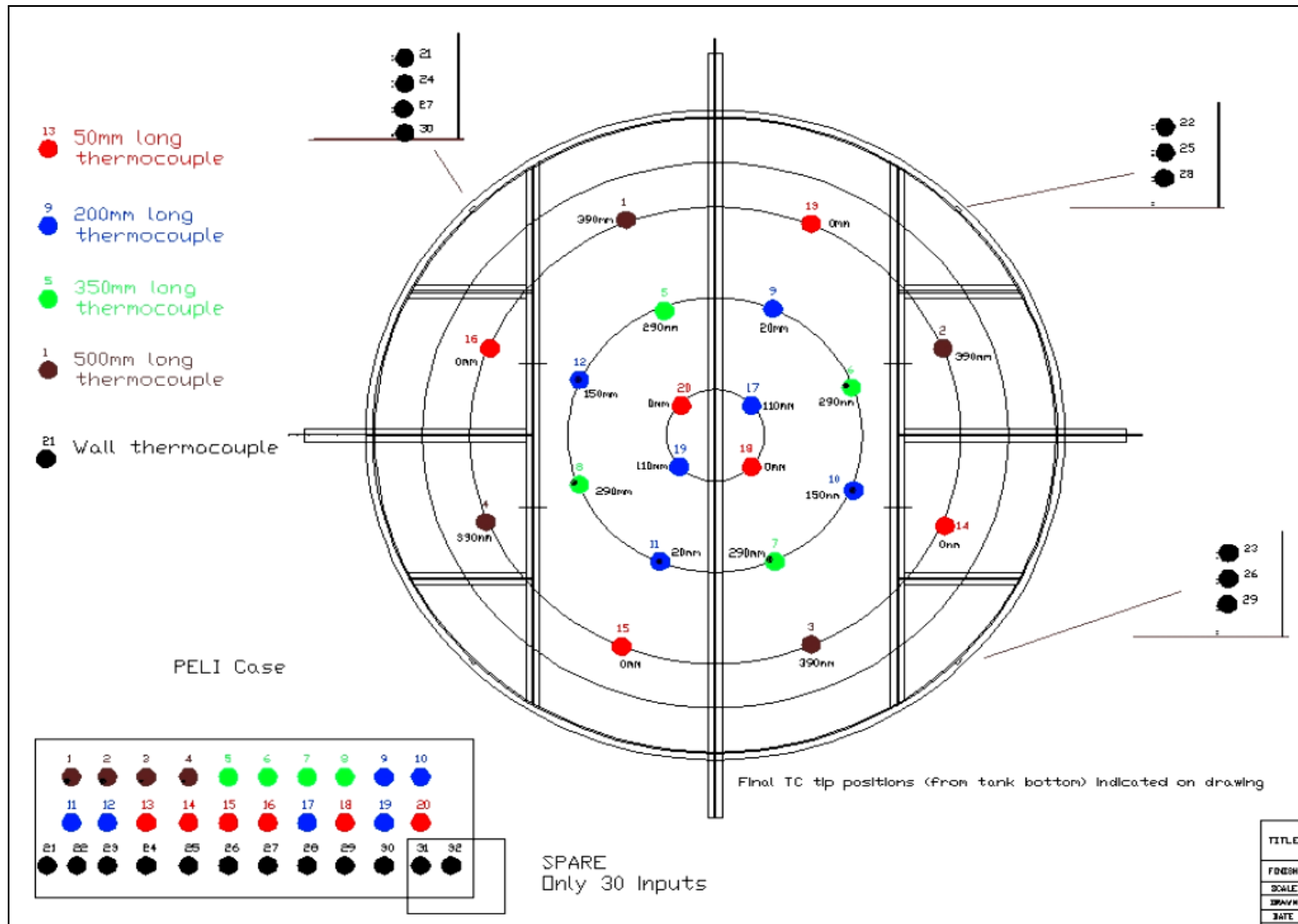


Figure 3-3: (c) Location of thermocouples in the 2.44 m diameter tank (RPI, 2005)

All the tests were undertaken with complete instrumentation to measure the temperature profiles in the fuel and water and to establish which parameters significantly affect the potential to boilover, time to boilover and the extent of fire spread. For each test, the specified height of water was placed in the tank, followed by the specified level of fuel, and left for a short period of time, to allow separation of the two layers. The ambient conditions during the tests were also noted. Details of the tests conducted are shown in Table 3-3.

Test No.	LASTFIRE Study	Crude Oil / Fuel	Tank Diameter (m)	Fuel Depth (mm)	Water Depth (mm)
FS Test 1	Phase 3 Test 2	AVTUR	1.2	250	20
FS Test 2	Phase 2 Test 8	Light Crude	1.2	80	20
FS Test 3	Phase 2 Test 10	Light Crude	1.2	100	40
FS Test 4	Phase 2 Test 9	Light Crude	1.2	115	20
FS Test 5	Phase 2 Test 6	Light Crude	1.2	150	40
FS Test 6	Phase 2 Test 7	Light Crude	1.2	150	20
FS Test 7	Phase 3 Test 17	Light Crude	1.2	180	0
FS Test 8	Phase 3 Test 18	Light Crude	1.2	180	0
FS Test 9	Phase 2 Test 2	Light Crude	1.2	230	40
FS Test 10	Phase 2 Test 5	Light Crude	1.2	230	40
FS Test 11	Phase 2 Test 1	Light Crude	1.2	250	20
FS Test 12	Phase 3 Test 4	Light Crude	1.2	250	20
FS Test 13	Phase 3 Test 5	Light Crude	1.2	250	20
FS Test 14	Phase 2 Test 3	Light Crude	1.2	255	15
FS Test 15	Phase 3 Test 11	Light Crude	2.44	270	20
FS Test 16	Phase 3 Test 14	Light Crude	2.44	270	55
FS Test 17	Phase 3 Test 16	Light Crude	2.44	290	40
FS Test 18	Phase 3 Test 3	Light Crude	2.44	380	20
FS Test 19	Phase 3 Test 10	Light Crude	2.44	440	40
FS Test 20	Phase 3 Test 8	Light Crude	2.44	475	25
FS Test 21	Phase 3 Test 7	Light Crude	2.44	485	25
FS Test 22	Phase 4b Test 3	Crude	2.44	500	20
FS Test 23	Phase 4b Test 5	Crude	2.44	500	40
FS Test 24	Phase 4a Test 1	Diesel	1.2	250	10
FS Test 25	Phase 4a Test 3	Diesel	1.2	250	20
FS Test 26	Phase 4a Test 4	Diesel	1.2	250	10

**Table 3-3: Summary of boilover tests conducted in the LASTFIRE Field Scale Tests**

**Table 3-3 (continued)**

Test No.	LASTFIRE Study	Crude Oil / Fuel	Tank Diameter (m)	Fuel Depth (mm)	Water Depth (mm)
FS Test 27	Phase 4a Test 2	Diesel	2.44	500	10
FS Test 28	Phase 4a Test 5	Diesel	2.44	500	20
FS Test 29	Phase 4b Test 1	Diesel	2.44	500	20
FS Test 30	Phase 4a Test 14	Gasoline	1.2	180	40
FS Test 31	Phase 4a Test 13	Gasoline	2.44	500	20
FS Test 32	Phase 4a Test 9	Jet A1	1.2	180	40
FS Test 33	Phase 4a Test 7	Jet A1	1.2	250	10
FS Test 34	Phase 4a Test 8	Jet A1	2.44	500	20
FS Test 35	Phase 4a Test 17	Light LFO	1.2	180	40
FS Test 36	Phase 4a Test 18	Light LFO	1.2	200	10
FS Test 37	Phase 4a Test 16	Light LFO	2.44	500	20
FS Test 38	Phase 4a Test 10	LFO	2.44	490	20
FS Test 39	Phase 4b Test 2	75 % Diesel + 25 % Gasoline	1.2	500	20

In line with the preliminary tests, boilover time, violence and fire spread were assessed. Each test was timed from the moment the full surface of the fuel was alight. The fire spread was estimated by observing how far burning fuel spread or was thrown around the tank.

Temperature measurements within the fuel and water layers were recorded at 1 second intervals throughout each test. Potential boilover indicators such as boiling, steam ejection, intensity of boiling and audible indicators were also noted.

### 3.1.3 Details of Abu Dhabi Field Scale Tests

Field scale experimental tests were carried out in the Jebel Dhanna terminal area by Abu Dhabi Company for Onshore Oil Operation (ADCO). The tests were managed by RPI, with support in the planning and performance of the tests of Loughborough University on behalf of the LASTFIRE project. ADCO, a member of LASTFIRE Group, carried out the boilover experimental study

(Shaluf & Abdullah, 2011) to look at the characteristics of the large oil tank fires in order to:

- i. Gain more knowledge of the boilover phenomenon of crude oil
- ii. Verify whether the crude oil stored by ADCO would boilover
- iii. Ascertain the rate of hot zone growth
- iv. Identify the time to boilover following ignition
- v. Record the radiant heat around the fire and the consequences of boilover

A series of tests using Murban crude oil was conducted in 2.4 m and 4.5 m diameter tanks. Thermocouples were installed inside both tanks; from the base to the top of the fuel layer to record the temperature within the liquid every second. For the 2.4 m diameter tank, 10 thermocouples were installed at the centre. In the 4.5 m diameter tank, two thermocouple trees were installed; one with 48 thermocouples on a central pole and another with 12 thermocouples close to the tank wall. There were also radiometers and video cameras placed around the tank to measure heat radiation and to record the tests. A summary of the tests conducted in Abu Dhabi is given in Table 3-4.

Test Number	LASTFIRE Test	Fuel Type	Test Diameter (m)	Fuel Depth (mm)	Water Depth (mm)
FS Test 40	Abu Dhabi Test 2	Crude Oil	2.44	520	40
FS Test 41	Abu Dhabi Test 4	Crude Oil	4.5	3524	174
FS Test 42	Abu Dhabi Test 1	75% Diesel + 25% Gasoline	2.44	520	40

**Table 3-4: Summary of boilover tests conducted in the Abu Dhabi Boilover Study**

The temperature at various heights within the tank, time to boilover, heat radiation at specific locations around the tank and the extent of fire spread were recorded during the tests.

### 3.1.4 Details of Asturias Field Scale Tests

The main purpose of this test series was to study fires involving biodiesel and an 80:20 v/v mixture of diesel and biodiesel and to compare the results with a diesel fire.

In addition, three tests involving a 75:25 v/v mixture of diesel and gasoline were performed. These tests were carried out, primarily, to demonstrate a boilover event to groups of invited observers.

Three further tests were undertaken to study the ability of a layer of small insulating spheres floating on the fuel to control a pool fire and to delay, or possibly prevent, a boilover by reducing the radiation feedback from the flame to the fuel surface. The details of the tests are shown in Table 3-5.

Test No.	LASTFIRE Study	Crude Oil / Fuel	Tank Diameter (m)	Fuel Depth (mm)	Water Depth (mm)
FS Test 43	Asturias 09/10 Test 9	Crude Oil (with 25 mm non conductor media)	1.2	150	100
FS Test 44	Asturias 09/10 Test 14	Crude Oil (with 50 mm non conductor media)	1.2	175	25
FS Test 45	Asturias 09/10 Test 18	Crude Oil	1.2	210	30
FS Test 46	Asturias 05/11 Test 4	75 % Diesel + 25 % Gasoline	1.2	200	40
FS Test 47	Asturias 05/11 Test 5	75 % Diesel + 25 % Gasoline	1.2	240	40
FS Test 48	Asturias 05/11 Test 8	75 % Diesel + 25 % Gasoline (with 75 mm non conductor material)	1.2	180	40
FS Test 49	Asturias 05/11 Test 7	Diesel	1.2	180	40
FS Test 50	Asturias 05/11 Test 1	Hydrotreated Vegetable Oil Diesel	2.44	400	40
FS Test 51	Asturias 05/11 Test 2	20% Hydrotreated Vegetable Oil Diesel + 80% Diesel	2.44	400	40

**Table 3-5: Summary of boilover tests conducted in the Asturias Boilover Study**



## 3.2 PRESENTATION OF THE OBSERVATIONS AND TEMPERATURE MEASUREMENTS

This section is devoted to presenting the results and main characteristics of the boilover event observed during the preliminary and field scale experiments. The initial section will describe the identification of the beginning of the phenomenon in the experiments. Then, once the identification of the phenomenon has been characterized, the temperature records will be discussed.

### 3.2.1 Presentation of the Observed Time to Boilover

#### 3.2.1.1 Preliminary Tests

Table 3-6 shows the observed time to boilover for the LASTFIRE boilover preliminary tests.

Test No.	Crude Oil	Equivalent Fuel Depth (mm)	Water Depth (mm)	Time to Boilover $t_{bo}$ (sec)
FS Prelim 1	420x1	171	100	5820
FS Prelim 2	420x1	171	5	3060
FS Prelim 3	420x4	171	50	4980
FS Prelim 4	420x4	171	25	3600
FS Prelim 5	420x4	171	5	3900
FS Prelim 6	420x4	171	100	2280
FS Prelim 7	420x4	171	5	3180
FS Prelim 8	420x4	342	50	4860
FS Prelim 9	420x4	342	50	4320
FS Prelim 10	420x4	342	25	5280
FS Prelim 11	650x1	291	50	6600

**Table 3-6: Observed Time to Boilover for the Preliminary Tests**

A wide range of boilover times was recorded for each crude type as shown in Table 3-6. In addition, flaring, splashing of water and crude droplets and boiling noises were all observed in many of the tests. Crude Oil 420x4 boiled over 8 out of 11 times with the onset time ranging from 33 – 88 minutes after ignition. In all of these boilovers, the burning was violent and the fire spread was extensive.

FS Prelim 8 and 9 tests, both with 342 mm layer of crude and a 50 mm layer of water, showed repeatable results with boilovers taking place at 72 and 81 minutes respectively. Similar agreement of the results was also observed, for repetitive tests involving 171 mm layer of crude and a 5 mm layer of water, in FS Prelim 5 and 7 tests. The boilover onset time was 65 and 53 minutes respectively.

### 3.2.1.2 Field Scale Instrumented Tests

The times to boilover observed in the field scale tests are given in Table 3-7.

Test No.	Crude Oil / Fuel	Tank Diameter (m)	Fuel Depth (mm)	Water Depth (mm)	Time to boilover (s)
FS Test 1	AVTUR	1.2	250	20	No boilover
FS Test 2	Light Crude	1.2	80	20	1222
FS Test 3	Light Crude	1.2	100	40	1268
FS Test 4	Light Crude	1.2	115	20	1401
FS Test 5	Light Crude	1.2	150	40	1962
FS Test 6	Light Crude	1.2	150	20	1992
FS Test 7	Light Crude	1.2	180	0	No boilover
FS Test 8	Light Crude	1.2	180	0	No boilover
FS Test 9	Light Crude	1.2	230	40	2220
FS Test 10	Light Crude	1.2	230	40	2880
FS Test 11	Light Crude	1.2	250	20	2770
FS Test 12	Light Crude	1.2	250	20	2470
FS Test 13	Light Crude	1.2	250	20	2380
FS Test 14	Light Crude	1.2	255	15	2910
FS Test 15	Light Crude	2.44	270	20	1881
FS Test 16	Light Crude	2.44	270	55	1679
FS Test 17	Light Crude	2.44	290	40	2973
FS Test 18	Light Crude	2.44	380	20	2760
FS Test 19	Light Crude	2.44	440	40	2824
FS Test 20	Light Crude	2.44	475	25	2940
FS Test 21	Light Crude	2.44	485	25	4282
FS Test 22	Crude	2.44	500	20	4530
FS Test 23	Crude	2.44	500	40	4494

**Table 3-7: LASTFIRE Field Scale Tests Results – Time to Boilover**

**Table 3-7 (continued)**

Test No.	Crude Oil / Fuel	Tank Diameter (m)	Fuel Depth (mm)	Water Depth (mm)	Time to boilover (s)
FS Test 24	Diesel	1.2	250	10	No boilover
FS Test 25	Diesel	1.2	250	20	No boilover
FS Test 26	Diesel	1.2	250	10	No boilover
FS Test 27	Diesel	2.44	500	10	No boilover
FS Test 28	Diesel	2.44	500	20	No boilover
FS Test 29	Diesel	2.44	500	20	No boilover
FS Test 30	Gasoline	1.2	180	40	No boilover
FS Test 31	Gasoline	2.44	500	20	No boilover
FS Test 32	Jet A1	1.2	180	40	No boilover
FS Test 33	Jet A1	1.2	250	10	No boilover
FS Test 34	Jet A1	2.44	500	20	No boilover
FS Test 35	Light LFO	1.2	180	40	No boilover
FS Test 36	Light LFO	1.2	200	10	No boilover
FS Test 37	Light LFO	2.44	500	20	No boilover
FS Test 38	LFO	2.44	490	20	No boilover
FS Test 39	75 % Diesel + 25 % Gasoline	1.2	500	20	1265

### 3.2.1.3 Abu Dhabi Field Scale Tests

Table 3-8 displays the observed times to boilover for the field scale tests conducted in the Jebel Dhanna terminal area by ADCO.

Test No.	Crude Oil / Fuel	Tank Diameter (m)	Fuel Depth (mm)	Water Depth (mm)	Time to boilover (s)
FS Test 40	Crude	2.44	520	40	1620
FS Test 41	Crude	4.5	3350	174	34982
FS Test 42	75 % Diesel + 25 % Gasoline	2.44	520	40	2188

**Table 3-8: LASTFIRE Abu Dhabi Field Scale Tests Results – Time to Boilover**

### 3.2.1.4 Asturias Field Scale Tests

Table 3-9 shows the observed time to boilover for the field scale experiments that were undertaken at Asturias, Spain.

Test No.	Crude Oil / Fuel (number in brackets represent the thickness of non conductor spheres layer)	Tank Diameter (m)	Fuel Depth (mm)	Water Depth (mm)	Time to boilover (s)
FS Test 43	Crude Oil (25 mm)	1.2	150	100	1980
FS Test 44	Crude Oil (50 mm)	1.2	175	25	5580
FS Test 45	Crude Oil	1.2	210	30	1500
FS Test 46	75 % Diesel + 25 % Gasoline	1.2	200	40	1200
FS Test 47	75 % Diesel + 25 % Gasoline	1.2	240	40	2400
FS Test 48	75 % Diesel + 25 % Gasoline (75 mm)	1.2	180	40	No boilover
FS Test 49	Diesel	1.2	180	40	No boilover
FS Test 50	Hydrotreated Vegetable Oil Diesel	2.44	400	40	No boilover
FS Test 51	20% Hydrotreated Vegetable Oil Diesel + 80% Diesel	2.44	400	40	No boilover

**Table 3-9: LASTFIRE Asturias Field Scale Tests Results – Time to Boilover**

Based on Table 3-7, Table 3-8 and Table 3-9, differences in boilover time were observed through changes in the crude oil or fuel depths. All tests where water was present at the tank bottom either resulted in slop over from some parts of the tank or full boilover. The two tests in which there was no water at the base of the tank i.e. FS Test 7 and 8 did not produce any boilover till the end of the burning. There is good evidence to conclude that the boilover occurs more quickly with low fuel depth and takes longer to occur the greater the depth of fuel.

The field scale tests results also show that an increased depth of water within the tank does not significantly affect the time to boilover, as observed between FS Test 5 - FS Test 6, FS Test 15 - FS Test 16 and FS Test 22 - FS Test 23.

The burning of the refined fuels such as the aviation fuel (AVTUR), diesel, gasoline and light fuel oil (LFO) did not result in boilover. The burning of biofuel also did not result in boilover as shown in Table 3-9. From the results shown, it could be summarized that the refined products/fuels used in the field scale tests did not produce a boilover.

### 3.2.2 Fire Spread during Boilover

Burning fuel spread ejected out from the tank during boilover was assessed with the use of 'markers' placed around tanks at 1m intervals for test FS Test 2, 3, 4, 5, 6, 9, 10, 11 and 14. Downwind, upwind and crosswind distances covered by the fire spread were estimated by observing the extent of any flaming in relation to them. The limited results of fire spread show that fuel quantities are critical. The results indicated that the extent of the fire spread depend on the amount of fuel remained in the tank prior to boilover. Based on the current observations, the greatest fire spread was seen during FS Test 9. Figure 3-4 shows the spread of the fire estimated due to the boilover.

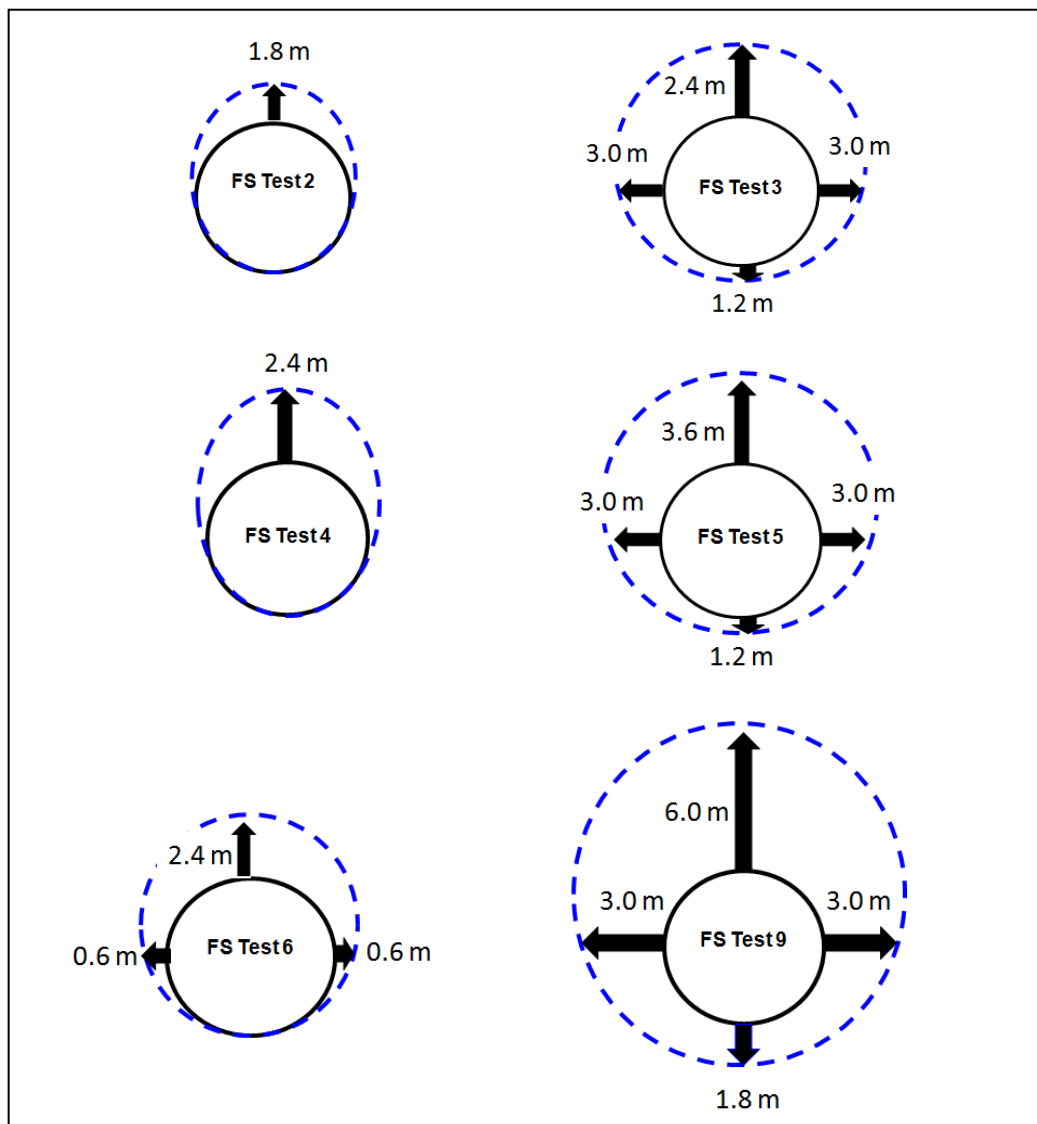
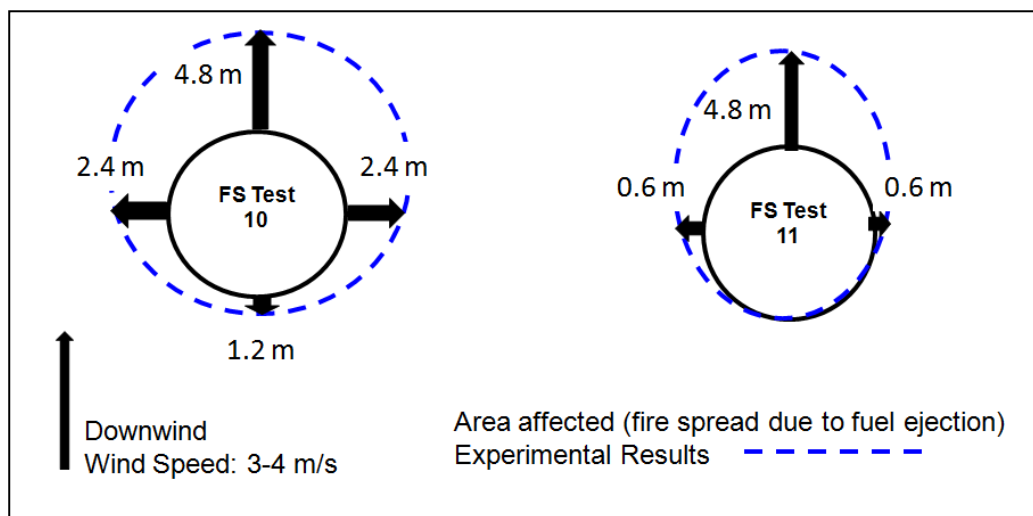


Figure 3-4: Spread of the fire estimated due to the boilover in FS Test 2, 3, 4, 5, 6, 9, 10 and 11



**Figure 3-4: Spread of the fire estimated due to the boilover in FS Test 2, 3, 4, 5, 6, 9, 10 and 11**

Note: The distances shown in Figure 3-4 are presented to indicate the extent of spread and are not following any proper scale

### 3.2.3 Indicators of the Onset of Boilover

Chapters 1 and 2 have discussed the definition and features of the boilover phenomenon. Potential 'indicators' such as boiling, fuel and steam ejection, intensity of boiling and audible indicators were listed as identification of the onset of boilovers. It has been mentioned in many literatures that the start of the boilover event is normally accompanied by a noise characteristic - a crackling sound - which relates to the explosion of vapour bubbles that carry the fuel into the flame. In addition, the appearance of boilover is also seen through fuel ejection due to the violent boiling of water and frothing over the whole tank content which resulted in an increase in the flame height two or three times larger than that during the steady burning period. The beginning of the phenomenon in a large-scale storage tank fire, therefore, has been characterized from the flame enlargement due to the fuel ejections and the noise level due to the water evaporation. Additionally, in a real boilover, an increase in the mass burning rate during the incident (as compared to the rate during steady burning) can also be observed through the analysis of fuel weight loss versus burning time. A sharp change in the slope of the weight-time curve indicates an increase/decrease in the burning rate.

In the LASTFIRE field scale tests, enlargement of flames during the study were observed in many cases. The flames were observed to be approximately 5 to 20 times the diameter of the tank and hot burning fuel was thrown out from the tank which landed several tank diameters away. As examples, Figure 3-5(a) and (b) show photos taken from the FS Test 3 indicating the changes of flame size during steady burning and during the boilover occurrence.

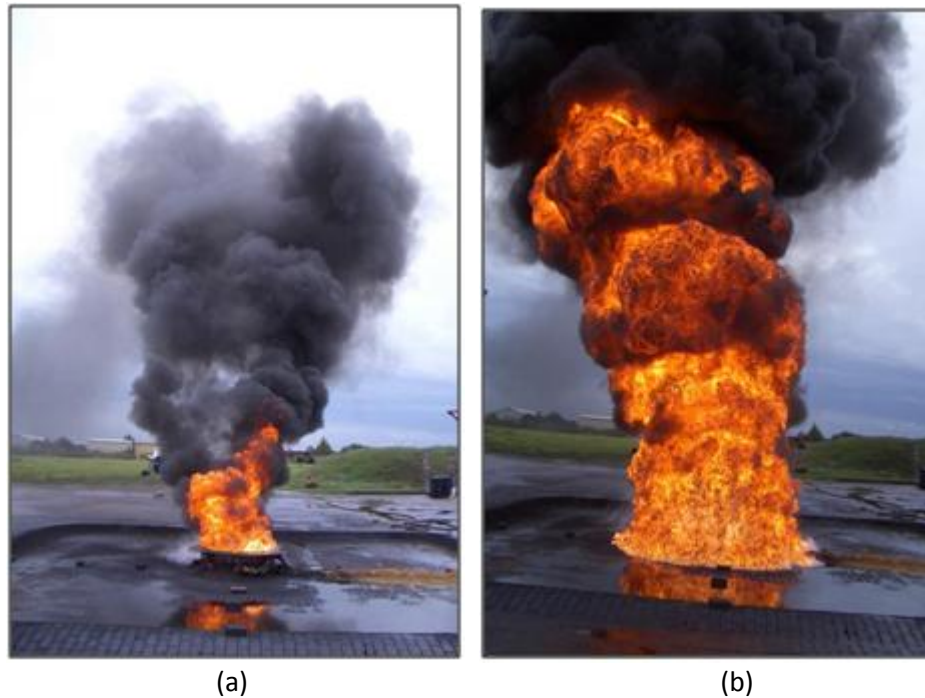


**Figure 3-5: Photo of FS Test 3 – Difference flame size (a) during steady burning and (b) during the boilover occurrence**

The appearance of the boilover is also seen in the graphs which represents the progress of temperature within the liquid with time. In the case of FS Test 6, as shown in Figure 3-6(a), a sharp change in the temperature profiles is observed in correspondence with the beginning of boilover, at 1997 s. As shown in Figure 3-6(b), boiling of water started when the thermocouple within the water layer (TC13) registered a value of about 110°C. At the same instant, the thermocouples within the fuel (TC5, 7 and 11) show a large decrease in the temperature. Due to the rise of relatively cold water vapour, these thermocouples are cooled and hence show a large decrease in the temperature. Hence the start of boilover for FS Test 6 occurs at 1997 s following ignition.

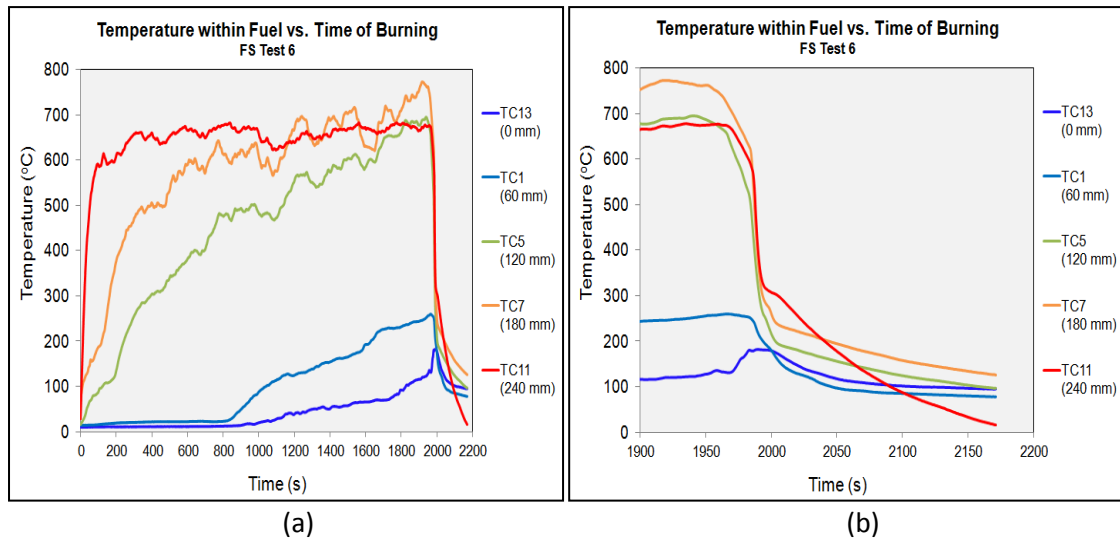


**Figure 3-6: Temperature profiles within liquid in the storage tank in the course of experiment for FS Test 6: (a) A sharp change in the temperature profiles is observed as boilover starts and b) Thermocouples within fuel show a large decrease in the temperature**

In summary, there are several methods of identifying the start of boilover which include the physical observation such as the presence of higher sound levels and flame enlargement, or through graphical analysis of measured data e.g. sharp change of slope in the height-time curve and change of temperature profiles in the temperature-time graph. In the context of this thesis, the beginning of the boilover is identified based on the:

- i. Changes in the temperature profiles in the temperature-time graph when the thermocouple at the fuel - water interface reached the temperature of water boiling, and
- ii. Physical changes observed i.e. changes of flame height for the field scale tests in the LASTFIRE Boilover studies.

### 3.2.4 Temperature Measurements within the Fuel and Water Layers

In this section, the behaviour of the liquid fuel temperature during the progress of the burning fire is presented. The temperature versus time was plotted for each test and the data records were examined at each stage of the fires



progression. This examination was essential to study the formation or not of a hot zone.

Figure 3-7 shows the evolution of the wall temperature for the preliminary test FS Prelim 9. The tank wall temperatures are taken as indication of the liquid temperatures inside the tank. Data from the tank wall temperature measurements show that the bottom-most tank wall temperatures (W2, W3 and W4) increased steadily throughout the burning period. Note that the temperatures of the upper part of the tank wall remain substantially hotter at all times due to direct heat input from the flame. The data show that if the bottom-most temperature zones reached the boiling point of water, then boilover was likely to occur as observed in the FS Prelim 9 test. This is indicated by the three temperature zones W2, W3 and W4, all converging above 100°C indicating the establishment of a hot zone prior to boilover as shown in Figure 3-7.

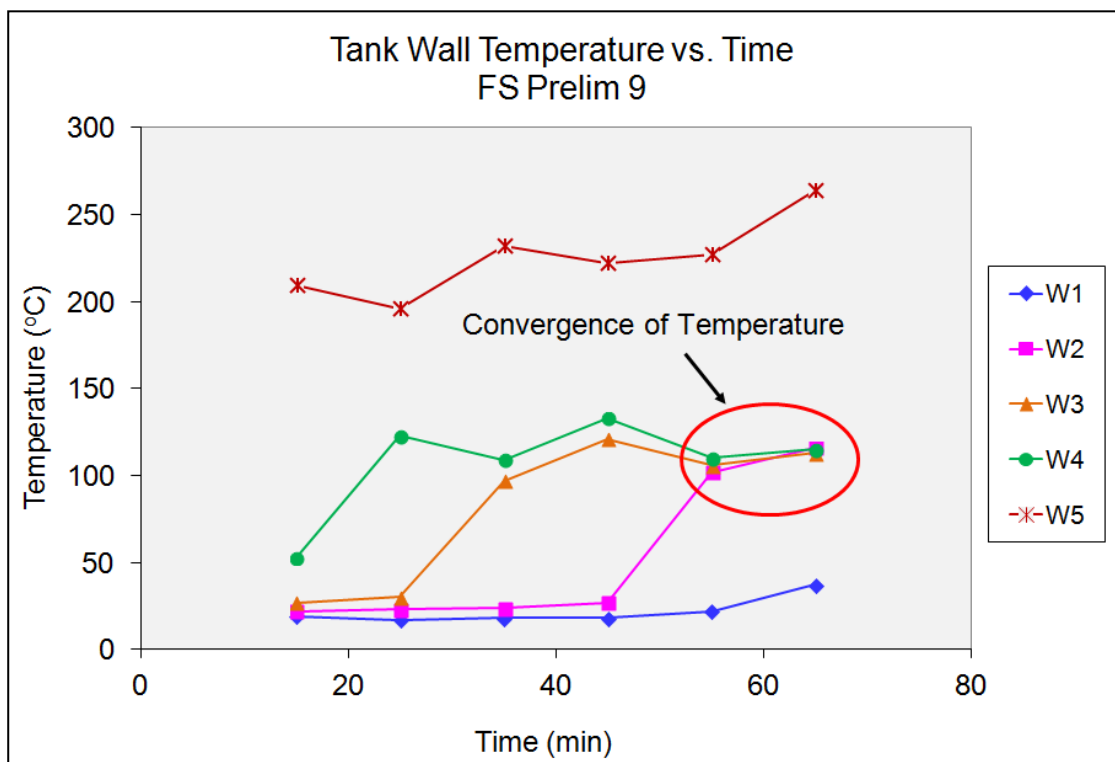
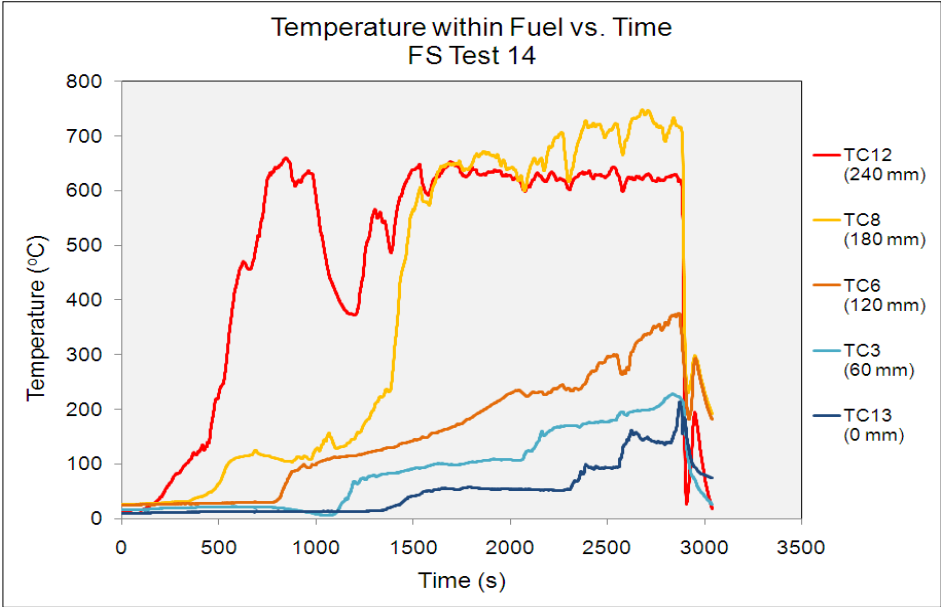


Figure 3-7: Tank wall temperature measurement for FS Prelim 9 (RPI, 2004).

The evolution of the fuel temperature for the field scale tests are shown in Figure 3-8, Figure 3-9, Figure 3-10 and Figure 3-11. Each figure represents the temperature profiles within the fuel during the progression of the experiment.

**3.2.4.1 Crude Oil Tests**

All the tests involving the crude oil showed a similar temperature evolution which is detailed by the following Figure 3-8(a) – (d).



**Figure 3-8: (a) Temperature profiles within the crude oil for the FS Test 14**

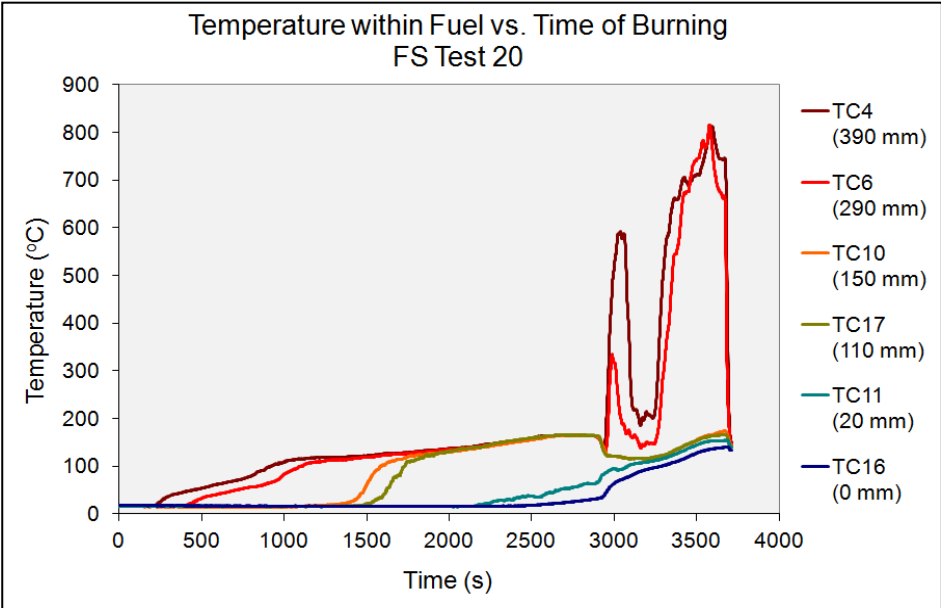


**Figure 3-8: (b) Temperature profiles within the crude oil for the FS Test 20**

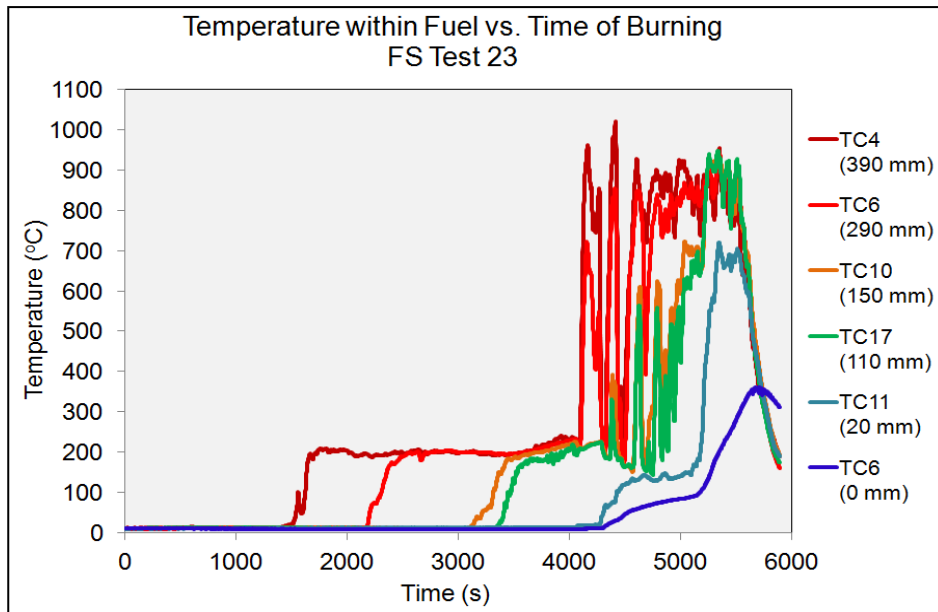


Figure 3-8: (c) Temperature profiles within the crude oil for the FS Test 23

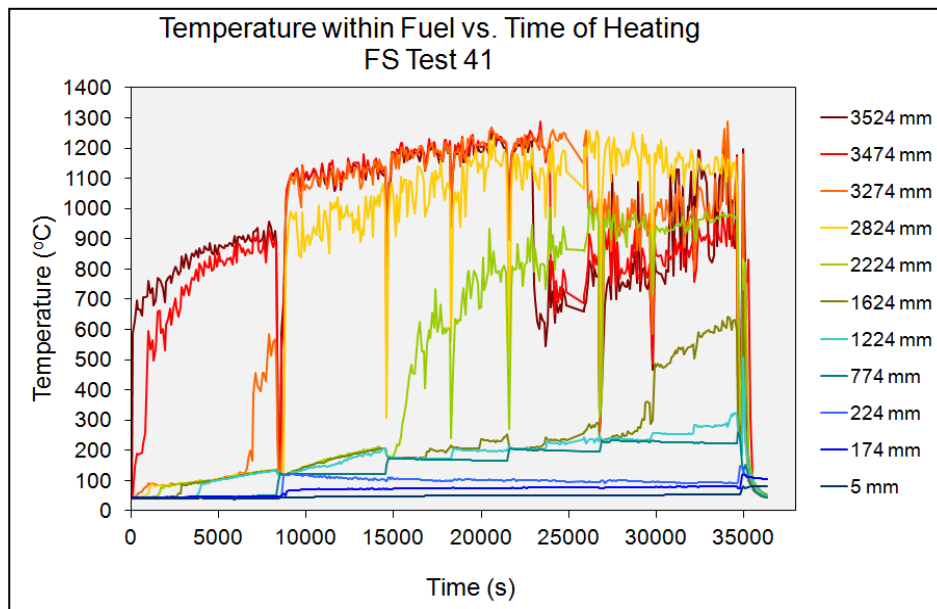


Figure 3-8: (d) Temperature profiles within the crude oil for the FS Test 41

The following paragraphs discuss the temperature development during the crude oil burning of the FS Test 41, based on the Figure 3-8(d).

The flames initially concentrated in the ignition area and then quickly spread over the whole of the fuel surface, at which time a fully developed fire was deemed to have been achieved. This process is characterised by a significant temperature increase at the fuel surface. The temperature just below the surface (recorded by thermocouples placed at 3527 and 3474 mm from the tank

base) increased rapidly to about 50°C upon ignition, and increased further to 200°C after 600 s of ignition. Lighter components vaporized during this period and hence the regression of the fuel surface began. When the surface regressed below the thermocouples, the temperatures increase rapidly up to about 350-400°C as indicated in the figure.

The fire had undergone an initial transient stage which was end-marked by the significant temperature increase. Simultaneously, the stationary burning period began. The characteristic behaviour of this stationary burning is that the thermocouples well below the fuel surface showed a gradual increase in the temperatures which then reached an approximately constant value before the start of boilover. The value reached was around 100 to 110°C i.e. a temperature within the known range of vaporisation of naphtha and gasoline. As shown in the Figure 3-8, following the onset of stationary burning, the temperature measured by the thermocouple at 3274 mm from the base of the tank increased to about 100 to 110°C during the first 1200 s of ignition. Temperatures at points 224 to 2824 mm from the tank base show similar tendencies. The thermocouples readings all converging to about 110°C indicate that a hot zone has been established.

The temperatures at all the points continue to increase with time. Then at some heights, eventually, the temperatures went beyond 400°C when the thermocouples were assumed to have come out of the fuel. Heavy components with high boiling points form the fluid layer down to a level of 224 mm from the base of the tank (as the thermocouples indicate that most of the lights have vaporised above that level). The temperature of the bulk fuel appears to become uniform with a value of about 100 to 110°C within the time range of 1200 s to 34800 s after ignition. Subsequently, a series of boilovers started. At this time, the temperature at the fuel-water interface (indicated by the thermocouple at 174 mm from the tank base) reached a value higher than the boiling point of water. The water vapour resulting from the boiling water cools the thermocouples above the fuel-interface, which shows a decrease in temperature. The boiling occurs for a short duration during which all the

thermocouples show values fluctuated around a fixed temperature. These events signal the end of stationary burning phase and the start of fully developed boilover. This occurred at approximately 34982 seconds (9 hours 43 minutes)

After examining the temperature records during the progression of FS Test 41, a detailed analysis was carried out to identify the maximum temperature reached for the pre-boilover (stationary burning), boilover and post-boilover periods. The maximum temperatures recorded for each of the periods are presented in Table 3-10. As regards to the maximum temperature for the stationary burning phase, the values are determined by extracting the largest number recorded within the period of 10 to 580 minutes of the test. The temperature for the period of boilover is taken averagely from the values measured during the fully developed stage of the phenomenon (in this test, within 581 to 583 minutes). In the final transition phase, the maximum temperature recorded by each of the thermocouples is taken from the measured data after the boilover period until the end of the test.

Thermocouple Height from Tank Base (mm)	Maximum Temperature in Stationary Burning (°C)	Average Temperature during Boilover (°C)	Maximum Temperature in the Post-boilover Period (°C)
3524	1340	1003	1044
3474	1300	796	838
2824	1301	601	662
2624	1222	591	744
2224	1036	565	842
1624	649	529	374
1224	334	424	322
774	271	264	152
224	233	144	122
174	91	128	122
124	79	112	117
74	74	77	89
5	53	71	81

**Table 3-10: Temperatures for each thermocouple at various stages of the crude oil fire in the FS Test 41.**

The values presented by the thermocouples located within the bulk fuel (height from 224 to 3524 mm), when moving across from pre-boilover to boilover period, show a sharp decrease. The drop in the temperatures is due to the cooling effects produced by the lighter ends vapour bubbles rising through the fuel.

The thermocouples immersed in the water layer (located at 5, 124 and 174 mm from the tank base) however show a temperature increase from one period to another. This is caused by the transfer of heat from the hot fuel to the cold water.

Note that the thermocouple closest to the interface - a level below the interface at 124 mm - displays a similar value of temperature during the boilover period i.e. above 100°C to the one at a level above (224 mm). This is explained by the turbulence produced during the boiling stage in which the fuel and water are well mixed.

The subsequent increase in the temperature measured by the thermocouples at levels 1624 mm up to 3524 mm between the boilover and final transition is because of their direct contact with the flames.

#### **3.2.4.2 Diesel-Gasoline Tests**

Figure 3-9 shows the evolution of temperature measured within the diesel-gasoline mixture during the progress of the boilover study conducted in the field scale tests of the LASTFIRE Boilover Study. In these experiments, similar to the crude oil tests, boilover was observed after a prolonged period of burning.

The temperature development throughout the tests was similar to that described for the studies involving crude oil. All the thermocouples immersed within the fuel showed an increase in the temperature measured from the start of the experiments and remained at a fixed value between 150 to 200°C, as clearly seen in the FS Test 42. There is a sharp increase in the values, up to 600 to 700°C, whenever the fuel surface has regressed below a thermocouple.

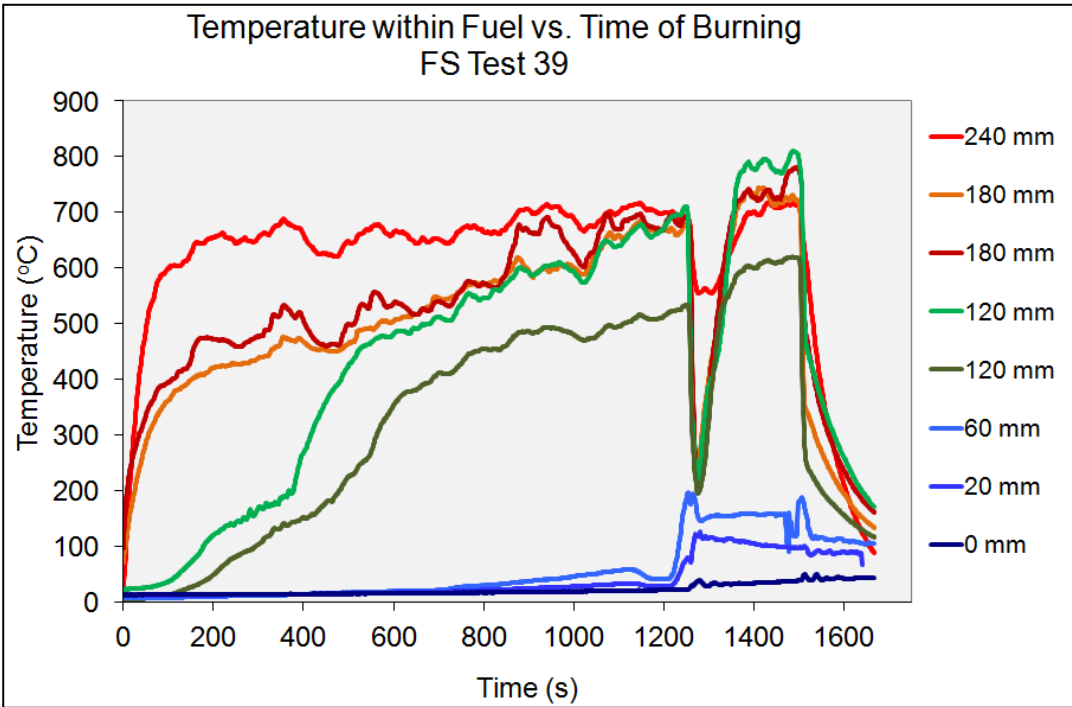


Figure 3-9: (a) Evolution of temperature in diesel-gasoline fuel mixture for boilover study of FS Test 39

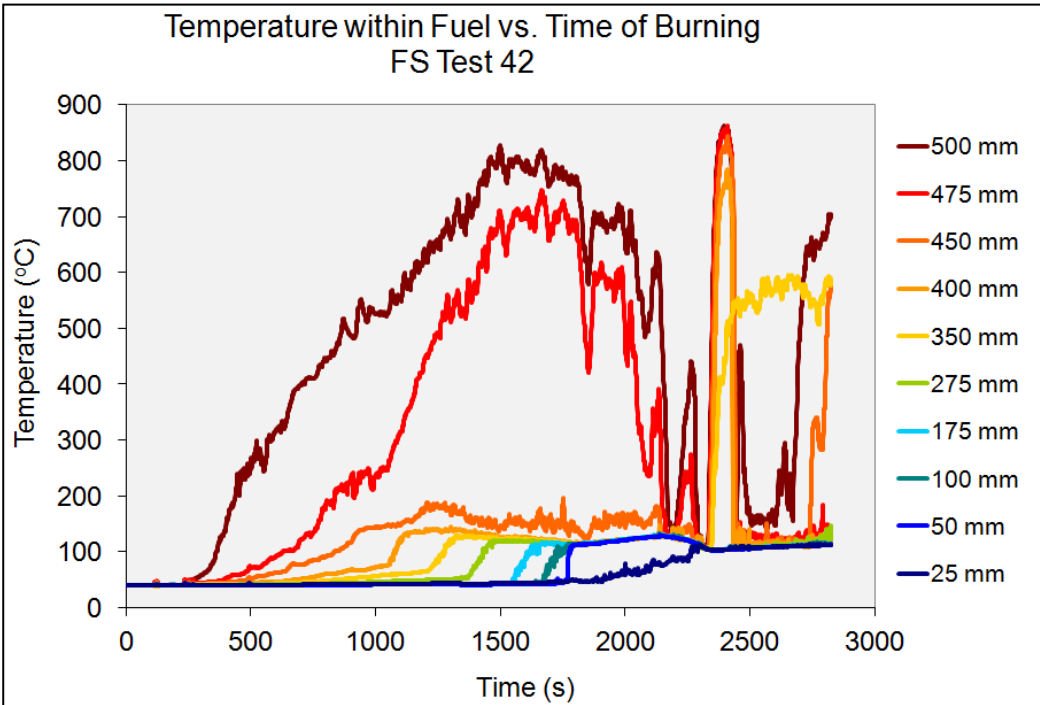


Figure 3-9: (b) Evolution of temperature in diesel-gasoline fuel mixture for boilover study of FS Test 42

A detailed analysis was carried out on the maximum temperature point reached for the pre-boilover, boilover and post-boilover period of the tests involving the diesel-gasoline fuel mixture. The values of the temperatures reached during the test for each thermocouple are presented in Table 3-11.

Boilover Test	Thermocouple Height (mm)	Max. Temperature in Pre-Boilover Period (°C)	Avg. Temperature during Boilover (°C)	Avg. Temperature in the Post-boilover Period (°C)
FS Test 39	240	717	678	718
	180	693	630	693
	120	611	549	611
	60	93	168	188
	0	23	24	51
FS Test 42	500	827	453	1016
	475	747	241	1025
	450	197	148	1012
	400	144	127	967
	350	130	127	901
	275	125	128	784
	175	125	128	554
	100	125	127	296
	50	125	127	244
	25	79	80	224

**Table 3-11: Temperatures for each thermocouple at various stages of the diesel-gasoline fuel mixture experiments**

From Table 3-11, the values presented by the top thermocouples located within the bulk fuel when changing over from pre-boilover to boilover period, illustrate a decrease in temperature. For the FS Test 39, the thermocouples located at the height of 120 to 240 mm from the base of the tank register a drop in the temperature measurements. In the FS Test 42, these observations are shown by the thermocouples located at the height of 350 to 500 mm from the tank base. Due to the rising of water vapour bubbles, the temperature of the bulk fuel drop during the boilover period. In the field scale experiments, these thermocouples then display higher temperatures since they are in direct contact with the flame.



The thermocouples immersed in the water layer show an increase in temperature when moving across from one period to another, as a result of heat transfer from the fuel to the water.

For tests in which boilover occurred, the behaviour of the temperature evolution was similar. One point to highlight is that, in these experiments, there is evidence of overheating of the water layer as the thermocouple at the fuel-water interface presented a temperature beyond the evaporation point of water.

### 3.2.4.3 Gasoline Test

Figure 3-10 shows the temperature evolution of a gasoline test FS Test 31. These results present the temperature evolution for the case in which there is no occurrence of boilover.

The behaviour in the early stage of gasoline fires is similar to that described for the crude oil fires. When the stationary burning period started, there was an increase in the temperature measured by the thermocouples especially the ones that were located near to the fuel surface.

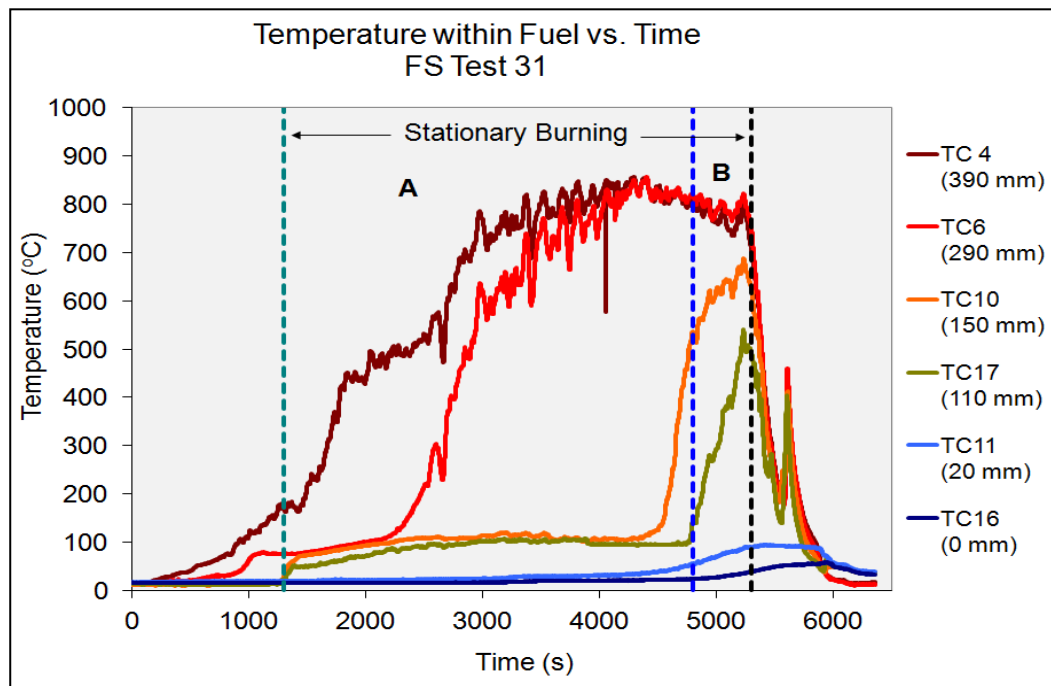


Figure 3-10: Evolution of temperature in gasoline for the FS Test 31

In Figure 3-10, the top thermocouple (at level 390 mm, very close to the fuel surface) recorded a steadily increasing temperature until it reached a value of about 100°C. Then the temperature showed a sudden increase up to about 700 to 800°C which indicates that the thermocouple had emerged from the fuel. The adjacent thermocouples (at level 110 to 290 mm) also show increase in temperatures up to about 100°C, after which time the temperature remains approximately constant. This period, within the period of 1400 to 4800 seconds, is taken as the stationary burning phase where the gasoline is burnt steadily. Moments later, the temperature measured by these thermocouples show a sudden rise. This rise is due to the fact that the thermocouples had emerged from the fuel and in direct contact with the flames.

The thermocouples immersed in the water did not show any significant increase in temperature until after about 4000 seconds of burning. Figure 3-10 shows that, after that time, the temperature at a level of 20 mm increased more rapidly to a value that remained stable through to the final transition period. The temperature rise, on the whole, continued until the start of the final transition which is manifested by the dramatic drop of temperature measured by the top thermocouples. All the thermocouples (from level 110 mm to 390 mm) were in contact with the flames but then show temperature decrease within the period of 5500 to 6000 seconds, as shown in Figure 3-10. The decrease could be linked to the reduction of the flame size and hence the heat received is substantially lower. The fire decreased in size as the fuel was depleted. The thermocouples immersed in the water layer (at level 0 and 20 mm) are not affected by the gradual decline in the size of the fire, as the water temperature remains constant.

A study was made of the temperature evolution for each thermocouple throughout the test. The determination of the temperatures was done differently, compare with the crude oil fires, because of the non-occurrence of boilover. The analysis was limited to stationary period which was divided into two parts, namely part A and B as shown in Figure 3-10. Table 3-12 presents the analysis of temperatures reached by each thermocouple during the gasoline test.

Boilover Test	Thermocouple Height (mm)	Max. Temperature in Stationary Period A (°C)	Max. Temperature in Stationary Period B (°C)	Max. Temperature in the Final Transition Period (°C)
FS Test 31	390	858	810	684
	290	857	822	747
	150	537	687	624
	110	143	540	486
	20	56	91	95
	0	24	39	58

**Table 3-12: Temperatures for each thermocouple at various stages of the gasoline experiments**

An important fact to note is that, in the experiments with gasoline, there is no evidence of overheating of the water layer. As shown in Table 3-12, the thermocouples at the fuel-water interface (at level 20 mm) did not reach the minimum temperature set for boilover occurrence (110°C, as mentioned in Section 3.2.3) and only sporadically reached 100°C. This could be associated with the fact that the boiling temperatures of most compounds in gasoline are below 100°C.

#### **3.2.4.4 Diesel Tests**

Figure 3-11 shows the temperature evolution of diesel tests for the FS Test 29 in which boilover did not occur.

An analysis was carried on the temperature evolution measured by each of the thermocouples in the diesel tests FS Test 29.

Table 3-13 presents the analysis of the temperatures reached by each thermocouple during the diesel test.

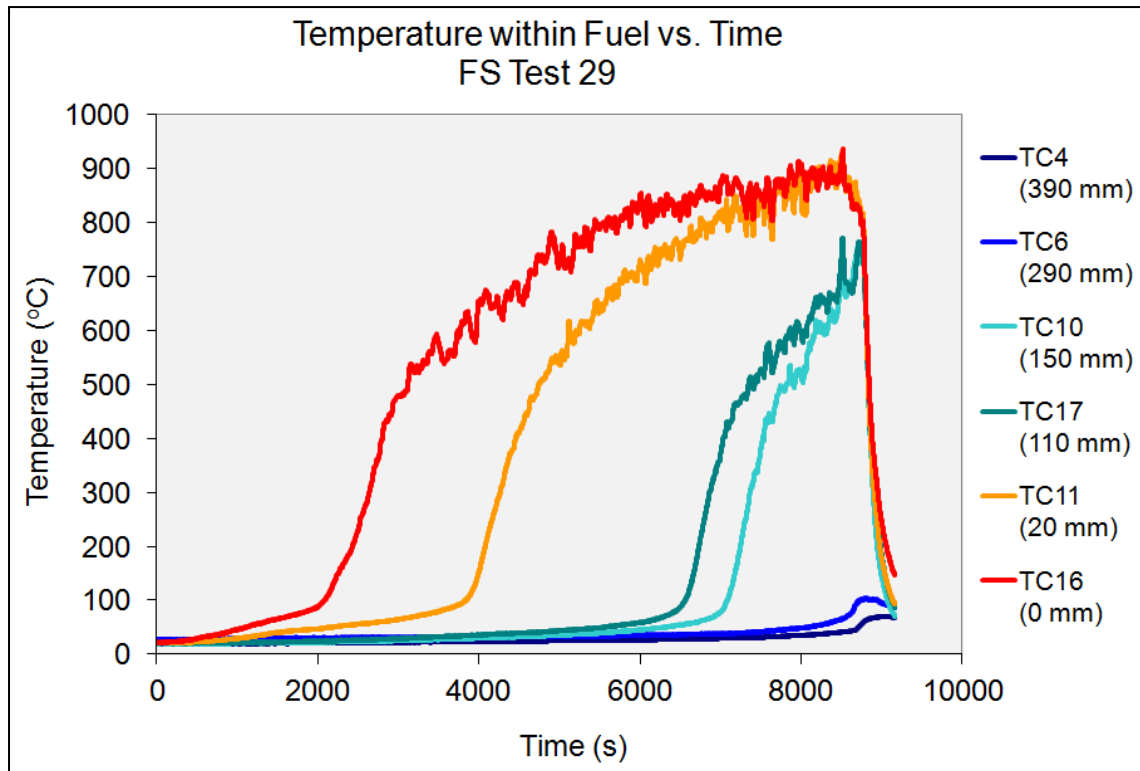


Figure 3-11: Evolution of temperature in diesel for the FS Test 29

Boilover Test	Thermocouple Height (mm)	Max. Temperature in Stationary Period A (°C)	Max. Temperature in Stationary Period B (°C)	Max. Temperature in the Final Transition Period (°C)
FS Test 29	390	875	912	935
	290	818	925	935
	150	371	741	771
	110	79	717	760
	20	39	65	104
	0	30	41	70

Table 3-13: Temperature reached by each thermocouple throughout the experiments on diesel

Based on Table 3-13, and similar to the gasoline tests, there is no evidence of water layer overheating in the FS Test 29. The thermocouple at the interface (at level 20 mm) only reached 100°C intermittently.

### 3.3 ANALYSIS OF THE TEST RESULTS

As set out in Section 3.1, the important questions to be addressed related to boilover phenomenon are:

- i. Can a boilover occur?
  - i.e. to identify if boilover could occur during fires involving a range of fuels commonly stored in large atmospheric storage tanks.
- ii. If a boilover occurs, when will it occur?
  - i.e. to identify when boilover could occur.
- iii. When a boilover occurs, what will be the consequences?
  - i.e. to identify and assess the consequences of a boilover event.

#### 3.3.1 Can a Boilover Occur?

Table 3-6, Table 3-7, Table 3-8 and Table 3-9 (Section 3.2.1) display the details and main results of field scale tests carried out during the LASTFIRE boilover studies which involved crude oil, refined fuels, biodiesel and mixtures of diesel and gasoline and diesel and biodiesel. As mentioned in Section 3.2.2, the time to boilover is determined based on the changes in the temperature profiles i.e. the thermocouple at the fuel-water interface reaching the boiling temperature of water and flame enlargement due to fuel ejections from the tank. Each test was timed from the moment the full surface of the fuel was alight.

All of the tests involving crude oil resulted in boilover as did the tests involving mixtures of diesel and gasoline. None of the tests involving refined fuels, biodiesel and the mixture of diesel and biodiesel resulted in boilover.

The conclusions from the results are that for boilover to occur it is necessary to have a fuel with wide boiling range and for the boiling points of the heavier components to be significantly greater than the boiling point of water. These requirements are necessary for a hot zone to be established and to ensure that when the hot zone comes into contact with and mixes with the water layer its

temperature is sufficient to ensure that large quantities of steam are generated extremely rapidly. The steam forces the hot burning fuel out of the tank resulting in an increase in flame length and the establishment of a pool fire outside the tank.

### **3.3.2 If a Boilover Occurs, When Will It Occur? (Time to Boilover)**

In the case of an accidental situation in which there is a possibility of boilover occurrence, it is essential to know the time at which the phenomenon will occur. One of the main factors influencing the onset of the boilover is the initial depth of the fuel layer. The following figure shows the influence of the initial fuel layer on the time to boilover.

Figure 3-12 shows the observed onset time of boilover as a function of the initial depth of fuel for the field scale tests conducted in the LASTFIRE Boilover Study involving crude oil. As can be seen, there is a large scatter in the data. However, the linear fit to the data (forced to pass through the origin) shows that boilover onset time increases with the initial depth of the fuel layer.

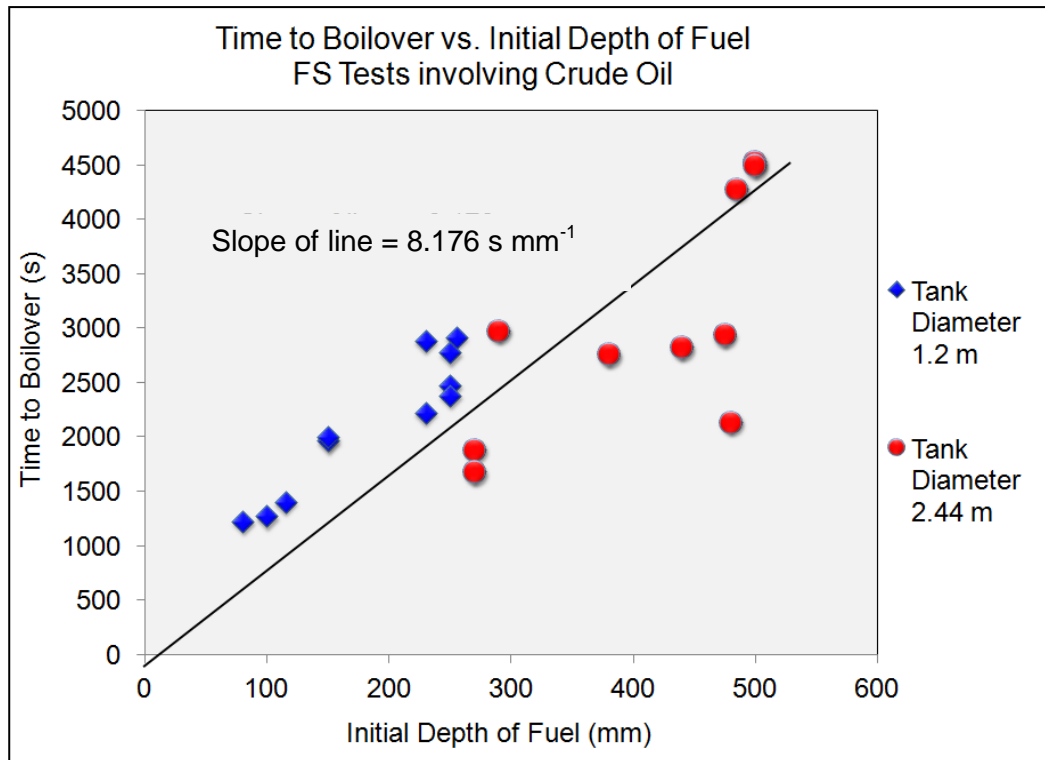


**Figure 3-12: Time to boilover against initial fuel depth for field scale tests for crude oil**

Experimental data from liquid hydrocarbon pool fire experiments on pools in excess of 1 m diameter by Garo & Vantelon (1999) and Koseki *et al.* (1991) show that the regression rate of the fuel surface is a constant. This indicates that the heat flux from the flame to the fuel surface is a constant. It follows that the creation and development of the hot zone can, similarly be considered to be constant and that for pools of 1 m size and greater the problem can be considered to be one-dimensional. Consequently, the inverse of the slope of the trend line on Figure 3-12 represents the constant speed with which the base of the hot zone progress down through the fuel. Multiplying the initial depth of the fuel by the slope of the trend line shown Figure 3-12 gives the time to boilover.

$$t_{bo} = 8.18 z_f$$

**Equation 3-1**

where  $t_{bo}$  is the time to boilover (s) and  $z_f$  is the initial depth of the fuel (mm).

Equation 3-1 provides a simple empirical relationship (Empirical Model 1) for the time to boilover based on the initial depth of the fuel.

Another approach to predict the time to boilover is to determine the speed at which the base of the hot zone travels down through the fuel using the thermocouple profiles.

The hot zone is a high temperature isothermal layer formed during the burning of the fuel as a result of a distillation process in which lighter components of the fuel are vaporised such that only the heavier components of the fuel mixture remain. The speed of the base of the hot zone represents the rate of heat propagation in the cold fuel below the hot zone. When the base of the hot zone reaches the layer of water at the bottom of the tank, rapid heating and vaporisation of the water occurs resulting in boilover. The base of hot zone refers to the region between the isothermal hot zone region and the water layer zone (as indicated in Figure 3-13).

The speed of the base of the hot zone is obtained through a detailed analysis of the temperature profiles in the fuel layer. Figure 3-13(a) – (d) show the temperature profiles inside the fuel at various times for tests FS Test 9, 20, 22 and 41.

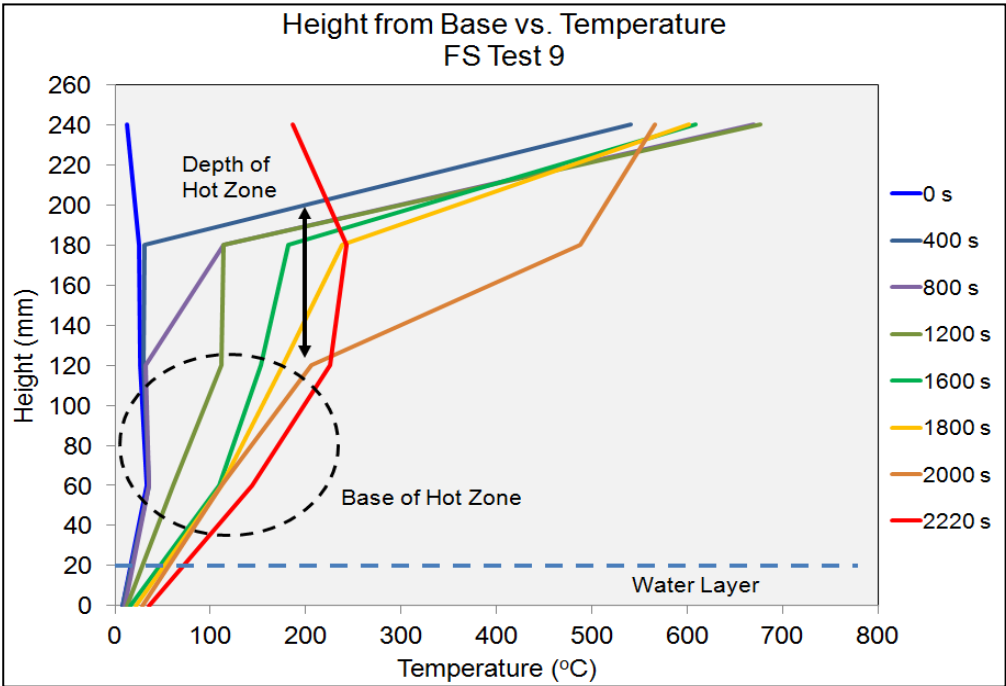


Figure 3-13: (a) Vertical temperature profile for FS Test 9



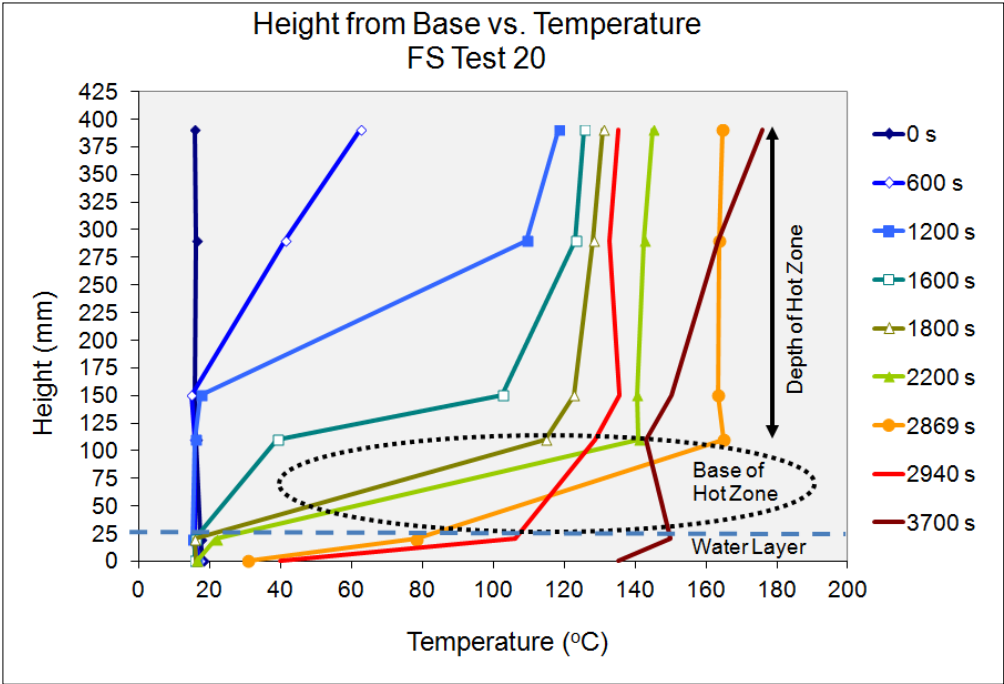


Figure 3-13: (b) Vertical temperature profile for FS Test 20

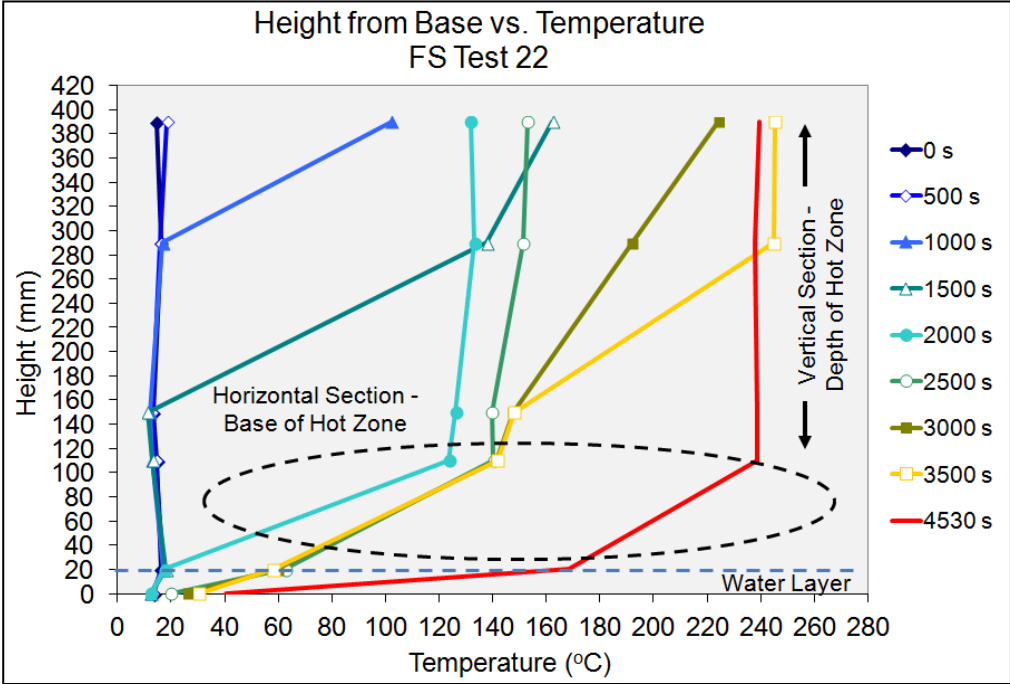


Figure 3-13: (c) Vertical temperature profile for FS Test 22

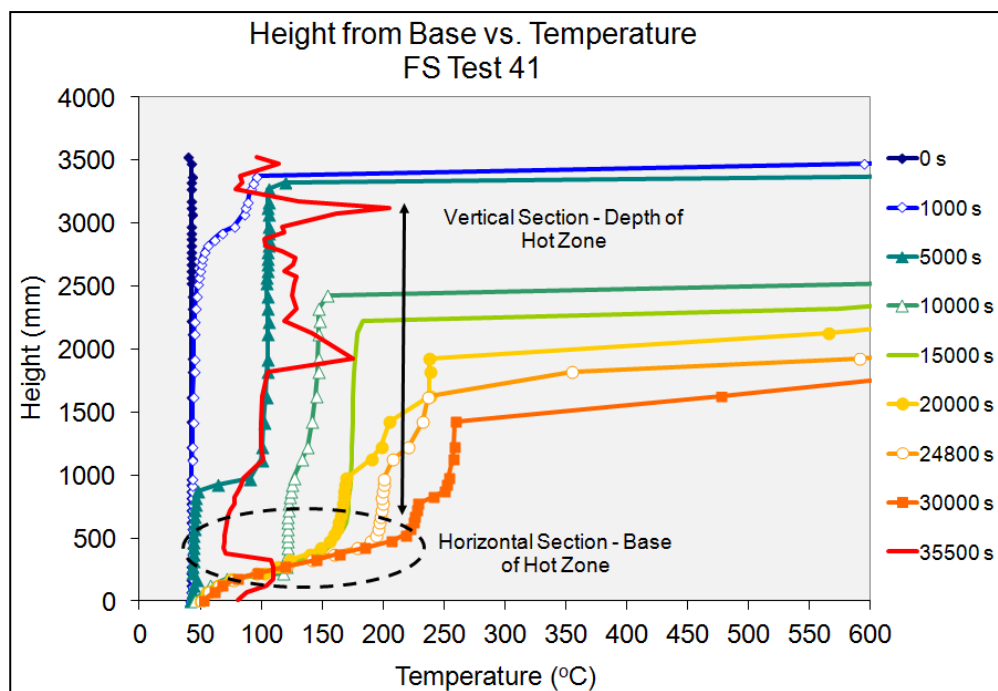


Figure 3-13: (d) Vertical temperature profile for FS Test 41

The temperature profiles shown in Figure 3-13(a) – (d) illustrate the formation of a hot zone and an interface between the hot and cold fuel zones. The vertical section of the temperature profiles gives the approximate depth of the hot zone. Since the figures do not distinguish clearly the interface between the hot zone and cold fuel zone, the horizontal section or the approximately horizontal section was assumed to be the bottom boundary of the hot zone i.e. the hot-cold interface. In addition, the average temperature of the uniform vertical section of the temperature profiles was taken as the temperature of the hot zone. Hence the temperature of the hot zone was taken to be about 100 - 150°C for tests FS Test 9 and 20 and 100 – 240°C for tests FS Test 22 and 41.

The red line in each of the figures represents the occurrence of boilover. In Figure 3-13(a), (b), (c) and (d), the boilover occurred when the temperature of the fuel-water interface was about 110°C. Therefore, it is assumed that the temperature at the bottom of the hot zone when boilover occurred in the field scale tests was about 110°C. This is close to the temperature at the bottom of the hot zone given in the literature i.e. 120°C (Inamura *et al.*, 1992; Garo *et al.*, 1999a; Koseki *et al.*, 2003 & 2006).

Consequently, when the base of the hot zone reached the water layer at the tank base, the temperature of the water was raised to its boiling point whilst a substantial depth of hot fuel remained above the water. Once the water started to boil, rapid mixing between the water and the hot fuel was initiated. This resulted in enhanced heat transfer and vigorous boiling in which large amounts of steam was generated. As a result, hot fuel was ejected out of the pool and hence flame enlargement and the formation of a pool fire around the tank.

### 3.3.2.1 Depth of Water Layer at Base of Tank

Figure 3-14 shows the observed time to boilover as a function of the depth of water at the tank base for the field scale tests involving crude oil. The field scale tests studied the effect of the depth of the water layer to the time to boilover through tests FS Test 5 - FS Test 6, FS Test 15 - FS Test 16 and FS Test 22 - FS Test 23.

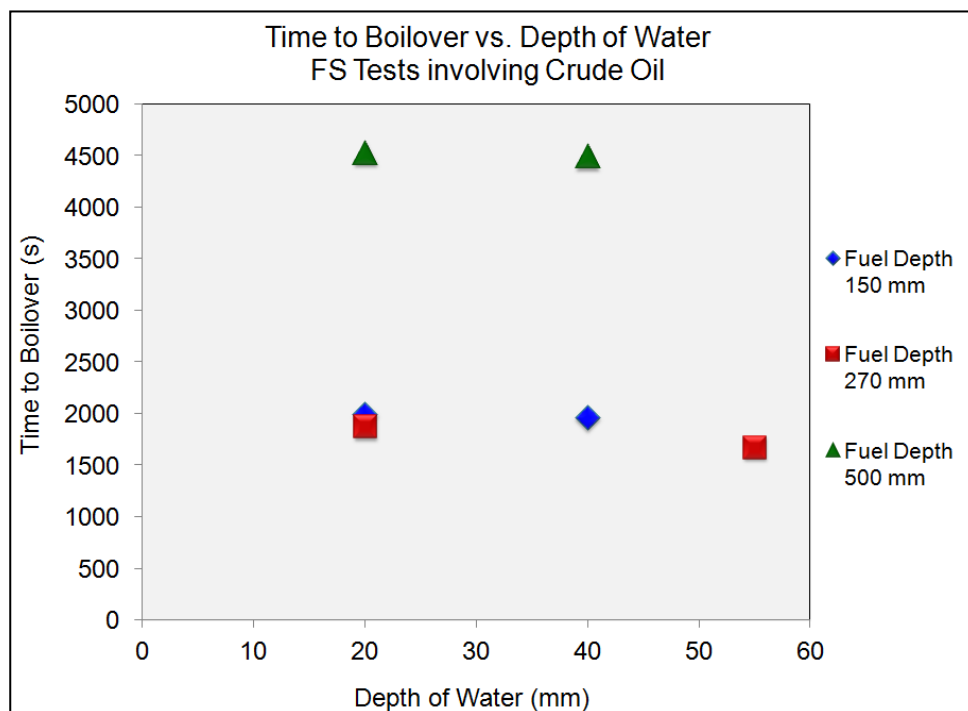


Figure 3-14: Time to boilover against depth of water at the tank base for field scale tests involving crude oil

The figure shows that the time to boilover is independent of the depth of the layer of water. The field scale tests results show that an increased depth of water within the tank does not significantly affect the time to boilover, as

observed between FS Test 5 - FS Test 6, FS Test 15 - FS Test 16 and FS Test 22 - FS Test 23.

### ***3.3.2.2 Distribution of Temperature in the Fuel Layer***

The objective of the analysis of temperature distribution in the liquid layer is to show the possible formation of hot zone and hence identify the triggering mechanism of boilover.

As seen in the Section 3.2.4, the fire behaviour and the temperature development within the burning fuel were similar for all experiments of the same fuel type. Crude oil fire is chosen as the benchmark for the test with boilover and gasoline fire for the test without boilover.

In each of the following graphs shown within this section, the temperature distribution in the liquid layer from the data recorded by the thermocouples is presented for a given instant of time. The abscissa of the graphs represents the depth of the liquid layer with values ranging from -20 mm (i.e. 20 mm below the fuel-water interface) to the highest thermocouple location of the described experiment (e.g. for the FS Test 23, the top thermocouple is at 370 mm above the interface). Each graphic is a curve indicating the time elapsed since the start of the experiments (either the start of burning or heating). The vertical red line that appears in some of the graphs represents the surface of the fuel during the progress of a test.

#### **Crude Oil Fire**

Figure 3-15 shows the temperature distribution within the liquid layer for the FS Test 22 involving the burning of 500 mm layer thickness of crude oil floating on 20 mm water layer in a 2.44 m diameter pan.

The period of 1100 s, as shown in Figure 3-15(a), is when the temperature experienced the first significant increase after an initial fire development phase. Analysing Figure 3-15(b), an exponential profile is first observed at the two top thermocouples after 1500 s of starting the fire. Then, after another 500 s of

burning, all the thermocouples above the interface register almost the same temperature of 130°C. This observation leads one to believe that a hot zone has been formed.

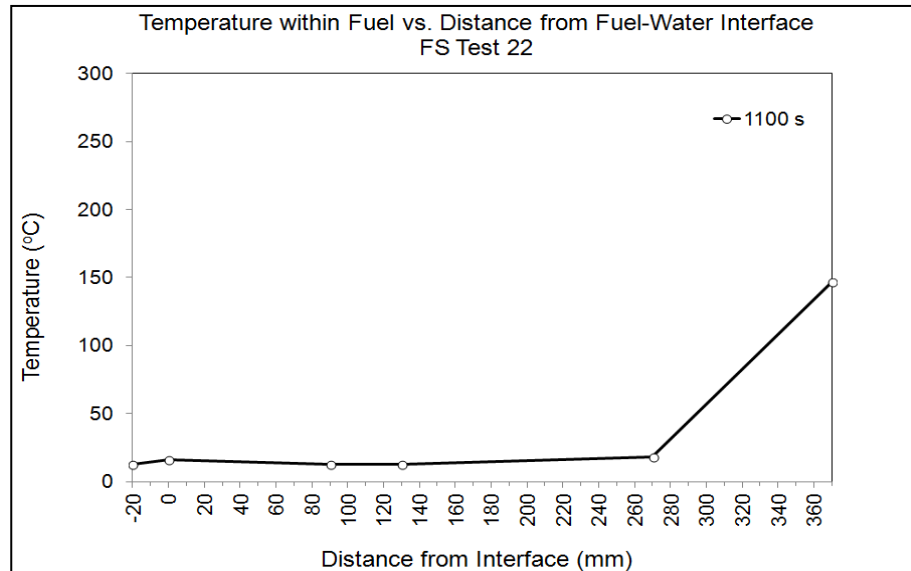


Figure 3-15: (a) Temperature distribution in the liquid at time 1100 s for FS Test 22

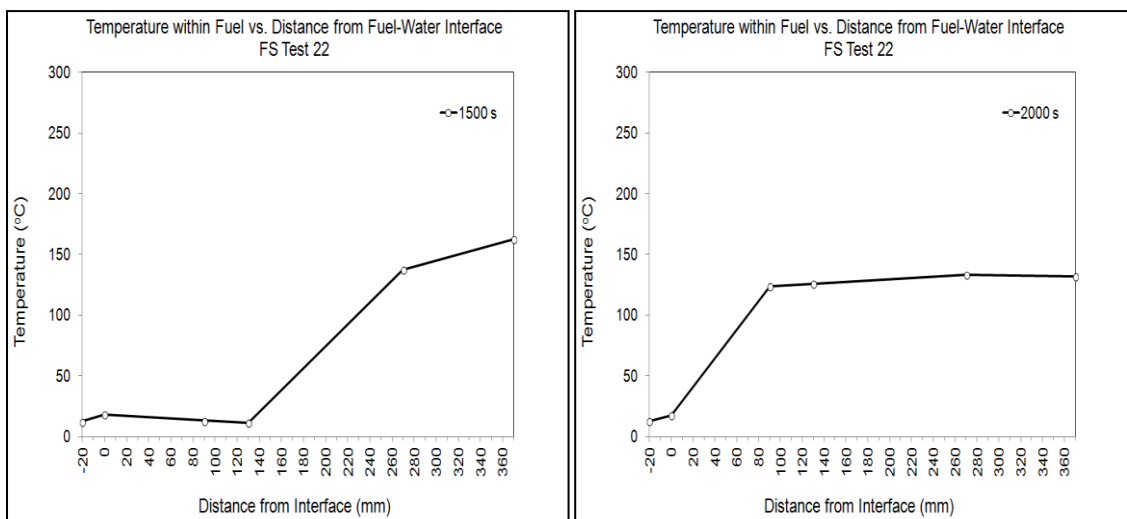


Figure 3-15 (b)

Figure 3-15 (c)

Figure 3-15: Temperature distribution in the liquid at time (b) 1500 s and (c) 2000 s for FS Test 22

Figure 3-16 shows the temperature distribution within the liquid layer between the periods of 3000 s to 4500 s since the start of the fire. Figure 3-16 shows that the constant temperature zone (between 90 mm to 370 mm above the interface) does not grow in size with time but moves with the liquid surface level. By the period of 4000 s, as shown by Figure 3-16(b), the temperature has increased to

about 250°C. The surface level is determined to drop from about 520 mm to about 260 mm from the interface. Figure 3-16(d) shows the temperature distribution at the instant when boilover occurred.

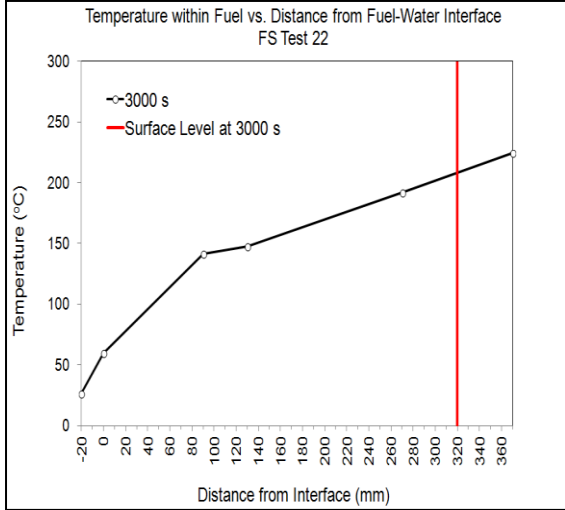


Figure 3-16 (a)

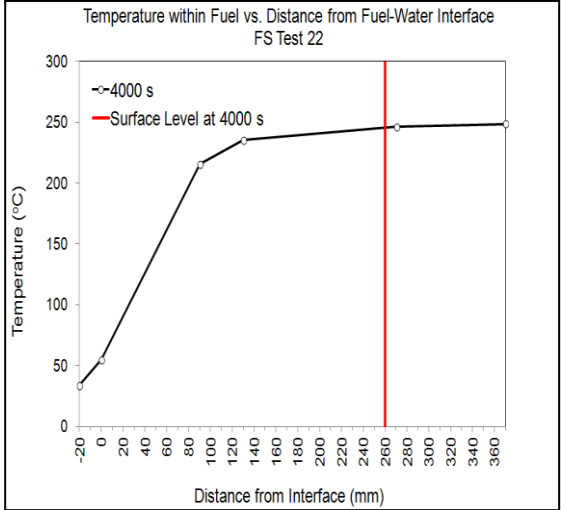


Figure 3-16 (b)

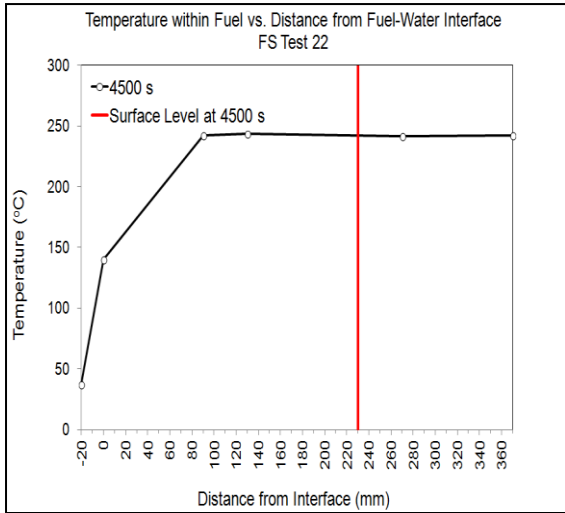


Figure 3-16 (c)

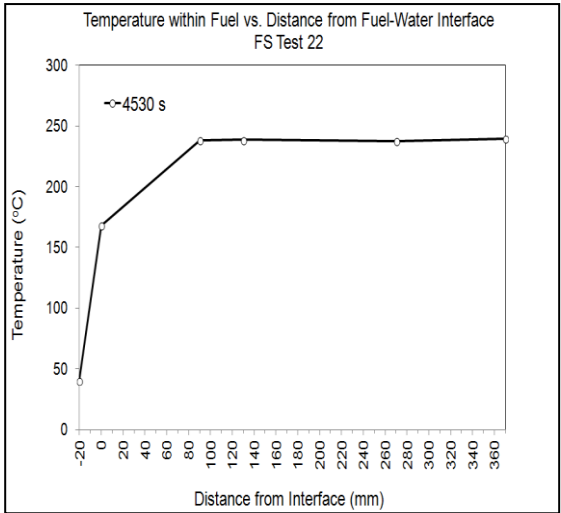


Figure 3-16 (d)

**Figure 3-16: Temperature distribution in the fuel at time of boilover (a) 3000 s, (b) 4000 s, (c) 4500 s and (d) 4530 s**

It is important to state that the thermocouple at the interface (0 mm) reaches a value of about 140°C at the period of 4500 s but boilover was not seen. This observation could be linked to the oscillations of the interface (Hasegawa, 1989 and Broeckmann & Schecker, 1995) and hence the thermocouple recorded an intermediate level temperature between the fuel and water.

It is also worth to state that, from the observation of the field scale tests; a boilover does not occurred immediately upon the interface reaching the water boiling point. It is noted that from the moment the thermocouple at the interface reached a temperature higher than 100°C, it takes about 40 seconds before the boilover fully started. This observation possibly relates to the longer heating required of the lowest fuel layer which consisted of components with very high boiling points.

Table 3-14 shows the time for the fuel-water interface to reach 100°C for some of the tests involving crude oil fires and the boilover onset time. As mentioned above, when the bottom of the fuel layer in contact with the water layer reaches a temperature of about 100°C, vaporization did not start immediately. Table 3-14 shows that it would take about 20 to 80 seconds before the boilover occurred.

Boilover Study	Initial Fuel Thickness (mm)	Time for Interface to reach 100°C (s)	Instant Start-up of Boilover (s)
FS Test 21	485	4275	4282
FS Test 22	500	4486	4530
FS Test 20	475	2920	2940
FS Test 23	500	4423	4494
FS Test 40	520	1565	1620
FS Test 41	3350	34900	34982

**Table 3-14: Comparison between time required for the fuel-water interface to reach boiling point of water and time of boilover start for the field scale tests involving crude oil tests**

Figure 3-17 shows the temperature distribution within the liquid layer upon the start and development of boilover phenomenon.

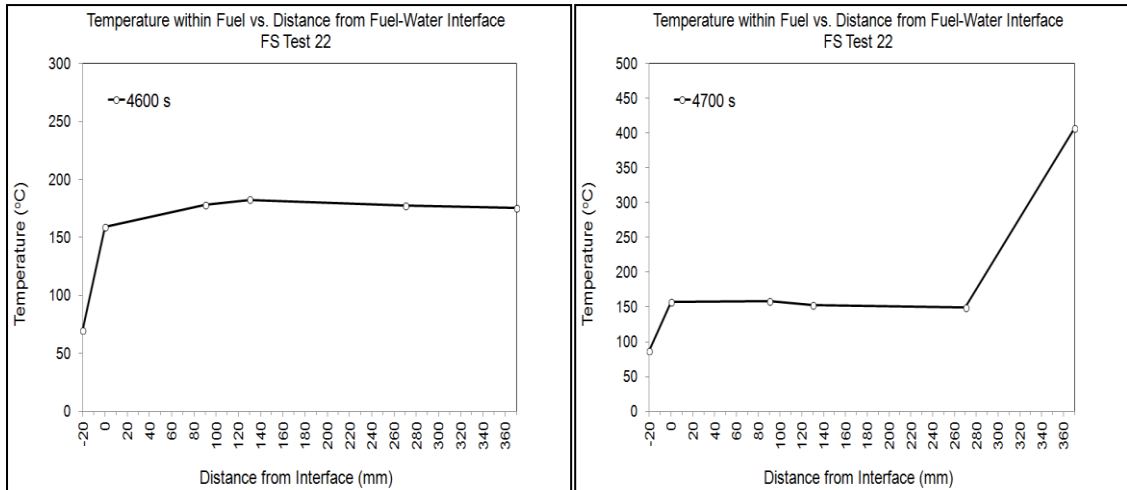


Figure 3-17 (a)

Figure 3-17 (b)

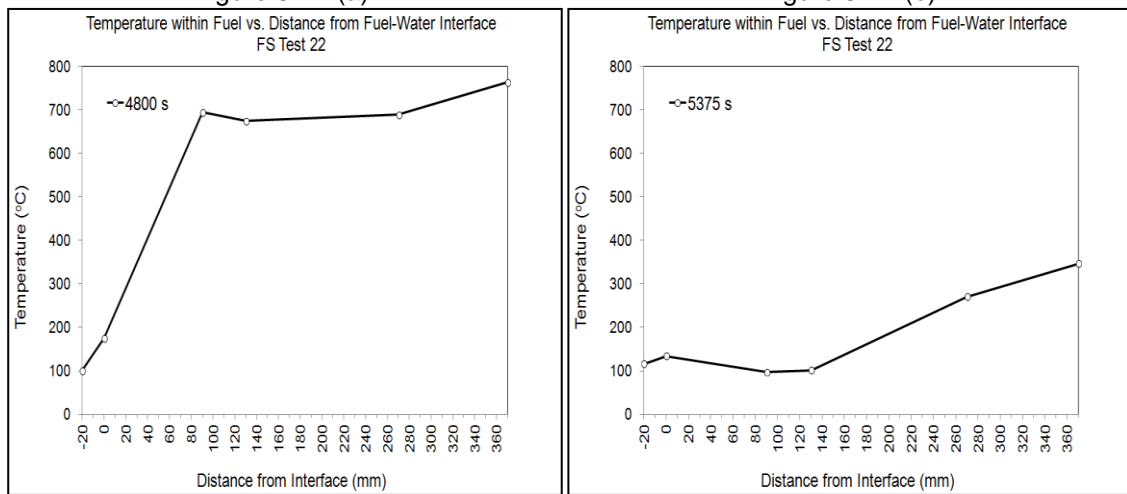


Figure 3-17 (c)

Figure 3-17 (d)

**Figure 3-17: Temperature distribution in the liquid at time of (a) 4600 s, (b) 4700 s, (c) 4800 s and (d) 5375 s for the FS Test 22**

At the instant after the boilover started, the temperature at the fuel-water interface reaches a value exceeding the point of water evaporation and crackling sounds are heard followed by vigorous production of vapour bubbles. The rising bubbles cool the fuel and hence the thermocouples in its path. The cooling is manifested by the decrease in the temperatures measured by the thermocouples as shown in Figure 3-17(a). The bubbles, mainly come from the conversion of liquid water to steam, force out the remaining fuel on the top layer. Consequently, more fuel is consumed by the flame and hence resulted in a larger and more intense fire. For this reason, the temperatures measured by the thermocouples at the upper part of the tank are higher, as presented by Figure 3-17(b) and (c), since the heat received is substantially higher. It should be noted that once the boilover starts, the surface level fluctuates very



irregularly due to turbulence and therefore could not be determined with precision. At about 5375 s after the start of the test, the fire subsided and hence the lower temperatures registered by the thermocouples.

### **Gasoline Fire**

In the case of gasoline fire, the behaviour is similar to that observed in the crude oil test in the early stage i.e. the temperature shows a well-defined exponential curve, as presented by Figure 3-18(a). The period of 900 s is when the temperature experienced the first significant increase after an initial fire development phase. The presence of this high temperature near the top part of the fuel layer can be attributed to the closeness of the flame and the heat transfer by convection, radiation and conduction from the fire.

In contrast, though the temperature is increasing as the time progresses from 900 s to 2220 s, there is no zone established between thermocouples as what has been observed in the crude oil fire (refer to Figure 3-15(c)). After about 1000 s later, the thermocouple located 270 mm above the interface displays almost the same temperature to the one measured at 370 mm. This could lead to the assumption that a hot zone has been formed. However, the constant temperature zone is outside of the liquid since it is crossed by the red line representing the fuel surface and therefore is measuring the flame temperature. All of the above can be seen in Figure 3-18(b) and (c), in which the temperature profiles represent the 2220 and 3500 seconds from the start of the burning respectively. Figure 3-18(b) presents the beginning of the regression of the fuel surface level within the availabilities of the thermocouples.

The fact that the isothermal layer does not spread to the bottom of the tank is because the rate of distillation of the components in the gasoline is very similar to the rate at which the liquid surface regresses. This observation is probably due to the relatively small range of boiling temperatures of the components that make up the gasoline.

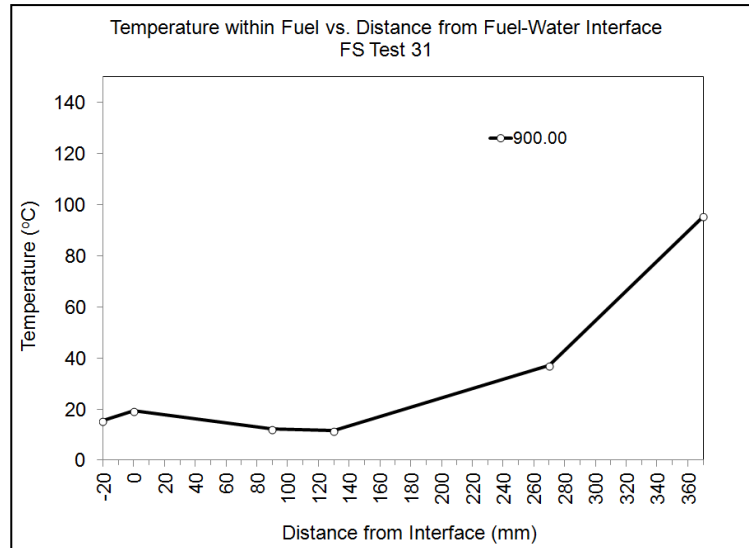


Figure 3-18: (a) Temperature distribution in the liquid at time of 900 s

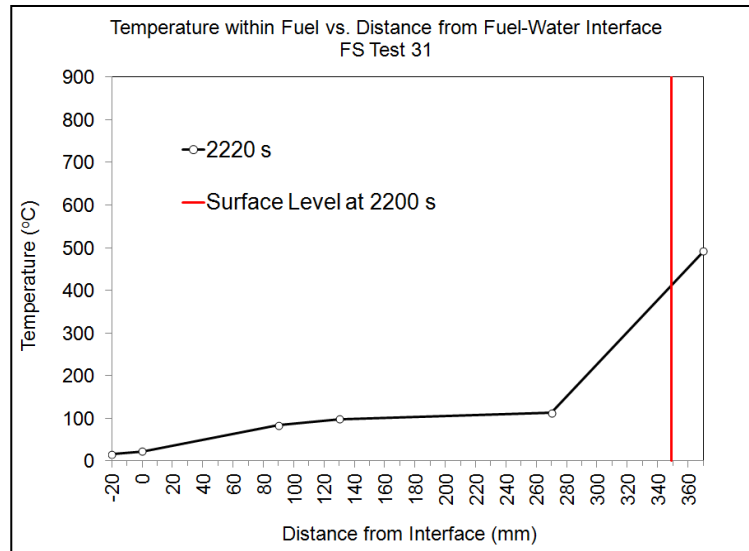


Figure 3-18: (b) Temperature distribution in the liquid at time of 2220 s

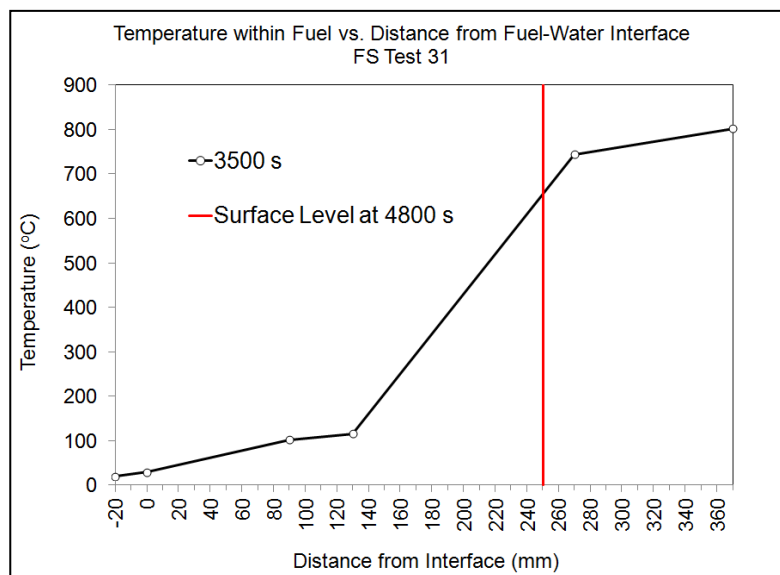


Figure 3-18: (c) Temperature distribution in the liquid at time of 3500 s for FS Test 31

Figure 3-19 shows the progressive evolution of the temperature distribution for the gasoline and the advancement of the fuel surface regression near the end of the experiment. Figure 3-19(e) shows the temperature distribution at the final moments of the test. Note that at any moment between 4800 to 6355 s after the fire started, the fuel-water interface (0 mm) does not reach the boiling temperature of water. The maximum temperature reached by the thermocouple is about 95°C. A point to highlight is that the temperature of the remaining fuel seems to drop when the surface approached near to the interface, as observed in Figure 3-19(c) to (e). This is probably due to the proximity of the water layer which acted as a cold sink.

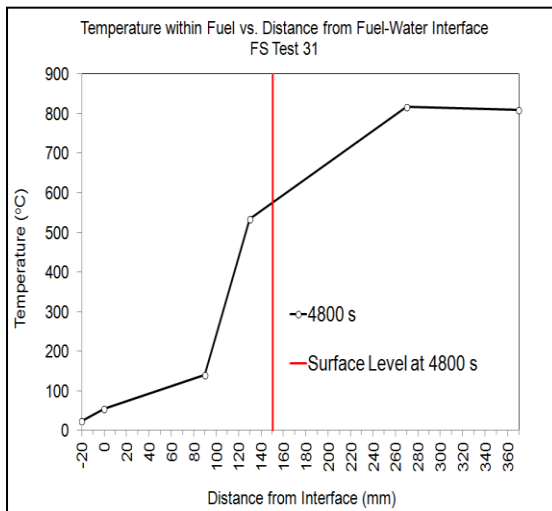


Figure 3-19(a)

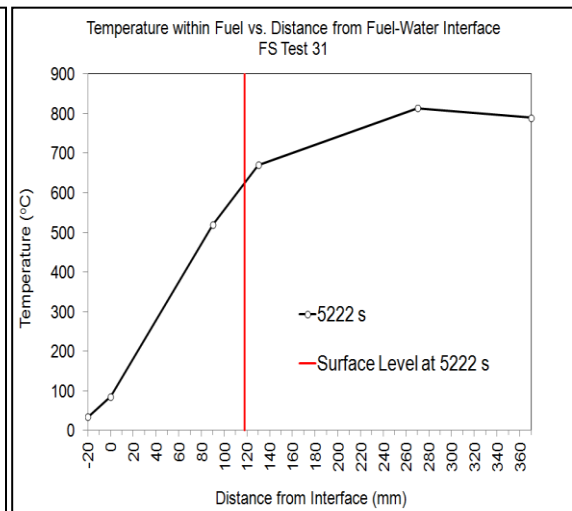


Figure 3-19(b)

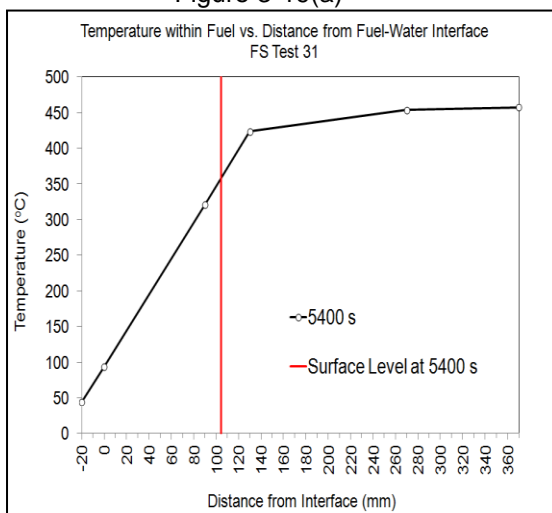


Figure 3-19(c)

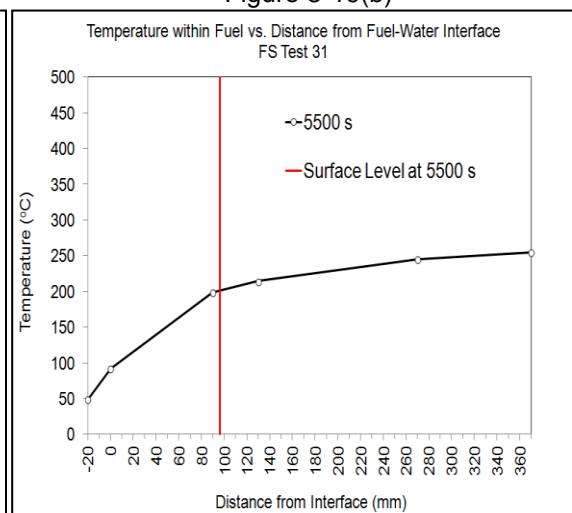
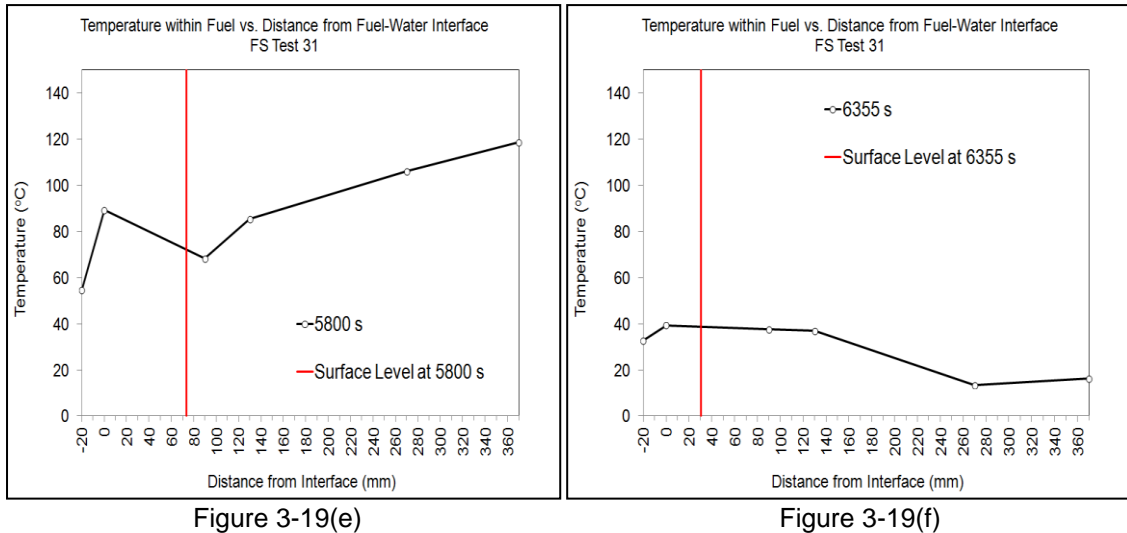


Figure 3-19(d)



**Figure 3-19: Temperature distribution in the liquid at time of (a) 4800 s, (b) 5222 s, (c) 5400 s, (d) 5500 s, (e) 5800 s and (f) the end of experiment – 6355 s; for the FS Test 31**

### 3.3.2.3 Speed of the Base of the Hot Zone

The speed of the base of the hot zone was estimated by determining the time required for the hot zone lower boundary to reach a specific depth. Based on the temperature profiles obtained for each of the field scale tests, the time for the base of the hot zone at 110°C reaching a specific depth could be determined. Table 3-15 shows the temperature measured within the crude oil at specific depths from the tank base at specific time interval for FS Test 23. The test involved the burning of 500 mm crude oil with 40 mm water at the tank base.

Based on the table, a hot zone could be seen to be formed below the fuel surface at about 1650 s after the establishment of a full surface fire. The base of the hot zone with the temperature of 110°C had reached the thermocouple at the depth of 390 mm from the bottom of the tank. The base of the hot zone at 110°C then regressed to the depth of 290 mm at about 2316 s after the establishment of a full surface fire. Subsequently, the base of the hot zone at a similar temperature regressed further to the depth of 150 and 110 mm from the tank base at about 3321 s and 3478 s after the full surface ignition, respectively.

Figure 3-20 shows the time at which the base of the hot zone reached a specific depth throughout the burning period. The average speed of the base of the hot zone was obtained from the slope of the trend line.

Time (s)	Depth of the fuel from the Tank Base (mm)					
	0	20	110	150	290	390
	Temperature (°C)					
0	10.47	9.22	10.69	11.39	9.26	10.45
500	10.10	9.83	11.28	11.59	10.24	10.61
1000	9.56	10.71	11.55	11.20	11.37	13.05
1500	8.80	10.89	12.07	11.76	11.83	66.55
1653	8.96	10.83	11.04	11.37	12.18	110.07
2000	8.77	11.05	11.40	10.49	12.09	203.22
2316	8.73	11.67	10.22	11.38	110.77	300.27
2500	8.36	11.40	10.50	10.28	189.52	113.52
3000	8.50	11.55	9.51	9.95	199.15	397.18
3321	8.12	12.47	11.16	110.30	196.25	198.51
3478	7.99	12.42	110.50	181.14	195.16	309.34
3500	7.95	12.51	127.32	187.62	196.21	93.48
4000	7.88	12.81	204.38	219.85	228.49	512.86
4494	44.63	120.33	163.44	166.30	181.33	172.55
4500	46.06	120.96	163.50	165.54	223.38	179.93
5000	84.65	140.92	426.36	596.63	822.22	928.01

Table 3-15: Temperature of crude oil at specific depth from the tank base at specific time for FS Test 23.

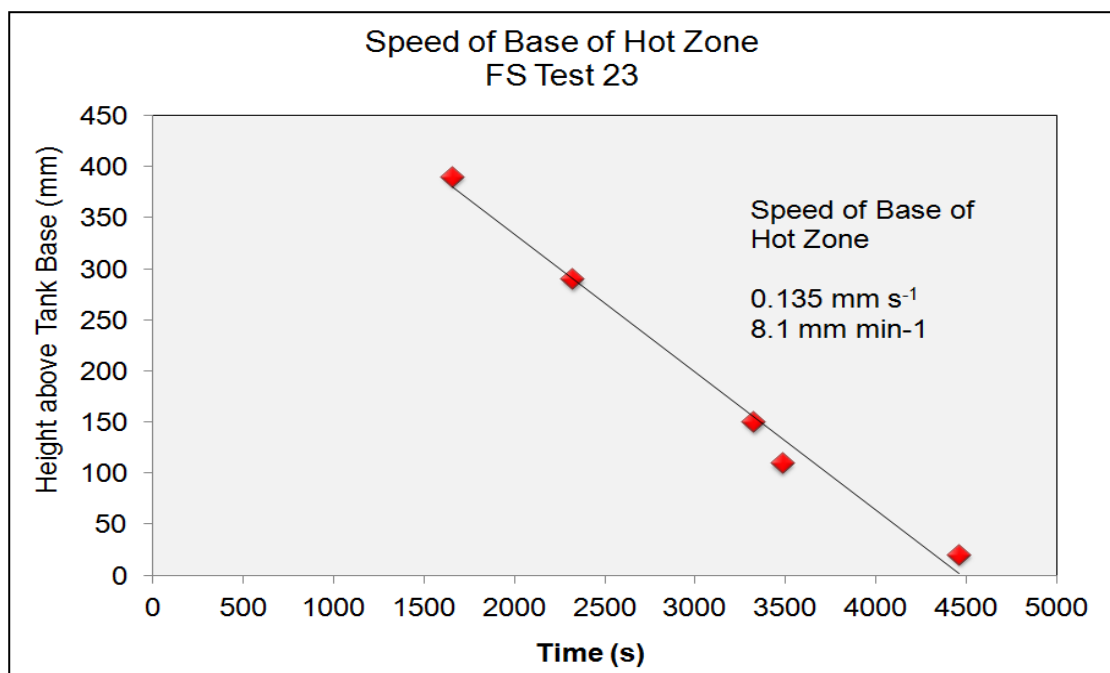


Figure 3-20: Time at which the base of hot zone with temperature of 110°C for FS Test 23 involving 500 mm crude oil

Similar methods were used to estimate the speed of the base of the hot zone for all the field scale tests. The average and maximum speed of the base of the hot zone for the field scale tests are shown in Table 3-16.

Test No.	Fuel Type	Tank Diameter (m)	Average Speed of Base of Hot Zone		Maximum Speed of Base of Hot Zone	
			(mm s <sup>-1</sup> )	(mm min <sup>-1</sup> )	(mm s <sup>-1</sup> )	(mm min <sup>-1</sup> )
FS Test 1	AVTUR	1.2	0.218	13.07	0.458	27.48
FS Test 2	Light Crude	1.2	0.120	7.23	0.241	14.46
FS Test 3	Light Crude	1.2	0.229	13.72	0.628	37.70
FS Test 4	Light Crude	1.2	0.310	18.60	0.870	52.17
FS Test 5	Light Crude	1.2	0.154	9.24	0.339	20.34
FS Test 6	Light Crude	1.2	0.158	9.47	0.313	18.75
FS Test 9	Light Crude	1.2	0.240	14.43	0.600	36.00
FS Test 10	Light Crude	1.2	0.139	8.36	0.458	27.48
FS Test 11	Light Crude	1.2	0.218	13.07	0.458	27.48
FS Test 14	Light Crude	1.2	0.134	8.03	0.293	17.56
FS Test 17	Light Crude	2.44	0.184	11.04	0.588	35.29
FS Test 19	Light Crude	2.44	0.312	18.70	0.654	39.22
FS Test 20	Light Crude	2.44	0.242	14.51	0.556	33.33
FS Test 21	Light Crude	2.44	0.208	12.46	0.610	36.59
FS Test 22	Crude	2.44	0.260	15.58	0.656	39.34
FS Test 23	Crude	2.44	0.135	8.10	0.235	21.24
FS Test 24	Diesel	2.44	0.048	2.85	0.078	4.68
FS Test 27	Diesel	2.44	0.051	3.08	0.090	5.39
FS Test 28	Diesel	2.44	0.052	3.11	0.099	5.93
FS Test 31	Gasoline	2.44	0.073	4.40	0.153	9.16
FS Test 34	Jet A1	2.44	0.060	2.16	0.067	4.03
FS Test 37	Light LFO	2.44	0.042	2.55	0.077	4.62
FS Test 38	LFO	2.44	0.039	2.35	0.074	4.45
FS Test 39	75% Diesel + 25% Gasoline	1.2	0.230	6.90	0.379	22.71
FS Test 40	Crude	2.44	0.201	12.03	0.544	32.61
FS Test 41	Crude	4.5	0.317	19.04	0.820	49.20
FS Test 42	75% Diesel + 25% Gasoline	2.44	0.320	19.17	0.833	50.00
FS Test 46	75% Diesel + 25% Gasoline	1.2	0.195	11.70	0.461	27.66
FS Test 47	75% Diesel + 25% Gasoline	1.2	0.183	10.98	0.632	37.92

**Table 3-16: Speed of the base of the hot zone of the field scale tests**

Table 3-16 shows that the average speed of the base of the hot zone for the crude oils that were used in the field scale tests were within the range of 0.12 to 0.317 mm s<sup>-1</sup>. Taking an average value of this range will give a speed of the base of the hot zone for the crude oils as 0.203 mm s<sup>-1</sup>. The average speed of the base of the hot zone for the tests involving the mixture of diesel and gasoline were within the range of 0.183 to 0.320 mm s<sup>-1</sup> (giving an average of the range as 0.232 mm s<sup>-1</sup>). The average speed of the base of the hot zone for diesel was within the range of 0.048 to 0.052 mm s<sup>-1</sup> (giving an average of the range as 0.050 mm s<sup>-1</sup>). The average speed of the base of the hot zone for gasoline fire test was about 0.073 mm s<sup>-1</sup>.

Knowing the speed of the base of the hot zone, the time to boilover for a particular fuel could be estimated if the initial depth of the fuel in the storage tank is known.

The time to boilover,  $t_{bo}$  for each crude oil in the field scale tests was predicted by dividing the original depth of the crude oil by the speed of the base of the hot zone determined (0.203 mm s<sup>-1</sup>):

$$t_{bo} = \frac{z_f}{v_{hz}} \qquad \text{Equation 3-2}$$

where  $z_f$  is the initial depth of fuel (m) and  $v_{hz}$  is the speed of the base of the hot zone (m s<sup>-1</sup>).

The values of observed against predicted times to boilover are plotted in Figure 3-21.

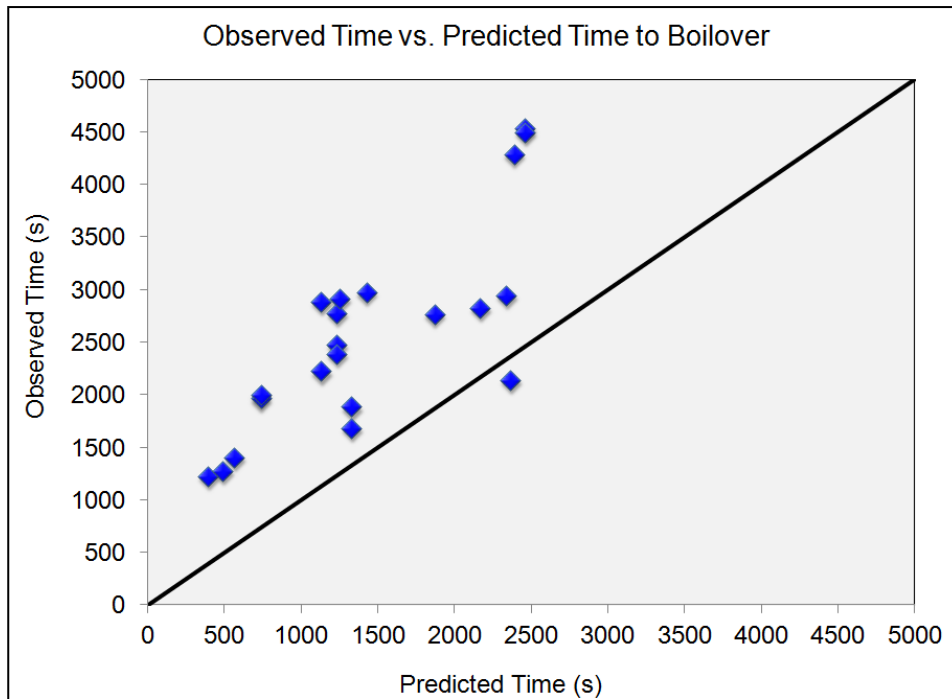


**Figure 3-21: Observed against predicted time to boilover for crude oil**

Figure 3-21 shows that the predictive model (Empirical Model 2) estimates faster time to boilover compared to the experimental results. The figure shows that the construction of such a model applicable to fires in full scale storage tanks is possible if the speed of the base of the hot zone could be determined as accurate as possible and if it can be shown that the assumptions adopted in the above model, such as a constant rate of penetration of the hot layer into the pool and discrete uniform layers of crude oil and water, *etc.* continue to be relevant.

In other words, an improved physically based model or empirical model can be developed, by having further understanding on the boilover process such as the mechanisms involved in:

- i. The transfer of heat from the fire to the pool
- ii. The transfer of heat down through the pool
- iii. The evolution of vapour consisting of the formation and movements of bubbles in the liquid
- iv. The formation of the hot layer



### 3.3.2.4 Average Surface Regression Rate vs. Speed of Base of Hot Zone

Comparing the average surface regression rate from Table 3-17 and average speed of the base of the hot zone in Table 3-16, it is observed that the latter provides higher values for those tests in which boilover was observed. This observation indicates that the thermal front moved faster than the regress of the fuel surface and hence a hot zone layer was formed.

The observation described above is true except for the FS Test 27, 28, 31, 34, 37 and 38. The average surface regression rate for all these tests was either similar to or higher than the heat front's average penetration velocity. This indicates that a hot zone was not generated. In the case where a hot zone was not generated, the plot of temperature distribution versus height from the tank base does not show any indication of the existence of a hot zone. There is no noticeable vertical section observed on the graphs showing the temperature profiles with the fuel layer. Figure 3-22 shows the time histories of the temperature at various points inside the fuel for FS Test 27 (diesel), 31 (gasoline) and 37 (light fuel oil).

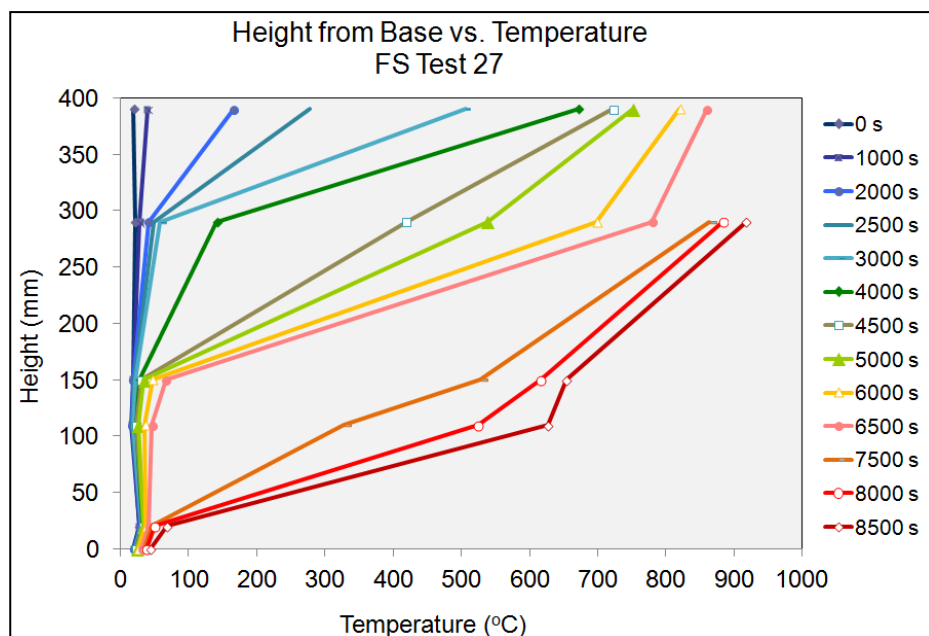


Figure 3-22: (a) Temperature profiles of fuel in field scale tests in which hot zone was not formed - FS Test 27 (diesel)

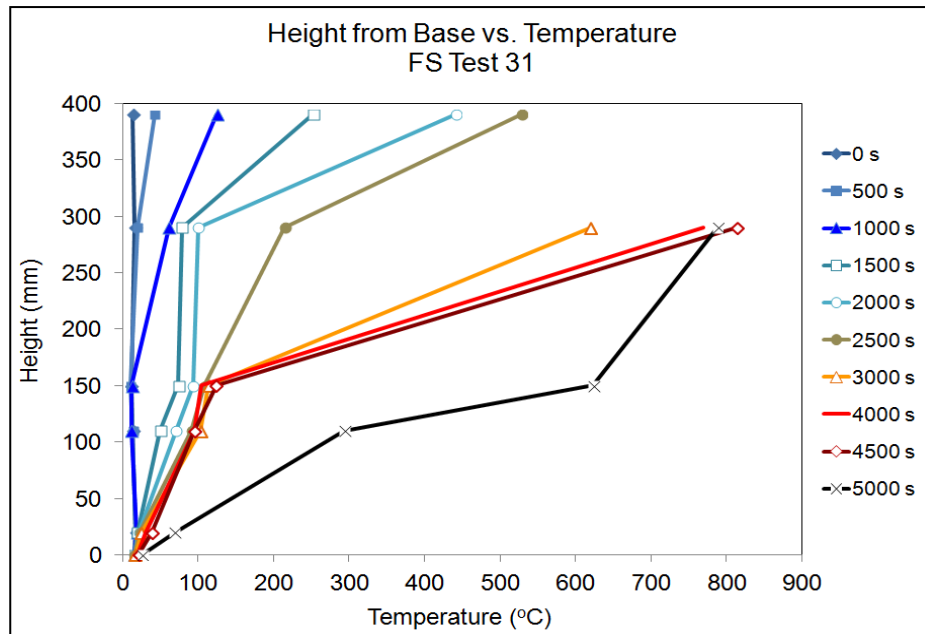


Figure 3-22: (b) Temperature profiles of fuel in field scale tests in which hot zone was not formed - FS Test 31 (gasoline)

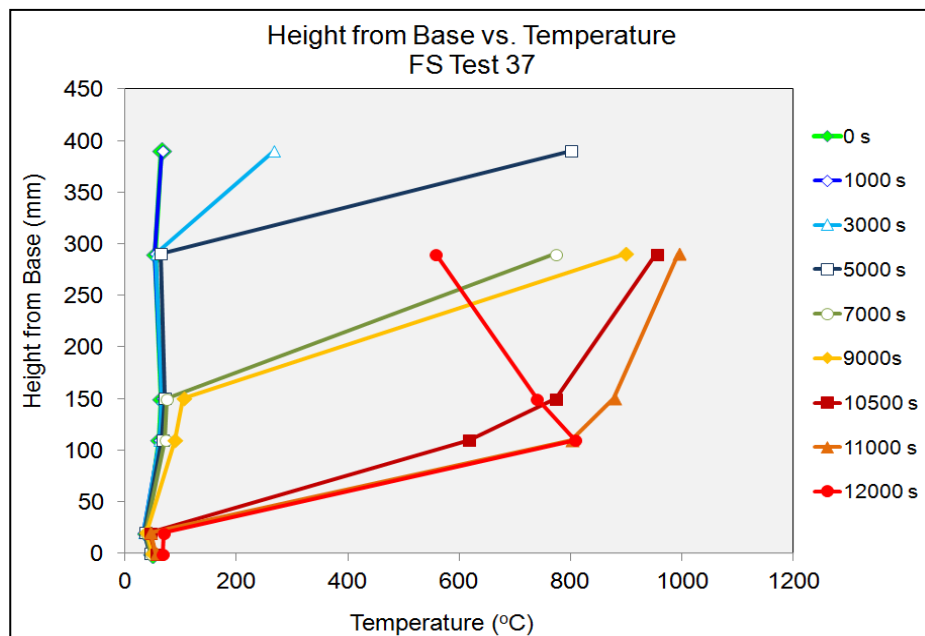


Figure 3-22: (c) Temperature profiles of fuel in field scale tests in which hot zone was not formed - FS Test 37 (light fuel oil)

### 3.3.3 When a Boilover Occurs, What Will Be the Consequences? (Consequences of Boilover)

The severity of the consequences will depend on the amount of burning fuel ejected from the tank when boilover occurs. The maximum amount of fuel that could be ejected is the amount of fuel remaining in the tank when boilover

occurs. If it is assumed that the fuel surface regression rate is constant, then the depth of fuel remaining in the tank when boilover occurs,  $z_{bo}$ , can be determined as follows:

$$z_{bo} = z_f - t_{bo} v_a \quad \text{Equation 3-3}$$

where

$z_f$  is the initial depth of fuel (m)

$t_{bo}$  is the time to boilover (s)

$v_a$  is the fuel surface regression rate ( $\text{m s}^{-1}$ )

If the depth of fuel remaining in the tank when boilover occurs is obtained, the maximum volume of fuel that could be ejected from the tank,  $V_E$ , as follows:

$$V_E = \frac{\pi D^2}{4} z_{bo} \quad \text{Equation 3-4}$$

where  $D$  is the tank diameter (m).

### 3.3.3.1 Fuel Surface Regression Rate

The fuel surface regression rate is essential to determine how much fuel left in tank when boilover occurs. The fuel surface regression rate for the experiments were obtained via an analysis of the thermocouple measurements since the experimental set up for the field scale tests was not equipped with the mechanism to measure the rate of mass loss from the tank. The fuel surface was taken to have regressed to a lower level when the temperature recorded by a particular thermocouple showed a sharp increase and registered unstable fluctuating readings i.e. the thermocouple had emerged from the fuel. Two examples showing the temperature development with respect to time recorded by different thermocouples at different heights within the tank are shown Figure 3-23 (a) and (b) which were taken from FS Test 22 and 23.

In FS Test 22, the fuel involved was 485 mm depth of crude oil with an initial fuel temperature of 25°C. After 900 s of ignition, the temperature near the fuel surface (level 390 mm from the tank base) first increased to 100°C and then increased further to about 200°C by 3200 s after ignition. A similar trend was recorded by the thermocouples in the fuel layer (at 290, 150 and 110 mm above the base of the tank, respectively). The temperature of 200°C was recorded by the three thermocouples after about 3200 s of burning. Then, the temperature at the highest thermocouple (at 390 mm) rose to about 300°C before increasing to 500°C whilst the lower thermocouples showed only a gradual increase in temperature to a value of 260°C. The boilover occurred after about 4282 s of burning. The sharp increase of temperature at 390 mm after about 3200 s of burning indicated that the thermocouple had appeared above the surface of the liquid fuel. The surface regression rate is then calculated through the division of the fuel initial depth and the observed time at which the highest thermocouple appeared above the liquid. In this specific example, the average fuel surface regression rate was determined to be 0.038 mm s<sup>-1</sup>.

Figure 3-23(b) shows the temperature development with respect to time for different thermocouple measurements for FS Test 23. The fuel involved was a 500 mm depth of crude oil with a 40 mm water layer at the tank base. After about 1600 s following the establishment of a full surface fire, the temperature measured by the upper most thermocouple TC4 (at a level of 390 mm from the base) first increased to 100°C and then increased further to about 200°C. The temperature then remained steady at approximately 200°C. After about 4100 s of burning, the temperature at the thermocouple TC4 increased to 300°C and then rapidly increased up to 800°C. Boilover then occurred after about 4494 s following the establishment of a full surface fire. The sharp increase of temperature to 300°C at TC4 after about 4100 s of burning indicated that the thermocouple had appeared above the surface of the fuel. For FS Test 23, the average fuel surface regression rate was determined to be 0.036 mm s<sup>-1</sup>. Similar calculations were repeated for the thermocouples which appeared subsequently above the fuel surface and an average of the rate was determined.

A similar method was used to determine fuel surface regression rate for all the field scale tests.

Figure 3-23(a), (b), (c) and (d) show the temperature development with respect to time for different thermocouple measurements in a large tank that involved the occurrence of a boilover. The field scale tests involved the burning of crude oil (FS Test 22 and 23) and diesel-gasoline mixture (FS Test 47). Figure 3-23(c) shows the temperature profile within the fuel for the test which did not produce any boilover. The fuel used in the burning test was diesel. In all cases, the thermocouple was considered to be out of the fuel when the temperature readings showed a sharp and rapid increase and registered very unstable fluctuated readings.

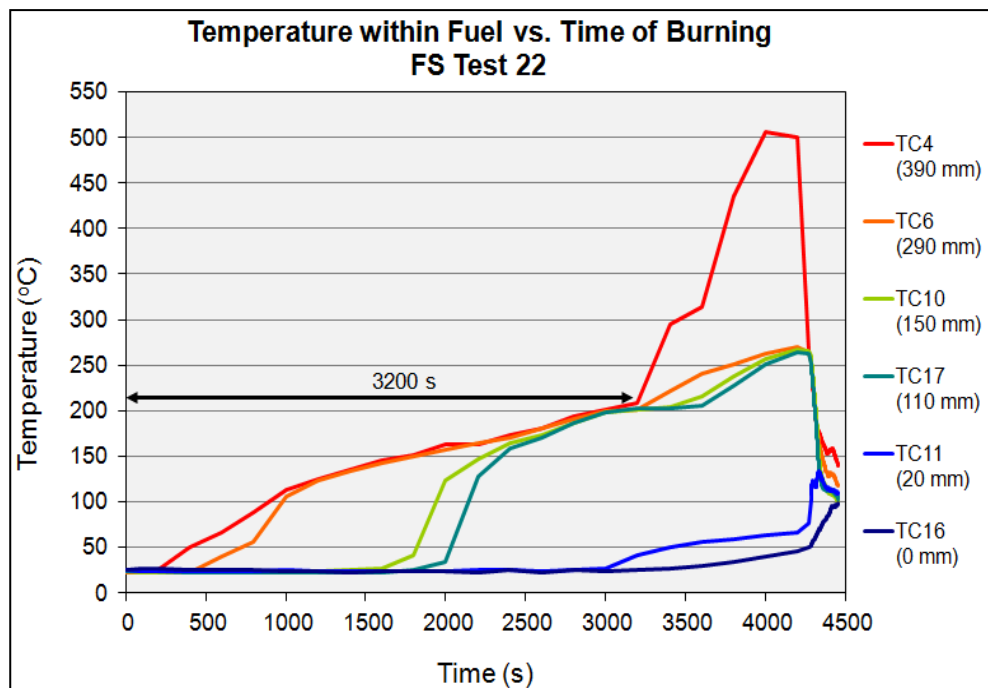


Figure 3-23: (a) Time histories of temperatures from crude oil test for FS Test 22

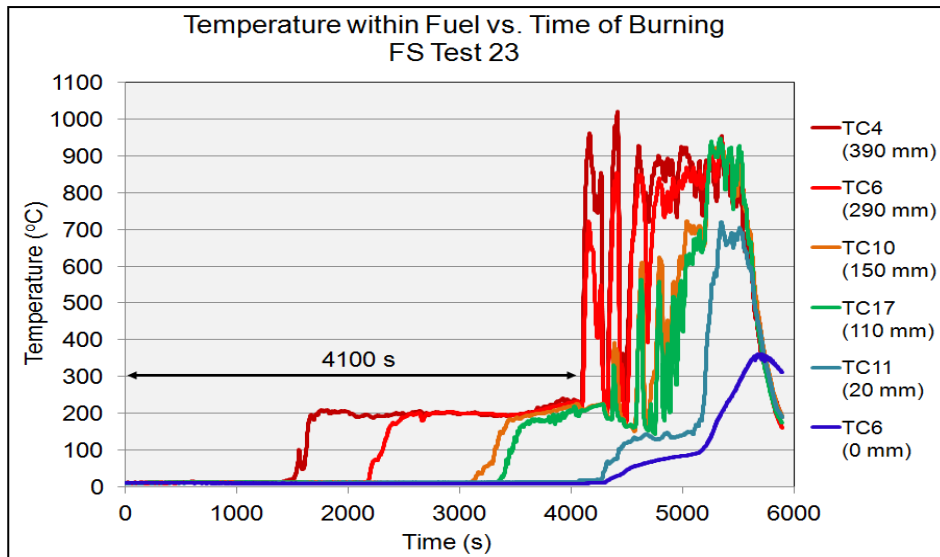


Figure 3-23: (b) Time histories of temperatures from tests involving crude oil FS Test 23

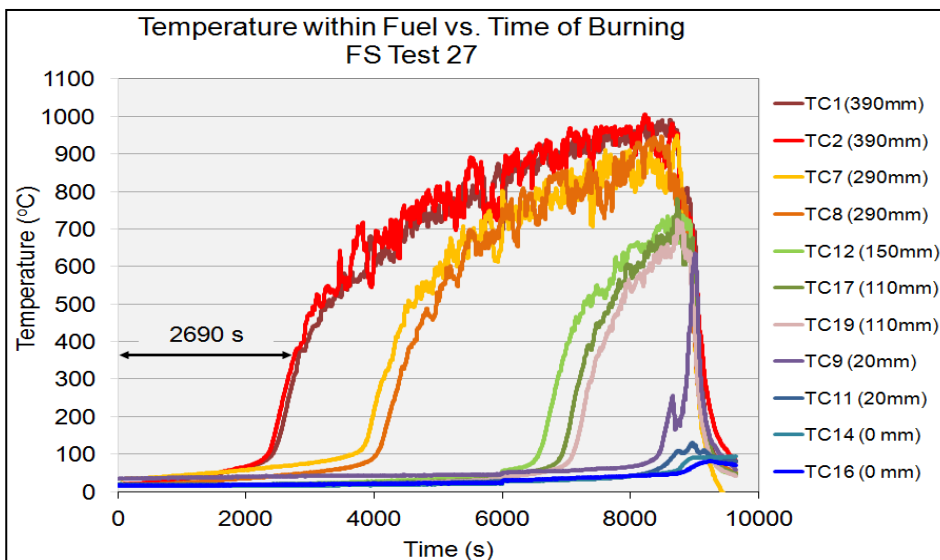


Figure 3-23: (c) Time histories of temperatures for diesel test FS Test 27

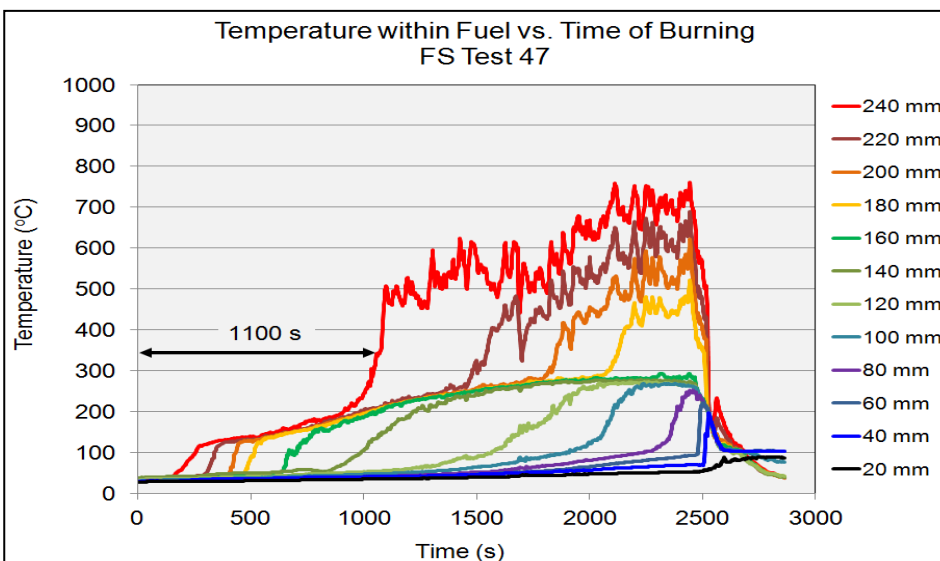


Figure 3-23: (d) Time histories of temperatures for diesel-gasoline mixture test FS Test 47

The average fuel surface regression rates for the field scale tests are shown in Table 3-17. As mentioned, the rates are determined through the analysis of the temperature versus time plots. For some of the experiments, the rate was not determined (or could not be deduced) due to some technical reasons, which include:

- i. Lacking of instrumentation for detailed measurement
- ii. Failure of thermocouples during the experiments which register negative temperature readings
- iii. Insufficient or incomplete recordings of data provided from the field test or test site

Test No.	Fuel Type	Average Surface Regression Rate, $v_a$ (mm s <sup>-1</sup> )
FS Test 2	Light Crude Oil	0.040
FS Test 5	Light Crude Oil	0.050
FS Test 6	Light Crude Oil	0.033
FS Test 9	Light Crude Oil	0.070
FS Test 10	Light Crude Oil	0.063
FS Test 11	Light Crude Oil	0.057
FS Test 14	Light Crude Oil	0.059
FS Test 17	Light Crude Oil	0.025
FS Test 19	Light Crude Oil	0.033
FS Test 21	Light Crude Oil	0.032
FS Test 22	Crude Oil	0.038
FS Test 23	Crude Oil	0.036
FS Test 27	Diesel	0.050
FS Test 28	Diesel	0.052
FS Test 29	Diesel	0.054
FS Test 31	Gasoline	0.084
FS Test 34	Jet A1	0.064
FS Test 37	Light Fuel Oil (lighter)	0.047
FS Test 38	Light Fuel Oil	0.040
FS Test 39	75% Diesel + 25% Gasoline	0.135
FS Test 40	Crude Oil	0.046
FS Test 41	Crude Oil	0.054
FS Test 42	75% Diesel + 25% Gasoline	0.077
FS Test 46	75% Diesel + 25% Gasoline	0.062
FS Test 47	75% Diesel + 25% Gasoline	0.057
FS Test 49	Diesel	0.046

**Table 3-17: Average surface regression rate for the field scale tests**

Table 3-17 shows that the average surface regression rates for the crude oils that were used in the field scale tests were determined to be within the range of 0.025 - 0.070 mm s<sup>-1</sup>. The average surface regression rates for the tests involving the mixture of diesel and gasoline were within the range of 0.057 to 0.135 mm s<sup>-1</sup>. The average surface regression rate for diesel was within the range of 0.050 to 0.054 mm s<sup>-1</sup>. Gasoline, being more volatile than diesel, had a higher surface regression rate. The surface regression rate for gasoline fire test was 0.084 mm s<sup>-1</sup>, as shown in Table 3-17.

The characteristic magnitude of the average fuel surface regression rates determined during the pre-boilover period for the experiments is in agreement with the results of the literature for similar fuels (as shown in Section 2.2.3 of Chapter 2). The average fuel surface regression rates are taken to be independent of the diameter of the pool, consistent with the experimental data for liquid hydrocarbon pool fires with diameters in excess of 1 meter. As shown in Table 2-3 of Section 2.2.3, the average fuel surface regression rates for similar kinds of fuel (i.e. crude oil) was within the range of 0.018 - 0.063 mm s<sup>-1</sup>. And the average surface regression rates for diesel, gasoline and a 75:25 v/v mixture of diesel and gasoline were in the range of 0.042 - 0.068 mm s<sup>-1</sup>, 0.077 - 0.117 mm s<sup>-1</sup> and 0.042 - 0.053 mm s<sup>-1</sup> respectively.

The results of fuel surface regression rates from the field scale tests show good agreement with the results presented in the literature. Hence using the thermocouple measurements to gauge the fuel surface regression is acceptable.

### **3.4 EFFECT OF REDUCING THE HEAT FLUX FROM THE FLAME TO THE FUEL SURFACE**

One of the main highlights of the literature review on boilover was that the energy for hot zone comes from the burning flame directly. About five per cent of the total heat energy release by combustion was transferred to the fuel from



the flame by radiation, and small amount of this energy was used for hot zone formation (Koseki, 1994 and 1999).

In work undertaken to develop a heat transfer model of a burning fuel floating on water so that temperature histories in the liquid and the time to boilover could be predicted, Garo, Gillard, Vantelon and Fernandez-Pello (1999a) established the dependence of the boilover onset time on the fuel's rate of burning, and thus the surface heat flux. As the surface heat flux increases (as the pool diameter increases), the fuel is heated faster and the boilover condition is reached sooner. These works, among others, have shown the importance of the surface heat flux and hence the radiative feedback from the flame to the fuel on the time to boilover. As described in Section 3.1.4 and Table 3-5, three tests were carried out in Asturias, Spain to study the effect of reducing the radiative feedback from the flame to the fuel by floating layers of small insulating spheres on the surface of the fuel. The aim of the Asturias FS tests was to study the significance of limiting the heat absorbed by the fuel from the fire and thus extending the time to boilover.

The fuel components with low boiling points are first vaporized and burned at the surface by the surface heat flux from the flame. This would result in the increase of the surface temperature. This is because the boiling temperature of the fuel at the surface depends on its composition. Consequently, this increase in surface temperature causes a temperature increase in deeper layers of the fuel. In these deeper layers, the fuel still has its original composition and thus its original boiling temperature. A boiling process might start within the bulk of the liquid when this original boiling temperature is exceeded. The process of vapour bubble formation connected with the homogenization of the fuel starts and a hot zone with uniform temperature is established. The hot zone formation and its regression would depend on the heat transferred from the flame and through the surface.

The effect of the surface heat flux on the time to boilover was examined by studying the effect of applying layers of non conducting material on the surface

of the burning fuel. It is assumed that by applying layers of non conducting materials on the surface, the heat transferred from the flame to the fuel would be reduced. Table 3-18 and Figure 3-24 show the effect of varying the depth of the non conducting media towards the penetration of heat within the fuel and hence the time to boilover.

Test No.	Fuel Type	Depth of Non Conducting Media (mm)	Fuel Depth (mm)	Time to boilover (s)	Fuel Depth/Time to Boilover ( $\text{mm s}^{-1}$ )
FS Test 45	Crude oil	0	210	1500	0.140
FS Test 43		25	150	1980	0.076
FS Test 44		50	175	5580	0.031
FS Test 46	75 % Diesel + 25 % Gasoline	0	200	1200	0.167
FS Test 48		75	180	No boilover	0

**Table 3-18: Effects of depth of the non conducting material towards time to boilover**

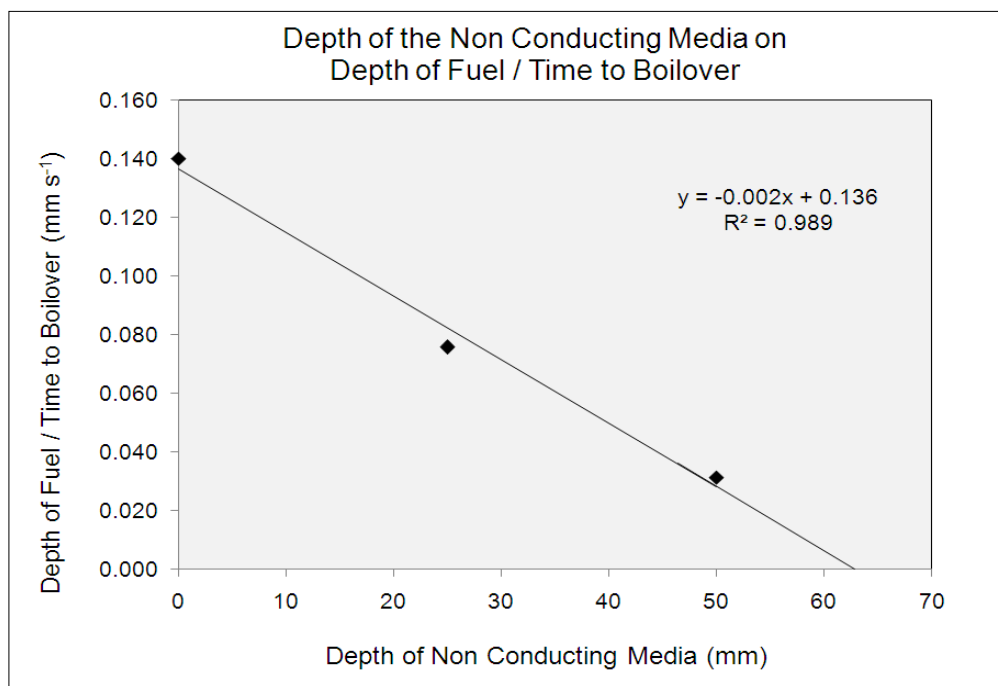


**Figure 3-24: Relations of the depth of the non conducting material with the ratio of depth of fuel-time to boilover for FS Test 43, 44 and 45**

In all the tests, generally, following the establishment of a full surface fire, the fire was observed to burn steadily for a few minutes. In some of the tests, as the non conducting medium was spread over the pool surface, the fire immediately subsided. The fire then recovered until it had reached a steady

burning condition at a size much smaller than during the initial steady burning period. The effect of the non conducting medium had been to reduce the surface heat flux transferred to the fuel which substantially reduced the fuel regression rate. Consequently the formation and regression of the hot zone would be slower due to the limited heat and hence longer time to boilover. Even in one of the test i.e. FS Test 48, it was assumed that the fire was controlled to an extent that prevented the formation of a hot zone and a boilover did not occur.

Figure 3-25(a) and (b) show the temperature histories for field scale tests involving crude oil. Both figures substantiate the formation of the hot zone in the FS Test 6 and 44; though in FS Test 44 the fuel surface was covered by the non conducting material.

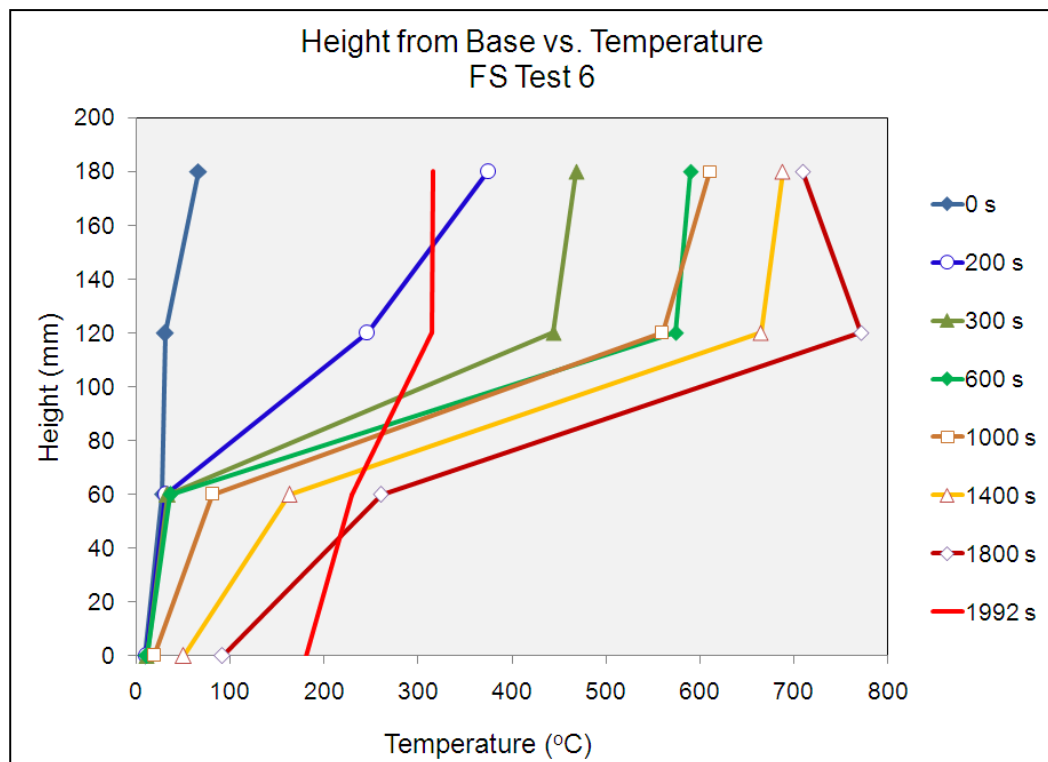


Figure 3-25: (a) Vertical temperature profile for FS Test 6 (crude oil only)

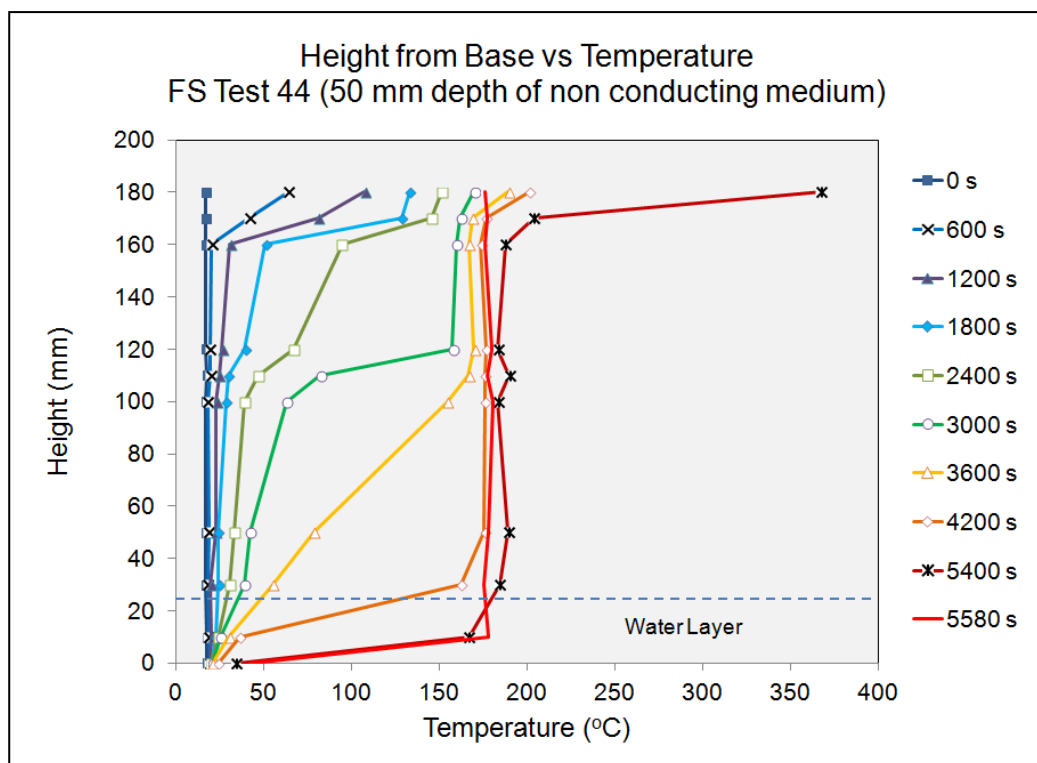


Figure 3-25: (b) Vertical temperature profile FS Test 44 (crude oil with 50 mm depth of non conducting material)

Based on Figure 3-25(a) and (b), a hot zone could be seen to be formed below the fuel surface between the period of 1800 to 2400 s after the establishment of a full surface fire in FS Test 44. The hot zone, on the other hand, was observed to be formed earlier in FS Test 6 i.e. within the period of 300 – 600 s after the full surface ignition. In addition, the temperature measured by the uppermost thermocouples in FS Test 6 showed higher values compared to FS Test 44. Through physical observation, the application of the non conductor media on the fuel surface had reduced the size of the flame and hence the intensity of the fire. Thus, the lower temperature measured by the thermocouples beneath the fuel surface. The effect of the non conductor media had been to reduce the feedback of heat from the fire to the surface.

Applying the same method as in Section 3.3.2.4 and 3.3.2.3, the average fuel surface regression rate and the average speed of the base of the hot zone for FS Test 44 on crude oil are estimated to be about  $0.034 \text{ mm s}^{-1}$  and  $0.063 \text{ mm s}^{-1}$  respectively. Comparatively, for similar type of fuel, the regression rate and the speed are lower with those observed in Section 3.3.2.4 and

Section 3.3.2.3. The significance of the results is that by limiting the heat absorbed by the fuel from the fire, the time to boilover could be prolonged and even to the extent of eliminating the phenomenon.

## 4 LABORATORY SCALE BOILOVER EXPERIMENT

Many recent studies on the conditions under which boilover occurs have been carried out using larger-scale pans of 5 to 20 m diameter by Koseki *et al.* (1992-94, 2003 and 2006) and Shaluf & Abdullah (2011). Various types of crude oils such as Murban and Arabian-light were used in these studies. Analysis on the temperature profiles inside the burning crude oil, measured by thermocouple trees embedded along a central pole and at the pan wall, showed the formation of hot zone in the oil. After ignition, the thickness of the hot zone increased with time, and developed to several meters deep before boilover.

The large-scale tests conducted have elucidated further the processes of the hot zone formation and its growth, and hence the occurrence of the boilover. However, it is difficult to carry out large-scale tests so often due to high costs and high safety concerns.

Undertaking field scale experiments, however, is very expensive, gathering details data is difficult and the experiments are subject to the vagaries of weather. In order to allow well defined and repeatable experiments to be performed and to obtain more detailed measurements and visual records of the behaviour of the liquids in the pool, a novel laboratory scale rig has been designed, built and commissioned. The viability of conducting a boilover test in a small-laboratory scale which would behave substantially the same way as in the larger size is one of the subjects of this research work.

In this section, the description of the experimental set-up in which the boilover tests were carried out, is discussed with a greater focus on the rig designs. Also, details of the temperature measurement tools, the data acquisition system and the heating mechanism used will be described. Finally, the chapter will also provide the characteristics of the fuels used and describes the way in which the experiments have been designed and carried out.

## 4.1 CONSIDERATION FOR DEVELOPMENT OF LABORATORY RIG

The development and the design of a laboratory scale rig for the boilover study are mainly to:

- i. Study the temperature distribution within fuel
- ii. Measure the time for heat to reach fuel-water interface and hence boilover
- iii. Observe and record physical changes within fuel and at the fuel-water interface when heat reached the interface

One of the main highlights of the literature analysis on boilover phenomenon is that the energy for hot zone formation within the bulk fuel came from the burning flame directly. In general, the thermal energy or heat flux from the flame to the fuel surface is absorbed at the surface and is transferred into the bulk of the fuel. The main criteria to be considered in conducting a boilover study is the source of the thermal energy or heat to be transferred into the fuel as to enable the formation of hot zone and hence a boilover occurrence.

Due to the high risk nature of the boilover phenomenon in the experimental works being proposed for the boilover study, many considerations have been measured in order to comply with the Loughborough University laboratory safety policy and to ensure the safe conduct of the works. The main considerations in the development and design of a rig for the laboratory scale boilover study are:

- i. No allowance to undertake a long duration pool fire with open flame in a laboratory
- ii. No allowance for vaporized fuels due to heating or burning to escape into the laboratory throughout the experimental works

Comprehensive risk assessments (RA) on the rig design, electrical works and chemical/fuels used were carried out by analyzing any risks related to the experimental requirements and thus proposing practicable actions to minimize

the impacts. As a result of the RA, various safety systems were included during the design of the rig. These systems were further discussed in the subsequent sections. A written detailed operation and shutdown procedure was also approved and strictly followed during execution of the experiments.

#### 4.1.1 Design of Heating Mechanism

The fact that it is prohibited to conduct the experimental works with open flame, a heating mechanism to vaporise the fuel is needed rather than burning the fuel. The provision of the heating mechanism in the laboratory scale boilover rig is to heat up and vaporize fuel used in the experimental works i.e. simulate the open top tank fire. The main characteristic of the heating source is that it should be able to provide sufficient thermal energy not only to raise the temperature at the fuel surface but also to vaporize the more volatile components of the fuel and hence to allow transfer of the heat within the bulk of the fuel. And as to simulate an open top tank fire, the source shall be located at the top of the pan or tank that contained the fuel.

Figure 4-1 shows the schematic of the proposed laboratory scale boilover tank which includes the heating source.

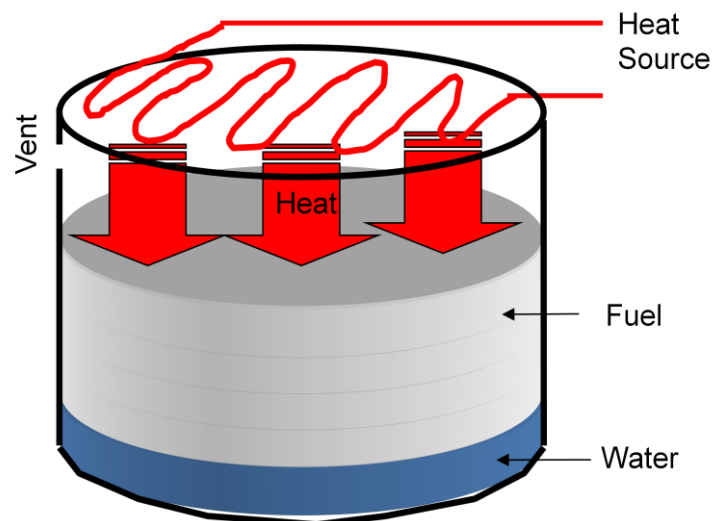


**Figure 4-1: Schematic of the proposed laboratory scale boilover tank with the heating source.**



Possible sources for the heating of the fuel that were considered include ceramic radiant heater, infrared heating element, hot plate or micro-heater / portable heating coil (similar to the under floor heating coil). Figure 4-2 shows one of the possible heating sources for the laboratory scale boilover study i.e. ceramic radiant heater.

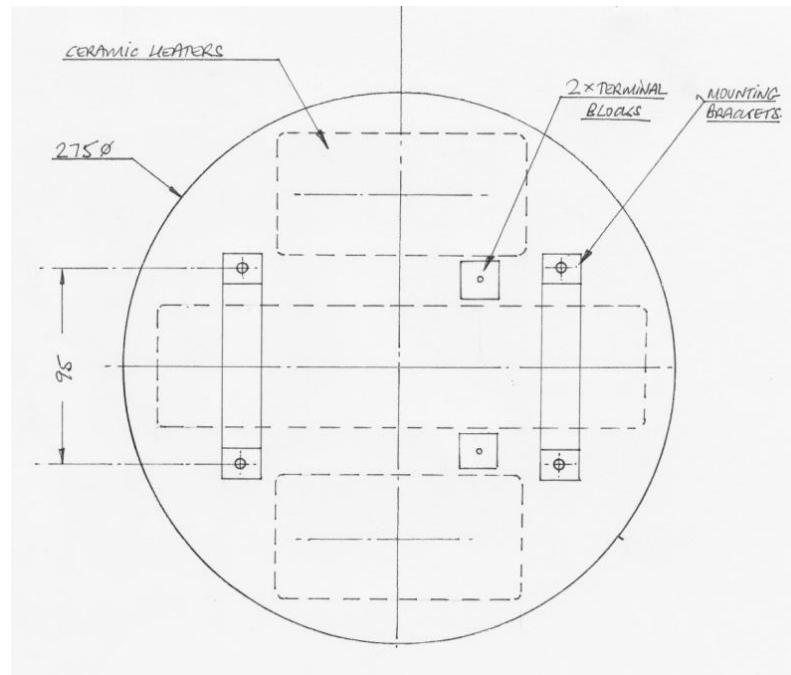


**Figure 4-2: Plan view of ceramic radiant heaters (Godfrey C., CMG Thermal, personal communication, Dec. 1, 2008)**

The ceramic radiant heater will be placed just above the fuel in the tank and would radiate thermal energy onto the surface. The large central and small side ceramic heaters were rated at 230V/1000 W and 230V/500W respectively (Godfrey C., CMG Thermal, personal communication, Dec. 1, 2008). The energy shall be able to heat up and vaporize the fuel which would result in the regression of the surface. The radiant heater will then be moved downwards to ensure that it is near to the fuel surface throughout the experiment.

Similar considerations were made for another potential source of heating i.e. the infrared heating element. Based on some technical discussion however, it was concluded that to obtain the required temperature as to vaporise the type of fuel

that would boilover, the time required would be long and the tank would need to be well insulated (Lewin, I., personal communication, Nov. 2008).

Based on further deliberation, it was decided to locate the heating source in a direct contact with the fuel to enable the heating and boiling of the fuel. The heating concept would imitate the mechanism of a water kettle but with the heating element placed at the top. The heating element will be immersed just beneath the surface of the fuel. The idea of putting the elements just underneath the fuel surface works well with the idea to simulate the absorption of thermal heat by the fuel in an actual open tank fire.

And as to achieve the heating mechanism described above for the laboratory scale boilover study, cartridge heaters are selected. In order to ensure well distributed heat production and transfer, the heater assembly would have a circular shape with ten cartridge heaters attached to the body. Figure 4-3 shows the schematic of the heater assembly.

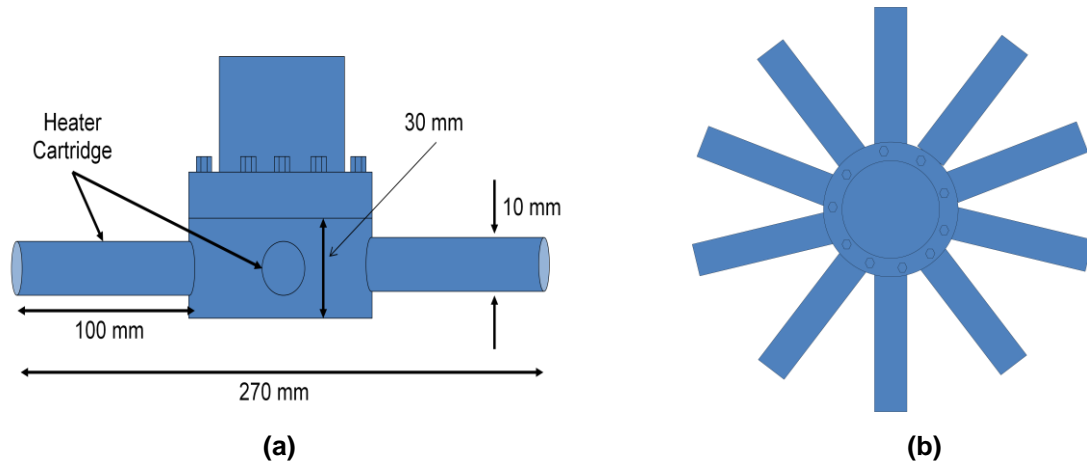


Figure 4-3: Schematic of cartridge heater assembly (a) Side view and (b) Plan view.

#### 4.1.2 Inerting of Boilover Tank

One of the main considerations in carrying out the laboratory scale boilover study is the prohibition for vaporized fuels due to the heating process to escape into the laboratory throughout the experimental works.

The presence of the fuel vapour at specific concentration in air in the laboratory will create an environment which favours ignition. In order to avoid such condition, the laboratory scale boilover tank shall be designed in a way that the vapour produced due to the heating will be discharged to the outside of the laboratory. The tank will be linked to the laboratory exhaust system that would remove the fuel vapour to the atmosphere. Furthermore, the fuel vapour will be condensed first to minimise the amount of vapour that needed to be removed.

In addition, to prevent the formation of flammable environment in the tank, nitrogen gas shall be introduced into the tank as inert in order to limit the presence of oxygen.

### **4.1.3 Observational Window**

One of the objectives of the laboratory scale boilover study is to monitor and record any physical changes within the fuel during the heating process and also to observe and record the occurrence of boilover. The observation is needed to identify whether any penetration of heat occur within the fuel (i.e. the formation of a hot zone) and to examine the behaviour at the fuel-water interface prior to boilover.

Considering that the boilover tests would involve the heating of fuel at high temperature, quartz glass panels were used and installed to the laboratory scale boilover tank. The glass panels are 130 mm (5.12 inch) wide, 440 mm (17.32 inch) high and 9 mm (0.35 inch) thick. Table 4-1 shows the properties of the quartz panel.

The quartz glass panels should be able to withstand the condition during the heating of the fuel and during the occurrence of the boilover. The heating of the fuel in this context of work simulated the process of the combustion of the fuel. Similar to the combustion process, the fuel will vaporize as the heating proceeds. Since the tests will be conducted in an experimental boilover tank, the vaporization of the fuel due to the confined heating will exert some pressure

on the observational window. The maximum pressure due to the confined heating is assumed to be similar to the maximum pressure for confined fuel combustion i.e. pressure due to combustion of stoichiometric mixture of fuel with air at which the adiabatic flame temperature is reached for burning the fuel.

Property	Data
Softening Point	1683 °C
Annealing Point	1215 °C
Strain Point	1120 °C
Poisson's Ratio	0.17
Design Compressive Strength	Greater than $1.1 \times 10^9$ Pa (160,000 psi)
Rigidity Modulus	$3.1 \times 10^{10}$ Pa ( $4.5 \times 10^6$ psi)
Young's Modulus	$7.2 \times 10^{10}$ Pa ( $10.5 \times 10^6$ psi)

**Table 4-1: Properties of Quartz Glass Panel (Gilmore, S., personal communication, June 2009)**

#### 4.1.3.1 Maximum Pressure during Confined Combustion

The maximum pressure generated during the fuel combustion is determined via (Hattwig and Steen, 2004):

$$P_{max} = P_{atm} EF \quad \text{Equation 4-1}$$

where  $P_{max}$  is the maximum pressure produced by the fuel combustion (MPa),  $P_{atm}$  is the atmospheric pressure (0.1 MPa) and  $EF$  is the expansion factor (unitless). The expansion factor due to the fuel combustion is calculated by the following expression:

$$EF = \frac{T_{flame, ad} n_{pdt}}{T_0 n_{rxt}} \quad \text{Equation 4-2}$$

where

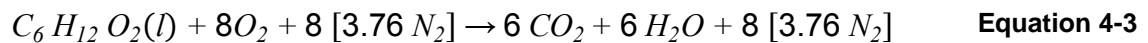
$T_{flame, ad}$  is the adiabatic flame temperature, K

$T_0$  is the initial (ambient) temperature, K

$n_{pdt}$  is the no. of moles of all the combustion products, mol

$n_{rxt}$  is the no. of moles of all the reactants, mol

One of the fuels that will be used in the laboratory scale boilover tests is the mixture of mineral oil and n-butyl acetate. The combustion reaction of n-butyl acetate is considered, as an example, in determining the maximum pressure in the tests. The adiabatic flame temperature of n-butyl acetate fire is 2798 K and the average ambient temperature is taken as 288 K. The reaction equation of n-butyl acetate combustion is:



The expansion factor is:

$$EF = \frac{2798 (6 + 6 + 30.1)}{288 (1 + 8 + 30.1)} = 10.46$$

The maximum pressure due to the combustion of n-butyl acetate is  $P_{max} = (0.1)(10.46) = 1.05$  MPa.

#### 4.1.3.2 Maximum Pressure during Boilover

Similar consideration has to be made during the occurrence of boilover. Boilover occurred due to the vaporisation of water at the fuel-water interface in a fuel storage tank fire. Hence, the maximum pressure produced at the instance of boilover occurrence is due to the expansion of liquid water to steam. Hence the expansion ratio for the boilover occurrence could be determined by the ratio of specific volume of steam to liquid water:

$$EF = \frac{v_g}{v_l} \quad \text{Equation 4-4}$$

where  $v_g$  is the specific volume of steam at 100°C (26.80 ft<sup>3</sup> lb<sub>m</sub><sup>-1</sup>) and  $v_l$  is the specific volume of liquid water at 20°C (0.016035 ft<sup>3</sup> lb<sub>m</sub><sup>-1</sup>). The expansion factor is 1671. Thus, the maximum pressure exerted during the occurrence of boilover is 167.1 MPa.

### 4.1.3.3 Limiting Pressure for Glass Window

The allowable pressure load or the limiting pressure,  $p_{lim}$  for a glass window with a thickness of  $z_{hw}$  (m) is determined via the expression (Brownell and Young, 1977):

$$p_{lim} = \left(\frac{16}{3}\right) \left(\frac{z_{hw}}{D_{wp}}\right)^2 f \quad \text{Equation 4-5}$$

Where

$f$  is the compressible strength of the window panel (MPa)

$D_{wp}$  is the diameter of the panel (m)

Since the window panel used in the laboratory scale boilover tank is rectangular, the equivalent diameter is determined and used in Equation 4-5. The glass window panel is 130 mm x 440 mm. The thickness,  $z_{hw}$  is 9 mm. The area of the glass window panel is 0.057 m<sup>2</sup>. The equivalent diameter is 0.27 m.

Based on Table 4-1, the quartz panel strength is greater than  $1.1 \times 10^9$  Pa. Hence, the limiting pressure for the quartz glass window panel is approximately:

$$p_{lim} = \left(\frac{16}{3}\right) \left(\frac{0.009}{0.27}\right)^2 (1100) = 6.5 \text{ MPa}$$

The limiting pressure of the glass window is greater than the pressure produced during the confined combustion of the fuel i.e. n-butyl acetate. The limiting pressure however is much lower than the pressure exerted during the occurrence of a boilover. In order to overcome the potential risk of the window failure, the boilover tank will be fabricated in such a way that the volume is sufficient to cater for the expansion of the liquid water to steam. In addition, the boilover tank will be connected to a 420 L volume secondary expansion tank.

## 4.2 BOILOVER LABORATORY SCALE RIG

Based on the considerations discussed in Section 4.1, the boilover experimental rig is fabricated that consists of a main boilover tank, an in-line condenser and a secondary container as shown in Figure 4-4. The schematic of the rig is shown in Figure 4-5.



Figure 4-4: Boilover Experimental Rig: (a) Main Tank, (b) Condenser & (c) Secondary Expansion Container

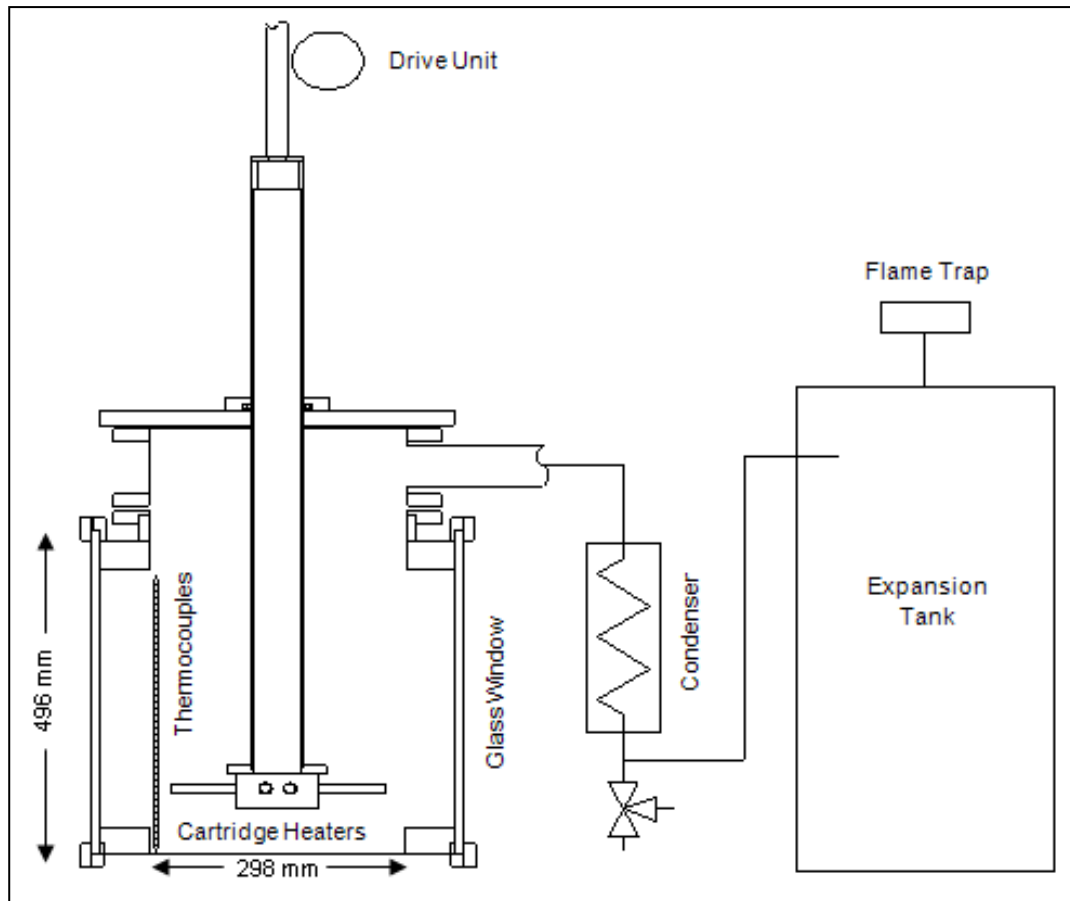


**Figure 4-5: Schematic of Boilover Experimental Rig**

The main tank is a 298 mm diameter and 496 mm high cylindrical tank fitted out with heating and temperature measurement system. The main tank is fully enclosed and connected directly to an in-line condenser and a secondary expansion tank. An assembly of a motor and a shaft, which controls the vertical movement of the heating system, is placed at the top of the tank. The tank is equipped with three glass panel windows which are 130 mm wide and 440 mm high in dimension. The windows are made of quartz glass with straining and softening points of 1120°C and 1683°C respectively.

The in-line condenser is embedded in the rig in order to cool down and condense any hot volatile vapour that would be produced via heating of fuel throughout an experimental work. This is to reduce the quantity of the flammable vapour and hence the risk of ignition; and prevent any fire occurrence. The in-line condenser consists of a 1.5 cm diameter copper tube coils placed inside a 22 cm diameter and 73 cm long cylindrical shell. The hot



vapour will enter through the shell and will be cooled down via contact with the coils, which is filled with flowing cold tap water (approximately at 6°C). The condenser is then connected to a secondary vertical container which is connected to an exhaust system.

The secondary container acts as an expansion tank which holds any vapour coming through the in-line condenser. The tank is approximately 60 cm in diameter and about 153 cm high. It is to also cool down the vapour further before discharging them out through the laboratory exhaust system.

## **4.2.1 Heating System**

### ***4.2.1.1 Cartridge Heater***

The main tank is equipped with a heating system which consists of ten RS 400 Watt cartridge heaters. These heaters, which would be positioned just beneath oil surface, are used to substitute the open flame in a storage tank fire i.e. to simulate an open tank fire due to safety factors. The cartridge heaters are placed with equivalent space in between the ten elements to ensure that a full surface heating is obtained. Each of the heaters is 10 mm in diameter and 100 mm in length. It has a high watt density element with the heating element located close to the sheath, which is swaged to improve heat conduction.

The heaters are moved by a drive unit located at the top of the main tank such that they were positioned at the top of the liquid, and were moved periodically during the experiments as the liquid level lowered. The heaters are able to raise the oil temperature up to about 1000°C.

Figure 4-6 shows the photo of the cartridge heaters.




**Figure 4-6: Cartridge heater assembly with ten cartridge heater elements**

#### ***4.2.1.2 Temperature Controller***

The heating temperature for the cartridge heaters is set manually at the main switchboard control panel. The heating temperature is maintained and controlled via TEMPATRON PID 500 temperature controller. The PID controller (proportional-integral-derivative controller) uses a generic control loop feedback mechanism and is the most commonly used feedback controller. The controller calculates the difference between the measured heating temperature and the set point and notes this difference as an “error”. The controller then attempts to minimize the error by adjusting the process control inputs i.e. manipulating the supply of the electrical current to the cartridges as to increase or stop the heating.

Table 4-2 provides brief characteristics and specifications of the TEMPATRON PID500 Controller.

Figure 4-7 shows the temperature controller system on the control panel.

Characteristics of the temperature controller		Module
<ul style="list-style-type: none"> <li>• Accuracy</li> <li>• Power Supply/Frequency</li> <li>• Control action</li> <li>• Display</li> </ul>	<ul style="list-style-type: none"> <li>• Greater of +/-0.25% FS or +/- 1°C</li> <li>• 85 – 270 VAC/DC (Optional 24 VAC/DC) / 50/60 Hz</li> <li>• PID (auto tune) or ON/OFF</li> <li>• Dual 4 digit LED</li> </ul> <p>Upper display: 10mm high Red (process value)</p> <p>Lower display: 7 mm high Green (selectable)</p>	 <p>PID500</p>

**Table 4-2: Characteristics of the PID500 Temperature Controller**



**Figure 4-7: Temperature Setting on the Heater System Control Panel**

#### 4.2.2 Temperature Measurement

Detailed observation on the temperature changes in the fuel and water in the main tank are carried out using 50 thermocouples of K-type composed of 1.5 mm probe diameter. They are suitable to be used in an oxidizing environment at the maximum operating temperature of up to 1000°C. The small probe diameter will guarantee a very low inertia, which is essential for fast measurements within the liquid. The thermocouples are named with a progressive numbering from TC0 to TC50, starting with the thermocouple placed at the base of the tank. They are placed at 10 mm height intervals from the base, which are linked with a data acquisition system (DAQ). The photo of the thermocouple tree is shown in Figure 4-8. The variation in the oil

temperature is measured every one second by the thermocouples and then stored on a computer through the DAQ. Because there is little difference in measured temperatures at various points in the same depth (Koseki *et al.*, 1992 and 2003), a thermocouple tree was not built for measuring radial temperature profiles.



**Figure 4-8: K-type thermocouples of 1.5 mm probe diameter placed at 10 mm height intervals from the tank base for detailed and fast measurements within the liquid**

### 4.2.3 Data Acquisition System

#### 4.2.3.1 Programming Software

National Instrument (NI) LabVIEW version 8.0 was used as the programming software to develop a data acquisition system for measurement of the temperatures within both fuel and water layers during the experimental works. The software was designed to automate the process of collecting data from all the thermocouples, displaying the results in real time and saving the results acquired during the course of the experiments for subsequent processing.




#### 4.2.3.2 Communication Network/Module

In addition to the software, the DAQ also consisted of:

- i. NI Compact FieldPoint 2120 (cFP-2120); a programmable automation controller hardware which is responsible for reading and converting digital

- data from the thermocouples and communicating them over the Ethernet to a PC that run the LabVIEW software.
- ii. NI Compact FieldPoint Thermocouple Module 120 (cFP-TC-120); a smart input/output (I/O) module that calibrates and scales raw sensor (thermocouple) signals to engineering units which will enable the software to produce linearized and scaled values hence reducing errors while converting binary values to temperature.
  - iii. NI Compact FieldPoint Connector Block 3 (cFP-CB-3); an integrated terminal which connects and wires the thermocouple signals to the input of the cFP-TC-120 Module.

Table 4-3 summarizes the characteristics and specifications of the Compact FieldPoint Modules cFP-2120, cFP-TC-120 and cFP-CB-3.

Characteristics of the Communication Network		Module
<ul style="list-style-type: none"> <li>• Processor</li> <li>• Communication</li> <li>• Serial Ports</li> </ul>	<ul style="list-style-type: none"> <li>• 188 MHz processor</li> <li>• Ethernet communication for distributed real-time systems</li> <li>• Up to 4 serial ports (three RS232 and one RS485) for communication</li> </ul>	 <p>cFP-2120</p>
<ul style="list-style-type: none"> <li>• Operating temperature</li> <li>• Input</li> <li>• Data scaling options</li> </ul>	<ul style="list-style-type: none"> <li>• - 40 to 70 °C</li> <li>• 8 temperature inputs i.e. thermocouple</li> <li>• Temperature (°C, °F, °K)</li> </ul>	 <p>cFP-TC-120</p>
<ul style="list-style-type: none"> <li>• Voltage Limit</li> <li>• Applications</li> </ul>	<ul style="list-style-type: none"> <li>• 250 V</li> <li>• Isothermal for thermocouples</li> </ul>	 <p>cFP-CB-3</p>

**Table 4-3: Characteristics and Specifications of Module cFP-2120, cFP-TC-120 and cFP-CB-3**

## 4.2.4 Safety System

### 4.2.4.1 Inert Gas

A nitrogen gas supply system is installed to the main tank to inject nitrogen gas in order to create an inert environment throughout an experiment as to reduce the chances of a vapour ignition.



Figure 4-9: Nitrogen ( $N_2$ ) Gas System –  $N_2$  cylinder is connected by the green tubing to the main tank

### 4.2.4.2 Gas Detector

An Analytical Technology Inc. Modular Gas Detector A14/A11-19 is fitted to the boiler rig to ensure that the oxygen concentration will always be at the safe minimum level to avoid ignition. A single point detecting mechanism is used for monitoring the oxygen concentration in the main tank and outlet of the secondary container of the boiler rig. The detector system consists of a NEMA 4X control setting-alarm module and remote mounted gas sensor/transmitters.



**Figure 4-10: Gas/Oxygen Detecting System (a) Control Setting + Alarm Module and (b) Sensor/Transmitter Module**

The alarm module contains one modular receiver, one power supply and an audible horn. The receiver modules provide an interface between the detection system and external alarming. The receiver module provides a high intensity digital LED display of gas concentration, plus alarm indicator LED's for "Warning" and "Alarm" set points. Two programmable alarm set points are being set to 2.0% for "Warning" and 1.5% for "Alarm" as to warn of the high levels of oxygen in the rig. These percentage limits are the factory adjusted to standard values, which are the minimum for oxygen as recommended by the manufacturer. Though the minimum oxygen concentration for combustion determined for each of the experiments is/may be higher, it is decided to maintain these values for overprotection. The alarm will be triggered if these set points are exceeded and will acquire a manual activation of emergency shutdown button to cut off the heating power.

The sensor/transmitter, as in Figure 4-10(b) provides the oxygen measurement function for the system. The sensor/transmitter consists of an electrochemical gas sensor that generates a signal linearly relative to the oxygen concentration. The sensors are closely joined to a digital transmitter for noise protection and to enhance the ability to transmit long distances using unshielded cable. The sensors are rated for ambient temperatures from  $-25^{\circ}$  to  $+50^{\circ}\text{C}$ , allowing both indoor and outdoor applications. The transmitter is powered from the receiver

module and uses a unique current pulse position technique to send information to the receiver over a two wire connection.

#### **4.2.4.3 High Temperature Glass Panel**

In order to avoid any accidental loss of containment of flammable oil, quartz glass panels with a straining point of 1120°C and a softening point of 1683°C are installed as the observation windows of the main tank. The description on the specification of the glass panel is provided in Section 4.1.3.

#### **4.2.5 Video Recording**

The physical changes within the oil in the main tank, formation of hot zone, effects of water evaporation and boilover occurrence are recorded by a video camera.

### **4.3 LABORATORY SCALE (LS) EXPERIMENTAL SERIES**

Series of experiments were carried out to establish the effects of several parameters upon the onset of the boilover event. In designing the plan of experiments, the consideration on the number of tests to be carried out depends largely on the parameters that influence the boilover onset e.g. fuel type, thickness, heating temperature and initial storage temperature. However, the numbers of tests to be performed are minimized, due to:

- i. Safety factors: a higher number of tests and the progress of the experimental campaign may/will deteriorate the rig and hence will increase the likelihood of accidents.
- ii. Economic factors: the quantities of fuel used will raise the cost of testing.
- iii. Environmental factors: it produces large quantities of waste to be handled (which may also contribute to the cost of testing).



It is important to highlight that the reason for building the laboratory scale rig was to develop a facility that could be used to undertake a study of boilover in a cost effective, safe and carefully controlled manner.

### **4.3.1 Fuels Used**

A mixture of mineral oil and n-butyl acetate was first used in preliminary experiments to determine whether the hot zone phenomenon could be reproduced using the laboratory rig (on a smaller scale). The selection of these fuels is mainly based on safety factor i.e. a fuel mixture that poses a mean boiling point higher than water and has the highest possible flash point and/or auto-ignition point. The flash point of the mineral oil (CAS# 8042-47-5) is more than 175°C. An auto-ignition point is not available for the mineral oil. It is a flash point of 22°C and an auto-ignition of 407°C for the n-butyl acetate (CAS#123-86-4). High flash and auto-ignition points would indicate a lower risk for a flash fire to occur during the experiments.

After the works with the mineral oil and n-butyl acetate which showed promising results, the subsequent experiments were carried out with more volatile fuels. Gasoline, diesel and a mixture of diesel and gasoline were used in the latter tests. In addition to the main objective, the purpose of using diesel and gasoline was to look at the effect of using lower boiling points fuels towards boilover onset. These two fuels were selected due to their significant advantages over other hydrocarbons:

- i. Diesel and gasoline fuels are representative of a wide range of hydrocarbons – gasoline presents the typical characteristics of light hydrocarbons and the diesel, heavy oil fractions.
- ii. Its use is widespread, both industrially and in the domestic sector, and it is easily available.

The latter tests then involved the usage of other fuels such as a mixture between kerosene and heptane, hydrotreated vegetable oil diesel, pseudo-crude (hexane-gasoline-kerosene-diesel-engine oil) and crude oil. The usage of

these fuels is to further assess the feasibility of using the rig to conduct a variety of boilover tests and hence improve knowledge of the phenomenon. The summary of the important properties of the fuels used in the experiments is shown in Table 4-4.

Fuel	CAS #	Boiling Point/Range (°C)	Relative Density (15/4 °C at which water = 1)
Mineral oil	8042-47-5	260 - 330	0.85 - 0.88
n-Butyl acetate	123-86-4	125	0.88
Diesel	68334-30-5	170 - 360	0.82 - 0.87
Gasoline	86290-81-5	50 - 200	0.70 – 0.78
Kerosene	64742-81-0	140 - 300	0.77 - 0.84
Heptane	142-82-5	98.4	0.68
Hydrotreated vegetable oil diesel	928771-01-1	180 - 320	0.77 - 0.79
Crude oil	8002-05-9	38 – 500+	0.70 – 0.95

**Table 4-4: Summary of properties of fuels used in the boilover experiments**

### 4.3.2 Number of Test

The number of tests carried out during this experimental programme was 23. The summary of the experimental programme is given in Table 4-5. The table shows information on the type of oil mixtures, the composition of the oil mixtures, the oil layer thickness (depth) and the water layer thickness.

No.	Test No.	Oil Mixture	Oil Thickness (mm)	Water Thickness (mm)	Initial Storage Temp. (Avg. °C)	Heating Temp. (°C)
1	LS Prelim 1	Water	0	130	22	150
2	LS Prelim 2	70% mineral oil + 30% n-butyl acetate	180	0	13	300
3	LS Prelim 3	80% mineral oil + 20% n-butyl acetate	180		12	300
4	LS Test 1	80% mineral oil + 20% n-butyl acetate	80	20	17	300
5	LS Test 2		80		45	
6	LS Test 3		150		16	
7	LS Test 4		200		37	
8	LS Test 5		200		17	

**Table 4-5: Summary of experimental programme**

Table 4-5 (continued)

No.	Test No.	Oil Mixture	Oil Thickness (mm)	Water Thickness (mm)	Initial Storage Temp. (Avg. °C)	Heating Temp. (°C)
9	LS Test 6	80% kerosene + 20% heptane	100	20	22	300
10	LS Test 7	80% diesel + 20% gasoline	80	20	16	300
11	LS Test 8		80	20	18	
12	LS Test 9		80	20	46	
13	LS Test 10		80	60	19	
14	LS Test 11		150	20	5	
15	LS Test 12		200	20	19	
16	LS Test 13	Gasoline	70	20	11	300
17	LS Test 14	Hydrotreated vegetable oil diesel	80	20	13	300
18	LS Test 15				10	375
19	LS Test 16				20	450
20	LS Test 17	Crude oil	80	20	19	500
21	LS Test 18		120		19	
22	LS Test 19		160		18	
23	LS Test 20		200		18	

### 4.3.3 Test Routine

At the beginning of the series of experiments, some preliminary tests were carried out in the rig, with the aim of studying the possibility of hot zone formation using the proposed oil mixture, checking the operation of the system and determining the optimal operation of equipment. The preliminary tests were also carried out in order to work out and produce a safe working procedure for the experimental works.

In carrying out the experimental campaign, the whole experiments are carried out according to the following routine:

- i. Based on the volume ratio, the individual fuels were first prepared in the required volume, as shown in Table 4-6 below, and then mixed in a conical flask. Then the flask would be swirled manually to ensure complete mixing.

Thickness of Fuel Layer (mm)	Equivalent Volume (L)	80% of Volume (L)	20% of Volume (L)
80	6.8	5.4	1.4
150	12.7	10.2	2.5
200	16.9	13.6	3.4

**Table 4-6: Volume based on the Thickness of Fuel Layer**

- ii. The required amount of oil mixture were then introduced into the main tank of the boilover rig and followed by 1.7 litres of water (equivalent to 20 mm layer thickness).
- iii. Initiation of nitrogen gas purging and oxygen percentage monitoring were carried out and followed by the supply of cooling water to the in-line condenser as the safety requirement of the work.
- iv. After that, cartridge heaters were shifted until they were fully immersed just beneath the surface of the oil mixtures.
- v. The heating temperature was then set as per the planning via the temperature controller. When setting of the heating temperature was carried out, the heating would simultaneously start. The timer is also initiated as to record the duration of the experiment.
- vi. Promptly, the DAQ was initiated via the NI LabVIEW software in order to start displaying and recording the thermocouple measurements of the temperature.

The preparation and conclusion of each of the tests also involved the completion of the following:

- Checking of the DAQ prior starting an experiment: After switching on the power supply to all the devices needed to operate the data acquisition system, the connections and operation of all the devices (e.g. thermocouples, communication module network, data logging software *etc.*) are checked to ensure that all the measurement and recordings of data work effectively.
- Cleaning of the main tank and in-line condenser after each experiment: When it is safe to do so, the oil mixture is removed from the main tank by

opening a discharge valve at the base of the tank. The oil is collected in a bucket and then transferred to a 25-litre container. The main tank is then repetitively soaked and rinsed with water to remove any residual oil. The tank is then being dried by blowing compressed air into the tank. Similarly, oil is also being remove from the in-line condenser via a valve into a bucket and then into the 25-litre container.

- Checking that the tank (glass window panels), thermocouples, sealants, wiring etc. were physically in good condition after repetitive exposure to high temperature. This was important as to ensure safety during the conduct of the experiment.

## **5 MAIN CHARACTERISTICS OF BOILOVER IN THE LABORATORY SCALE EXPERIMENTS WORKS**

Chapter 5 presents the main characteristics of the boilover events observed in the laboratory experiments works. The initial section will describe the identification of the beginning of the boilover phenomenon in the experiments. Identification of the onset of boilover is important in order to standardize the decision regarding whether boilover did or did not occur. Once the onset of boilover was characterized, the following properties were determined:

- i. Speed of the base of hot zone
- ii. Onset time of boilover following the start of the heating process

In the subsequent section, the experimental results are presented and analyzed according to the range of parameters considered during the experimental program as described in Chapter 4 i.e. the initial thickness of the fuel layer, the type of the fuel and the preset temperature of the cartridge heaters. Table 4-5 shows information on the type of oil mixtures, the composition of the oil mixtures, the initial depth of fuel and the water layer thickness.

The laboratory scale boilover rig is to be used primarily to determine whether or not a fuel will boilover. Hence the tests listed in Table 4-5 were carried out in order to determine the conditions necessary for boilover to occur and conditions for boilover not to occur.

### **5.1 Conditions Necessary for Boilover**

Preliminary tests LS Prelim 1, 2 and 3 were carried out in the laboratory scale boilover rig, with the aim of studying the possibility of hot zone formation using the proposed fuel mixture, checking the operation of the system and determining the optimal operation of equipment. The preliminary experiments were carried out to determine whether the hot zone phenomenon that occurred

in the larger scale tests could be reproduced on a smaller scale using the laboratory rig.

## 5.1.1 Preliminary Test Observations

### 5.1.1.1 LS Prelim 1

From the fire test results in the literature and from the field scale test results presented in Section 3.2.1, it has been established that the burning of the pure or refined fuels did not form any hot zone and did not result in boilover. The test LS Prelim 1 was then conducted using water (to represent a pure fuel) to characterize the conditions necessary for hot zone not to form (and hence conditions for boilover not to occur). Figure 5-1 shows the temperature changes in the heating of 130 mm depth of water.

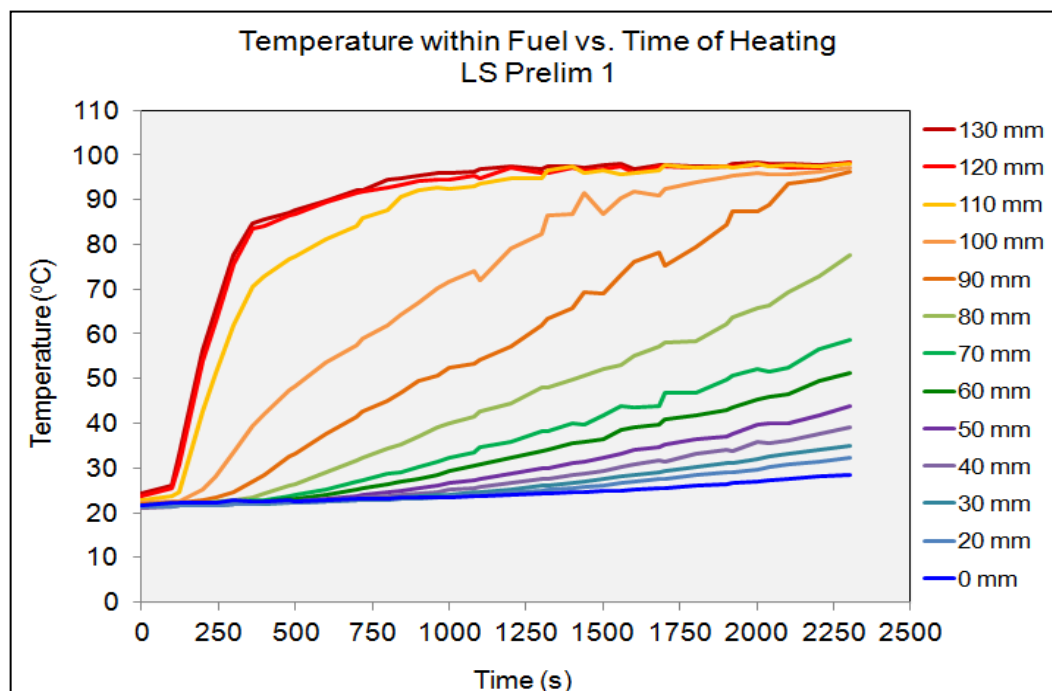
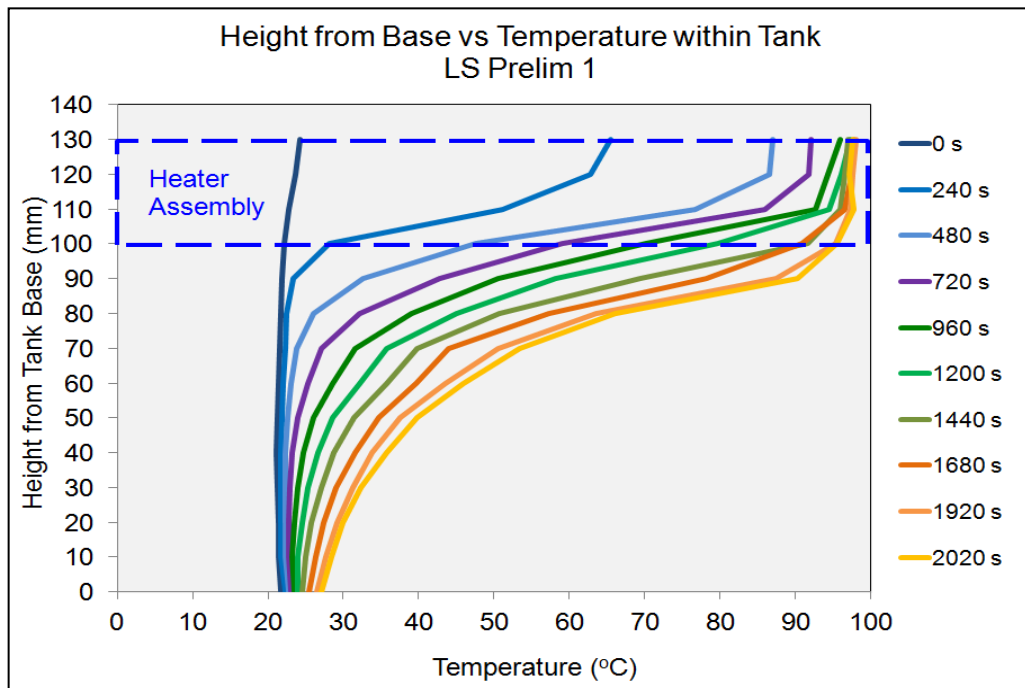


Figure 5-1: Temperature profiles within fuel in the tank in the course of test LS Prelim 1

Figure 5-1 shows that the thermocouples recorded increases in the temperature from the start of the test until the heating was terminated. The top three thermocouples (TC10 – TC13) display a steady increase in the temperature from about 20°C to 100°C. The thermocouple readings then converge to about

100°C at 1000 s after the heating started indicating the formation of a hot zone. A closer look at Figure 5-2 however indicates that the thermocouples were within the region of the cartridge heaters. Figure 5-2 shows the plot of temperature distribution versus height from tank base for the laboratory scale preliminary test LS Prelim 1.



**Figure 5-2: Vertical temperature profiles during heating of water for test LS Prelim 1**

Based on Figure 5-2, there is no noticeable vertical section on the curves showing a uniform temperature region in the fuel below the heater assembly. Though the figure shows the existence of vertical isothermal line, it was observed only within the fuel layer in which the heater assembly was located. The observations demonstrate that for a pure fuel (in this case water), a hot zone is not formed. In addition, the thickness of the isothermal region through the heater assembly is determined to be about 3 cm which covered the region of three thermocouples.

#### **5.1.1.2 LS Prelim 2**

LS Prelim 2 involved the heating of a 180 mm layer of mineral oil and n-butyl acetate mixture i.e. representing a simple binary fuel mixture. Figure 5-3 shows



the temperature changes in the heating of the mixture. The figure exhibits that the thermocouples recorded increases in the temperature from the start of the test until the heating was terminated. The top three thermocouples (TC16 - TC18) display a rapid increase in the temperature from about 15°C to 140°C within 500 s after the heating started. The temperatures measured by these three thermocouples then increased to 180°C before gradually decreased to 160°C. The thermocouples readings converge to 140°C after approximately 400 s of heating indicating the possibility of the hot zone formation.

At the points TC13 (130 mm from the base), TC14 (140 mm from the base) and TC15 (150 mm from the base), a similar trend was observed. For TC14 and TC15, the temperatures initially increased to 140°C. The temperature at TC15 then increased and remained close to 180°C whilst for TC14, the temperature increased to 160°C before jumping to 180°C. The reading at TC13 showed an initial increase to 80°C after about 1200 s of heating. The temperature at TC13 then increased rapidly to 180°C. The thermocouples (TC13 - TC15) readings all converging to about 180°C after 1500 s of heating indicate that a hot zone has been established. The remaining thermocouples (TC7-TC12) also displayed similar trend in the temperature changes as the heating progressed. The thermocouples readings all converged to about 160°C at a later period of time.

A closer look at Figure 5-4 supports the observation of the hot zone formation. Figure 5-4 shows the plot of temperature distribution versus height from tank base for the laboratory scale preliminary test LS Prelim 2. Initially, vertical isothermal lines were observed within the fuel layer in which the heater assembly was located i.e. within 3 cm beneath the fuel surface. The fuel within this region was being heated until it reached a uniform temperature i.e. about 140°C. This is approximately the temperature of n-butyl acetate that was boiling off. The boiling point of n-butyl acetate is near to 130°C. Hence the vertical isothermal lines were observed.

The heat then penetrated into the fuel below the cartridge heaters. As the heating progressed, a uniform temperature across the thickness of the fuel layer

below the heater assembly was reached. As an example; after about 1800 s of heating, a temperature of about 160°C was measured within 40 mm region below the heater assembly (from 110 mm to 150 mm from the base of the tank). This observation demonstrates that a hot zone has been formed in this test.

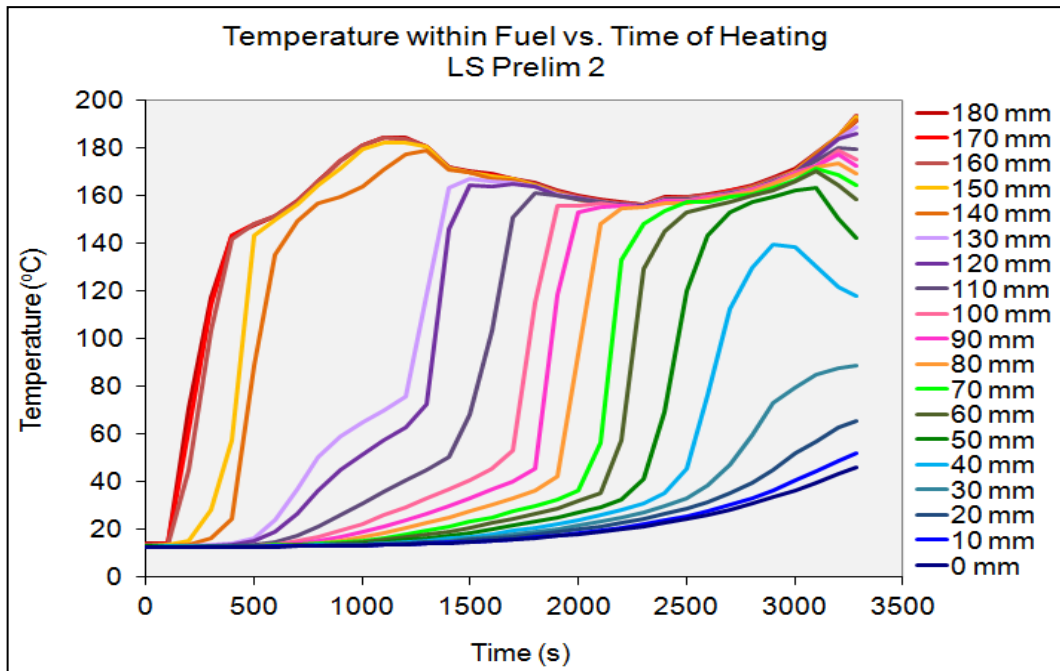


Figure 5-3: Temperature profiles within fuel in the tank in the course of test LS Prelim 2

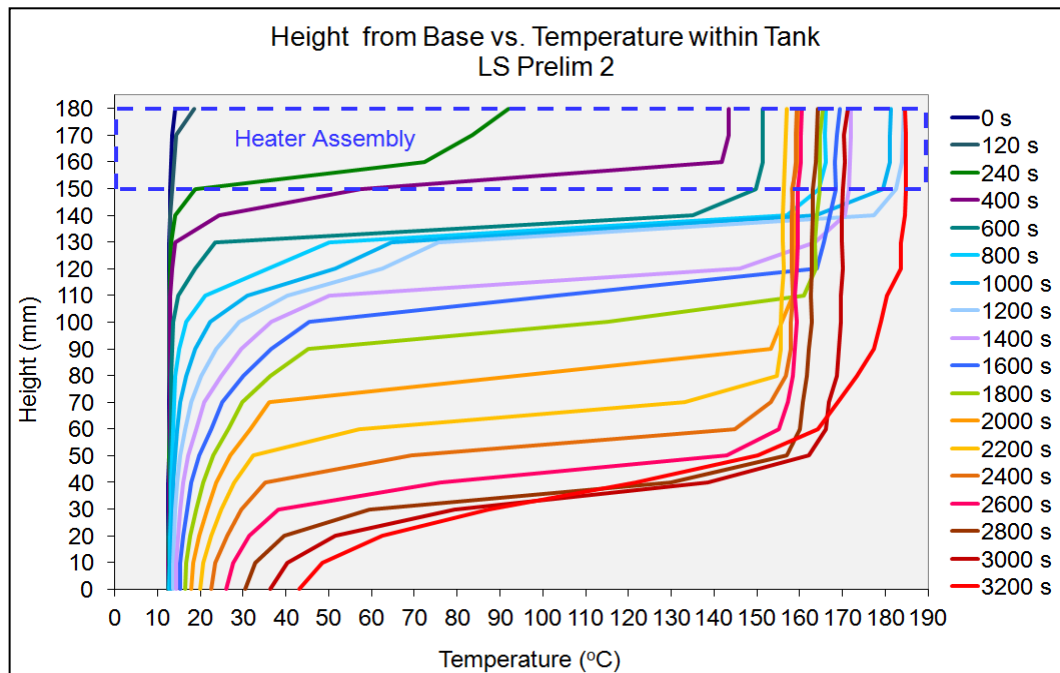


Figure 5-4: Vertical temperature profiles during heating of water for test LS Prelim 2

The photographs during the progress of the experiment are shown in Figure 5-5(a) – (d). These photographs provide physical observation on the formation of the hot zone.

Near the surface, bubbles are bursting creating turbulence as the heating progresses as shown in Figure 5-5(a). This is caused by the rapid evaporation of the lighter component of the mixture, i.e. n-butyl acetate which has a lower boiling point.

Photograph in Figure 5-5(b) was taken 600 s after the heating had started and the hot zone can be clearly seen. An interface separating two distinct layers which are the hot zone and the cold fuel also can be clearly detected. The hot zone layer was observed to be a bit blurry compared to the clear layer of cold oil. This condition may be due to the stirring effect of convective currents resulted from the vaporising of the low boiling point component of the fuel. The hot zone consists mainly of the high boiling point component through which passes vapour bubbles of the low boiling point component generated in the region of the hot-cold interface.

The hot-cold interface then moved downwards and reached 100 mm above the base of the tank at 1500 s after the start of heating, as shown in photograph Figure 5-5(c). Corresponding time histories of the temperatures plot at later times are also shown. Photograph (d) shows that the hot zone continues to grow further down after 2100 s of heating. The temperature profile plot indicates that the hot zone lower boundary is about 60 mm from the base. The experiment was stopped after 3300 s of heating and the hot zone-cold fuel interface was detected at approximately 30 mm from the base of the tank.

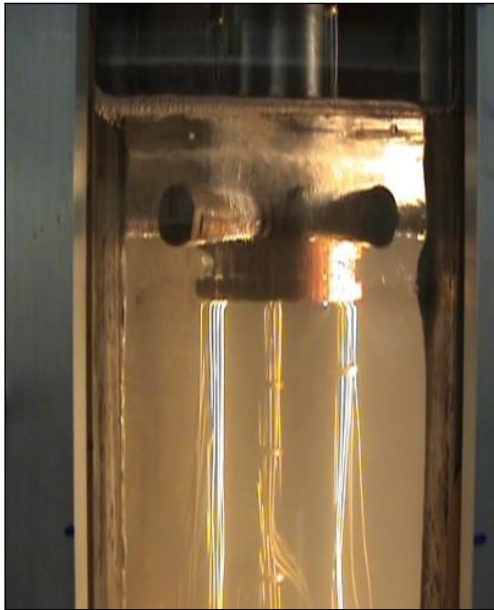


Figure 5-5: (a) Formation of hot zone: Bubbling at surface upon start of heating



Figure 5-5: (b) Formation of hot zone: Hot zone started to be visible. Base of the hot zone regresses below the heater assembly after about 600s of heating

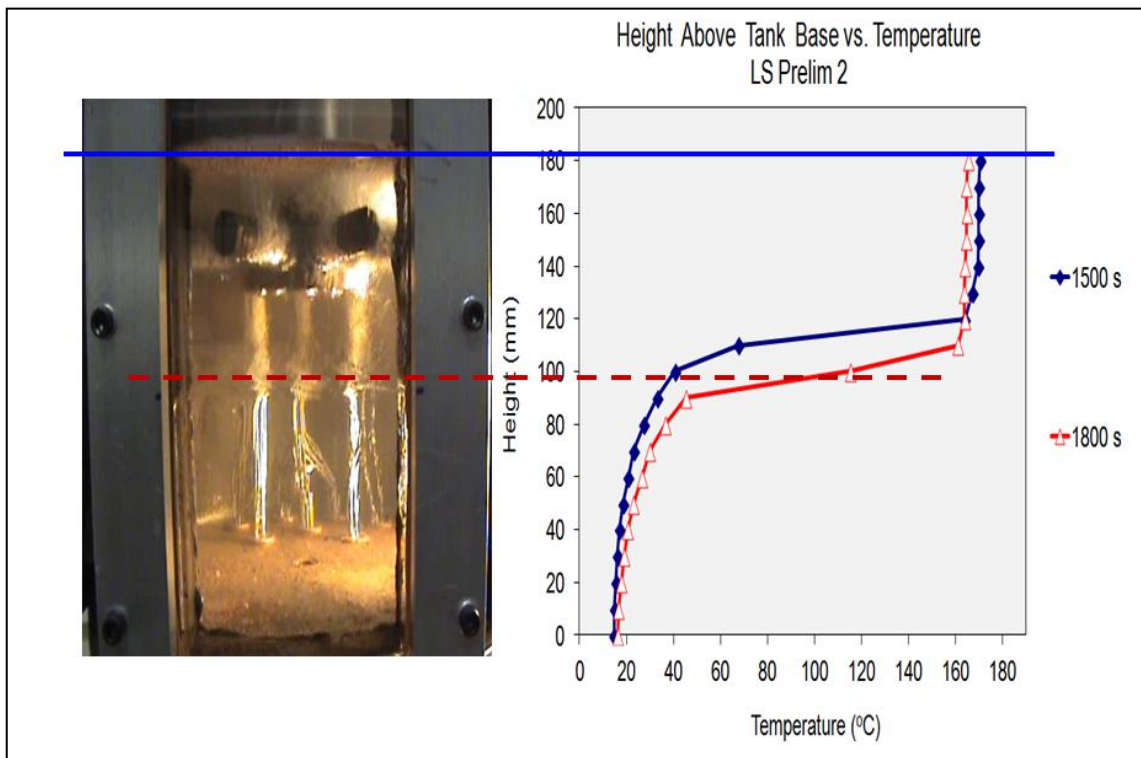
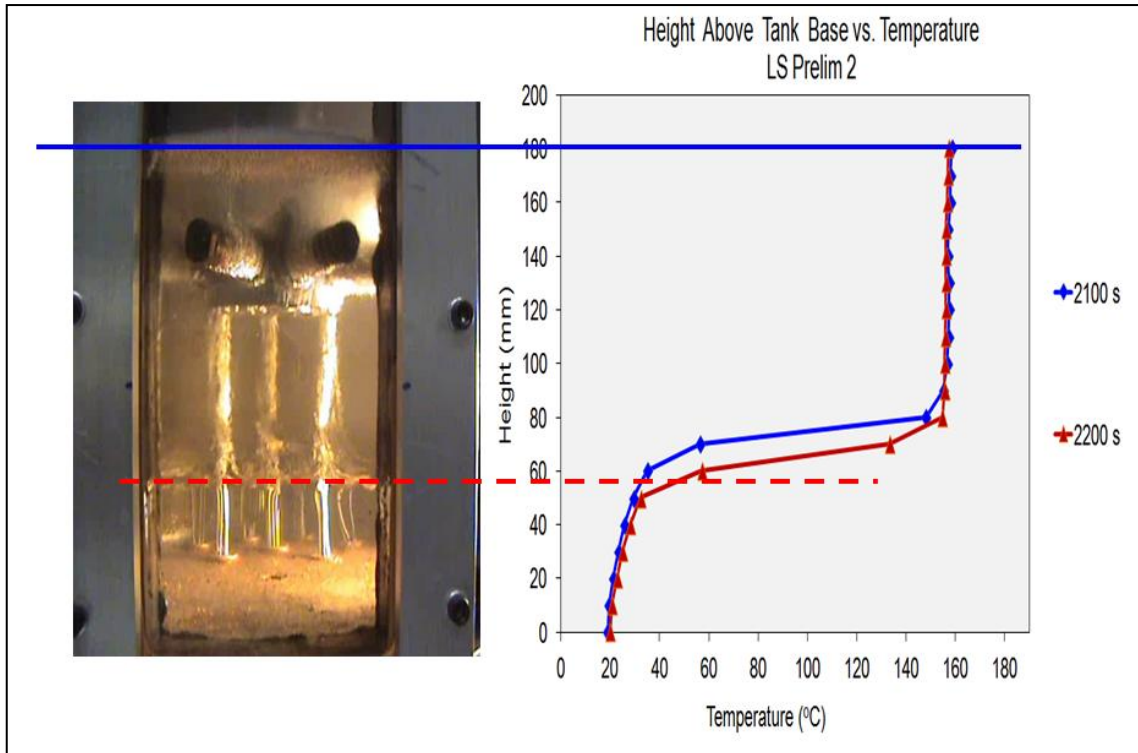


Figure 5-5: (c) Formation of hot zone: Interface of hot-cold fuel approximately at 100 mm from the base of the tank observed within the period of 1500 s to 1800 s of heating



**Figure 5-5: (d) Formation of hot zone: Hot zone has grown further downwards of the tank after about 2100 s to 2200 s of heating**

The above observations demonstrate that for a simple binary fuel mixture, a hot zone is formed. Taking into consideration the thickness of the isothermal region through the heater assembly, the vertical section of the temperature profiles below the region of the heater assembly in Figure 5-5 can be used to approximate the hot zone thickness. Figure 5-5 also shows that the temperature of the hot zone is about 160°C. This temperature is greater than the boiling point of water. If water is present and the hot zone came into contact with the water, consequently, vigorous boiling and boilover will occur.

Section 5.1.2 further discusses the formation of the hot zone observed during the progression of the laboratory scale experiments that end with a boilover.

### 5.1.2 Observations on Tests with Boilover

The laboratory scale boilover tests were carried out in a closed vessel and with the absence of an open flame. These features prevented the observation of flame enlargement during boilover as in the field scale tests. However, the rig

was designed with three glass windows which allowed the physical changes within the liquid in the tank to be observed throughout the experiments and to be recorded using a video camera.

The behaviour of the liquid fuel temperature during the progress of the heating is presented. The temperature versus time was plotted for each test and the data records were examined at each stage of the heating progression. This examination was essential to study the formation of a hot zone and the occurrence of a boilover.

#### **5.1.2.1 Temperature Profiles of Temperature-Time Curve**

Figure 5-6 shows the temperature changes in the heating of a 150 mm depth of mineral oil and n-butyl acetate mixture with a 20 mm depth of water at the base of the tank. The figure shows that the thermocouples recorded increases in the temperature from the start of the test until about 9500 s of the heating when the thermocouples within the fuel (TC4-TC17) showed sharp drops in temperature (see bottom of Figure 5-6). At this point, the thermocouple at the fuel-water interface (TC2) registered a value of about 100°C and thus the boiling of water started. The thermocouples within the fuel (TC4-TC17) were cooled by the rise of water vapour and show a large decrease in temperature. The temperatures measured by thermocouples TC0 and TC2, which were placed in the water layer, continued to rise up to 110°C. All the thermocouples then recorded values that oscillated around 110°C. In LS Test 3, these occasions, which will be referred to as the beginning of a fully developed boilover, started at 9510 s.

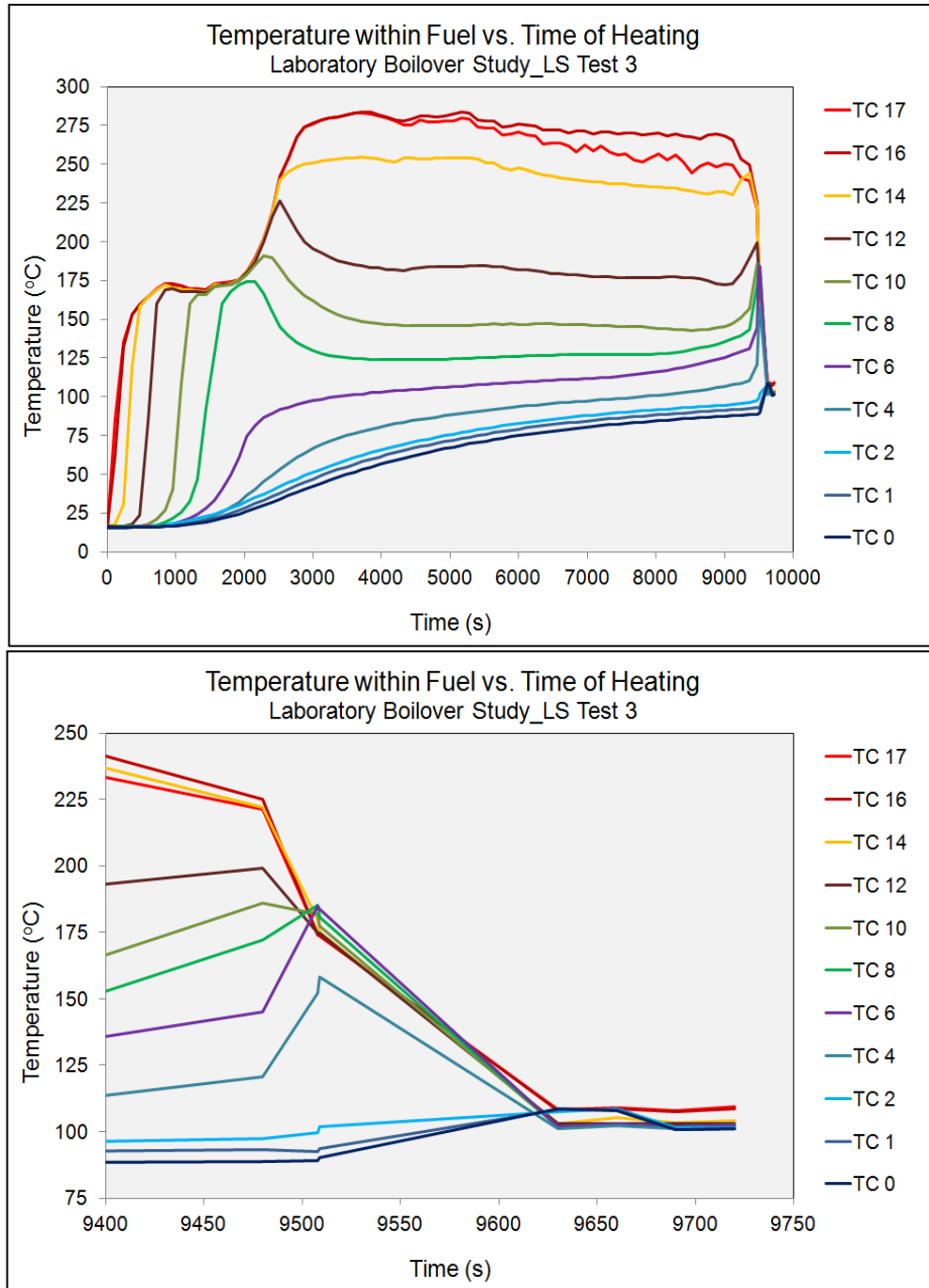


**Figure 5-6: Temperature profiles within liquid in the tank in the course of LS Test 3. The sharp drops in the temperature indicate vaporisation of water layer at the tank base.**

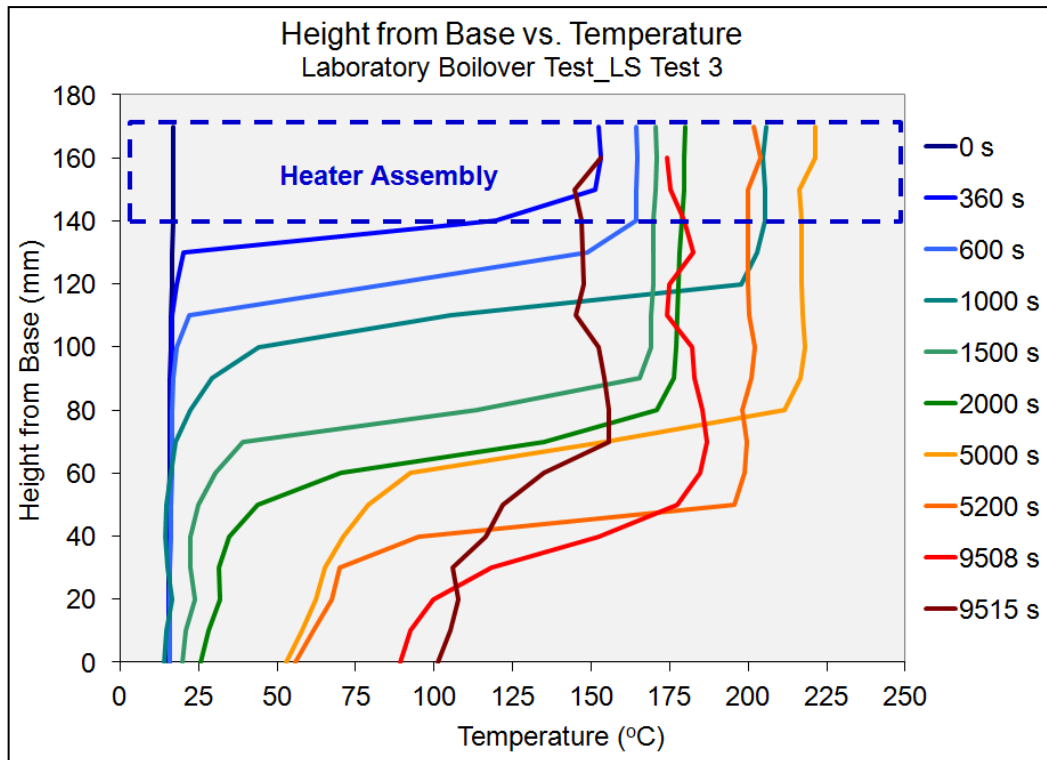


**Figure 5-7: Vertical temperature profiles during heating of mineral oil and n-butyl acetate mixture for LS Test 3**

Figure 5-7 shows the plot of temperature distribution versus height from tank base for the laboratory scale preliminary test LS Test 3 which supports the observation of the hot zone formation. The data could be used to determine the interface between the hot and cold fuel zone. The vertical section of the temperature profiles below the region of the heater assembly in the figure was used to approximate the hot zone thickness. Since the interface between the hot zone and cold fuel zone could not be distinguished directly from the figures, the horizontal section was assumed as the base of the hot zone i.e. the hot-cold interface. As the hot-cold interface approached the water layer at the tank base (in this case, the water level was at 20 mm from the tank base), the temperature of the water was raised to its boiling point whilst a substantial depth of hot fuel remained above the water. At this instance, the temperature of the hot zone was observed to be about 175°C. Once the water started to boil, rapid mixing between the water and the hot fuel was initiated. These mechanisms were observed at about 9500 s after the heating started and is shown by the red curve in Figure 5-7. Due to the rapid mixing, the fuel above the water layer was



cooled by the rise of water vapour and showed a decrease in temperature (see brown line at 9515 s of heating in Figure 5-7).

### 5.1.2.2 Photographs of Hot Zone Formation and Boilover

Figure 5-8(a) – (f) displays a series of photographs taken during experiment LS Test 3 which shows the hot zone formation and boilover occurrence.

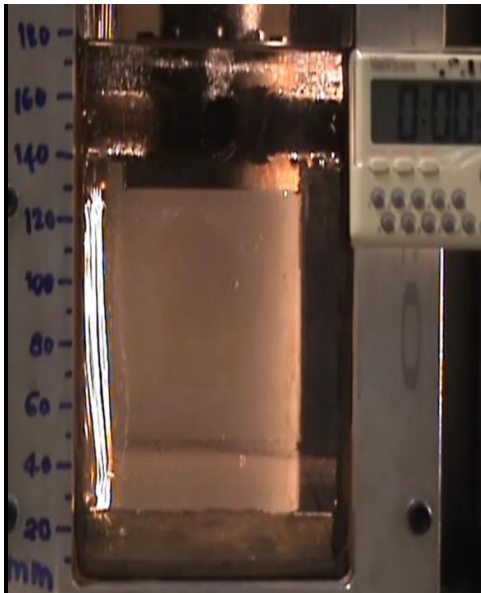


Figure 5-8: (a) Bubbling at surface at the start of the test

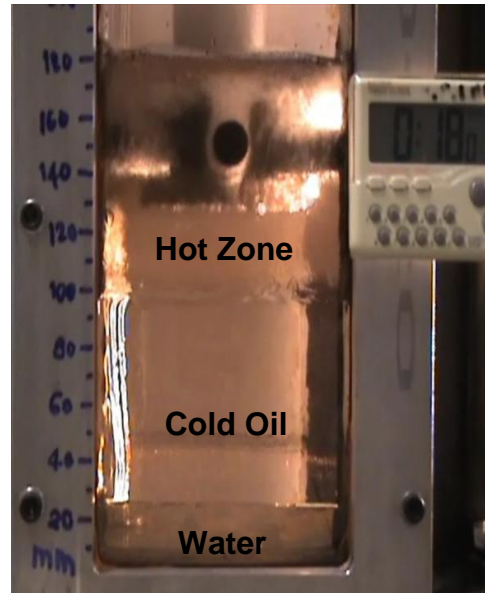


Figure 5-8: (b) Hot zone, cold fuel and water layer clearly visible after about 18 minutes of heating

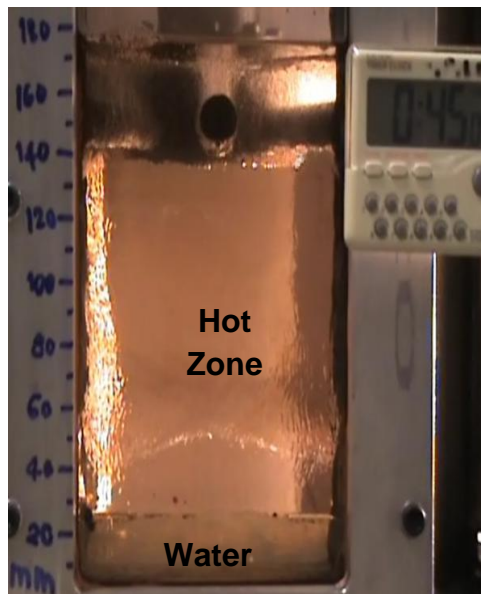


Figure 5-8: (c) Hot zone clearly visible after about 45 minutes of the test

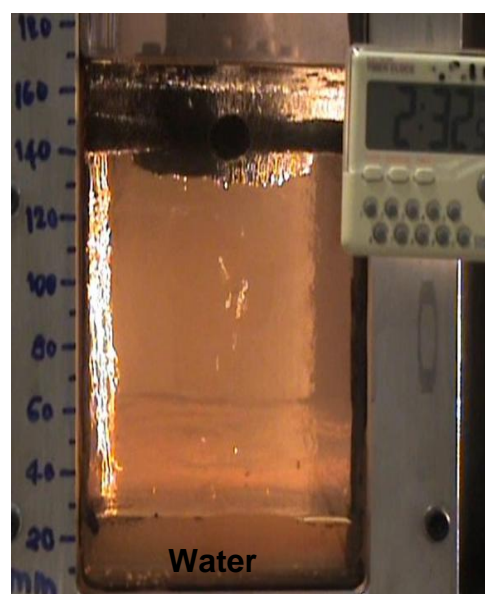


Figure 5-8: (d) Bubbles ascend from fuel-water interface after about 2 hours and 30 minutes of heating

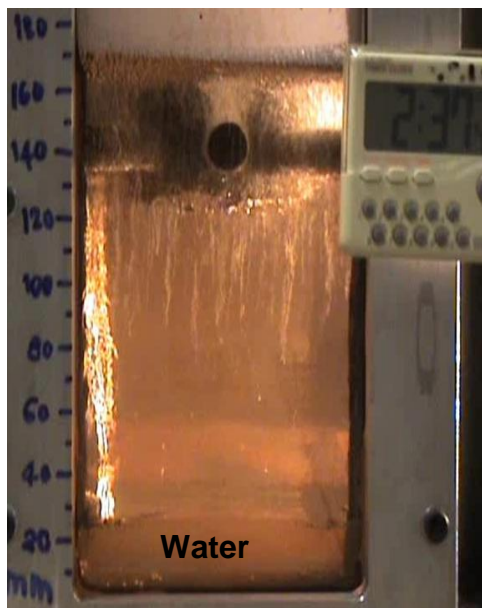


Figure 5-8: (e) Bubbles ascend from fuel-water interface with increasing intensity as heating progress



Figure 5-8: (f) Boilover occurred after about 2 hours and 38 minutes of heating (9510 s)

**Figure 5-8: Formation of hot zone and boilover occurrence for LS Test 3**

From photograph (a) taken after few seconds of heating, it can be clearly seen that there are a lot of bubbles floating on the fuel surface, which is due to the rapid evaporation of the lighter component, n-butyl acetate as the cartridge heaters reach their set temperature. Photograph (b) recorded about 1000 s after heating shows clearly the formation of a hot zone. In the photograph, a layer of cold fuel and the water layer are also observed. The hot zone continues to grow and heats up all the cold oil after 45 min of heating. At this instance, the hot zone is above the water layer, as shown in photograph (c).

After about two hours of heating with the temperature of the hot zone-water interface approaching  $100^{\circ}\text{C}$ , vapour bubbles form. Initially the bubble size is small with a low generation rate, and they are seen to form at middle sections of the interface, as shown in (d) and (e). At this instance, micro-vapour-explosions (Hua *et al.*, 1998; Arai *et al.*, 1990), which produce a 'crackling' sound, similar to the sound created when water is added to hot frying oil, is detected. As the heating continues, the temperature at the interface rises beyond  $100^{\circ}\text{C}$ , boiling of water become stronger, the bubble size increases, the generation rate becomes higher, and bubbles are formed over the entire interface. Photographs

(d) and (e) demonstrate this process which occurred after about 7200 s of heating. The micro-explosions also intensified as more and more bubbles rose up to the surface. The effects of bubble formation plus the stirring and mixing effects while moving upwards through the oil layer enhance the heat transfer process. More heat is fed back to the hot zone-water interface, which enhances the water's boiling process. Finally after 9510 s of heating, boilover occurred as shown in photograph (f). In the end of the experiment, it was observed that almost the entire tank contents have been evacuated into the secondary tank by the boilover event.

Observation shows that the water's boiling effects on the hot zone-water interface consists of two stages, i.e. weak and strong agitation. The former causes the phenomena of the emission of micro-explosion noise and the second leads to the occurrence of boilover (Hua *et al.*, 1998). The observations demonstrate that boilover, of the type in which this study is interested, requires a hot zone to be formed at a temperature substantially greater than the boiling point of water. The hot zone is identified based on the vertical section on the curves showing a uniform temperature region in the fuel below the heater assembly.

### **5.1.3 Observations on Tests with No Boilover**

In the case where a hot zone was not generated, the plot of temperature distribution versus height from the tank base does not show any indication of the hot zone existence below the region of the cartridge heaters. There is no noticeable vertical section on the curves showing a uniform temperature region in the fuel below the cartridge heaters.

#### **5.1.3.1 Temperature Profiles of Temperature-Time Curve**

Figure 5-9(a) - (b) show the temperature changes in the heating of a 70 mm layer of gasoline with a 20 mm layer of water in LS Test 13. Sharp changes in the temperature profiles are not visible in the LS Test 13. The thermocouples display a steady increase in temperature from the start of heating. A drop in the

temperature readings from about 125°C to 100°C was observed at about 1200 s. At this instant of time, the thermocouple at the fuel-water interface (TC2) registers a value of about 100°C but a vigorous boiling and mixing of gasoline and water did not occur. The temperature drop recorded by the top thermocouples (TC5-TC9) is due to the fact that they have been exposed outside the gasoline.

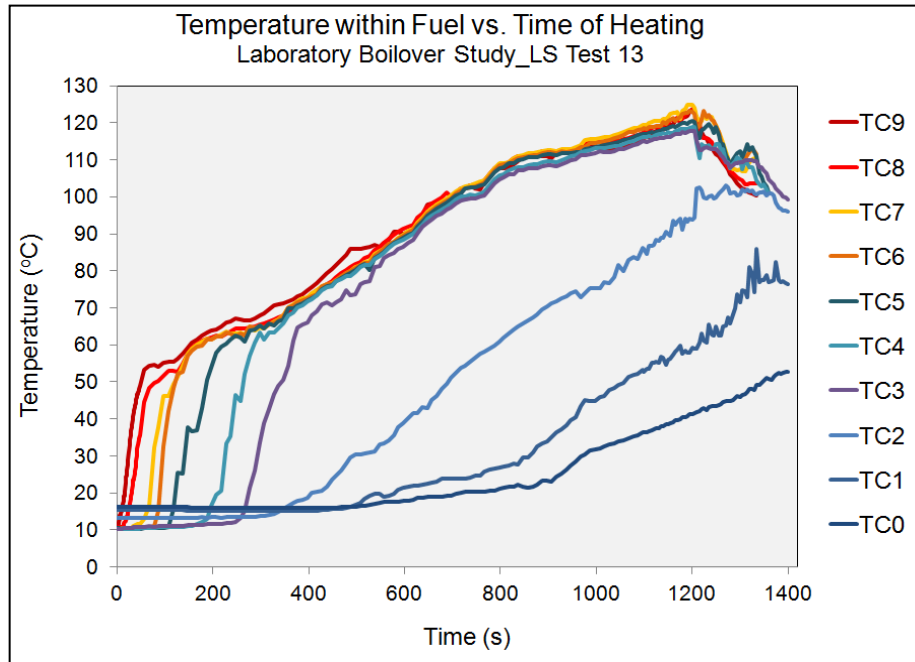


Figure 5-9: (a) Temperature profiles within liquid in the tank in the course of experiment for LS Test 13

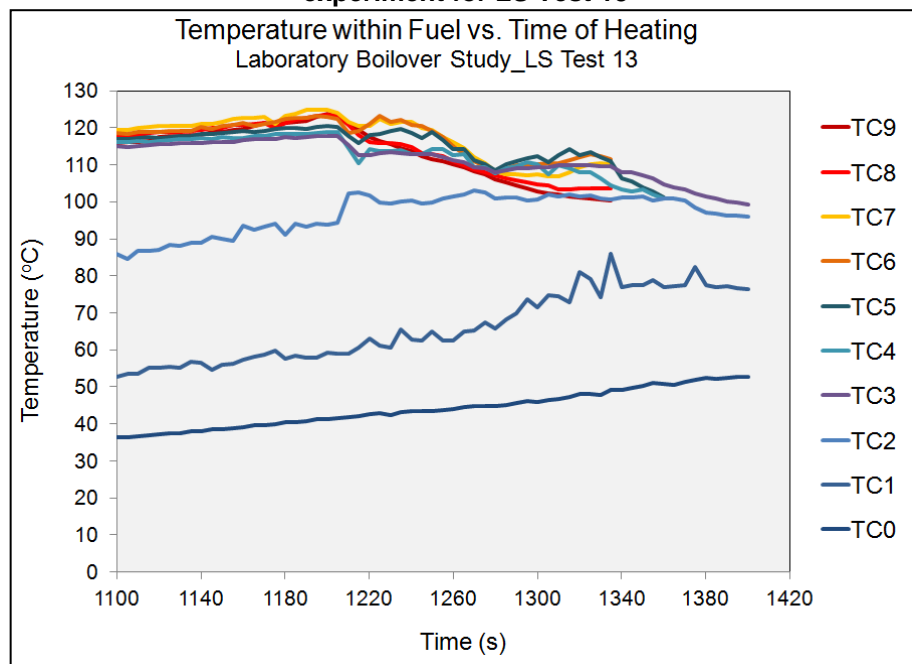
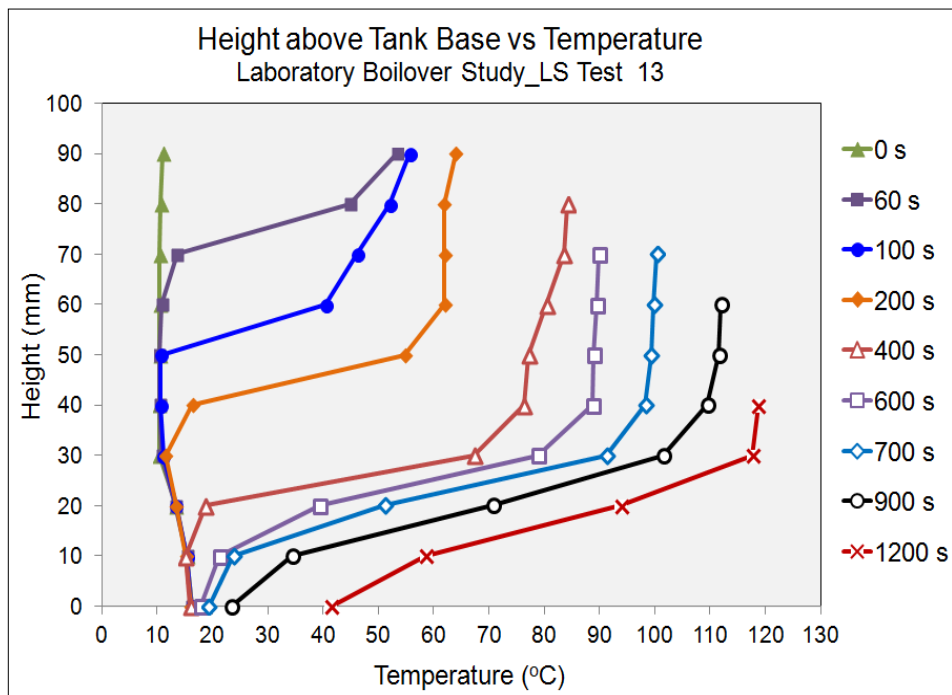


Figure 5-9: (b) Temperature profiles within liquid in the tank in the course of experiment for LS Test 13

Figure 5-10 shows the time histories of the temperature at various points inside the fuel for laboratory boilover study LS Test 13. Though the figure shows the existence of vertical isothermal line, it was observed only within the fuel layer in which the heater assembly was located.



**Figure 5-10: Vertical temperature profiles according to height of fuel in which hot zone were not formed for laboratory scale boilover studies.**

Figure 5-11 shows the temperature evolution of a gasoline test LS Test 13 with the photographs taken during the course of the test. The test with gasoline presents information regarding the temperature evolution in which there was no occurrence of boilover.

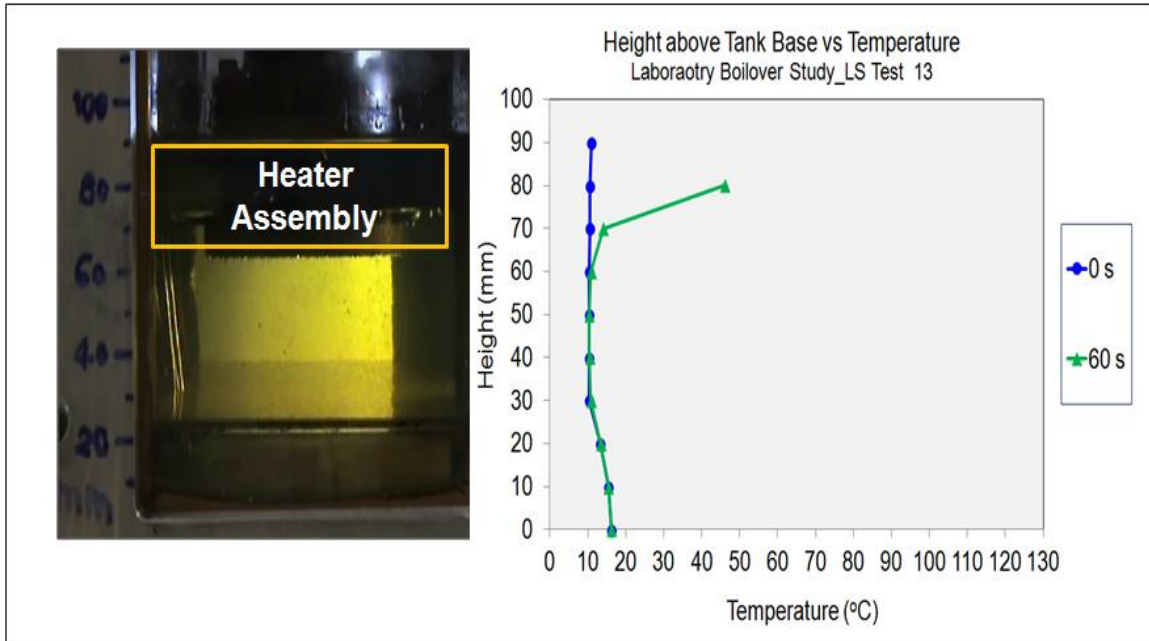


Figure 5-11: (a) Photographs of fuel surface regression and vertical temperature profiles during heating of gasoline for LS Test 13: At the beginning of the test with the surface at 90 mm

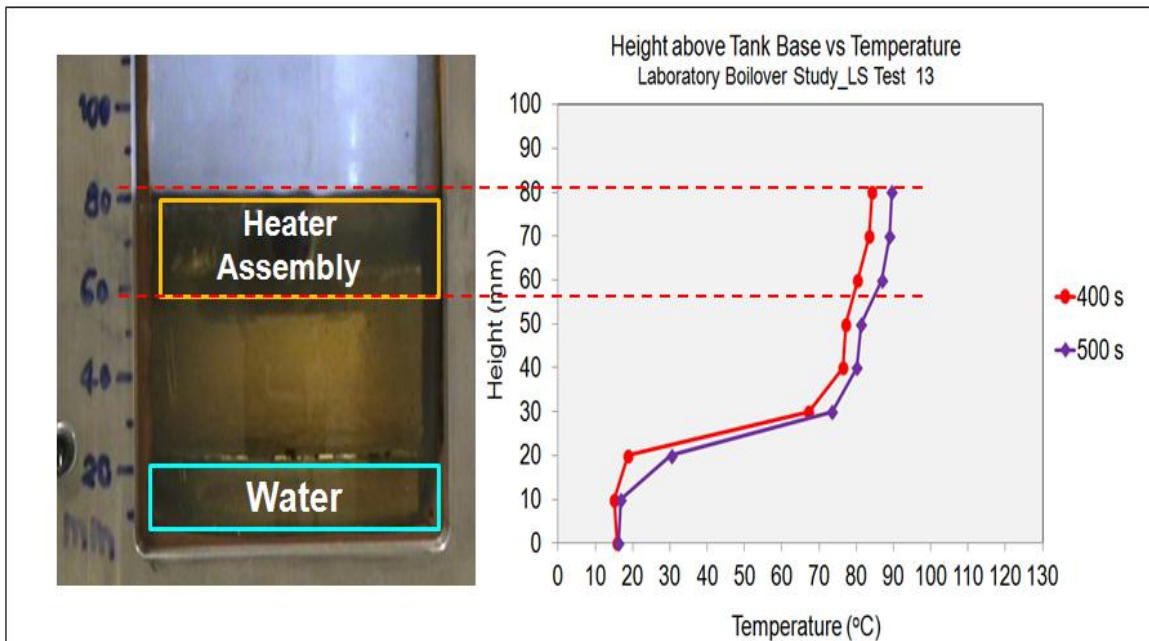


Figure 5-11: (b) Photographs of fuel surface regression and vertical temperature profiles during heating of gasoline for LS Test 13: After about 420 s of heating at which the surface has regressed to 80 mm

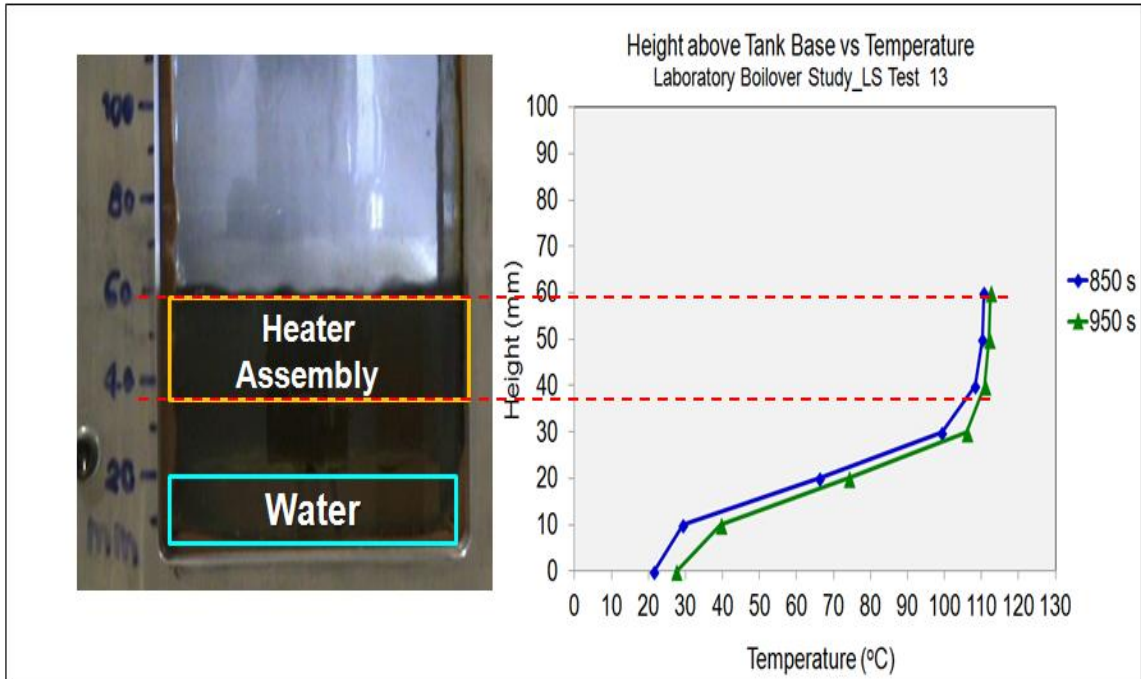


Figure 5-11: (c) Photographs of fuel surface regression and vertical temperature profiles during heating of gasoline for LS Test 13: After about 840 s with the surface at 60 mm

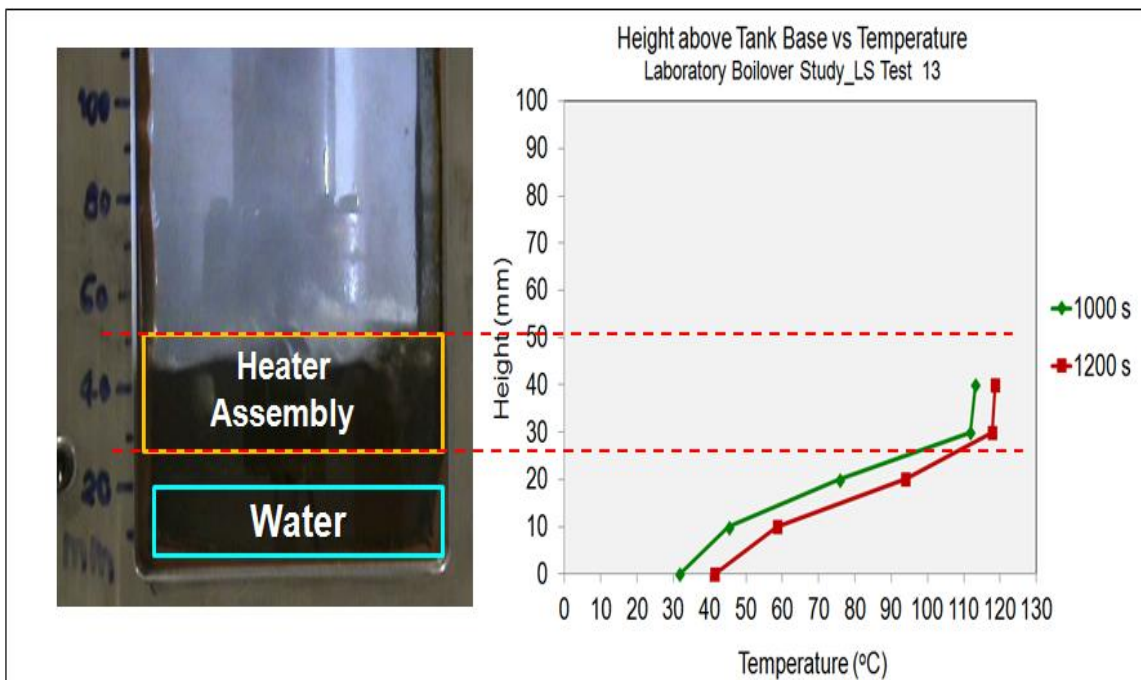


Figure 5-11: (d) Photographs of fuel surface regression and vertical temperature profiles during heating of gasoline for LS Test 13: At the end of the test at which the surface has regressed to 50 mm from the base.

At the beginning of the test, the temperature profile was a well-defined exponential curve, as presented by Figure 5-11(a). At about 60 s, the temperature profile showed the first significant increase after the heating had

started. The high temperature measured near the top part of the fuel layer was in the region of the heater assembly.

The temperature was observed to increase as the time progressed from 400 s to 950 s but no isothermal zone was established between thermocouples similar to that observed in Figure 5-4 and Figure 5-7. Between 850 s to 950 s after the heating started, the thermocouples located at 40 mm, 50 mm and 60 mm from the tank base displayed approximately the same temperature. Although this gives the impression that a hot zone had formed, the isothermal zone was observed only to reside within the region in which the heater assembly was located.

### 5.1.3.2 Photographs of Gasoline Test

Figure 5-12 shows a series of photographs taken during experiment LS Test 13.

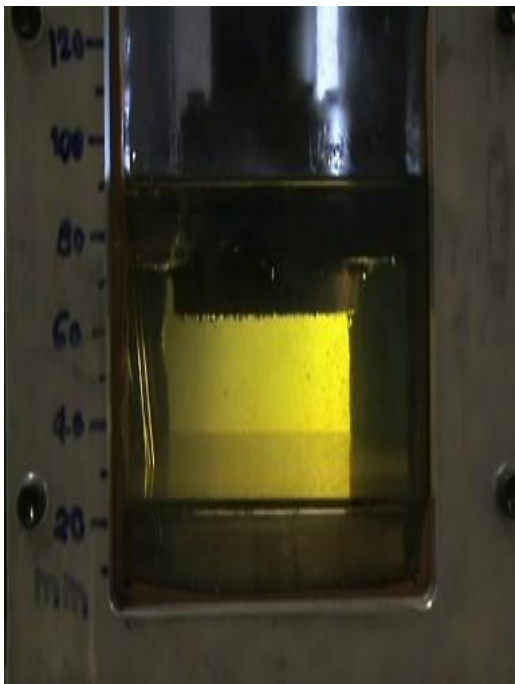


Figure 5-12: Photo of Laboratory Boilover Test LS Test 13 involving gasoline (a) During the start-up of heating – bubbling near cartridge heaters



Figure 5-12: Photo of Laboratory Boilover Test LS Test 13 involving gasoline (b) After 420 s of heating – surface level is approximately at 80 mm from tank base





Figure 5-12: Photo of Laboratory Boilover Test LS Test 13 involving gasoline (c) After 900 s of heating – surface level is approximately at 60 mm from tank base



Figure 5-12: Photo of Laboratory Boilover Test LS Test 13 involving gasoline (d) At the end of the experiment – surface level has dropped to about 40 mm level mark. Vigorous boiling/bubbling did not occur.

**Figure 5-12: Photo of Laboratory Boilover Test LS Test 13 involving gasoline**

Figure 5-12 shows the conditions in which boilover did not occur in a laboratory scale test. The figure shows physical changes recorded during LS Test 13. The photographs show that the gasoline surface level dropped as the heating proceeded until the experiment was stopped when the heater almost reached the tank base. The vigorous boiling of water and hence boilover did not occur although the heater came very close to the fuel-water interface.

The observations from LS Test 13 demonstrate that for a pure fuel, a hot zone is not formed. In addition, though the heater came very close to the fuel-water interface, the vigorous boiling of water and hence boilover did not occur. Based on Figure 5-11(d), the temperature of fuel layer below the heater assembly was about 90°C. This thin layer of fuel is at a temperature below that which is sufficiently above the boiling point of water for boilover to occur.

## **5.2 IDENTIFICATION OF BOILOVER PHENOMENON IN THE LABORATORY SCALE EXPERIMENT**

As described in Chapter 3, the potential ‘indicators’ of boilover include fuel and steam ejection, flame enlargement and audible indicators. The appearance of boilover is seen through vigorous fuel ejection due to the violent boiling of water and frothing over of the whole tank content which resulted in increases of the flame height two or three times larger than that at the steady-state burning. The beginning of the phenomenon in a large-scale open tank fire, therefore, has been characterized from the vigorous fuel ejection to the tank surrounding, the flame enlargement due to the fuel ejections and the noise level due to the water evaporation. In the laboratory-scale boilover rig, however, similar characteristics could not be used as the indication of the boilover start-up and appearance.

Nevertheless, the observations and discussions conducted in Section 5.1.1, 5.1.2 and 5.1.3 have demonstrated the conditions need for boilover to occur and the conditions under which boilover will not occur for the laboratory scale tests. The identification of the conditions need to boilover to occur for the laboratory tests is important in order to characterize the onset of boilover. Section 5.2.1 and 5.2.2 emphasize further the conditions need for boilover to occur to standardize the decision regarding the start of the phenomenon.

### **5.2.1 Temperature Profiles of Temperature-Time Curve**

The appearance of boilover can be seen in the graphs which represents the progress of temperature within the fuel with time. As shown in Figure 5-13, in the case of LS Test 11 and in correspondence with the beginning of boilover at 4366 s, a sharp change in the temperatures measured is observed. The figure shows that the thermocouples recorded increases in the temperature throughout the course of the experiment. Then, boiling of water started when the thermocouple at the fuel-water interface (TC2) registered a value of about 100°C after 4366 s of heating (see bottom figure of Figure 5-13). Due to the turbulence resulted by the rise of water vapour, the thermocouples within the fuel (TC4-TC17) are hence cooled and show a large decrease in the

temperature. In the case of the thermocouples TC0 and TC2 which were placed in the water layer, the recorded temperature continues to rise up to 140°C. All the thermocouples then record values that oscillated around 120°C. In LS Test 11, these occasions – which will be referred to as the beginning of a fully developed boilover – started at 4366 s.

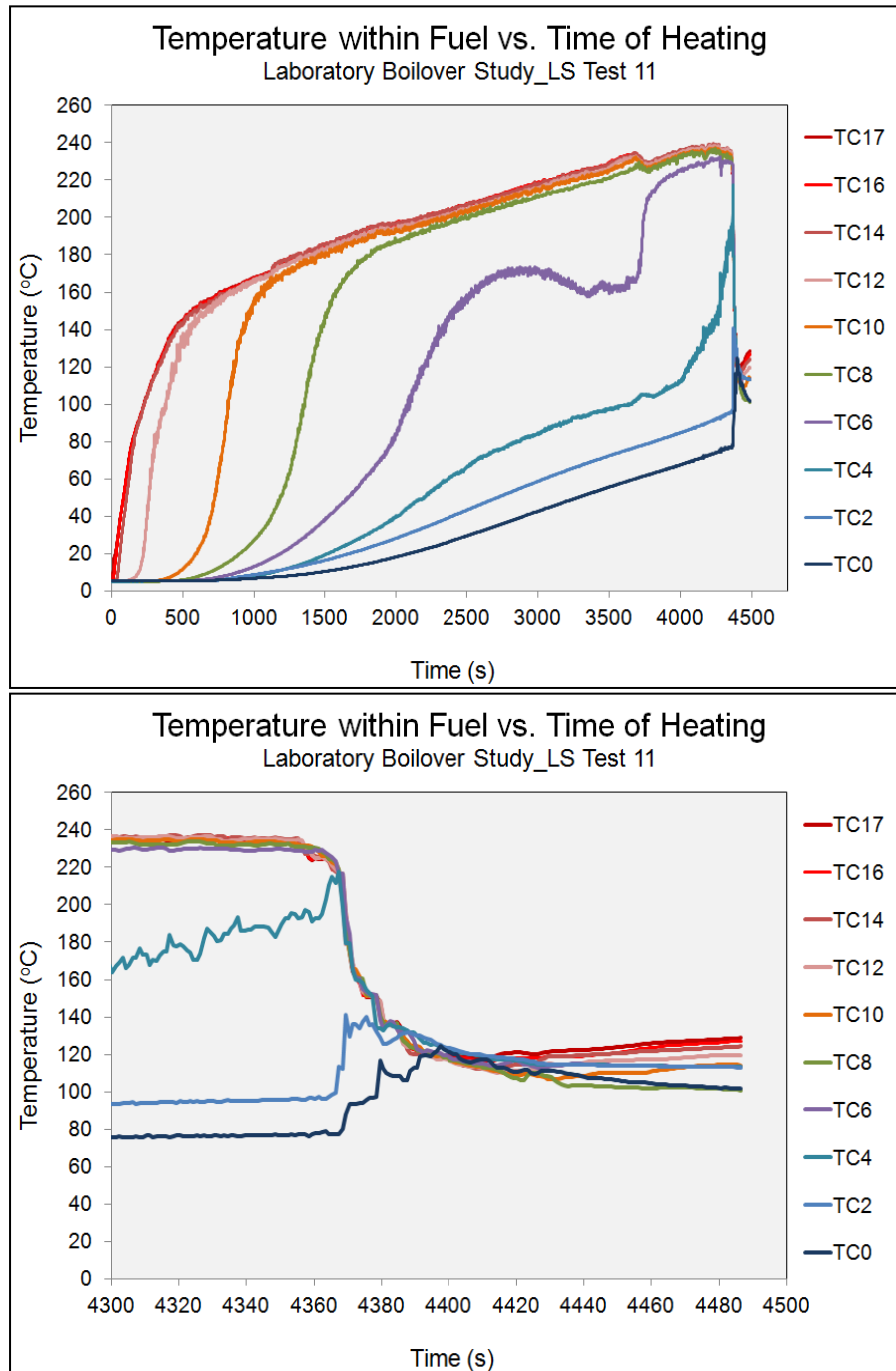


**Figure 5-13: Temperature profiles within liquid in the tank in the course of experiment for LS Test 11.**

## 5.2.2 Violent Boiling of Fuel-Water Interface

Section 5.1.2.2 indicates that the violent boiling of the water at the fuel-water interface could be observed and characterized as the beginning of the boilover phenomenon. Photographs taken from the LS Test 7 (for an 80 mm layer of diesel and gasoline mixture with a 20 mm water layer thickness at the tank base) are shown in Figure 5-14 to demonstrate the onset of boilover. Figure 5-14 shows two conditions indicating the start of the heating process at the beginning of the test and the occurrence of boilover.

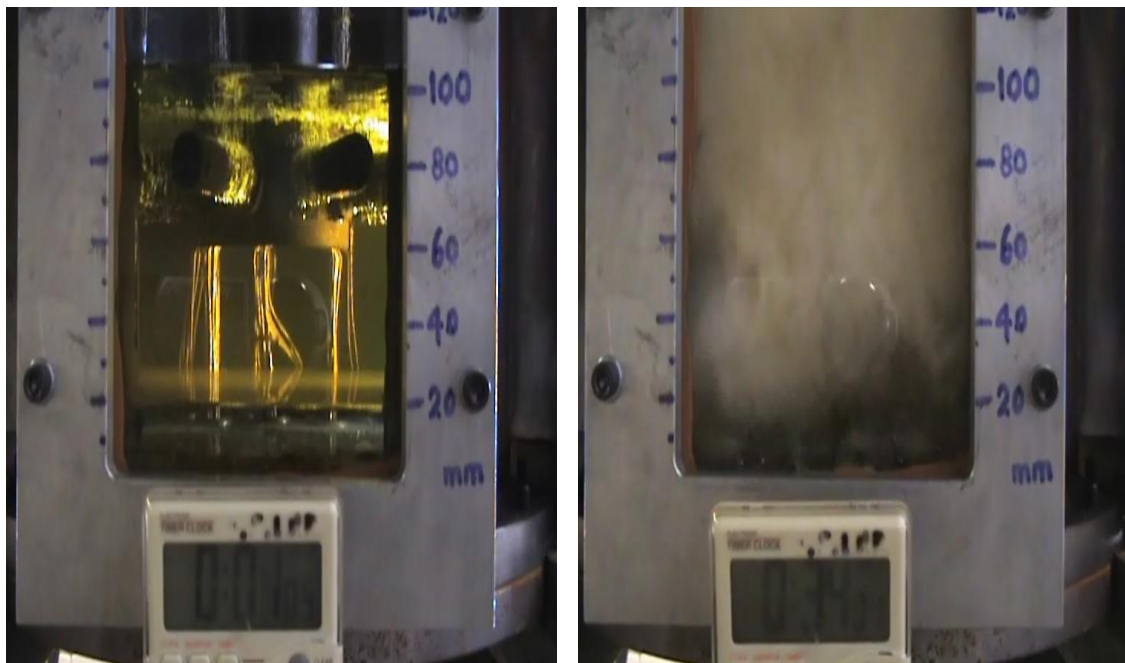


**Figure 5-14: Photo of Laboratory Boilover Test LS Test 7 (a) During the start of heating – bubbling is observed near the heaters and (b) During the start of boilover – boiling of water occurred where vigorous bubbling (mixing of fuel and water) was observed.**

In summary, the start of boilover in the laboratory scale tests was identified through changes in the temperature profiles and the observation of violent boiling of the water.

## 5.3 CHARACTERISTIC PARAMETER AND OBSERVATION

This section summarizes the characteristics of the tests conducted and the value of the main parameters that describe the boilover phenomenon i.e. average fuel surface regression rate and the speed of the base of the hot zone.

This section is also devoted to presenting the results on the boilover onset time observed during the preliminary and laboratory scale experiments. As mentioned in Chapter 4, the preliminary experiments i.e. LS Prelim 1, 2 and 3 were carried out to determine whether the hot zone phenomenon that occurred in the larger scale tests could be reproduced on a smaller scale using the laboratory rig. The fuels used in the preliminary tests were mineral oil and n-butyl acetate. Since the works with the mineral oil and n-butyl acetate showed very promising results, the subsequent experiments were carried out with more volatile fuels.

### 5.3.1 Time to Boilover

Table 5-1 provides the time to boilover for those experiments in which boilover was observed. The time to boilover was determined based on the changes in the temperature profiles i.e. the thermocouple at the fuel-water interface reaching the boiling temperature of water followed by the violent boiling of the water.

No.	Test No.	Fuel Thickness (mm)	Initial Storage Temp. (Avg. °C)	Time to Boilover $t_{bo}$ (sec)
1	LS Prelim 1	180	13	No boilover
2	LS Prelim 2	80	12	No boilover
3	LS Prelim 3	0	22	No boilover
4	LS Test 1	80	17	4520
5	LS Test 2	80	45	968
6	LS Test 3	150	16	9508
7	LS Test 4	200	37	12473
8	LS Test 5	200	17	15706
9	LS Test 6	100	22	1245
10	LS Test 7	80	16	1605
11	LS Test 8	80	18	1999
12	LS Test 9	80	46	1184
13	LS Test 10	80	19	2284
14	LS Test 11	150	5	4366

**Table 5-1: Laboratory Scale Boilover Study Experimental Results**

**Table 5-1 (continued)**

No.	Test No.	Fuel Thickness (mm)	Initial Storage Temp. (Avg. °C)	Time to Boilover $t_{bo}$ (sec)
15	LS Test 12	200	19	5569
16	LS Test 13	70	11	No boilover
17	LS Test 14	80	13	3725
18	LS Test 15	80	10	2666
19	LS Test 16	80	20	2324
20	LS Test 17	80	19	1746
21	LS Test 18	120	19	3706
22	LS Test 19	160	18	5106
23	LS Test 20	200	18	5627

Based on Table 5-1, for a similar fuel type, differences in boilover time were observed through changes in the amount of fuel. The two tests in which there was no water at the base of the tank did not produce a boilover.

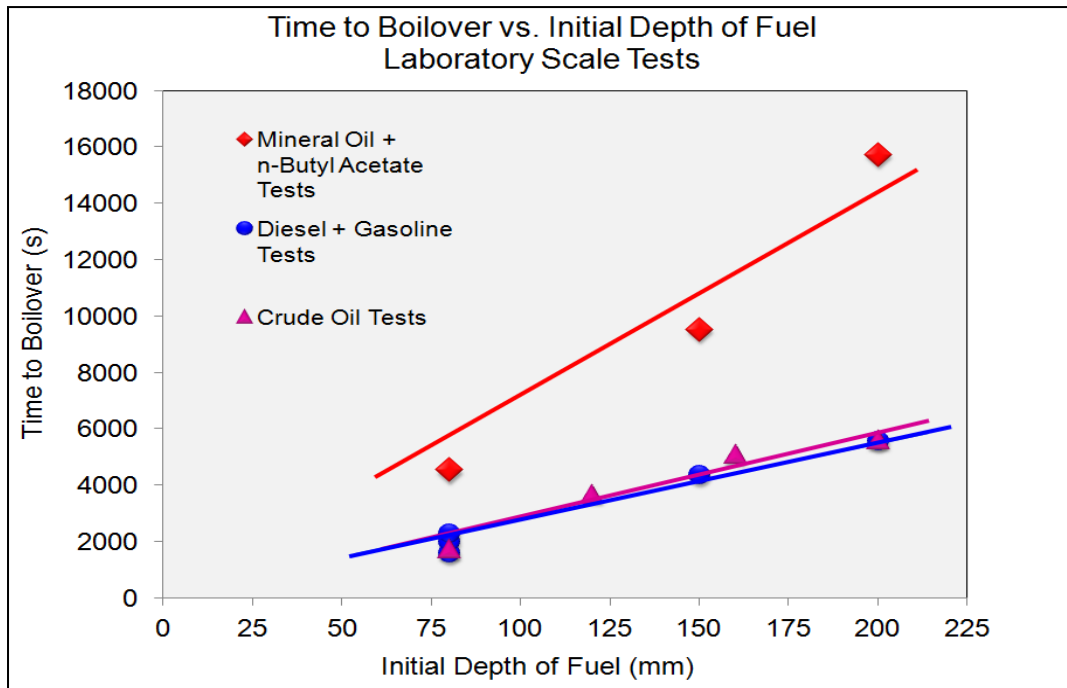
### 5.3.2 Initial Fuel Layer Thickness on Boilover Onset

Figure 5-15 studies the influence of the initial fuel thickness on the time to the onset of boilover for the experimental works conducted in the laboratory scale boilover tests that involved the fuel mixture of mineral oil + n-butyl acetate (LS Test 1, 3 and 5), mixture of diesel + gasoline (LS Test 7, 8, 10, 11 and 12) and crude oil (LS Test 17, 18, 19 and 20). Similar to the observations during the field scale tests, it is also seen that the dependence of the boilover onset time on the initial fuel depth is linear.

Figure 5-15 also shows trend lines that have been outlined to pass through the origin. All the lines have a correlation coefficient greater than 0.90. The equations of the lines take the form shown in Equation 5-1, where  $t_{bo}$  (s) is the time to boilover after the start of heating,  $a$  (s mm<sup>-1</sup>) is the constant of proportionality and  $h_0$  (mm) is the initial depth of fuel.

$$t_{bo} = a h_0$$

**Equation 5-1**



**Figure 5-15: Boilover Onset Time vs. Initial Thickness of Fuel Layer for Laboratory Scale Tests involving mixture of mineral oil + n-butyl acetate, mixture of diesel + gasoline and crude oil**

Table 5-2 below shows the values of the constant of proportionality,  $a$  for the three fuels.

Test	Fuel	$a$ (s mm <sup>-1</sup> )
LS Test 1, 3, 5	Mineral oil + n-butyl acetate	71.54
LS Test 7, 8, 10, 11, 12	Diesel + Gasoline	27.41
LS Test 17, 18, 19, 20	Crude oil	29.25

**Table 5-2: Constant of proportionality for the fuels of Figure 5-15**

As described earlier, boilover starts when the temperature at the fuel-water interface reaches a given value and hence the straight lines in Figure 5-15 can be considered to be representative of a constant, average, apparent thermal penetration rate. Values of the apparent thermal penetration rate, which represent the velocity of heat propagation in the fuel layer, are equal to the inverse of the slope of the boilover onset time versus fuel layer thickness plot (Garo & Vantelon, 1999). The straight line obtained from Figure 5-15 for the diesel + gasoline mixture gives a slope of 27.41 s mm<sup>-1</sup> whilst for the mineral oil + n-butyl acetate, a slope of 71.54 s mm<sup>-1</sup> is obtained. The crude oil test

produced a straight line with a slope of  $29.25 \text{ s mm}^{-1}$ . Therefore, the apparent thermal penetration rates for diesel + gasoline mixture, mineral oil + n-butyl acetate mixture and crude oil are  $0.037$ ,  $0.014$  and  $0.034 \text{ mm s}^{-1}$  respectively. The higher rates of the thermal heat penetration for the diesel + gasoline mixture and crude oil are possibly as a result of the high volatility (i.e. low boiling point of the lighter components of the fuel). High volatility means a faster rate of consumption of the fuel layer and hence will increase the rate of heat production, causing the water to require less time to reach its boiling temperature. Consequently, for the same thickness of fuel layer, the boilover onset occurs sooner for fuel with more volatile light components fuel.

### **5.3.3 Fuel Surface Regression Rate**

Fuel surface regression rates for the experiments were obtained from the analysis of the thermocouple results since the experimental set up for the laboratory scale boilover studies was not equipped with the mechanism to measure the weight loss. The heater cartridges ensured a steady amount of heat supply to the fuel. Hence, temperature measurements were stable once the heating reached the preset temperature. Obviously this temperature had to be higher than the vapour above the surface (vaporised lighter components of the fuel). Consequently whenever a thermocouple at a specified height showed a clear reduction in the measured temperature compared to its lower thermocouple, it was considered that the thermocouple had emerged above the fuel. The fuel surface was hence taken to have regressed to a lower level when the temperature recorded by a particular thermocouple showed a reduction/decrease (with respect to the thermocouple beneath it) and registered unstable fluctuated readings i.e. the thermocouple had emerged from the fuel.

Examples showing the temperature development with respect to time for different thermocouple measurements in the laboratory scale tests are shown in Figure 5-16, Figure 5-18 and Figure 5-20. These results were obtained during laboratory scale test LS Test 5, LS Test 12 and Test 20, respectively.



In LS Test 5, the fuel involved was a 200 mm layer of mineral oil + n-butyl acetate mixture with an initial fuel temperature of 17°C. The temperature near the fuel surface (level 220 mm from the tank base) increased considerably to about 150°C after about 7 minutes of heating. The temperature then displayed a gradual temperature increase to about 180°C before the temperature jumped to about 280°C. Similar trend was observed at lower thermocouples i.e. at the levels of 200 and 190 mm from the tank base. The temperature of 280°C was recorded by the top three thermocouples at about 4800 s after the start of the heating process. The temperature then dropped gradually until it reached the value below 240°C at about 8400 s after the heating started. The drop in the temperature indicated that thermocouples TC22, TC20 and TC19 had appeared outside the liquid fuel. The surface regression rate was then calculated knowing the original depth of liquid and by determining the time at which the highest thermocouple appeared above the liquid.

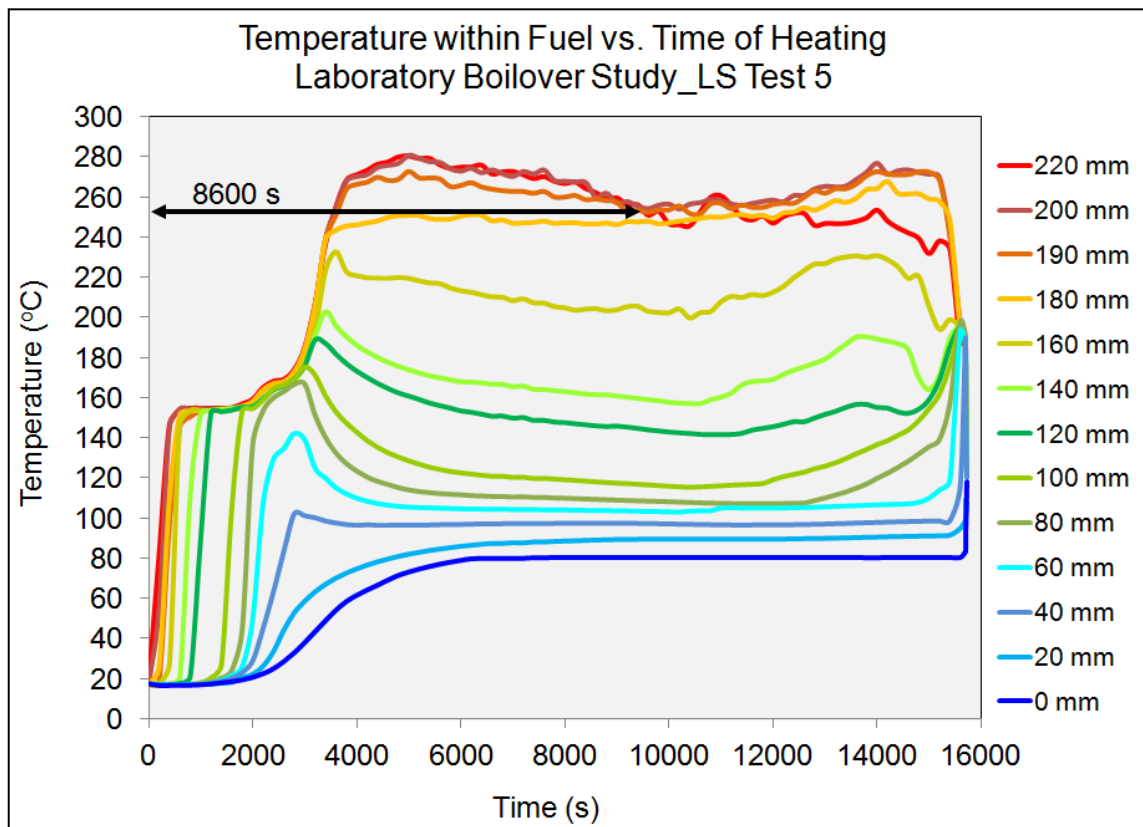
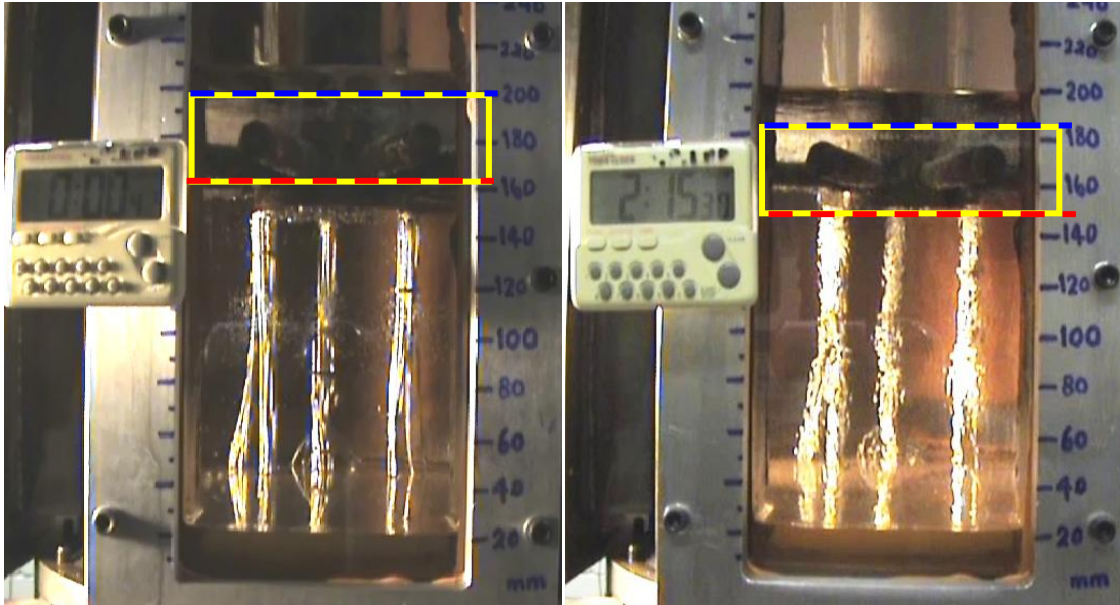


Figure 5-16: Time histories of temperatures for LS Test 5 involving mineral oil + n-butyl acetate



**Figure 5-17: Photos taken during the progression of LS Test 5: (a) Left: Photo taken at the beginning of the test and (b) Right: Photo taken after 8100 s of heating.**

Figure 5-17 shows the progression of the fuel surface throughout the LS Test 5. The figure shows the photo taken at the beginning of the LS Test 5 and at the 8100 s after the heating had started. The yellow box represents the layer of fuel in which the heater elements were immersed. The blue dashed line represents the fuel surface and the red dashed line indicates the bottom of the heater elements. Based on Figure 5-17(b), the fuel surface was observed to have regressed to 190 mm level after about 8100 s of heating. At this point, the thermocouples TC22, TC20 and TC19 had appeared above the liquid fuel.

Similar observations were identified for LS Test 12 as shown in Figure 5-18. The fuel involved was 200 mm layer of diesel + gasoline mixture. Upon heating, the temperature near the fuel surface (TC22 - 220 mm from the tank base) increased to about 175°C after 900 s. Then, after another 3000 s, the temperature increased to about 225°C. Upon reaching this point, the thermocouple showed very unsteady and oscillatory temperature measurements. The temperature measured by the thermocouples TC22, TC20 and TC18 were observed to have dropped below the measured temperature by the TC16. The thermocouples had come out of the fuel and the fuel surface had regressed to a lower level i.e. 180 mm from the base. The top thermocouples TC22, TC20 and TC18 had appeared outside the liquid fuel.

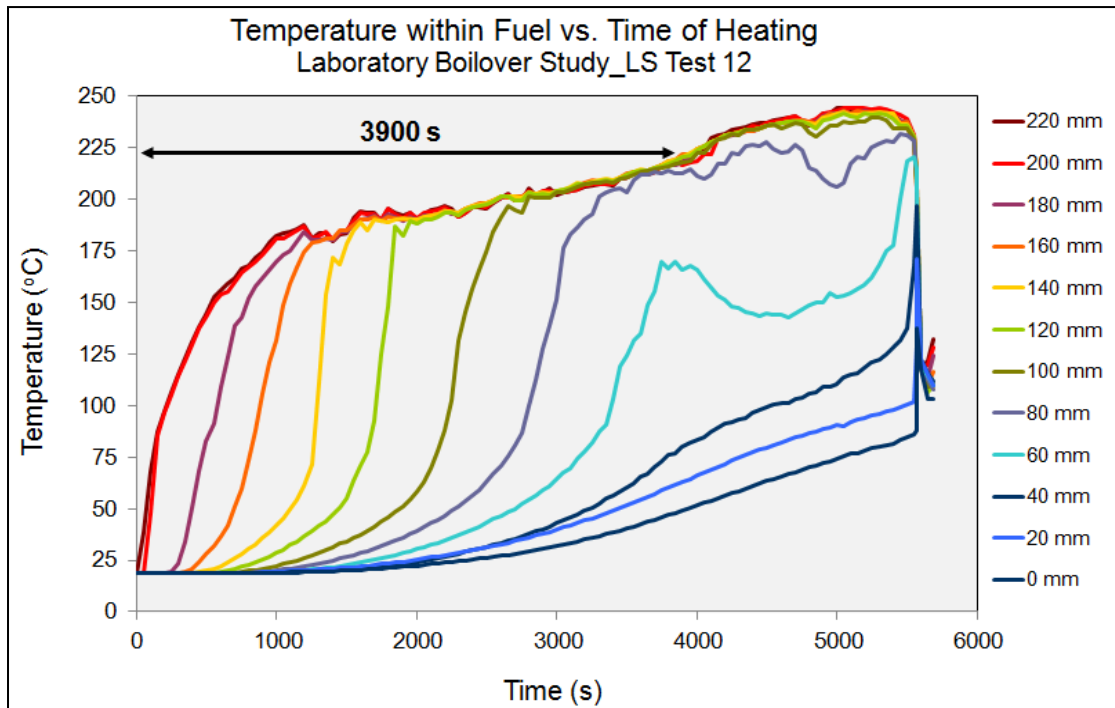


Figure 5-18: Time histories of temperatures for LS Test 12

Figure 5-19 shows the progression of the fuel surface throughout the LS Test 12. The figure shows the photo taken at the beginning of the LS Test 12 and at 4080 s after the heating had started. Based on Figure 5-19(b), the fuel surface was observed to have regressed to a level below 200 mm after about 3900 s of heating.

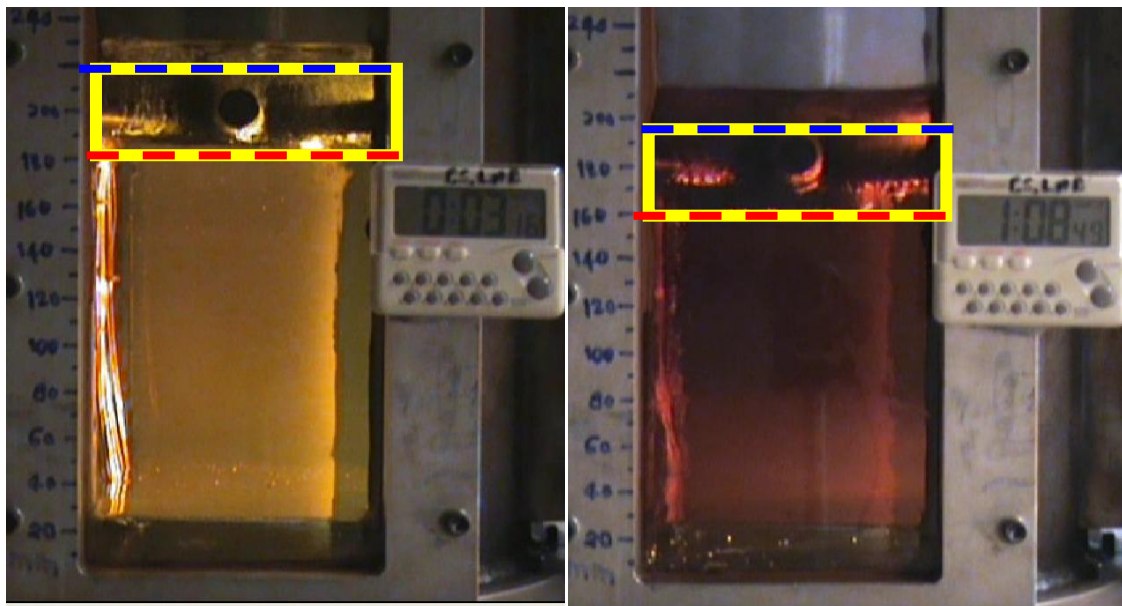


Figure 5-19: Photos taken during the progression of LS Test 12: (a) Left: Photo taken at 180 s after the heating started and (b) Right: Photo taken after 4080 s.

For LS Test 23, in which 200 mm layer of crude oil with an initial fuel temperature of 18.7°C was heated in the boilover rig, the temperature near the fuel surface (TC22 - 220 mm from the tank base) initially increased to about 175°C after about 1020 s of heating. The thermocouple then displayed a gradual temperature increase to about 220°C after 2700 s of heating. Then a drop in the temperature measurement was recorded until the boilover occurred. Similar trends were observed at the subsequent thermocouples i.e. at the levels of 200 and 190 mm from the tank base. The temperature of 260°C was recorded by TC19 at about 3900 s after the start of the heating process. The temperature then dropped gradually until boilover occurred. The drop in the temperature indicated that thermocouples TC22, TC20 and TC19 had appeared outside the liquid fuel.

Figure 5-20 shows the temperature development with respect to time for different thermocouple measurements in LS Test 20 and Figure 5-21 shows the photo of the fuel surface regression throughout the test. Note that the fuel surface had regressed to a level of 170 mm from the base of the tank, as shown in Figure 5-21(b).

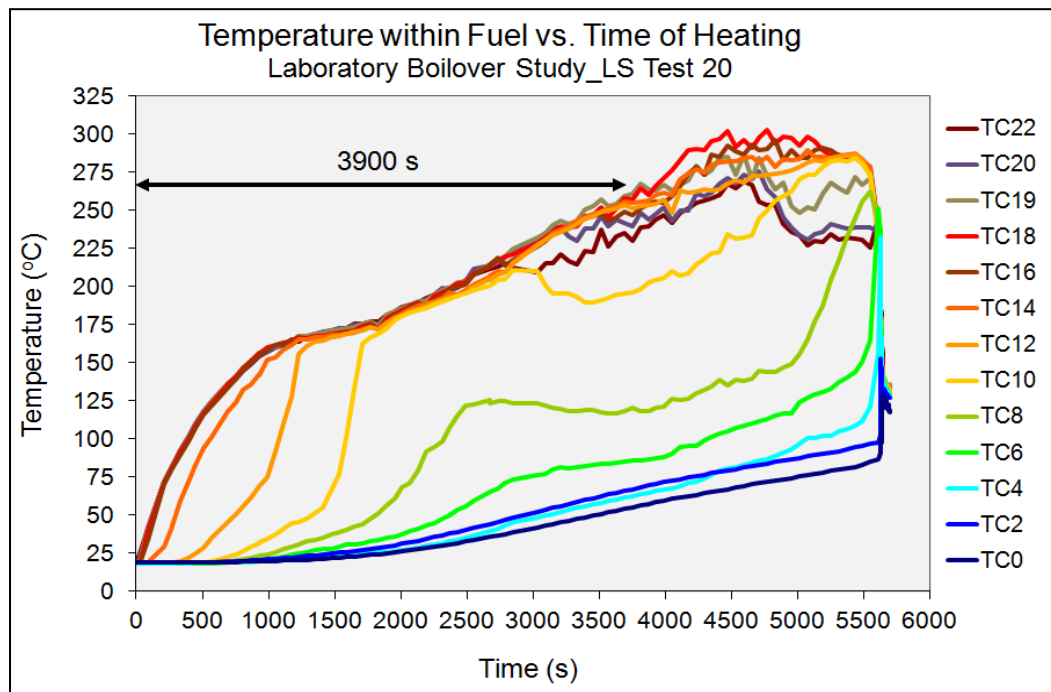


Figure 5-20: Time histories of temperatures for LS Test 20

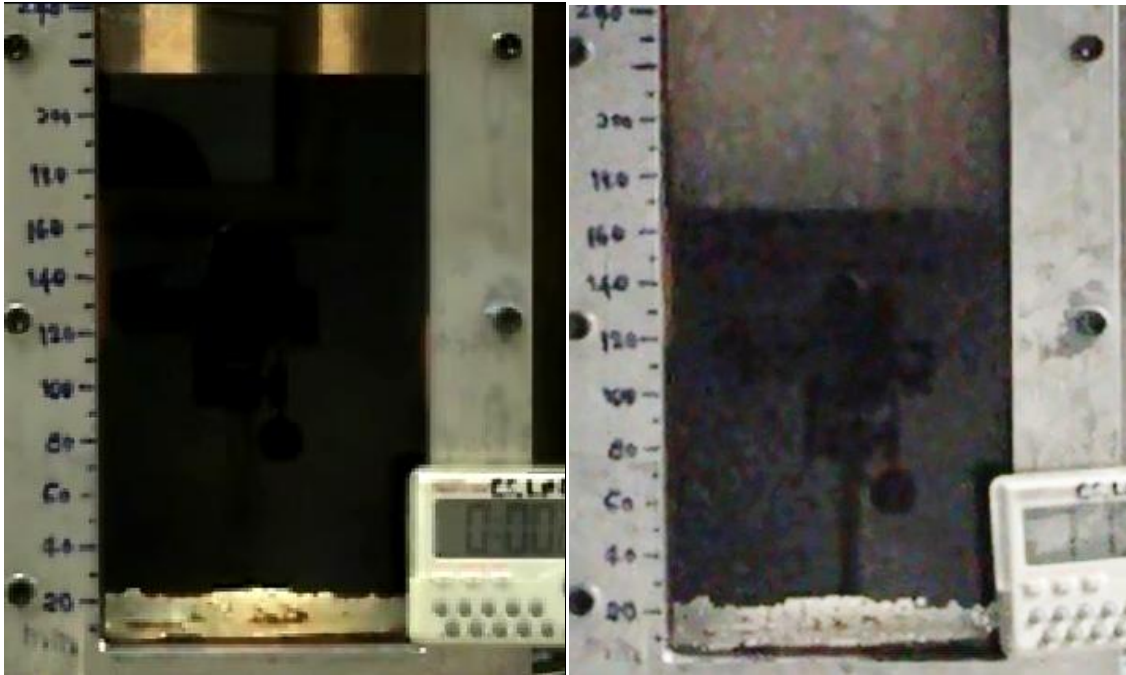


Figure 5-21: Photos taken during the progression of LS Test 20: (a) Left: Photo taken at the beginning of the test and (b) Right: Photo taken after 4500 s

Similar method was applied in determining the surface regression rate for all the laboratory scale tests. Table 5-3 shows the average fuel surface regression rate,  $v_a$  determined for each of the laboratory scale boilover tests.

Test No.	Fuel Mixture	Fuel Thickness (mm)	$v_a$ (mm s <sup>-1</sup> )
LS Prelim 1	70% mineral oil + 30% n-butyl acetate	180	0.008
LS Prelim 2	80% mineral oil + 20% n-butyl acetate	80	0.008
LS Test 1		80	0.009
LS Test 2		80	No regression observed
LS Test 3		150	0.002
LS Test 4		200	0.004
LS Test 5		200	0.005
LS Test 6	80% kerosene + 20% heptane	100	0.028
LS Test 7	80% diesel + 20% gasoline	80	No regression observed
LS Test 8		80	No regression observed
LS Test 9		80	No regression observed
LS Test 10		80	0.017
LS Test 11		150	0.008
LS Test 12		200	0.010

Table 5-3: Average Fuel Surface Regression Rates for the Laboratory Scale Boilover Study

**Table 5-3 (continued)**

Test No.	Fuel Mixture	Fuel Thickness (mm)	$v_a$ (mm s <sup>-1</sup> )
LS Test 13	Gasoline	70	0.024
LS Test 14	Hydrotreated vegetable oil diesel	80	No regression observed
LS Test 15			No regression observed
LS Test 16			No regression observed
LS Test 17	Crude oil	80	No regression observed
LS Test 18		120	0.008
LS Test 19		160	0.008
LS Test 20		200	0.010

The fuel surface regression rates for the laboratory scale tests were found to be low. For the mixture of mineral oil and n-butyl acetate, the surface regression rates were in the range of 0.002 - 0.009 mm s<sup>-1</sup>. The fuel surface regression rates for the mixture of diesel + gasoline were observed to be within the range of 0.008 - 0.017 mm s<sup>-1</sup>. The regression rates for crude oil were in the range of 0.008 - 0.010 mm s<sup>-1</sup>. Both the mixture of diesel + gasoline and crude oil have volatile light components hence showed higher surface regression rates compared with the regression rates for the mixture of mineral oil + n-butyl acetate. Gasoline and mixture of kerosene + heptane are the most volatile fuels amongst those used in the laboratory scale boilover tests and hence showed the highest surface regression rates i.e. 0.024 mm s<sup>-1</sup> for gasoline and 0.028 mm s<sup>-1</sup> for the kerosene + heptane mixture.

The characteristic magnitude of the average fuel surface regression rates determined during the pre-boilover period for the experiments is in agreement with the results of the literature for similar fuels as shown in Table 5-4 below. The results of fuel surface regression rates from the lab scale tests show good agreement with the results presented in the literature. Hence using the thermocouple measurements to gauge the fuel surface regression i.e. the fuel surface was taken to have regressed to a lower level when the temperature recorded by a particular thermocouple showed a reduction/decrease (with respect to the thermocouple beneath it), is acceptable.

Author	Pool Diameter (m)	Fuels	Average Burning Rate (mm s <sup>-1</sup> )
Hasegawa (1988)	0.57	Gasoline	0.053
		80% Diesel + 20% Gasoline	0.030
	0.10 0.20 0.50	80% Diesel + 20% Gasoline	0.010
			0.015
0.023			
Garo <i>et al.</i> (1999b)	0.15	Crude Oil ( $\rho = 845 \text{ kg m}^{-3}$ )	0.011
Torero <i>et al.</i> (2003)	0.15 0.23 0.30 0.50	Crude Oil ( $\rho = 845 \text{ kg m}^{-3}$ )	0.011
			0.014
			0.015
			0.020

Table 5-4: Experimental values of burning rate (surface regression rate) for tanks with diameter below than 1.0 m)

### 5.3.4 Speed of the Base of the Hot Zone

The speed of the base of the hot zone can be estimated through detailed analysis of the temperature profiles in the fuel layer. The temperature profiles within the fuel were determined from time histories of the temperatures at fixed points as shown noted in Figure 5-22 for four tests conducted during laboratory scale boilover study.

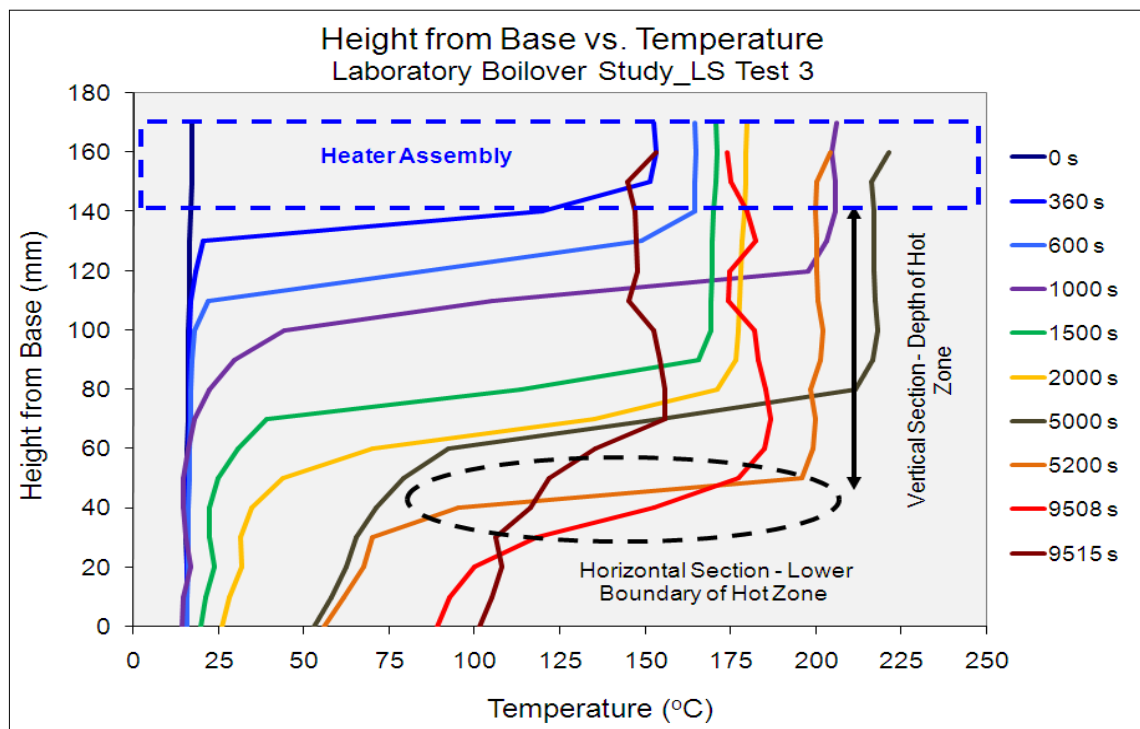


Figure 5-22: (a) Vertical temperature profiles during heating of fuel for LS Test 3: Mineral oil + n-butyl acetate

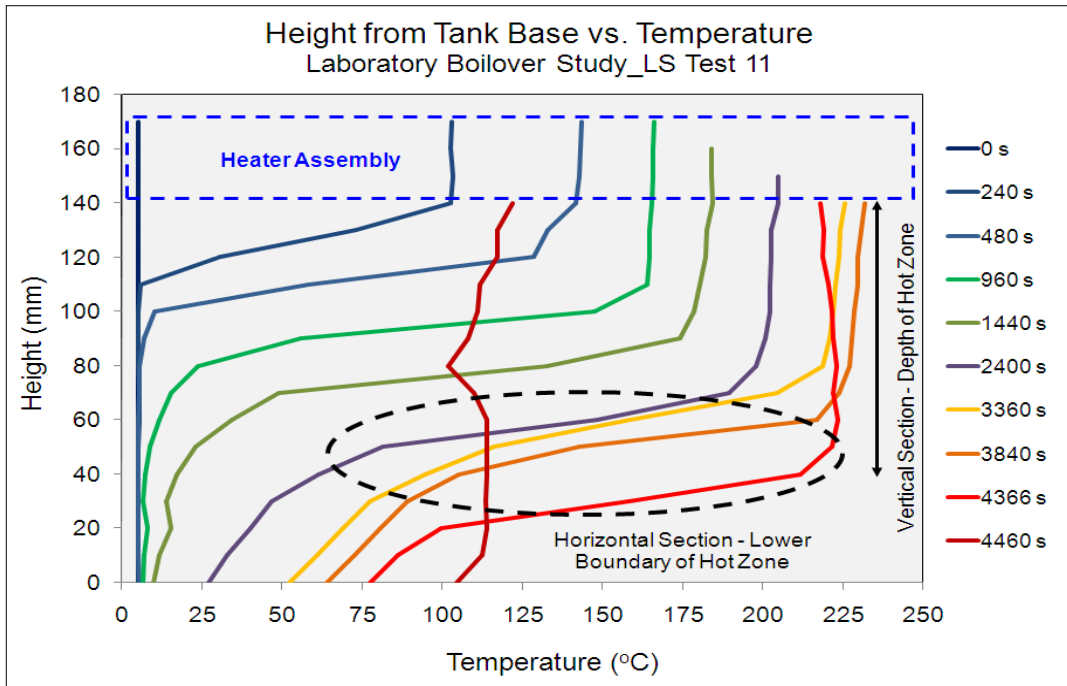


Figure 5-22: (b) Vertical temperature profiles during heating of fuel for LS Test 11: Mixture of Diesel and Gasoline

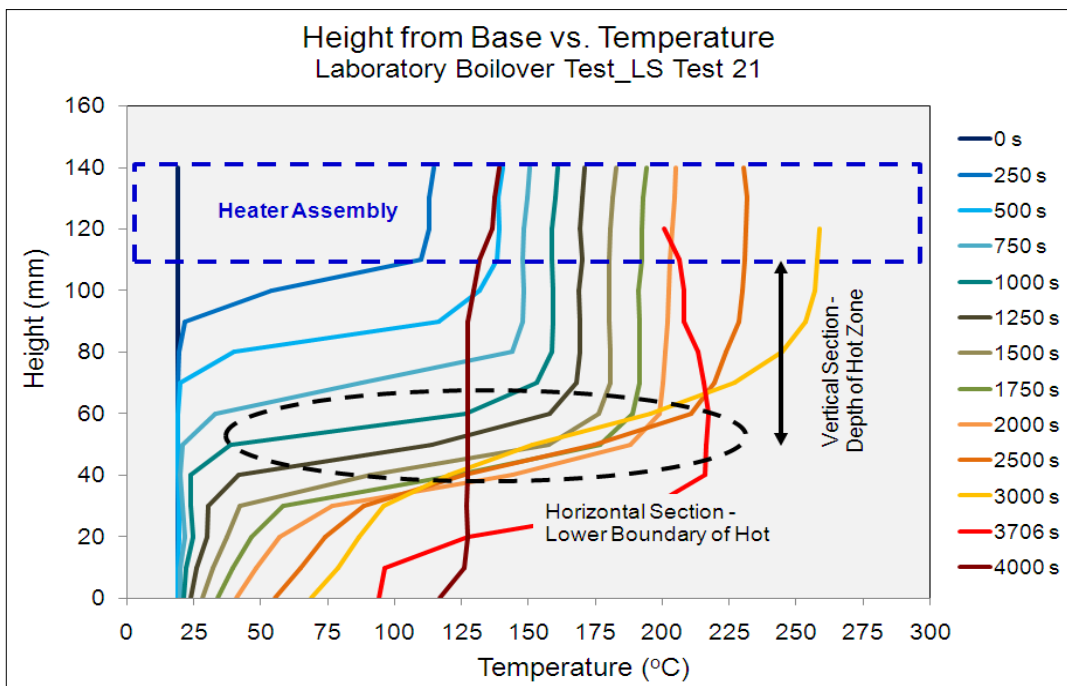
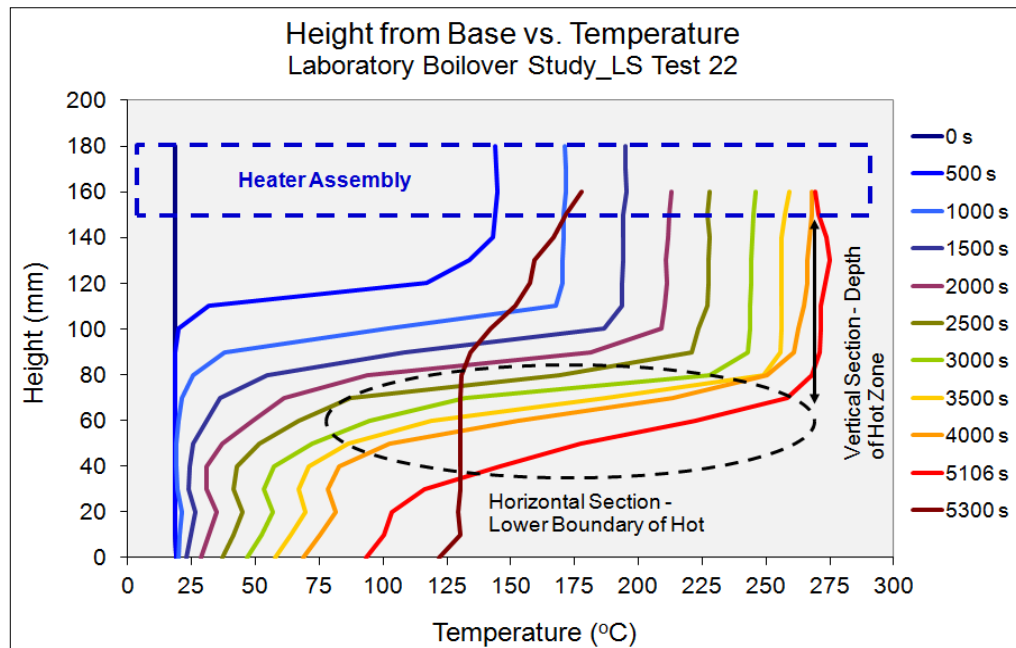


Figure 5-22: (c) Vertical temperature profiles during heating of fuel for LS Test 21: Crude Oil





**Figure 5-22: (d) Vertical temperature profiles during heating of fuel for LS Test 22: Crude oil.**

Data of Figure 5-22 show the formation of a hot zone in the fuel which is a requirement for a boilover to occur. The data could be used to determine the thickness of the hot zone and the interface between the hot and cold fuel zone. The vertical section of the temperature profiles below the region of the heater assembly in the figures was used to approximate the hot zone thickness. Since the interface between the hot zone and cold fuel zone could not be distinguished directly from the figures, the horizontal section (or the approximately horizontal section) was assumed as the base of the hot zone i.e. the hot-cold interface.

Consequently, as the hot-cold interface approached the water layer at the tank base, the temperature of the water was raised to its boiling point whilst a substantial depth of hot fuel remained above the water. Once the water started to boil, rapid mixing between the water and the hot fuel was initiated. This resulted in enhanced heat transfer and vigorous boiling in which large amount of steam were generated. As a result, hot fuel was ejected or was pushed upwards. The time for the hot-cold interface to reach the water layer after the heating started will depend on the velocity of heat propagation into the fuel layer. This velocity is represented by the speed of the base of the hot zone.

The speed of the base of the hot zone was estimated by determining the time required for the hot zone lower boundary to reach a specific depth. The base of the hot zone was said to reach certain depths of the fuel when a temperature of 110°C was measured and recorded by the thermocouple at a specific height from the tank base. Boilover occurrence was also observed when the temperature at the fuel-water interface reached such a temperature. The speed of the base of the hot zone was then calculated on the basis that the assumed temperature of 110°C reached specific depths of the fuel at specific times. Table 5-5 shows the average and maximum hot zone growth rates of the boilover tests for the laboratory scale boilover study.

Test	Fuel Type	Fuel Thickness (mm)	Average Speed of Base of Hot Zone	Maximum Speed of Base of Hot Zone
			(mm/s)	(mm/s)
LS Prelim 2	70% Mineral Oil + 30% n-Butyl Acetate	180	0.075	0.169
LS Prelim 3	80% Mineral Oil + 20% n-Butyl Acetate	80	0.054	0.081
LS Test 1		80	0.047	0.117
LS Test 2		80	0.055	0.127
LS Test 3		150	0.060	0.132
LS Test 4		200	0.039	0.111
LS Test 5		200	0.071	0.119
LS Test 6		80% Kerosene + 20% Heptane	120	0.109
LS Test 7	80% Diesel + 20% Gasoline	80	0.110	0.370
LS Test 8		80	0.093	0.385
LS Test 9		80	0.152	0.556
LS Test 10		80	0.101	0.385
LS Test 11		150	0.098	0.371
LS Test 12		200	0.056	0.185
LS Test 13	Gasoline	70	0.035	0.038
LS Test 14	Biodiesel	80	0.048	0.172
LS Test 15			0.045	0.161
LS Test 16			0.086	0.172
LS Test 17	Crude Oil	80	0.224	0.556
LS Test 18		120	0.135	0.769
LS Test 19		160	0.141	0.625
LS Test 20		200	0.156	0.833

**Table 5-5: Data of Speed of the Base of the Hot Zone for Laboratory Scale Boilover Study**

Comparing the fuel surface regression rate from Table 5-3 to the speed of the base of the hot zone in Table 5-5, it is observed that the latter, mostly, provides higher values. This observation indicates that the thermal front moved faster than the fuel surface and hence an isothermal layer was formed due to the distillation process taking place within the fuel. The observation described above is true except for the LS Test 13. The burning rate for the test was not significantly different from the heat front's average penetration velocity. This seems to indicate that only a thin hot zone was formed just beneath the location of the heater assembly.

Table 5-5 shows that the average speed of the base of the hot zone for crude oil is  $0.135 - 0.224 \text{ mm s}^{-1}$ , diesel is  $0.044 - 0.058 \text{ mm s}^{-1}$ , gasoline is  $0.035 \text{ mm s}^{-1}$  and for the mixture of diesel + gasoline is  $0.056 - 0.152 \text{ mm s}^{-1}$ .

### **5.3.5 Influence of Initial Fuel Temperature**

There is a concern in different geographical areas that high (or low) ambient (storage) temperature could affect the boilover occurrence and hence contribute to serious safety issue concerning fuel storage facilities. In order to understand further the boilover phenomenon, tests were carried out to study whether the initial fuel storage temperature would influence the boilover onset time.

Since it is difficult to preset the fuel storage temperature for tests conducted outdoor, experiments to analyse the effect of the initial storage temperature were conducted in the laboratory scale study. The experiments were conducted for 80 mm of fuel layer thickness of mineral oil + n-butyl acetate and diesel + gasoline mixture respectively.

LS Test 1 and LS Test 2 were carried out involving the mixture of mineral oil and n-butyl acetate at the initial storage temperature of  $17^{\circ}\text{C}$  and  $45^{\circ}\text{C}$  respectively. As shown Table 5-1, the boilover onset time for LS Test 1 was 4520 s and for LS Test 2 was 968 s.

LS Test 7, LS Test 8 and LS Test 9 which involved the mixture of diesel + gasoline were carried out with the initial temperature of 16°C, 18°C and 46°C respectively. Table 5-1 shows the boilover onset time for LS Test 7 was 1605 s, for LS Test 8 was 1999 s and for LS Test 9 was 1184 s.

The results, though limited, indicate that in a case of storage tank fires with a possibility of boilover occurrence, a higher initial fuel temperature will contribute to a shorter onset time. A boilover occurs sooner if the initial temperature is higher because of the heat transfer – less heat is required to raise the temperature of the fuel to the boiling points of its components.

### **5.3.6 Heating Temperature vs. Boilover Onset**

One of the main highlights from the literature analysis on boilover includes the findings that the energy for hot zone came from the burning flame directly. About five per cent of the total heat release from the flame was transferred to the fuel, and a small amount of this energy being transferred was used for the hot zone (Koseki, 1994 and 1999).

During the development of a heat transfer model of a burning fuel floating on water in order to predict the time to boilover, Garo, Gillard, Vantelon and Fernandez-Pello (1999a) established the dependence of the onset time on the fuel's burning rate, and thus the surface heat flux. As the surface heat flux increased (because the pool diameter was increased), the liquid is heated up faster and the water reached the boiling condition sooner. These works, among others, have shown the importance of the surface heat flux and hence the radiative heat feedback to the fuel on the time to boilover. Because the radiative feedback from the flame to the fuel sustaining a fire is difficult to calculate or measure, or to be predetermined prior to the conduct of a burning test, laboratory scale experiments were performed to investigate the effects of varying the heat absorbed by the fuel on the boilover onset time.

The effects of varying the heating temperature, simulating changes in the radiative heat feedback to the fuel in an actual fire were examined by comparing the time to boilover of the three experiments on biodiesel, namely LS Test 14, LS Test 15 and LS Test 16. The results in Table 5-1 show that a boilover event occurred for all the experimental works involving the biodiesel. It was noted that the time to boilover increased as the temperature of the heating was decreased. By reducing the heating temperature, a longer time elapses before boilover occurs. Figure 5-23 shows the effect of varying the heating temperature on the boilover onset time.

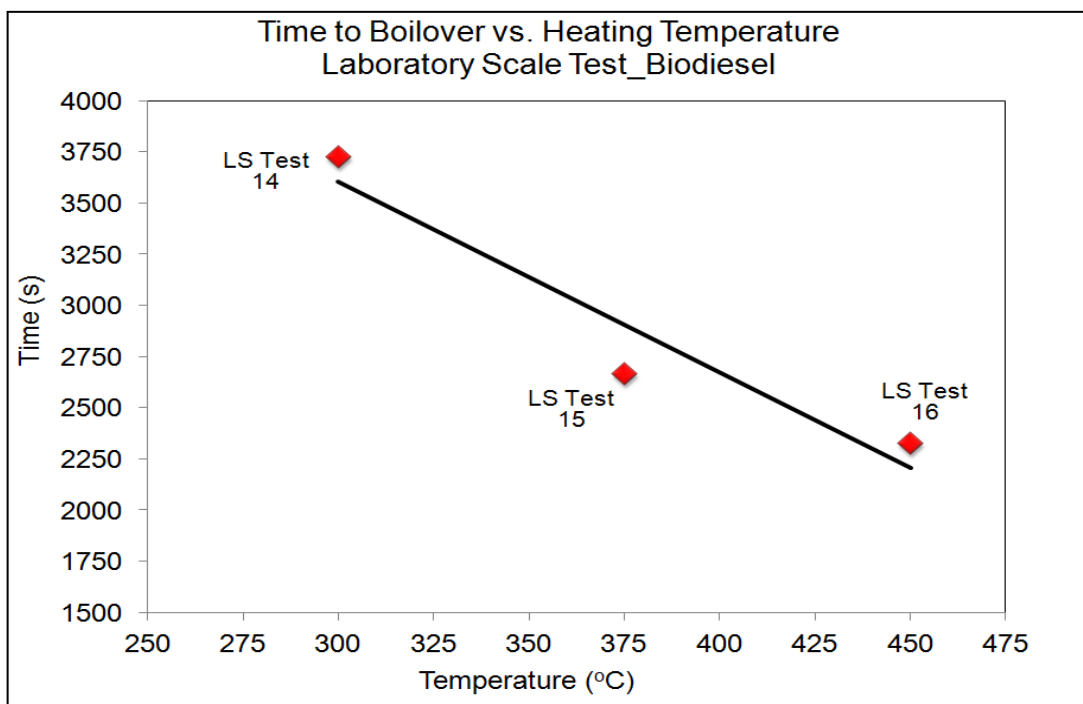


Figure 5-23: Effect of heating temperature on the time to boilover

The significant of the results is that by reducing the heating temperature i.e. by limiting the heat absorbed by the fuel from the fire, the time to boilover could be prolonged and even to the extent of eliminating the phenomenon.

#### 5.4 TEMPERATURE PROFILES WITHIN THE LIQUID LAYER – EVOLUTION OF TEMPERATURE WITH TIME

In this section, the behaviour of the fuel temperature during the progress of the heating process is analysed by considering the evolution of the temperature

with time within the fuel. The aim is to investigate whether or not the laboratory scale tests produce similar results and behaviour as that observed in the field scale tests. For the analysis, the fuel temperature was plotted versus the heating time for each test and the data recorded by the thermocouples were reviewed based on the progression of the heating process.

The evolutions of the fuel temperature during laboratory scale boilover tests are shown in Figure 5-24, Figure 5-25, Figure 5-26 and Figure 5-27. Each figure represents the temperature profiles within the fuel during the progression of the experiments.

### 5.4.1 Crude Oil Tests

All the tests involving the crude oil have shown a similar temperature evolution which is detailed by the following Figure 5-24.

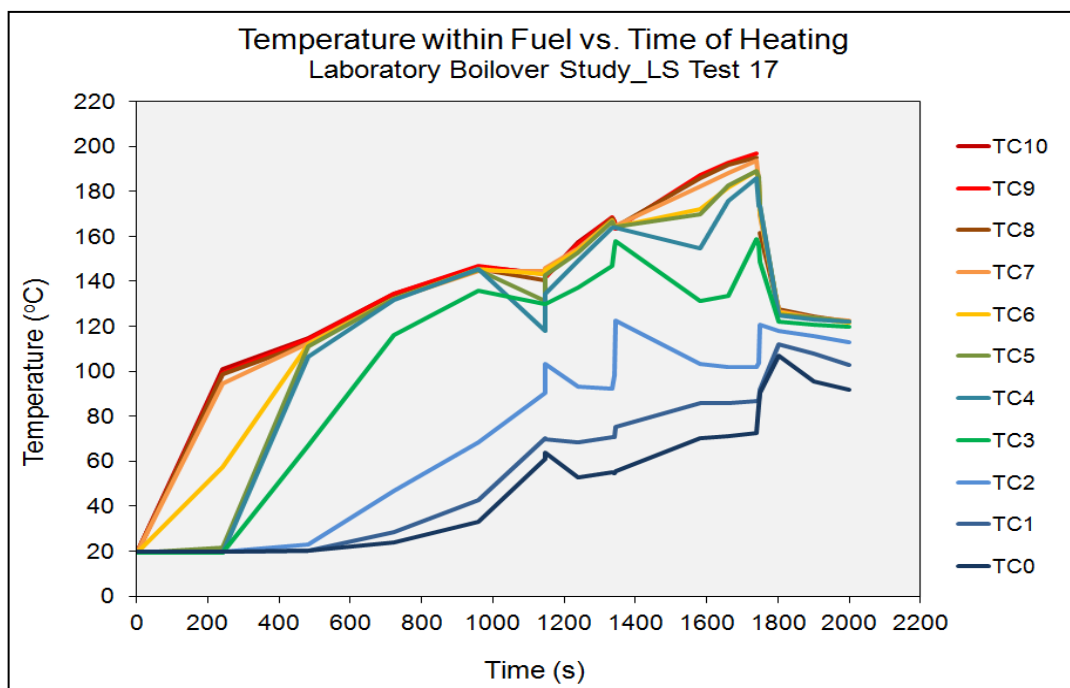
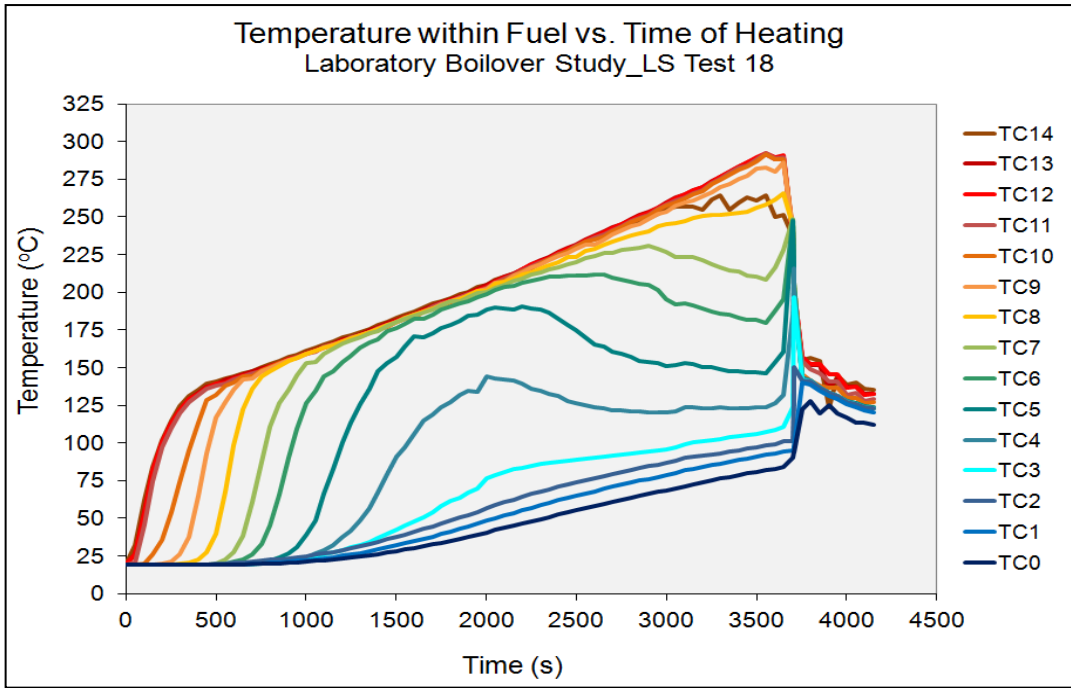
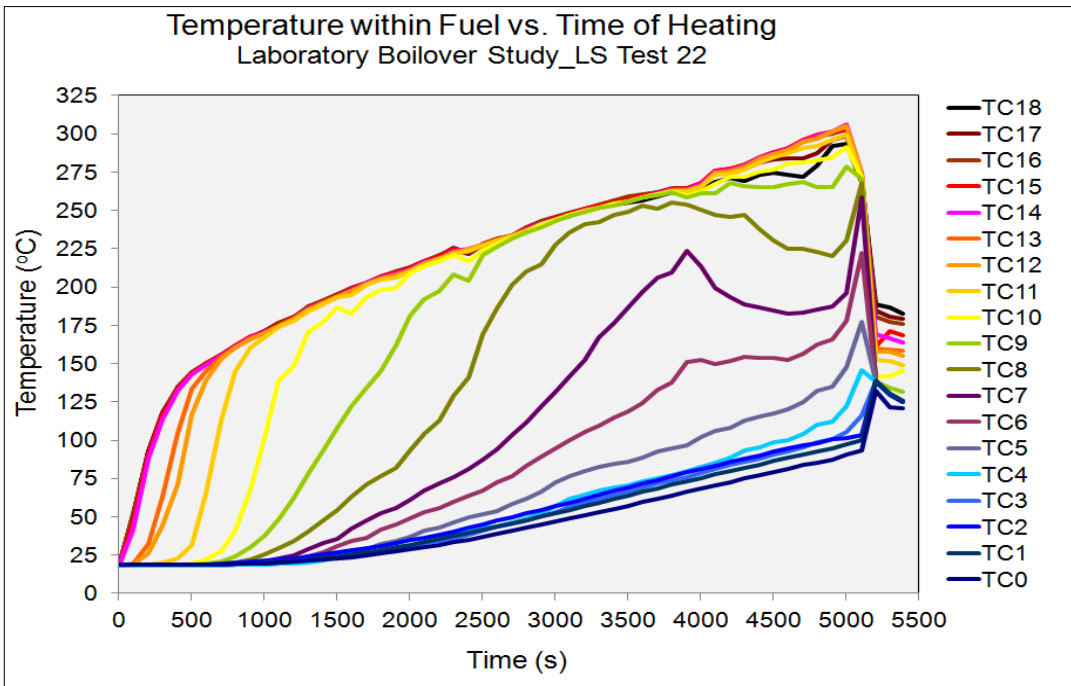


Figure 5-24: (a) Evolution of temperature in the crude oil for Laboratory Boilover Study LS Test 17



**Figure 5-24: (b) Evolution of temperature in the crude oil for Laboratory Boilover Study for LS Test 18**



**Figure 5-24: (c) Evolution of temperature in the crude oil for Laboratory Boilover Study for LS Test 22**

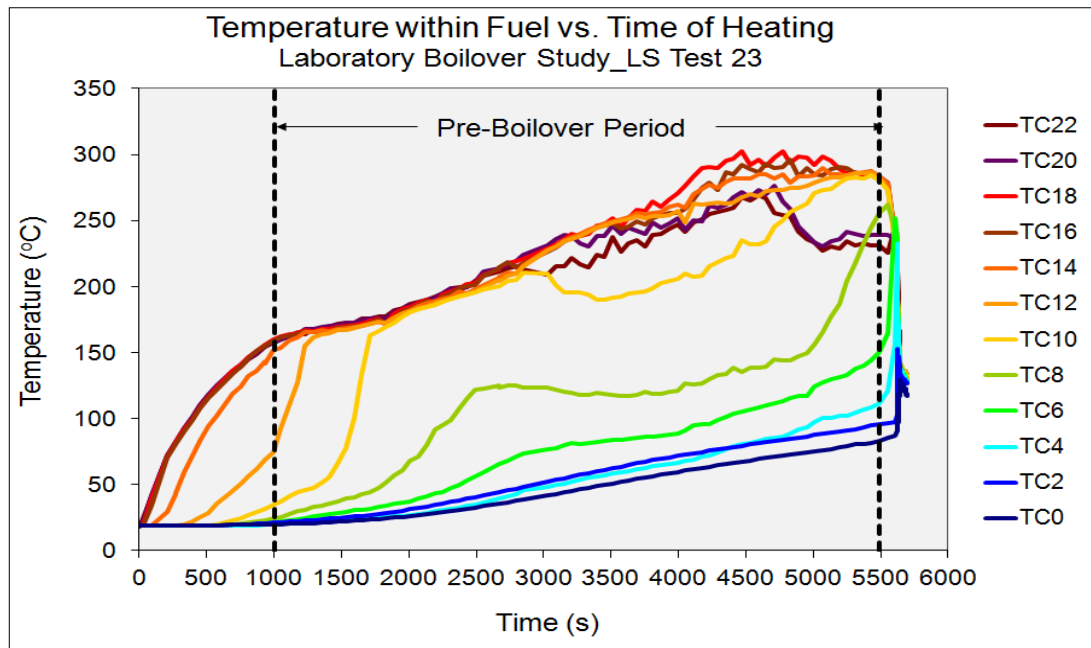


**Figure 5-24: (d) Evolution of temperature in the crude oil for Laboratory Boilover Study for LS Test 23**

In order to compare the observation of the large scale test with the laboratory boilover study, the next paragraphs will discuss the temperature development for the LS Test 23 conducted in the lab as shown by Figure 5-24(d).

The temperature near the surface (recorded by TC16 - TC22) increased up to about 160 - 170°C after 900 s of heating. Most of the lighter components within this layer of fuel (about 60 mm thickness) had vaporized during this period. As a basis for comparison with the equivalent large scale test, this instance would be considered the start of the pre-boilover period or the stationary burning period. Fifteen minutes later, the lower thermocouples (TC10 - TC14) also show similar temperature rises. The temperature continues to increase to about 220°C, after about 3900 s of heating, when the upper thermocouples started to show a decrease with sharp fluctuation in the values measured. The thermocouples (TC20-TC22) would be assumed to have come out of the fuel.

The temperature of the bulk fuel continues to increase gradually. This slow increase in the temperature indicates that within this layer, the lighter components have been vaporised and hence, the other components require more heat for evaporation. After more than 5400 s of heating, thermocouples



TC10 - TC18 show value of about 280°C and TC3, the thermocouple close to the fuel-water interface, displays a value of 120°C. Moments later, a boilover occurred. At this instance, the thermocouple at the interface TC2 has reached the boiling point of water. The boiling lasts for a short period during which all the thermocouples showed values fluctuating around a fixed temperature of 130°C. In this particular test, this phase, which is the end of the pre-boilover phase and the start of fully developed boilover, begins at 5627 seconds (1 hour 34 minutes).

The values of temperature reached by the thermocouples during the pre-boilover, boilover and post-boilover periods for LS Test 23 are presented in Table 5-6. As regards to the maximum temperature for the stationary burning phase, the values are determined by extracting the largest number recorded within the period of 900 to 5400 s of the test. The temperature for the period of boilover is taken as the average of the values measured during the fully developed stage of the phenomenon (in this test, within 5580 to 5640 s). In the final transition phase, the temperature values of each thermocouple are reached by averaging the measured data from 5640 s to the end of the test (the heating was stopped at 5700 s).

Thermocouple TC (Height in mm)	Maximum Temperature in Pre- Boilover Period (°C)	Average Temperature during Boilover (°C)	Average Temperature in the Post-boilover Period (°C)
22 (220)	272	197	134
20 (200)	280	184	135
18 (180)	306	187	136
16 (160)	300	185	136
14 (140)	294	186	138
12 (120)	287	185	140
10 (100)	286	189	141
8 (80)	260	188	139
6 (60)	153	186	138
4 (40)	114	184	137
3 (30)	100	171	134
2 (20)	96	130	133
1 (10)	91	111	133
0 (0)	84	103	128

**Table 5-6: Temperatures for each thermocouple at various stage of LS Test 23**

The values presented by the thermocouples located within the bulk fuel (TC3 – TC22), when changing over from pre-boilover to boilover periods, show a decrease in temperature. The drop is due to the cooling effects produced by the water vapour bubbles. The thermocouples immersed in the water layer (TC0 – TC2), show an increase in temperature when moving across from the pre-boilover to boilover periods. A significant observation from all the laboratory scale experiments on crude oil, was that the average temperature measured at the fuel-water interface during the boilover period was about 110°C. This is similar to the minimum temperature of the fuel-water interface set for the occurrence of the boilover in previous studies (Inamura *et al.*, 1992; Garo *et al.*, 1999a; Koseki *et al.*, 2003 & 2006).

#### 5.4.2 Diesel-Gasoline Test

Figure 5-25 shows the evolution of temperature measured within the diesel-gasoline fuel mixture during the progress of the boilover study conducted in laboratory experiments. In these experiments, similar to the crude oil tests, boilover was observed after long period of heating.

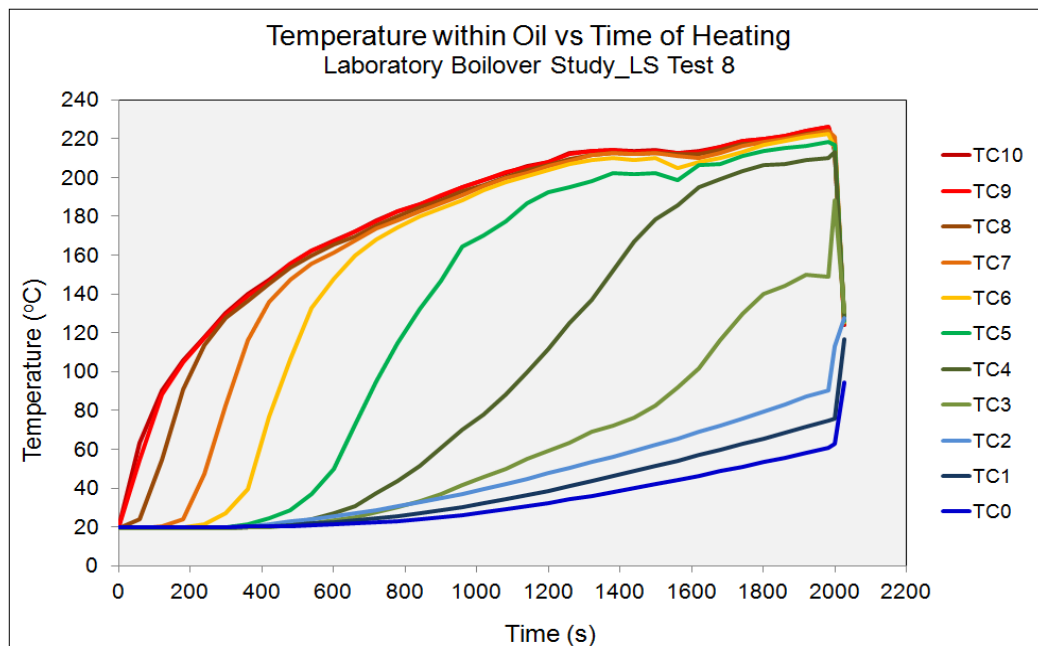


Figure 5-25: (a) Evolution of temperature in diesel-gasoline fuel mixture for laboratory scale boilover test LS Test 8

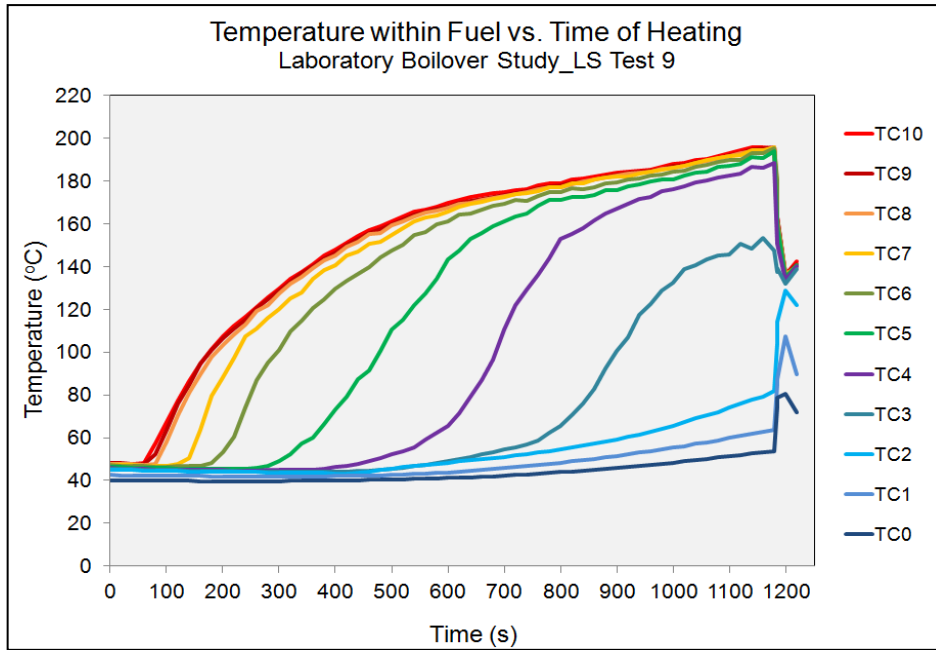


Figure 5-25: (b) Evolution of temperature in diesel-gasoline fuel mixture for laboratory scale boilover study LS Test 9

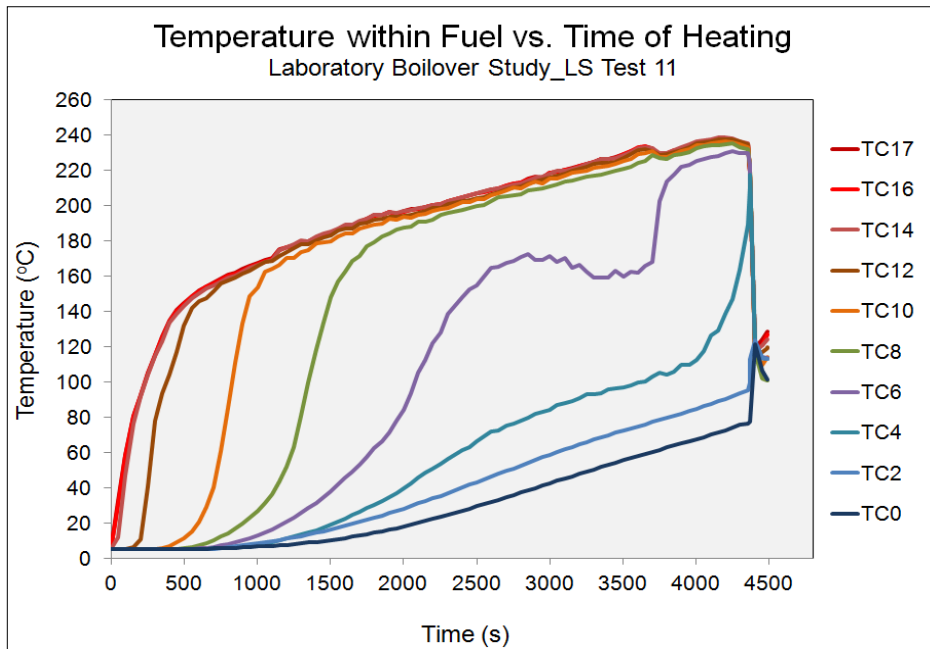
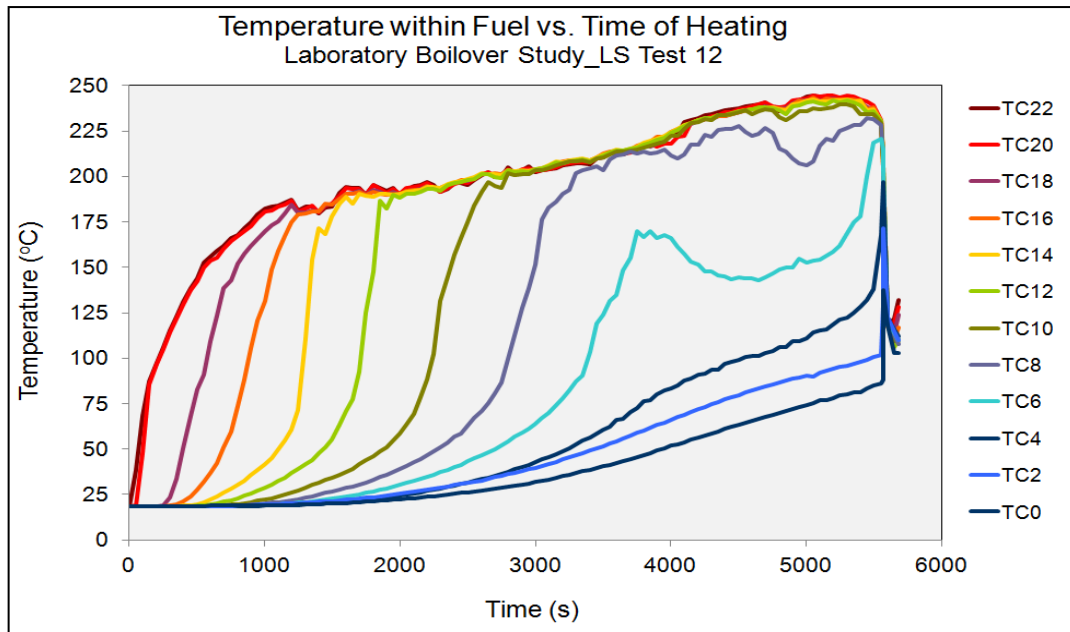


Figure 5-25: (c) Evolution of temperature in diesel-gasoline fuel mixture for laboratory scale boilover study LS Test 11



**Figure 5-25: (d) Evolution of temperature in diesel-gasoline fuel mixture for laboratory scale boilover study LS Test 12**

The behaviour of temperature development throughout all the tests with the mixture of diesel + gasoline was not very different from that described for the tests involving crude oil. All the thermocouples immersed within the fuel showed an increase in the temperature measured from the start of the experiments and remained at a fixed value between 175 to 200°C up to about 3000 s of heating, as clearly seen in laboratory test LS Test 12. There was a temperature drop detected at the top thermocouples at about 4000 s at which time the fuel surface was deduced to have regressed from the initial position to below thermocouples TC20-22.

The values of temperature reached by the thermocouples during the pre-boilover, boilover and post-boilover periods for the diesel-gasoline fuel mixture test LS Test 12 are presented in Table 5-7.

The values presented by the top thermocouples located within the bulk fuel, in all the experiments, when changing over from pre-boilover to boilover period, show a decrease in temperature as presented by Table 5-7. This observation is in agreement with the results obtained in the field scale tests involving the burning of the diesel + gasoline mixture as reported in Section 3.3.2. The

reason for this observation was due to the rising of water vapour bubbles, the temperature of the bulk fuel drop during the boilover period.

Thermocouple Height (mm)	Max. Temperature in Pre-Boilover Period (°C)	Avg. Temperature during Boilover (°C)	Avg. Temperature in the Post-boilover Period (°C)
220 (TC22)	245	230	141
200 (TC20)	245	233	142
180 (TC18)	244	233	141
140 (TC14)	243	232	139
100 (TC10)	241	231	140
60 (TC6)	193	221	142
30 (TC3)	109	122	147
20 (TC2)	98	112	138
10 (TC1)	92	94	125
0 (TC0)	83	85	121

**Table 5-7: Temperatures for each thermocouple at various stages of the LS Test 12**

The thermocouples immersed in the water layer (TC0, TC1 and TC2) show an increase in temperature when moving across from the pre-boilover to boilover periods.

### 5.4.3 Gasoline Test

Figure 5-26 shows the temperature evolution during a gasoline test LS Test 14. The test with gasoline presents information regarding the temperature evolution in a test in which there was no occurrence of boilover.

The behaviour in the early stage of the gasoline test was similar to that described for the crude oil and the diesel + gasoline mixture. When heating was started, there was an increase in the temperature measured by the thermocouples.

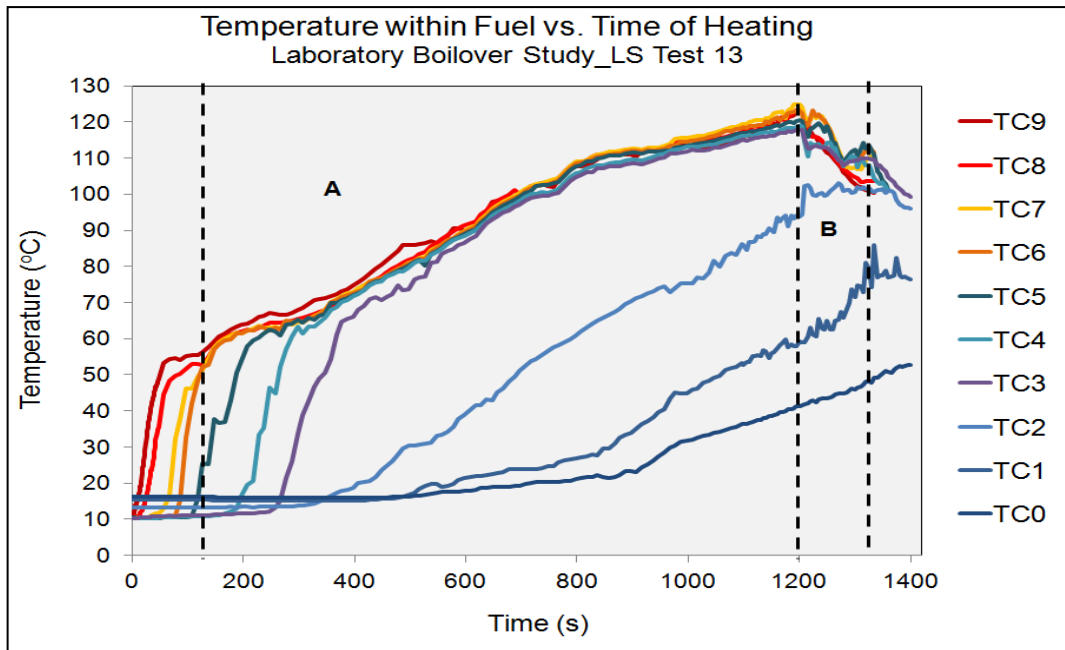


**Figure 5-26: Evolution of temperature in gasoline for LS Test 13**

In Figure 5-26, the top thermocouple TC9 (at level 90 mm) initially recorded a sharp increasing value until it reaches a temperature of about 60°C. Then the temperature showed a steady increase up to about 110 to 120°C.

The adjacent thermocouples TC3 - TC8 (at level 30 to 80 mm) also showed a steep increase in temperatures up to about 60°C initially, from which the subsequent temperature increase then became less steep. This period, from 100 to 1000 seconds, indicated that the gasoline was vaporising steadily. Moments later, the temperature measured by these thermocouples showed a sudden drop. This drop indicated that the fuel level had fallen below the thermocouples were by now had been exposed outside the fuel.

The thermocouples immersed in the water did not show any significant increase in temperature until after about 600 seconds of heating. Figure 5-26 shows that after about 600 seconds, the temperature at level 20 mm increased more rapidly to a value that was stable through to the final period of the heating process. The temperature rise, on the whole, continued until the start of the final transition which is manifested by the dramatic drop of temperature measured by most of the thermocouples. The thermocouples display temperature increases from the start of heating. A drop in the temperature readings from about 125°C

to 100°C then was observed at about 1200 s. The temperature drop recorded by the top thermocouples (TC5-TC9) was a result of them appearing above the gasoline surface.

A study was made of the temperature evolution for each thermocouple throughout the test. The determination of the temperatures was done differently because of the non-occurrence of boilover. The analysis was divided into two parts: (i) Part A, for the period at which the temperature increase was less steep, and (ii) Part B, after the temperature drop had occurred, as shown in Figure 5-26. Table 5-8 presents the maximum temperatures reached by each thermocouple during the gasoline test.

Thermocouple Height (mm)	Max. Temperature in Stationary Period A (°C)	Max. Temperature in Stationary Period B (°C)	Max. Temperature in the Final Transition Period (°C)
90 (TC9)	124	112	96
80 (TC8)	124	113	99
70 (TC7)	125	119	104
60 (TC6)	124	119	103
50 (TC5)	120	119	102
40 (TC4)	119	114	101
30 (TC3)	118	113	105
20 (TC2)	96	103	101
10 (TC1)	61	86	82
0 (TC0)	41	50	55

**Table 5-8: Temperatures for each thermocouple at various stages of the gasoline experiments**

An important fact to note is that, in the experiments with gasoline, there was no evidence of overheating of the water layer. As shown in Table 5-8, the thermocouples at the fuel-water interface TC2 (at level 20 mm) did not reach the minimum temperature assumed for boilover occurrence (110°C as mentioned in Subsection 5.3.4) and only sporadically reached 100°C. This could be related to the fact that the boiling temperatures of most compounds in gasoline are below 100°C.

#### 5.4.4 Biodiesel Test

Figure 5-27 shows the temperature evolution of biodiesel test LS Test 15. The figure shows the progression of the test with a boilover. The figure shows that as the heating was started, there was an increase in the temperature measured by the thermocouples. All the top thermocouples from the height of 80 mm to 100 mm from the base of the tank showed a gradual increase in temperature up to 260°C within 1200 - 1300 s of the heating process. The temperature readings then remained between 260°C to 270°C before the boilover occurred at about 2666 s after the heating started.

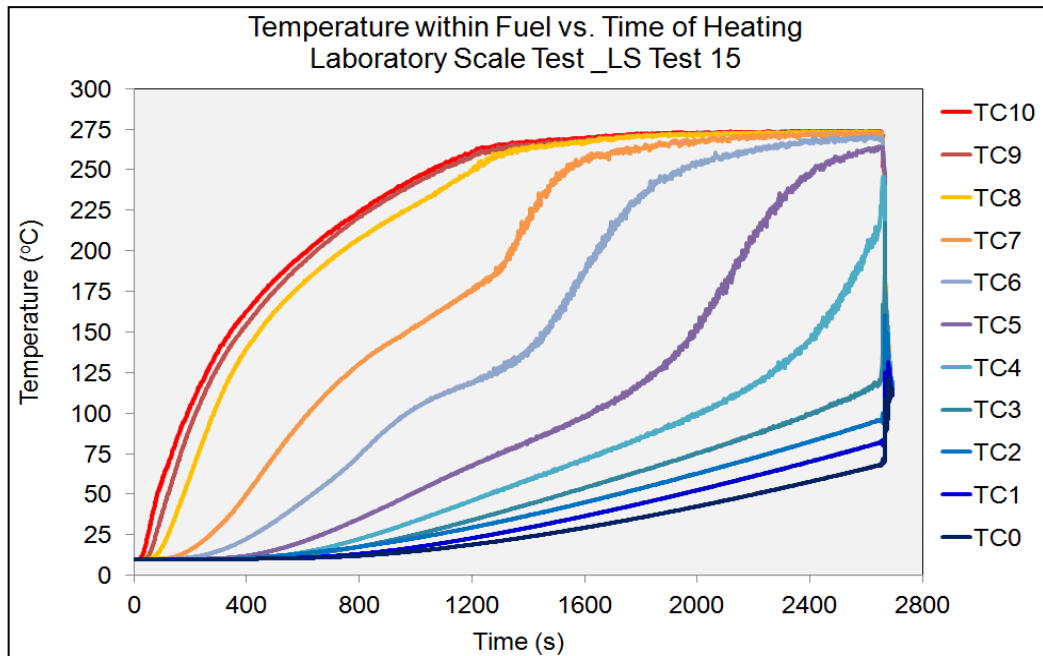


Figure 5-27: Evolution of temperature in biodiesel for LS Test 15

An analysis was carried out to look in more details at the temperature evolution for each of the thermocouples in the diesel test. Table 5-9 presents the temperatures reached by each thermocouple during the diesel test. The pre-boilover period was between the start of heating until the period of 2655 s. The boilover period was between 2660 s to 2675 s of heating. The post-boilover period was between 2975 s until the 2690 s when the heating was terminated.

Based on Table 5-9, the thermocouple at the interface (TC2) reaches a value up to about 160°C. As in all the tests in which a boilover occurred, there is



evidence of overheating of the water layer as the thermocouple at the fuel-water interface in LS Test 15 presented a temperature beyond the evaporation point of water.

Thermocouple Height (mm)	Max. Temperature in Pre-Boilover Period (°C)	Avg. Temperature during Boilover (°C)	Avg. Temperature in the Post-boilover Period (°C)
100 (TC10)	274.093	251.93	152.195
90 (TC9)	273.813	253.984	152.381
80 (TC8)	273.502	259.058	152.568
70 (TC7)	273.004	261.58	153.284
60 (TC6)	270.732	260.054	153.097
50 (TC5)	264.568	257.907	152.942
40 (TC4)	222.732	245.673	152.661
30 (TC3)	120.848	217.502	148.148
20 (TC2)	95.914	160.381	137.782
10 (TC1)	82.125	125.486	131.556
0 (TC0)	68.335	108.739	121.128

**Table 5-9: Temperature reached by each thermocouple throughout the experiments on diesel in LS Test 19**

The occurrence of boilover in the laboratory scale tests involving biodiesel required further analysis. Similar tests conducted at the field scale using the same fuel did not produce any boilover. Figure 5-27 shows that the thermocouples recorded increases in the temperature from the start of the test until the heating was terminated. The top three thermocouples (TC8 – TC10) display a steady increase in the temperature until about 1200 s after heating when the readings then converge to about 260°C indicating the formation of a hot zone.

A closer look at Figure 5-28 however indicates that the thermocouples were within the region of the cartridge heaters. Figure 5-28 shows the plot of temperature distribution versus height from tank base for the laboratory scale test LS Test 15. The figure does not show a noticeable vertical section on the curves showing a uniform temperature region in the fuel below the heater assembly to indicate that a hot zone was formed. Nevertheless there is a layer of hot fuel layer in the biodiesel slightly below the heater assembly. In Section 5.1.2, it was demonstrated that boilover, of the type in which this study is

interested, requires a hot zone to be formed at a temperature substantially greater than the boiling point of water. The hot zone is identified based on the clear vertical section on the curves showing a uniform temperature region in the fuel below the heater assembly.

As in the case of LS Test 15, the vertical section on the curves below the heater assembly was not clearly in evidence. The boilover occurred could not be categorised as the boilover that is of interest to this project. This type of boilover would be considered as thin film boilover. For thin film boilover, fire heats only a thin layer of fuel which gradually descends to the bottom of the tank at the same speed as the regression rate of the fuel surface (Broeckmann & Schecker, 1992, 1995). For this reason, when the water boils, only a very small layer of fuel remains, hence the consequential effects of boilover are greatly reduced. It was further suggested by Broeckmann and Schecker that a fuel that does not form a hot zone, whatever the initial thickness, can only lead to thin layer boilover because when the water is brought to its boiling point, there will always only be a small amount of fuel remaining.

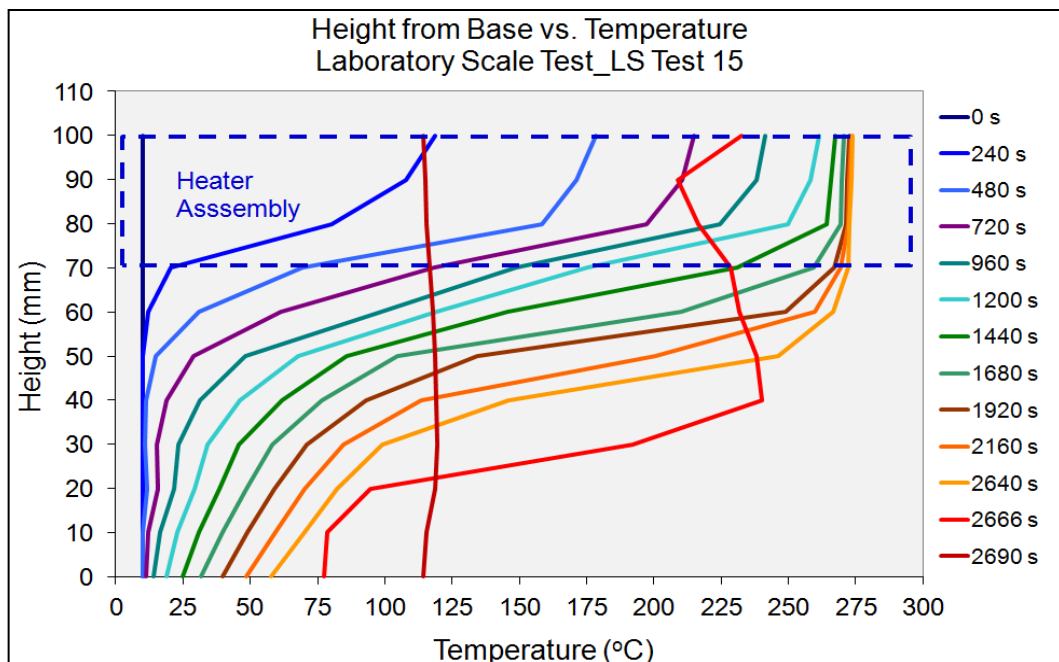


Figure 5-28: Temperature profiles within fuel in the tank in the course of test LS Test 15

#### 5.4.4.1 Photographs of Biodiesel Test

Figure 5-29(a) – (f) displays a series of photographs taken during experiment LS Test 15 which shows the boilover occurrence. The figure shows physical changes recorded during the progression of LS Test 15.

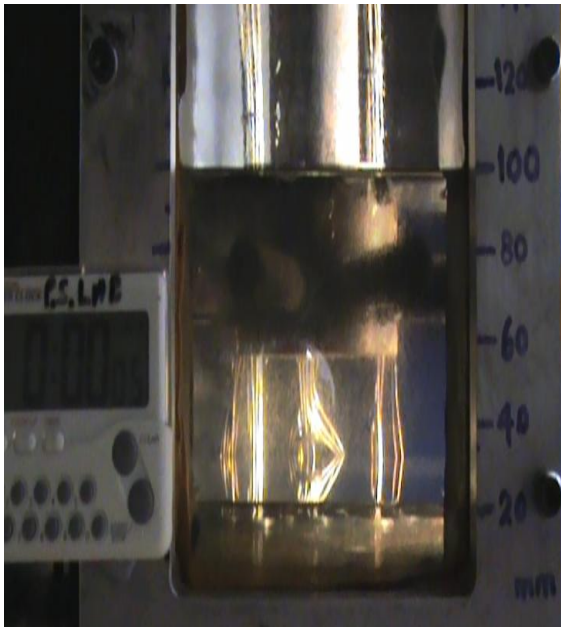


Figure 5-29: (a) Start of heating for LS Test 15



Figure 5-29: (b) Vigorous bubbling within the fuel layer in which the heater assembly was located was observed after 1200 s of heating

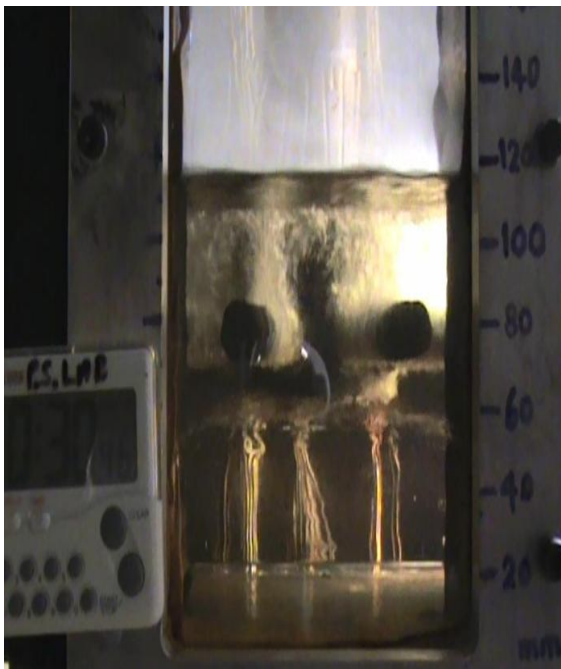


Figure 5-29: (c) Isothermal layer still within the heater assembly region at 1800 s after heating



Figure 5-29: (d) Isothermal layer penetrated thin layer of fuel just below the heater assembly at 2520 s after heating



Figure 5-29: (e) Initiation of boilover occurrence at 2640 s after heating



Figure 5-29: (f) Full boilover at 2666 s after heating

**Figure 5-29: Photo of Laboratory Boilover Test LS Test 15 involving biodiesel**

Photograph (a) shows the start of the test. Photograph (b) shows that boiling is occurring at heater surfaces. This is caused by the rapid evaporation of the lighter component within the biodiesel. Photograph (b) recorded about 1200 s after heating shows the formation of an isothermal layer or hot zone within the region where the heater assembly was located. As the heating progressed, the isothermal layer was clearly visible but still just through the heater assembly, as shown in photograph (c). After 2520 s of heating, the hot zone was seen to penetrate into the fuel beneath the heater assembly but the depth was minimal (see photograph (d)). After another 120 s of heating, the temperature at the interface rises beyond  $100^{\circ}\text{C}$ , boiling of water become stronger, the bubble size increases and the generation rate of bubbles becomes higher. Finally after 2666 s of heating, boilover occurred as shown in photograph (f).

The vigorous boiling of water and hence boilover was observed although a sizeable hot zone was not clearly seen. The boilover occurred could not be categorised as the boilover that is of interest to this project. In a real fire this would be thin film boilover at the bottom of the tank.

## 5.5 VALIDITY OF LABORATORY SCALE RIG RESULTS

The laboratory scale rig was designed to study in detail the temperature distribution within fuel and from the temperature records to determine whether or not a particular fuel would boilover. In addition, it was possible to investigate the effects of changes in the test conditions which would be difficult to control at field scale such as changing the heat input to the fuel and varying the initial temperature of the fuel and water. In addition, the validity of conducting a boilover test in a small-laboratory scale and drawing conclusions that are relevant to full-surface boilover event was also one of the objectives of this research work.

The data obtained and their subsequent analyses have been discussed. This has demonstrated that the laboratory scale boilover rig has enabled the study of the boilover to be conducted in a controlled and safe manner and that repeatability of the experimental results are acceptable. The observations from the laboratory scale tests show very promising results in imitating the findings obtained from the field scale tests. The results indicate the possibility of reproducing the performance and observations of the field scale boilover studies using the laboratory scale boilover rig. The observations and the trends of the results of the laboratory scale tests were similar to those described for the field scale boilover tests in Chapter 3.

The highlights of the laboratory scale boilover tests are:

1. Thermocouple measurement showed the creation of a hot zone
2. When the isothermal region through the heater was discounted they also showed the lack of creation of a hot zone for those fuels that did not boilover
3. Boilover was observed for fuels in which a hot zone was established with a temperature significantly above the boiling point of water
4. Boilover, as of interest to this project, was not observed for fuels described by point (2), although something like boilover occurred since there was a depth of hot fuel above water that was through the heater

5. What is described in point (4) could be considered thin film boilover in a real fire
6. If the hot zone temperature is less than the temperature indicated in point (3), boilover was not observed.
7. For boilover as is of interest to this project is concerned, to occur:
  - a) A hot zone must be created which extends below the region of the heaters
  - b) It must be at a temperature substantially above the boiling point of water
8. For boilover, as is of interest to this project is concerned, not to occur:
  - a) A hot zone that extends below the region of the heaters is not formed, or
  - b) The temperature of the hot zone is not at a temperature substantially above the boiling point of water
  - c) If point (a) occurs then it may appear that boilover has occurred because there is layer of hot fluid  $\approx 250^{\circ}\text{C}$  in the biodiesel within the region of the heaters. In a real fire this would be thin film boilover at the bottom of the tank.
9. The laboratory scale test results, though limited, indicate that in the case of storage tank fires with a possibility of boilover occurrence, a higher initial fuel temperature will contribute to a shorter onset time.
10. By reducing the heating temperature i.e. by limiting the heat absorbed by the fuel from the fire, the time to boilover could be prolonged and even to the extent of eliminating the phenomenon.

In addition to the above, it is important to take note that the fuel surface regression rate and speed of the base of the hot zone are not comparable with the field scale tests. The time to boilover observed in the laboratory scale tests is also not comparable with the field scale tests.

## 6 PREDICTIVE TOOL FOR BOILOVER PHENOMENON

The important aspects when dealing with a boilover and its consequences, as noted by Michaëlis *et al.* (2005) are:

- i. The time to boilover and hot zone temperature at boilover time
- ii. The quantity of liquid fuel remaining in the tank at boilover time

Hence, the development of the predictive tool was divided into two sections. The first section concentrated on the prediction of the onset time of the boilover phenomenon and the hot zone temperature within the bulk fuel prior to boilover. In the second part, the mass of fuel remaining in the tank prior to boilover was quantified. This mass was then used to quantify the amount of fuel vapour involved in the fireball-effect flame and the amount of liquid fuel ejected from the tank during boilover.

The first part of the predictive tool is based on the theory that a distillation process is created and that heat is transferred from the surface down into the bulk of the liquid as a result of convective currents arising as a result of this distillation process (Hall, 1925). At the surface, heat is transferred from the flame to the liquid fuel primarily by radiation. This heat vaporises the liquid at the surface raising its temperature to the boiling point of the heaviest component of the fuel. Heat is then transferred to the liquid immediately below by conduction. Below the surface, a layer is formed in which a distillation process develops. The lighter more volatile components of the fuel are vaporised and the bulk temperature of the liquid is raised to the boiling point of these lighter components. These vapours move upwards to the fuel surface where they feed the fire. The hot heavier components sink vaporising the lighter components and increasing the temperature of the heavier components in which they come into contact. Consequently, strong convective currents are formed resulting in the creation of a uniform temperature layer known as the hot zone. The temperature of the hot zone increases as the lighter components of

the fuel are consumed. Below the hot zone the liquid is heated by conduction from the hot zone and thus becomes part of the hot zone. By these mechanisms the depth of the hot zone grows and gradually increases in temperature as the lighter components are depleted. Provided the temperature of the hot zone is sufficiently above the boiling point of water, boilover will occur when the hot zone reaches the layer of water residing at the bottom of the tank. The assumptions described above allow the use of simple equations based on physical and thermodynamic laws. These equations avoid complex modelling of convective flows during hot zone formation. The important parameter to be predicted by the model is the time, from the start of the fire, at which the boilover occurs. Similar to the hot zone expansion work (Broeckmann and Schecker, 1995), the proposed prediction calculation uses a basic heat balance surrounding the burning fuel to determine the time to boilover.

The second part of the predictive tool is concerned with the consequences of a boilover event. An important aspect is to determine the amount of fuel that is ejected from the tank. Part of this fuel enhances the size of the fire through the formation of a relatively long duration fireball-like event. At the same time, the remainder of the fuel is ejected over the tank wall as hot burning liquid and forms a pool on the ground around the tank, and, for a relatively short duration, results in an increase in the size of the pool fire. The second part is to model the size of the fuel eruption in order to determine the amount of fuel being ejected, the flame size and the radiant heat during boilover.

The main criterion of the model is that it should produce accessible results to guide a wide range of emergency response personnel on handling the boilover phenomenon. Hence a model based on physical and thermodynamic principles has been developed. This model is capable of providing timely predictions that can be used to understand what could happen during a tank fire involving a particular fuel and to guide the actions of emergency responders during an actual event.



Modelling and simulation of the boilover phenomenon will allow the prediction of the important characteristics features of such an event and enable corresponding safety measures to be prepared. Of particular importance when managing the emergency response operations in tank farms in which fuels are stored that have the potential for boilover to occur, is the time from ignition to the occurrence of boilover. As mentioned in Sections 1.2.2 and 2.3, very few of the previous studies focussed on the practical application of heat transfer theory to the problems associated with fighting tank fires with boilover potential. Hence there remains a lack of predictive tools for emergency planning or for use at the time of an incident.

The prediction of boilover onset is very important in terms of fire safety assessment. The main objective of this chapter is to develop a tool capable of predicting boilover phenomenon. The model should be capable of predicting:

- i. Whether, in the event of a fire, a stored fuel can undergo a boilover;
- ii. If a fuel can undergo a boilover, at what time after the start of the fire would a boilover occur;
- iii. If a boilover occurred, what would be the magnitude of the consequences? That is, the increase in fire size (fireball effect) and the amount of fuel ejected out of the tank resulting in an increased size of pool fire.

Based on the discussion of the Section 3.2.3, it could be deduced that there are three stages observed in the mechanism of boilover incidence. At the start of the fire there is a stage when the hot zone is formed. This is followed by a period when the bottom of the hot zone moves downwards at a pseudo constant rate in which the distillation process (vaporisation of the fuel's lighter ends) is taking place. The final stage is when the hot zone reaches the fuel-water interface but no boilover is observed. There appears to be a delay between the hot zone arriving in the vicinity of the fuel-water interface and boilover occurring. It is assumed that the hot zone is heating up further the lowest fuel layer consisting of components with very high boiling points which must be heated to a temperature sufficiently above that of the boiling point of

water so that the water is superheated and rapid vaporization of the water occurs.

In order to establish a tool for the prediction of the boilover events, it is necessary to understand what happens within the fuel during a fire. Such understanding is important in order to recognize and determine the mechanisms for the hot zone formation and growth which are essentials, especially for predicting the onset time of boilover.

## **6.1 BEHAVIOUR WITHIN THE BURNING LIQUID**

Results of the field scale test involving crude oil and mixtures of diesel and gasoline e.g. FS Test 22 and FS Test 39 respectively, are used to describe the behaviour within the fuel during a storage tank fire that result in a boilover.

### **6.1.1 Boilover Fire**

Figure 6-1 shows the temperature profiles for test FS Test 22. In the experimental works involving crude oil (a multi-component fuel), the results of the temperature development showed an initial sharp increase in the surface temperature after an initial fire development phase (see Figure 6-1). It can be seen that a well-defined exponential temperature profile is established under the surface of the fuel. As observed in FS Test 22, during the initial stages of the fire the surface temperature reached about 150°C. This phase, referred to as the heat-up phase by Broeckmann & Schecker (1995), lasted for about 1100 s. The burning fuel had undergone an initial transient stage which was end-marked by a sharp temperature increase. Simultaneously, the beginning of the stationary burning period started. The characteristic behaviour of the stationary burning period is that the thermocouples beneath the fuel surface showed a gradual increase in the temperatures which then reached an approximately constant value. This phase also indicated the beginning of the hot zone formation and growth.

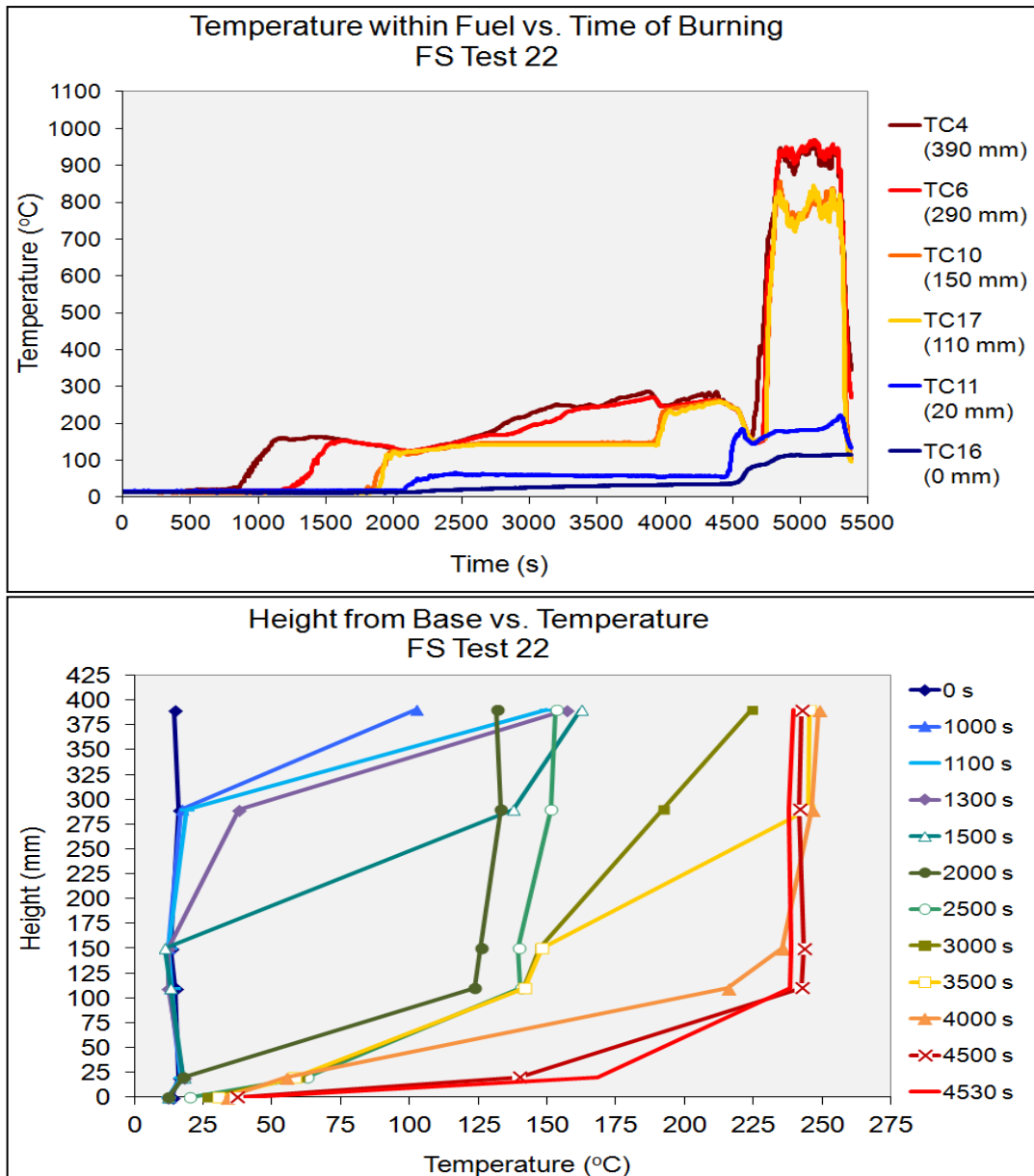


Figure 6-1: Temperature profiles within crude oil for test FS Test 22

After the heat-up phase, the exponential temperature profile under the surface of the fuel then transformed to a uniform temperature profile (i.e. the temperature of the hot zone) as indicated by two or more thermocouples having similar temperatures. Both the hot zone thickness and temperature increased slowly as burning progressed (clearly seen between 1500 s to 2500 s of burning). The thickness growth was seen via the gradual movement of the hot zone lower boundary (hot-cold fuel interface) towards the base of the tank at a rate faster than the regression rate of the fuel surface. As observed in test FS Test 22, the hot zone temperature increased to about 250°C. Based on the

temperature development, this hot zone growth phase lasted for about 2500 to 3500 s. The time of hot zone growth must depend on the depth of the fuel.

When the hot zone lower boundary reached the fuel-water interface, at approximately 1000 s after the end of the previous phase, the temperature was about 140°C. However, a boilover did not occur immediately. A time delay was observed. It is possible that heat was required to raise the temperature of the lowest fuel layer (consisting of components with very high boiling points which settle during storage) and the water layer to the boiling point of the latter. This observation indicates the end of the hot zone growth phase (pre-boilover phase) and the commencement of fully developed boilover. Based on the results of the field scale tests involving crude oil, it would take about 20 to 80 seconds before boilover occurred.

The behaviour of the burning fuel in the diesel-gasoline fire was similar to the crude oil fire. Figure 6-2 displays the temperature profiles for test FS Test 39. The temperature profile within the fuel showed an initial sharp increase in the surface temperature after an initial fire development phase. It can be seen that a well-defined exponential temperature profile has been established under the surface of the oil. The exponential temperature profile under the surface of the fuel is then transformed to a uniform temperature profile (i.e. the temperature of the hot zone) as indicated by two or more thermocouples having similar temperature. Such development of a uniform temperature layer could be observed, in test FS Test 39, after 500 s following ignition. The hot zone thickness increased to more than 120 mm thick and its temperature rise slowly to about 600°C as the burning progressed prior to the boilover. The thickness growth was seen via the gradual movement of the hot zone lower boundary (hot-cold fuel interface) towards the base of the tank. Based on the temperature development, this hot zone growth phase lasted for about 700 to 1250 s. The time of hot zone growth must depend on the depth of the fuel. By the period of 1300 s of burning, a boilover occurred.

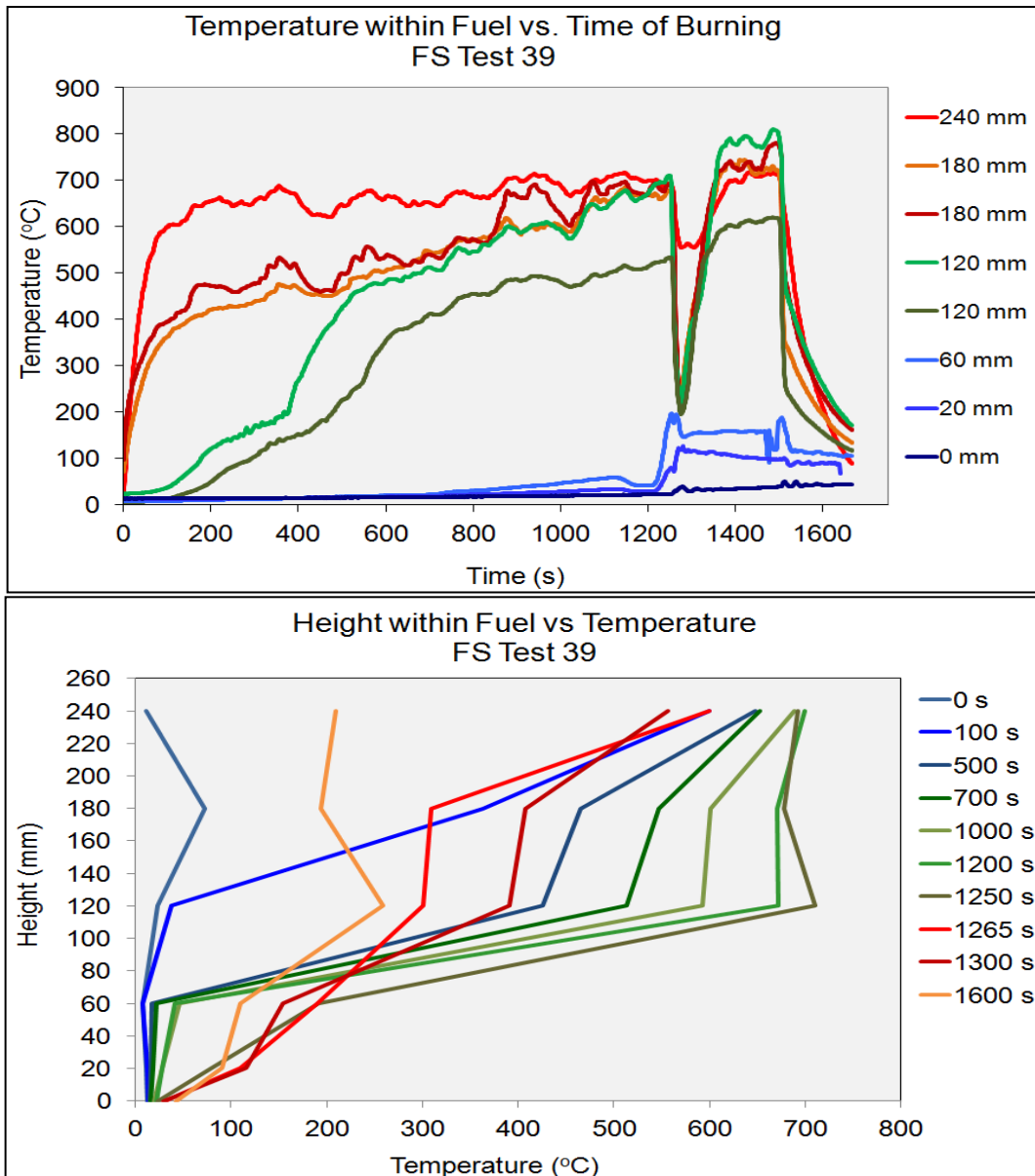


Figure 6-2: Temperature profiles within diesel and gasoline mixture for test FS Test 39

### 6.1.2 Non-boilover Fire

The behaviour within the burning fuel during a storage tank fire in which boilover did not occur was also examined. For this purpose, results of the tests involving gasoline and diesel e.g. FS Test 31 and FS Test 29 respectively are described.

Figure 6-3 shows the temperature evolution during a gasoline test FS Test 31. The bottom figure of Figure 6-3 shows the vertical temperature profile for the test.

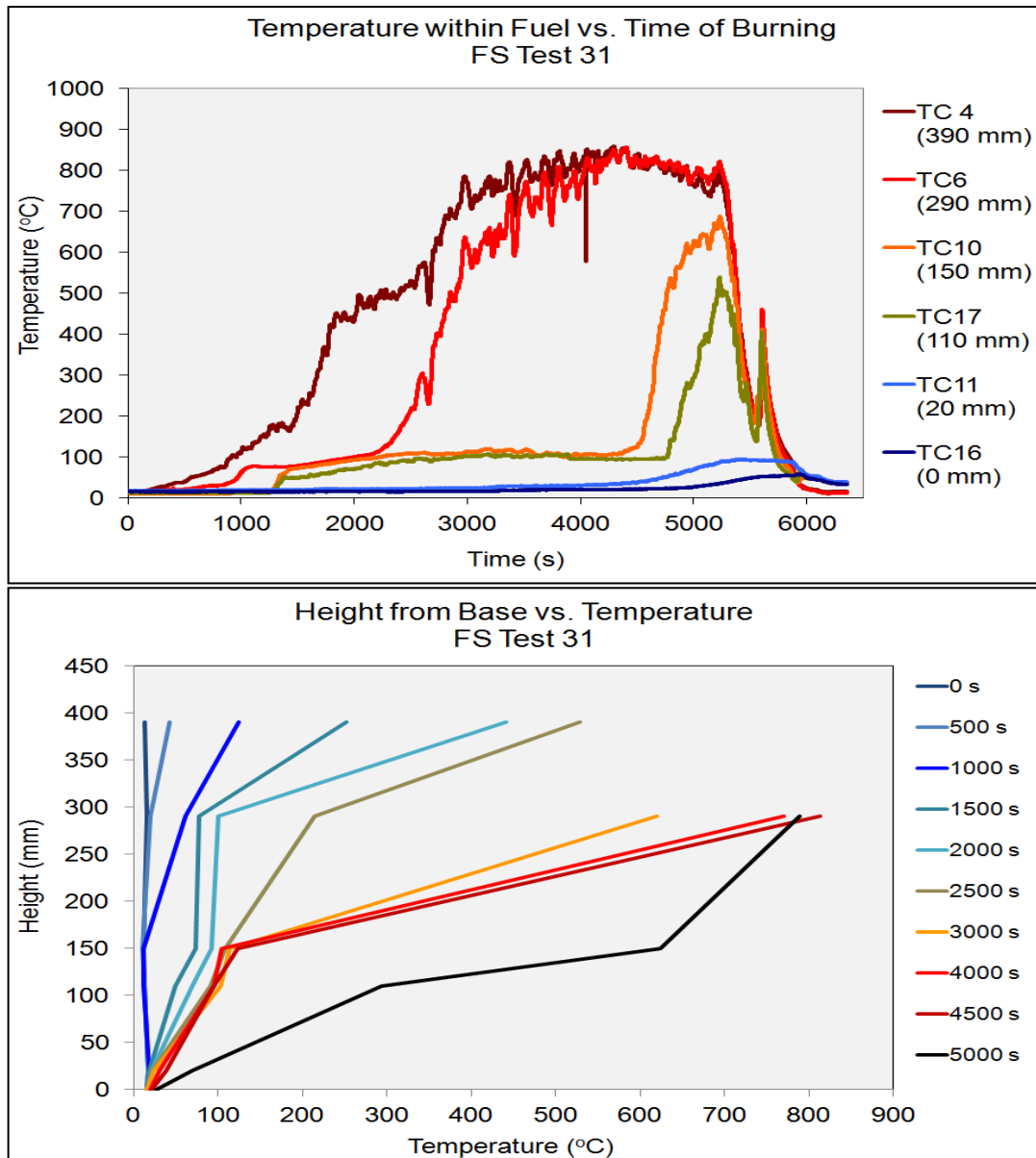


Figure 6-3: Temperature profiles within gasoline for test FS Test 31

In the gasoline fire, the behaviour is similar to that observed in the crude oil test in the early stage i.e. the temperature shows a well-defined exponential curve under the fuel surface. The period at about 1000 s is when the temperature experienced the first significant increase (up to about 110°C) after an initial development phase, as observed in the FS Test 31. An exponential rise in temperature was measured as the thermocouple approached the fuel surface. At about 1500 s after burning, the thermocouples TC6 and TC10 readings converge to a temperature just below 100°C. This observation is supported by the bottom figure of Figure 6-3 which displays two or more thermocouples having similar temperatures between 1500 s to 2000 s after the burning started.

This observation indicates the formation of a hot zone. As the burning progresses, the exponential curve under the surface remained to be seen as beneath the surface of the fuel. This process was observed within the period of 1000 – 4500 s after the full surface ignition. Towards the end of the gasoline fire, the thermocouples showed lower temperature as the flame were extinguished. Though there is an indication that a hot zone was formed, the temperature of the hot zone is not at a temperature substantially above the boiling point of water. Hence, a boilover, that is of interest to this project is concerned, not observed.

Figure 6-4 shows the temperature evolution during a diesel test FS Test 29.

For the diesel fire, in test FS Test 29, an initial sharp increase in the surface temperature after an initial fire development phase was also observed. It can be seen that a well-defined exponential temperature profile has been established under the surface of the diesel approximately 2500 s after ignition. The temperature shown by the thermocouple approaching the surface was at about 200°C. The exponential temperature profile under the diesel surface remained to be seen as the burning progressed and no clear indication of similar temperature readings by the adjacent thermocouples underneath the surface. As the surface regressed, the exponential temperature curve could still be observed underneath the surface but no isothermal layer was formed beneath the exponential profile. These were observed within the period of 2000 till 8000 s of the burning. The temperature then dropped to 200°C at about 9000 s of burning when the flame size became smaller. The boilover phenomenon was not observed until the end of the test.

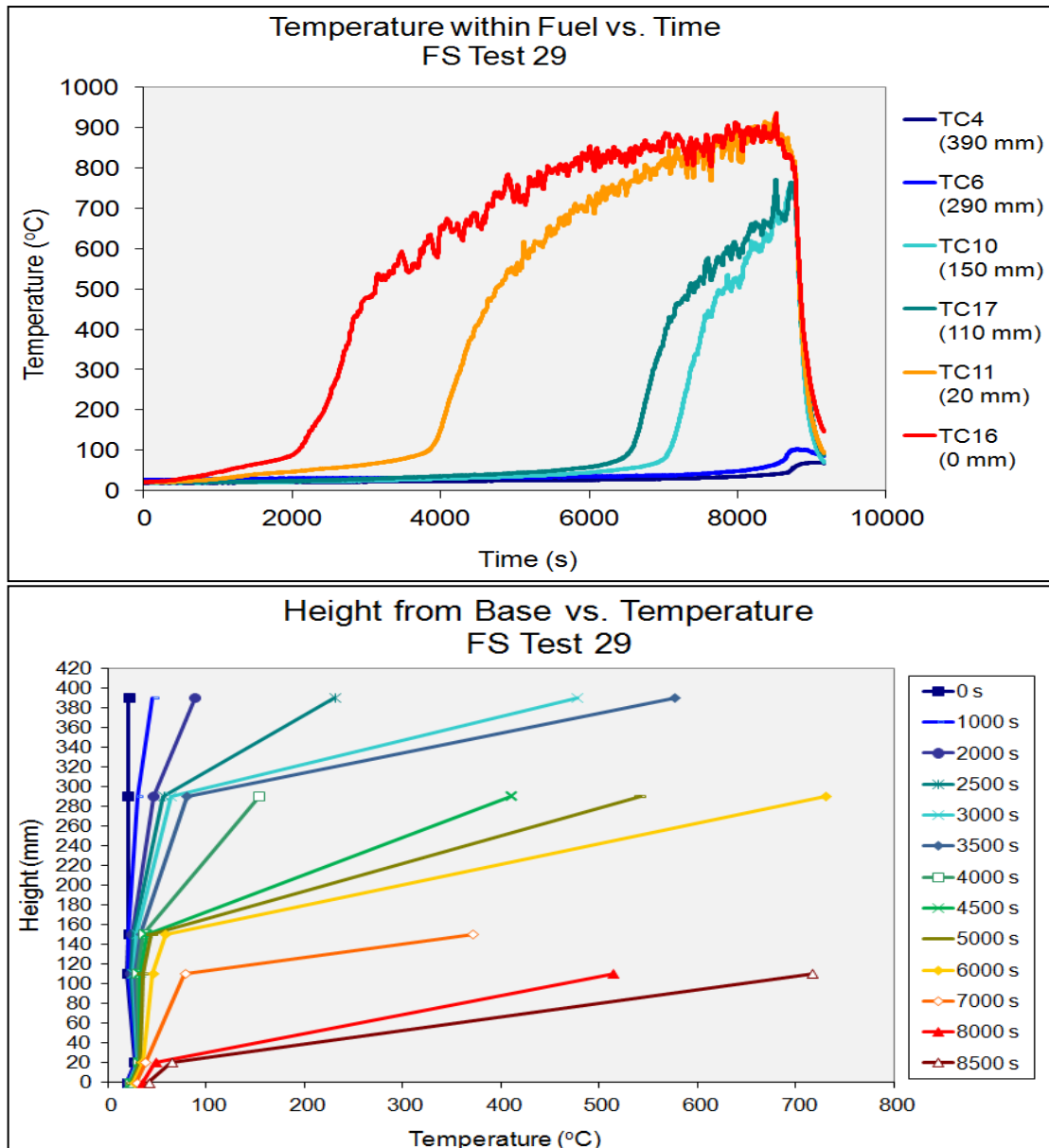


Figure 6-4: Temperature profiles within diesel for test FS Test 29

## 6.2 TEMPERATURE PROFILES OF BURNING LIQUID

Based on what has been described in Section 6.1, for the case of a fire ending with a boilover, an initial sharp increase in the surface temperature were observed during the initial stage of burning. Consequently, a well-defined exponential temperature profile was established under the surface of the burning fuel. From the start of the fire, it was deduced that the heat from the flame is transferred to the fuel surface, primarily by radiation, resulting in the rise in the temperature. Heat is then transferred downwards into the pool by the



mechanism of conduction and hence the exponential temperature profile. As the burning progresses, the heat is further transferred downwards into the pool mainly by convection, as the light components are vaporised and the uniform temperature layer i.e. the hot zone is formed. The process continues downwards as the heat vaporises the cold fuel's lighter components and the cold region becomes part of the hot zone. This process continues until the base of the hot zone approaches the fuel/water interface. Once the base reaches the interface, there appears to be a delay before the occurrence of boilover, even though the temperature of the fuel is at the vaporisation point of water. The delay is linked to the longer time required to heat the remaining heavy components of the fuel to enable the water to be heated to its boiling point.

Figure 6-5, Figure 6-6, Figure 6-7 and Figure 6-8 show what happened during tests FS Test 22 and LS Test 23 within the liquid fuel bulk when boilover occurs. The figures indicate the development of the temperature profiles throughout the burning of the fuel in a storage tank fire incident.

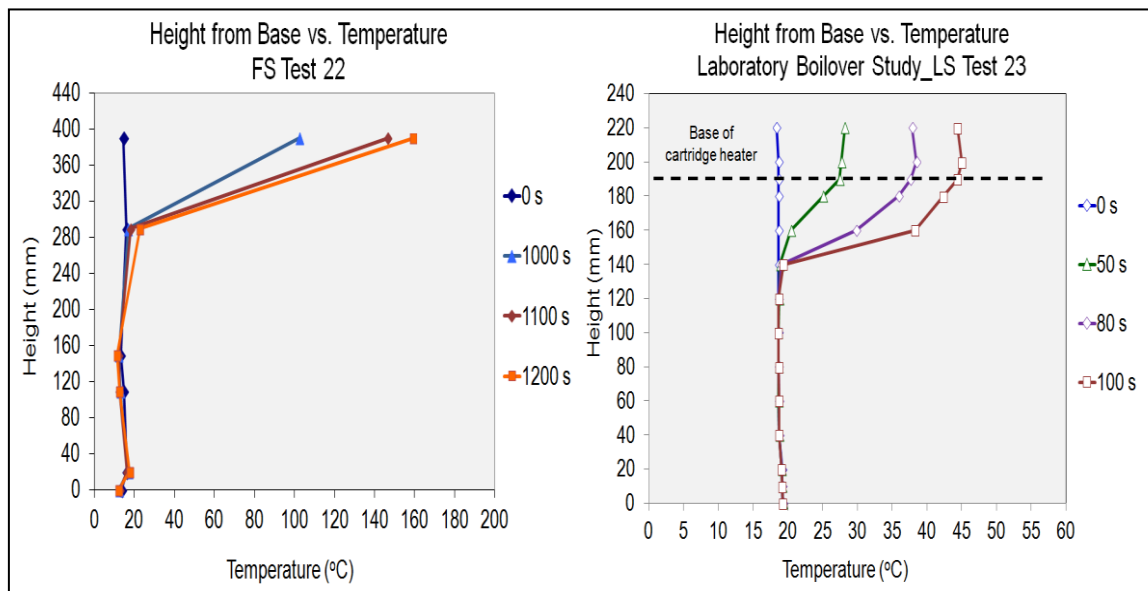


**Figure 6-5: Plot of height against temperature for the field scale testing and laboratory scale experimental work during the initial stage of burning when heat transfer is assumed to be conduction. Note the exponential temperature profile measured by the top thermocouples**

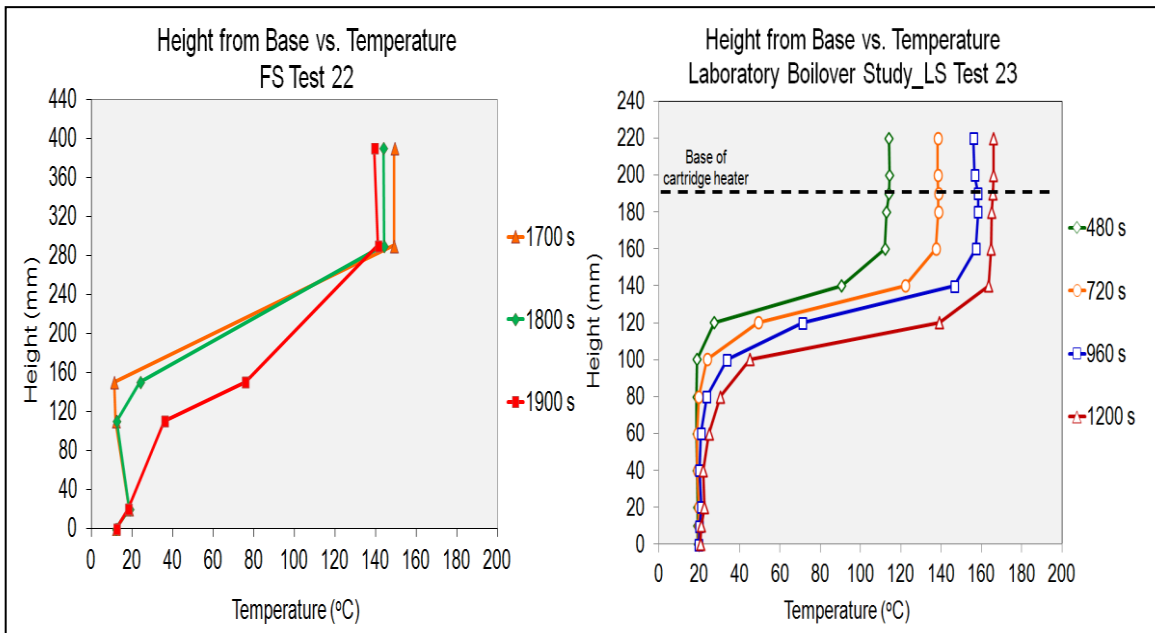


**Figure 6-6: Plot of height against temperature for field scale testing and laboratory scale experimental work during the subsequent stage of burning when the hot zone is forming. Note the similar temperature readings by two or more of the top thermocouples**

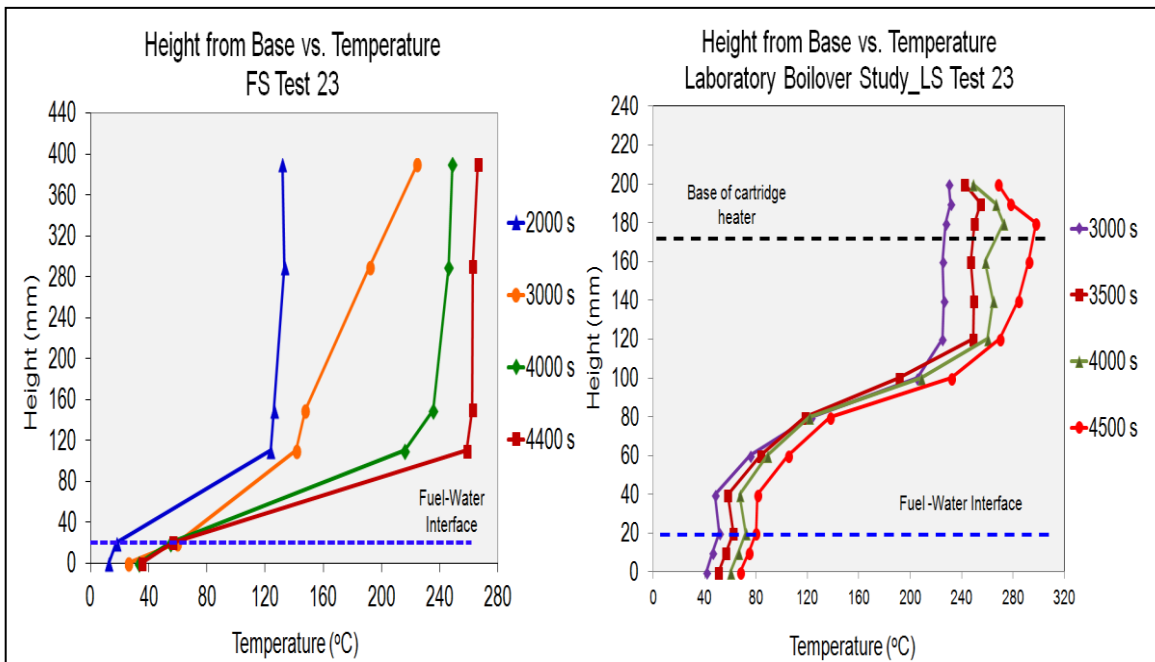


**Figure 6-7: Plot of height against temperature during the period when the base of the hot zone is moving downwards towards the fuel/water interface. Note the horizontal section of the temperature profile regresses gradually towards the tank base. The temperature of the hot zone is also increasing gradually.**

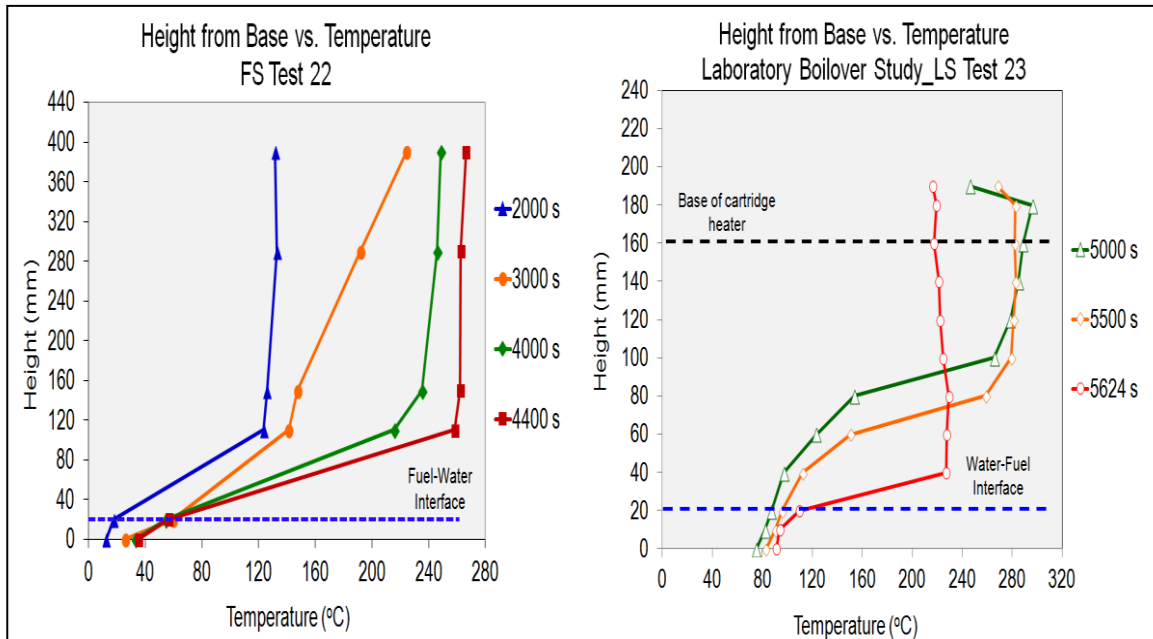


**Figure 6-8: Plot of height against temperature when the base of the hot zone has reached the fuel/water interface. The red line indicates the boilover occurrence. Note that the boilover did not occur immediately though the hot zone base reached the interface at the vapourisation point of water.**

Based on the above figures, it can be summarised that at any point of the storage tank fire (in which a boilover is possible), an exponential temperature profile will be observed just underneath the fuel surface. Then, beneath the exponential profile, a vertical temperature profile representing an isothermal layer is established. What follows is another exponential temperature profile which represents the base of the isothermal layer i.e. hot zone.

Figure 6-9 below shows the summary of the temperature profile within the fuel observed throughout the overall processes of burning prior to the boilover occurrence.

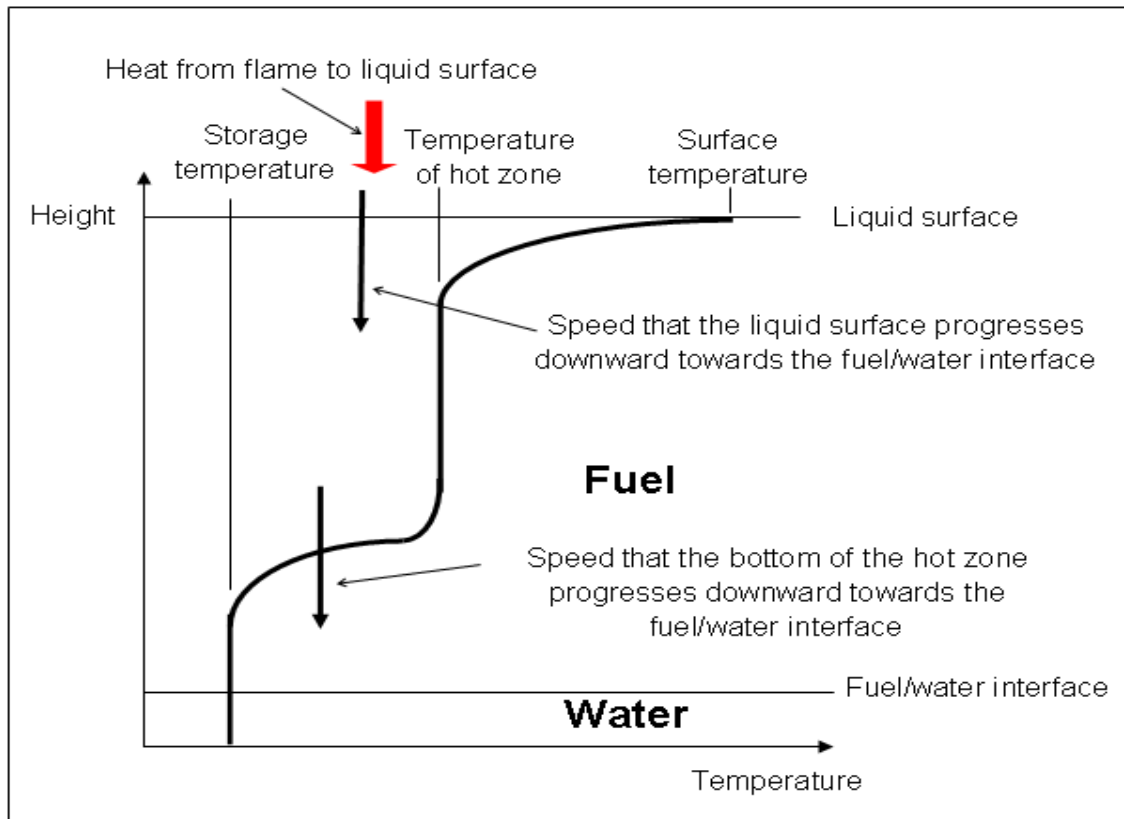


**Figure 6-9: The temperature profile of the overall mechanism observed during a fire prior to the boilover occurrence.**

Based on the observations of the mechanisms involved in the boilover occurrence, the following points need to be looked upon during a liquid hydrocarbon storage tank fire:

- i. Could a boilover occur?
  - Will a hot zone be formed?
  - Will the temperature of the hot zone be sufficient to vaporise water in sufficient quantities to result in boilover?
- ii. When could a boilover occur?
  - At what time after ignition will the base of the hot zone reach the fuel/water interface?
- iii. How much fuel will be in the tank when boilover occurs?
  - How much fuel will have been vaporised and entered the fire between ignition and boilover?

The points mentioned above are the major concerns relevant to boilover occurrence particularly related to the critical consequences of the event. Hence any effort linked to managing such a scenario, e.g. prediction of the boilover onset, should take into considerations those important points.

In the context of this thesis, the predictive calculations will focus on the provision of the two latter points i.e. provision of an estimate on the time to boilover upon the establishment of a full surface fire and an estimate of the amount of fuel remaining in the tank prior to the occurrence of the boilover. A determination of the remnants of the fuel is essential in estimating the consequences of the event.

### **6.3 PREDICTION OF TIME TO BOILOVER AND HOT ZONE TEMPERATURE**

Of particular importance when managing the emergency response operations in tank farms in which fuels are stored that have the potential for boilover to occur, is the time from ignition to the occurrence of boilover.

#### **6.3.1 Heat Balance Equation**

For a case of a storage tank fire, it has been shown that the heat flux from the flames of the burning fuel raises the temperature and vaporises the fuel (Hamins *et al.*, 1995). The heating mechanism of the three-stage process as discussed in Section 6.2 is achieved via the transfer of heat from the flame through the surface and into the liquid fuel. It is assumed that part of the heat is used to form and sustain the hot zone via vaporising some of the components (i.e. the lighter ends of the fuel) in the hot zone which is at the boiling point of the lighter component being vaporised. The remainder is used to raise the temperature of some of the previously unheated fuel located immediately below the hot zone to the boiling point of the component currently vaporising in the hot zone.

In order to aid the development of a predictive tool for boilover onset, the heating mechanism is simplified by considering that the heat involved in the process is only used for vaporising the component in the hot zone and for raising the temperature of the unheated fuel to the hot zone temperature. The temperature profile given in Section 6.2 is then simplified as shown in Figure 6-10.

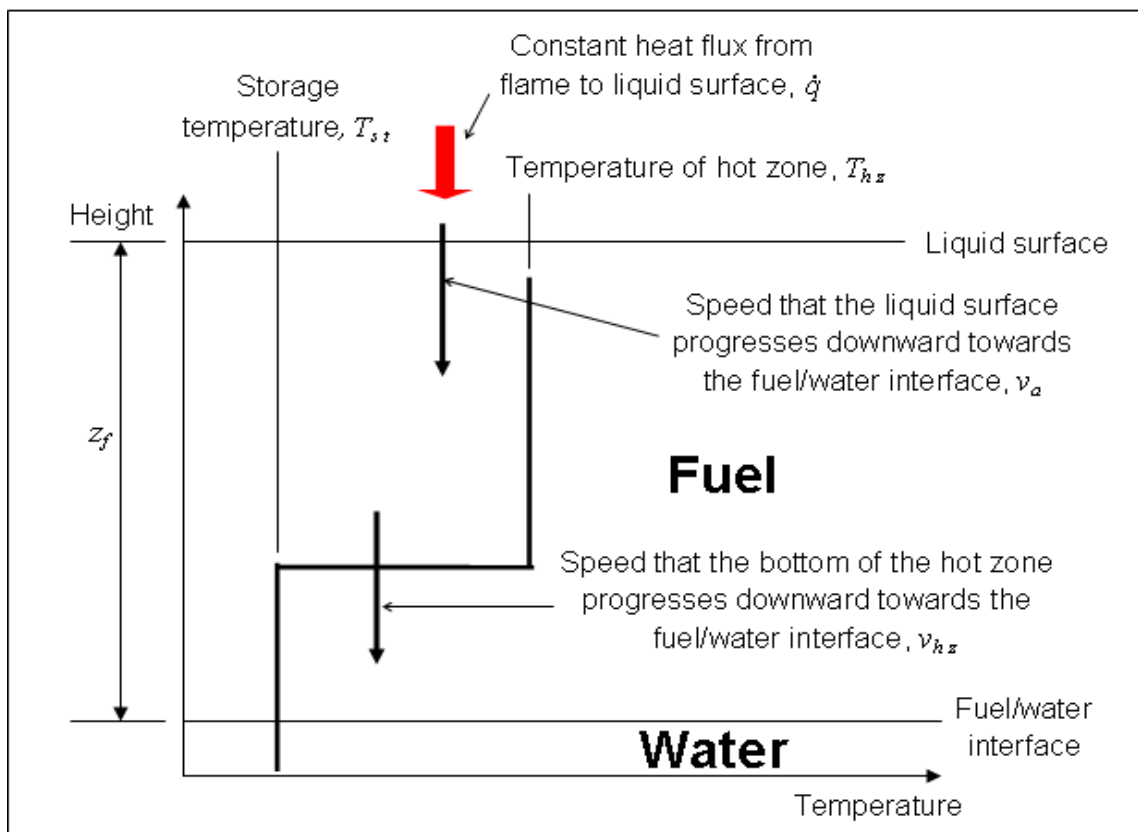


**Figure 6-10: Simplified temperature profile within burning liquid as a basis for boilover onset predictive tool development**

During a particular time interval,  $\Delta t$ , the amount of heat received by the fuel from the fire,  $\Delta Q$ , is:

$$\Delta Q = \dot{q} A \Delta t \quad \text{Equation 6-1}$$

where

$\dot{q}$  is the constant rate of heat flux to the fuel surface,  $\text{W m}^{-2}$

$A$  is the cross sectional area of storage tank,  $\text{m}^2$

It is assumed that some of this heat,  $\Delta Q_{sh}$  is used to raise the temperature of some of the previously unheated fuel located immediately below the hot zone to the boiling point of the component currently vaporising in the hot zone. This newly heated fuel serves to increase the size of the hot zone.

$$\Delta Q_{sh} = \dot{m}_L \Delta t C_p (T_{hz} - T_{st}) \quad \text{Equation 6-2}$$

where

$\dot{m}_L$  is the rate of reduction of mass of the previously unheated fuel layer,  $\text{kg s}^{-1}$

$C_p$  is the specific heat of the fuel,  $\text{J kg}^{-1} \text{K}^{-1}$

$T_{st}$  is the storage temperature, K

$T_{hz}$  is the hot zone temperature, K

The remainder of this heat,  $\Delta Q_{lh}$  is used to vaporise some of the component in the hot zone that is at its boiling point:

$$\Delta Q_{lh} = \dot{m}_V \Delta t \Delta h_{lh} \quad \text{Equation 6-3}$$

where

$\dot{m}_V$  is the constant rate of vaporisation of the component currently vaporising in the hot zone,  $\text{kg s}^{-1}$

$\Delta h_{lh}$  is the latent heat of vaporisation of the component in the hot zone that is being vaporised,  $\text{J kg}^{-1}$

Now, the total heat received by the fuel is:

$$\Delta Q = \Delta Q_{sh} + \Delta Q_{lh}$$

Introducing Equation 6-2 and Equation 6-3 gives the heat balance as:

$$\begin{aligned} \dot{q} A \Delta t &= \dot{m}_V \Delta t \Delta h_{lh} + \dot{m}_L \Delta t C_p (T_{hz} - T_{st}) \\ \dot{q} A &= \dot{m}_V \Delta h_{lh} + \dot{m}_L C_p (T_{hz} - T_{st}) \end{aligned} \quad \text{Equation 6-4}$$

### 6.3.2 Prediction of Boilover Onset

The time to boilover is related to the time taken for the lower boundary of hot zone to reach the fuel-water interface and boil the water. The growth of the hot zone depends on the rate of the cold (unheated) fuel being heated and incorporated into the hot zone hence its increase in size. Rearranging Equation 6-4 provides the relationship between the rate of cold/unheated fuel incorporated into the hot zone,  $\dot{m}_L$  and the amount of heat received by the fuel from the flame.

The relationship between the rate of cold/unheated fuel incorporated into the hot zone,  $\dot{m}_L$  with the amount of heat received by the fuel from the flame is:

$$\dot{m}_L = \frac{(\dot{q} A - \dot{m}_V \Delta h_{lh})}{(C_p (T_{hz} - T_{st}))} \quad \text{Equation 6-5}$$

The vaporisation rate of the component boiling in the hot zone or simply the fuel mass burning rate,  $\dot{m}_V$  ( $\text{kg s}^{-1}$ ) is given by

$$\dot{m}_V = v_a A \rho_{LV} \quad \text{Equation 6-6}$$

where  $\rho_{LV}$  is the density of the liquid that has been vaporised,  $\text{kg m}^{-3}$

The rate at which the cold fuel is incorporated into the hot zone,  $\dot{m}_L$  could also be linked to the speed that the lower boundary of the hot zone progresses downward:

$$\dot{m}_L = v_{hz} A \rho_L \quad \text{Equation 6-7}$$

where  $\rho_L$  is the density of the liquid in the storage tank,  $\text{kg m}^{-3}$



Combining Equation 6-5, Equation 6-6 and Equation 6-7 provides an estimate of the speed of the lower boundary of hot zone:

$$v_{hz} = \frac{\dot{m}_L}{A \rho_L} = \frac{\dot{q} A - \dot{m}_V \Delta h_{lh}}{A \rho_L C_p (T_{hz} - T_{st})} \quad \text{Equation 6-8}$$

The speed of the lower boundary of hot zone is linked to the distance travelled by the base of the hot zone,  $z$  within certain period of time,  $t$ .

$$v_{hz} = \frac{z}{t} = \frac{q A - \dot{m}_V \Delta h_{lh}}{A \rho_L C_p (T_{hz} - T_{st})} \quad \text{Equation 6-9}$$

When the lower boundary of the hot zone reaches the fuel-water interface (and assuming a boilover happens at that instant),  $t$  is taken as the time to boilover,  $t_{bo}$ . If  $z_f$  is taken as the initial depth of the fuel layer, then:

$$t_{bo} = \frac{z_f A \rho_L C_p (T_{hz} - T_{st})}{\dot{q} A - \dot{m}_V \Delta h_{lh}} \quad \text{Equation 6-10}$$

This predictive calculation on the time to boilover, as stated in Section 6.3.1, is based only on the stage at which the base of the hot zone is moving downwards towards the fuel-water interface at a pseudo constant rate at a temperature of  $T_{hz}$ . Once the base of the hot zone reaches the interface, a boilover is assumed to occur instantaneously.

In order to solve Equation 6-10 for determining the time to boilover, the model requires the following information:

- i. Storage conditions prior to fire:
  - Cross sectional area of storage tank,  $A$ ;
  - Height, above the water layer, of the fuel in storage tank,  $z_f$ ;

- ii. Properties of the fuel:
  - Temperature of stored fuel,  $T_{st}$  ;
  - Density of the stored fuel,  $\rho_L$ ;
  - Specific heat of the stored fuel,  $C_p$ ;
  
- iii. Parameters during fire:
  - Rate of heat flux from the flame to fuel,  $\dot{q}$ ;
  - Latent heat of vaporisation of the fuel that is vaporised,  $\Delta h_{lh}$  ;
  - Mass flow rate of vapours from pool to flame = mass burning rate,  $\dot{m}_V$ ;
  - Temperature of the hot zone,  $T_{hz}$ .

Some of the information required are measurable properties such as the tank dimensions and some are available from material property sheet e.g. fuel density. However, some of the information, especially the thermo-physical properties of fuel are not readily available and need to be calculated through certain thermodynamic relations or generalized correlations such as the heat capacity and latent heat of vaporisation. For this work, generalized correlations that require certain input properties which include boiling point and density (or specific gravity) of a given fuel are used to estimate the relevant thermo-physical properties. The criterion to use such correlations is to achieve simplicity in the predictive calculations and produce conservative, yet acceptable, results.

### **6.3.3 Estimates of Specific Heat, Latent Heat of Vaporisation, Heat Flux Radiated (from flame to fuel) and Heat of Combustion**

Empirical models are used to calculate the parameters directly related to consequence assessment, such as size and shape of the fire and the radiant heat flux received at particular locations external to the fire: they are not used to describe the combustion process. Empirical modeling relies on experimental data and the correlations that can be derived from this data can be used to predict the relevant parameters. Empirical models are preferred for use

especially in hazard assessment, due to their reliability and speed. Some advantages are that the predictions gleaned from empirical models provide good agreement with the experimental data and their computer programs can also be easily built with short run times. The main disadvantage of empirical models is that correlations should only be used within their range of applicability: this is the range over which the experiments were based on or carried out. Unfortunately, it is rarely possible to undertake full-scale experiments, so the use of empirical models inevitably requires extrapolation.

In the following sections, the literature is reviewed and predictions are made, in terms of the most commonly-used empirical models.

### 6.3.3.1 Specific Heat

Specific heat is defined as the quantity of heat required to raise a unit mass of material through one degree of temperature. The specific heat is often required in estimating the net heat fluxes necessary to heat a liquid prior to vaporisation. Estimation methods are an obvious choice to provide heat capacities for compounds when there is a complete lack of data. Additivity schemes that relate thermo-physical and thermodynamic properties with molecular structure have been widely used for data estimation. Under such schemes, a molecular property is calculated by summing up atomic, bond or group contributions.

One relatively simple atomic group contribution approach proposed by Chueh and Swanson in 1973 for liquid heat capacity at 293.15 K is presented as below (Perry and Green, 1997):

$$C_p = \sum_{i=1}^n N_i \Delta_{cpi} + 18.83 m$$

Equation 6-11

where  $C_p$  is the heat capacity of a liquid hydrocarbon at 293.15 K ( $\text{J mol}^{-1} \text{K}^{-1}$ ),  $n$  is the number of different atomic groups in the compound,  $N_i$  is the number of atomic groups  $i$  in the compound,  $\Delta_{cpi}$  is the numeric value of the contributing

atomic element  $i$  and  $m$  is a number of carbon groups requiring additional contributions.

Using a similar scheme, a group additivity method was developed for the estimation of the heat capacity of a liquid hydrocarbon ( $\text{J mol}^{-1} \text{K}^{-1}$ ) as a function of temperature in the range from the melting temperature to the normal boiling point (Růžička and Domalski, 1993):

$$\frac{C_p}{R} = \sum_{i=1}^k n_i \Delta c_i \quad \text{Equation 6-12}$$

In Equation 6-12,  $R$  is the gas constant ( $8.314 \text{ J mol}^{-1} \text{K}^{-1}$ ),  $n_i$  is the number of additivity units of type  $i$  and  $k$  is the total number of additivity units in a molecule. The additivity unit includes groups and structural corrections. The dimensionless value of the additivity unit of type  $i$ ,  $\Delta c_i$  is expressed as:

$$\Delta c_i = a_i + b_i \frac{T}{100} + d_i \left( \frac{T}{100} \right)^2$$

where  $T$  (K) is the temperature and  $a_i$ ,  $b_i$  (unit of  $\text{K}^{-1}$ ) and  $d_i$  (unit of  $\text{K}^{-2}$ ) are adjustable parameters.

Estimations of the heat capacity based on additivity methods, though very useful and with low errors, are somewhat complicated. The aim of this work is to produce a predictive tool that can produce readily accessible results to guide a wide range of emergency response personnel on handling the boilover phenomenon and is easy to use. Hence, the essence of the additivity methods which require on-hand information on the additivity unit and appropriate adjustable parameters contradicts the requirement of being able to carrying out quick and easy predictive calculations.

There are other correlations available for liquid heat capacities of hydrocarbons that are in general use. Equation 6-13 is a correlation for the specific heat within

the prescribed temperature range of  $145 \text{ K} < T < 0.8 T_c$  (critical temperature) proposed by Lee and Kesler (1975):

$$C_p = a (b + c T) \quad \text{Equation 6-13}$$

where

$C_p$  is the heat capacity of the liquid hydrocarbon,  $\text{J mol}^{-1} \text{K}^{-1}$

$T$  is the temperature of the hydrocarbon material,  $^{\circ}\text{F}$

$SG$  is the specific gravity of the liquid hydrocarbon ( $60^{\circ}\text{F}/60^{\circ}\text{F}$ )

$a = 1.4651 + 0.2302 K_w$

$b = 0.306469 - 0.16734 SG$

$c = 0.001467 - 0.000551 SG$

$K_w$  is the Watson characterisation factor

The Watson characterisation factor is the ratio of the cube root of the molal average boiling point,  $T_b$  in degrees Rankine to the specific gravity at  $60^{\circ}\text{F}/60^{\circ}\text{F}$ :

$$K_w = \frac{\sqrt[3]{T_b}}{SG}$$

Another relationship is recommended by the American Petroleum Institute covering the condition of reduced temperature,  $T_r < 0.85$  (Daubert & Danner, 1997):

$$C_p = A_1 + A_2 T + A_3 T^2 \quad \text{Equation 6-14}$$

In the above equation,  $C_p$  is the heat capacity of liquid hydrocarbon ( $\text{J mol}^{-1} \text{K}^{-1}$ ) and the constants are determined as follows:

$$A_1 = -4.90383 + (0.099319 + 0.104281 SG) K_w + \left( \frac{4.81407 - 0.194833 K_w}{SG} \right)$$

$$A_2 = (7.53624 + 6.214610 K_w) \times \left( 1.12172 - \frac{0.27634}{SG} \right) \times 10^{-4}$$

$$A_3 = - (1.35652 + 1.11863 K_w) \times \left( 2.9027 - \frac{0.70958}{SG} \right) \times 10^{-7}$$

In this work, the specific heat is estimated through a correlation proposed by Speight (2001). Based on many experimental measurements made on various hydrocarbon materials, the specific heat data ( $\text{kJ kg}^{-1} \text{ }^\circ\text{C}^{-1}$ ) for liquid hydrocarbon at temperature  $T$  (in  $^\circ\text{C}$ ) were generalized by the following equation:

$$C_p = \frac{I}{SG^{0.5}} (1.685 + 0.039 T) \quad \text{Equation 6-15}$$

with empirical constants of  $1.685 \text{ kJ kg}^{-1} \text{ }^\circ\text{C}^{-1}$  and  $0.039 \text{ kJ kg}^{-1} \text{ }^\circ\text{C}^{-2}$ .

Equation 6-15 is used in the estimation of fuel's specific heat due to its simplicity and empirical basis.

### 6.3.3.2 Heat of Vaporization

Another property related to the heat capacity is the heat of vaporization of the liquid hydrocarbon fuel. The heat of vaporization represents the heat required to vaporise a given mass or volume of liquid into vapour. There are several correlations to calculate the heat of vaporization in the literature. Among the commonly used correlations are the Riedel correlation (Poling *et al.*, 2000; Wisniak, 2001), the Chen and the Vetterer methods (Poling *et al.*, 2000).

The Riedel correlation proposed that:

$$\Delta h_{lh} = 1.093 R T_c T_{br} \frac{\ln P_c - 1.013}{0.93 - T_{br}} \quad \text{Equation 6-16}$$

where

$\Delta h_{lh}$  is the latent heat of vaporisation of the liquid hydrocarbon at normal boiling point expressed in  $\text{J kg}^{-1}$

$P_c, T_c$  are the critical pressure, bar and critical temperature, K

$T_{br}$  is the reduced boiling temperature =  $T_b T_c^{-1}$

$T_b$  is the normal boiling point, K

The Chen method showed that the latent heat of vaporisation at the normal boiling point could be estimated via:

$$\Delta h_{lh} = R T_c T_{br} \frac{3.978 T_{br} - 3.958 + 1.555 \ln P_c}{1.07 - T_{br}} \quad \text{Equation 6-17}$$

For both correlations, the critical pressure and temperature must be known or estimated.

The Vetere correlation provided an estimation of the latent heat of vaporisation when  $P_c$  and  $T_c$  are not available:

$$\Delta h_{lh} = A + B + \frac{C T_b^{1.72}}{M W'} \quad \text{Equation 6-18}$$

In Equation 6-18,  $A$ ,  $B$ , and  $C$  are numerical constants and  $MW'$  is a fictitious molecular weight that is equal to true molecular weight for most compounds. The numerical constants are given in the Table 6-1 below.

Compound	$A$	$B$	$C$
Hydrocarbons and $\text{CCl}_4$	3.298	1.015	0.00352
Alcohols	-13.173	4.359	0.00151
Esters	4.814	0.890	0.00374
Other polar compounds	4.542	0.840	0.00352

**Table 6-1: Numerical constants for Equation 6-18**

The latent heat of vaporisation,  $\Delta h_{lh}$  can also be estimated using the following relation which was proposed based on an investigation conducted on a series of 12 petroleum fractions with boiling points ranging from 67 to 300°C (Washburn, 2003).

$$\Delta h_{lh} = (93.4 - 0.187 T_b) \quad \text{Equation 6-19}$$

with empirical constants of 93.4 cal g<sup>-1</sup> and 0.187 cal g<sup>-1</sup> °C<sup>-1</sup> and where  $\Delta h_{lh}$  is in cal g<sup>-1</sup> (1 cal g<sup>-1</sup> = 4.184 J g<sup>-1</sup>) and  $T_b$  is the normal boiling temperature in °C.

Riazi and Daubert (1987) developed a simple two-parameter equation for the prediction of physical properties of undefined hydrocarbon mixtures. The proposed expression for estimating the latent heat of vaporisation of a compound with a boiling point within the range of 80-650°F is as follows:

$$\Delta h_{lh} = 8.206 T_b^{1.141} SG^{9.771 \times 10^{-3}} \quad \text{Equation 6-20}$$

where  $\Delta h_{lh}$  is in Btu lb·mol<sup>-1</sup> and  $T_b$  is the normal boiling temperature in °F

The simplest form of expression for quick estimation of the heat of vaporisation is given by the Trouton's rule (Wisniak, 2001):

$$\Delta h_{lh} = 88 T_b \quad \text{Equation 6-21}$$

The latent heat of evaporation for a hydrocarbon liquid can also be calculated by the following equation proposed by Speight (2001), once the boiling temperature,  $T_b$  and specific gravity of the liquid are known:

$$\Delta h_{lh} = \frac{251.47 - 377.136 \times 10^{-3} T_b}{SG} \quad \text{Equation 6-22}$$

Equation 6-16, Equation 6-17, Equation 6-18, Equation 6-20 and Equation 6-22 provide good estimates results for hydrocarbons with an average error of 2.0% (Poling *et al.*, 2000; Riazi & Daubert, 1987). Equation 6-22 is used in the estimation of fuel's latent heat of vaporisation in this work.

### 6.3.3.3 Radiant Heat Flux (from flame to fuel)

The prediction on the boilover onset as shown in Equation 6-10 relies on the rate of heat flux radiated from the flame to the fuel,  $\dot{q}$  (W m<sup>-2</sup>).

The heat flux radiated from the flame to the burning fuel surface can be quantified based on the total heat release rate from the fire. And the total heat release rate can be quantified based on the measured experimental flame temperature.



The heat release rate,  $\dot{Q}$  (W) from a pool fire (take note that a storage tank fire is considered as a confined pool fire) can be expressed as (Drysdale, 1999):

$$\dot{Q} = \rho_{air} C_{p,air} [T_{\infty} g (T_{flame} - T_{\infty})]^{1/2} D^{5/2} \quad \text{Equation 6-23}$$

where

$\rho_{air}$  is the air density at ambient temperature,  $\text{kg m}^{-3}$

$C_{p,air}$  is the is the specific heat at ambient temperature for air,  $\text{J kg}^{-1} \text{K}^{-1}$

$T_{flame}$  is the average flame temperature, K

$g$  is the acceleration of gravity ( $9.81 \text{ m s}^{-2}$ )

$D$  is the diameter of the fuel pool, m

$\infty$  is the subscript that stands for ambient conditions.

The heat flux,  $\dot{q}$  ( $\text{W m}^{-2}$ ) reaching the surface of the burning fuel represents a small fraction of the total heat release rate of the pool fire and can be expressed as (Torrero *et al.*, 2003; Hristov *et al.*, 2004):

$$\dot{q} = \frac{4}{\pi} \chi_R \dot{Q} = \frac{4}{\pi} \chi_R \rho_{air} C_{p,air} [T_{\infty} g (T_{flame} - T_{\infty})]^{1/2} D^{1/2} \quad \text{Equation 6-24}$$

where

$\chi_R$  is the fraction of the heat release rate from the flame that is radiated back to the fuel surface that contribute to the formation of hot zone

For a generic correlation where the experimental flame temperature data is not available, the heat flux radiated from the flame to the fuel surface is often expressed as (Hamins *et al.*, 1991, 1995; Zalosh, 2002; Engelhard, 2005):

$$\dot{q} = \chi_R m_V'' \Delta h_c \quad \text{Equation 6-25}$$

where

$m_V''$  is the mass burning flux or mass burning rate per unit area,  $\text{kg m}^{-2} \text{s}^{-1}$

$\Delta h_c$  is the heat of combustion of the fuel,  $\text{J kg}^{-1}$

### 6.3.3.4 Mass Burning Flux

The mass burning flux,  $m_V''$ , is an important parameter related to the heat flux to the fuel surface. The heat flux to the fuel is supplying heat to raise its temperature and vaporise the more volatile component (lower boiling point) that leads to the formation of the hot zone. Hence the mass burning flux ( $\text{kg m}^{-2} \text{s}^{-1}$ ) is linked to the vaporisation rate of the component boiling in the hot zone or simply the fuel mass burning rate,  $\dot{m}_V$  (Equation 6-6) and the cross sectional area of storage tank,  $A$ :

$$m_V'' = \frac{\dot{m}_V}{A} = v_a \rho_{LV} \quad \text{Equation 6-26}$$

For cases where the fuel mass burning rate is not readily available, the burning rate per unit area as a function of the pool fire diameter,  $D$  can be determined by the following expression (Babrauskas, 1983; Drysdale, 1999; Chatris *et al.*, 2001):

$$m_V'' = m_{V,max}'' [1 - \exp(-k\beta D)] \quad \text{Equation 6-27}$$

where  $m_{V,max}''$  is the asymptotic burning rate for large pools,  $\text{kg m}^{-2} \text{s}^{-1}$ ,  $k$  is the extinction coefficient,  $\text{m}^{-1}$  and  $\beta$  is the mean-beam-length correction.

This requires determining two empirical factors:  $m_{V,max}''$  and the product ( $k\beta$ ) (represented as a single value). The empirical factors are not universal geometrical factors, but vary widely with the type of fuel considered. In the case that the relevant empirical factors are not available, the mass burning flux could be estimated by (Gottuk and White, 2002; Engelhard, 2005; Fay, 2006):

$$m_V'' = \frac{1 \times 10^{-3} \Delta h_c}{\rho_{LV} [\Delta h_{lh} + C_p (T_b - T_{st})]} \quad \text{Equation 6-28}$$

with the numerical constant of  $1 \times 10^{-3} \text{ kg}^2 \text{ m}^{-5} \text{ s}^{-1}$ . The temperatures are expressed in Kelvin.

An estimate of the mass burning flux can also be determined via the speed of regression of the liquid fuel surface,  $v_a$  ( $\text{m s}^{-1}$ ). In the absence of experimental data,  $v_a$  can be estimated by the following equation (Gottuk and White, 2002):

$$v_a = 1.27 \times 10^{-6} \frac{\Delta h_c}{\Delta h_{lh} + C_p (T_b - T_{st})} \quad \text{Equation 6-29}$$

with the numerical constant of  $1.27 \times 10^{-6} \text{ m s}^{-1}$ . The temperatures are in Kelvin.

The result of Equation 6-29 is then used to solve for the mass burning flux via Equation 6-26.

### 6.3.3.5 Heat of Combustion

The solution for the heat flux radiated to fuel requires the value of the heat of combustion of fuel as indicated by Equation 6-25. The calculation of the heat of combustion, in practise, can be carried out using the principle of molar additivity of the heats of formation of the combustion products and reactants i.e. by subtracting the heat of formation of the products from the heat of formation of the reactants.

If the enthalpies of formations of the combustion reaction products and reactants are not known, the following correlations can be used to estimate the heat of combustion,  $\Delta h_c$  (Chulkov, 1968; Bugai *et al.*, 1998):

$$\Delta h_c = 50462.7 - 8546.1 SG \quad \text{Equation 6-30}$$

$$\Delta h_c = 46423.2 + 3169.4 SG - 8792.3 SG^2 \quad \text{Equation 6-31}$$

where  $\Delta h_c$  is the heat of combustion ( $\text{kJ kg}^{-1}$ ) and  $SG$  is the fuel's specific gravity.

Oxygen consumption is another method commonly used for calculating the heat of combustion for known chemical structures (Walters, 2001). Heats of combustion estimated from oxygen consumption rely on the empirical

observation that a wide range of organic compounds have approximately the same heat of complete combustion per gram of diatomic oxygen consumed. As burning common fuels in a fire involves breaking chemical bonds involving hydrogen, carbon and oxygen, the heat generated per unit mass of oxygen consumed,  $E$  appears to be a constant (approximately  $13.1 \pm 0.7 \text{ kJ g}^{-1}$  of oxygen consumed)(Chow and Han, 2011). Hence, the net heat of complete combustion of the fuel with all products in the gaseous state is expressed as:

$$\Delta h_c = E \frac{n_{O_2} M_{O_2}}{n_f M_f} = (13.1 \pm 0.7) \frac{n_{O_2} M_{O_2}}{n_f M_f} \quad \text{Equation 6-32}$$

In Equation 6-32,  $n_f$  and  $M_f$  are the number of moles (mol) and molecular weight of the fuel ( $\text{g mol}^{-1}$ ), respectively,  $n_{O_2}$  is the number of moles of  $O_2$  consumed in the balanced combustion equation, and  $M_{O_2}$  ( $= 32 \text{ g mol}^{-1}$ ) is the molecular weight of diatomic oxygen.

### 6.3.3.6 Fraction of Radiative Heat Feedback for Hot Zone

For a case of a storage tank fire, it has been shown that part of the total heat release from the flames of the burning fuel raises the temperature and vaporises the fuel (Hamins *et al.*, 1995). The heat flux is transferred from the flame through the surface and into the liquid fuel. And in the case of boilover in which a hot zone is a key requisite, a fraction of this heat contributes to the formation of the hot zone.

Koseki (1994) stated that multi component materials with a wide boiling point range such as crude oil have the greatest tendency to undergo boilover, and the energy for hot zone formation came directly from the flame via radiation.

The fraction of radiative heat feedback is important in the determination of the heat flux radiated from the flame to the fuel. The fraction which is essential for the solution of Equation 6-25, is then assumed to be within the range of 1-5% from the total heat release rate of the burning fuel. Such an assumption is

proposed based on the analysis conducted by Koseki (1994) and Garo *et al.* (1999).

The estimated values of all these intermediate parameters are then used to solve Equation 6-10 in order to predict the time to boilover.

### 6.3.4 Fraction of Fuel Vaporised

The fraction of the fuel vaporized in a storage tank fire represents the amount of light components of the fuel mixture that have been consumed from the beginning of the fire until the occurrence of boilover. From the start of the fire, heat from the flame is transferred to the fuel surface, primarily by radiation. It is then transferred downwards into the pool by the mechanisms of conduction (initially) and then by convection as the light components are vaporised and the hot zone is formed. Heat is transferred to the fuel below the hot zone again by conduction (initially) and then by convection as the light components are vaporised and that region of the pool also becomes part of the hot zone. This process continues until the base of the hot zone reaches the fuel/water interface and the water temperature is raised to its boiling point. At this point steam is produced. Vigorous mixing between the fuel at the temperature of the hot zone and water at or close to its boiling point takes place resulting in water being converted into steam at a very high rate and the ejection of burning oil out of the tank.

The fraction of fuel vaporised, is quantified based on fuel surface regression rate,  $v_a$  ( $\text{m s}^{-1}$ ) and time to boilover,  $t_{bo}$  (s) as shown by the following Equation 6-33. The surface regression rate prior to boilover relies to the consumption of the light components of the fuel.

$$x_V = \frac{v_a t_{bo}}{z_f} \quad \text{Equation 6-33}$$

where  $z_f$  is the initial depth of the fuel, m.

### 6.3.5 Hot Zone Temperature prior to Boilover

The fraction of fuel vaporised indicates the amount of light components of the fuel that have been vaporised since the start of the fire until the instance at which boilover occurs. The temperature at which most of the light components of the fuel mixture have been vaporised is taken as the hot zone temperature. Therefore the hot zone temperature can be linked to the fraction of fuel vaporised.

This temperature is also considered to be the average temperature of the remaining hot fuel that has been heated by the radiative heat flux from the flame prior to the boilover occurrence. Hence the temperature, at which a boilover occurs i.e. the hot zone temperature immediately prior to boilover,  $T_{hz}$  could be estimated by means of a correlation between temperature,  $T$  and the fraction of fuel vaporised,  $x$ . Such correlation is taken from Riazi & Daubert (1987).

$$T = a_0 + a_1 x + a_2 x^2 + a_3 x^3 + a_4 x^4 + a_5 \ln(x + 0.5) \quad \text{Equation 6-34}$$

In the case of occurrence of a boilover,  $T$  (which is taken to be  $T_{hz}$ ) is the hot zone temperature immediately prior to boilover ( $^{\circ}\text{F}$ ) and  $x$  (which is taken to be the fraction of fuel vaporised prior to boilover,  $x_V$ ) is the volume fraction of fuel that have been vaporised during the fuel burning. The correlation constants  $a_0, a_1, a_2, a_3, a_4, a_5$  were experimentally obtained by means of a hydrocarbon volatility/distillation curve. In order to solve for the temperature, the constants are selected from Table 6-2 according to the initial boiling point of the fuel.

Initially, an assumption for the hot zone temperature immediately prior to boilover ( $T_{hz,initial}$ ) is made to determine the time to boilover. A value of  $T_{hz,initial} = 100^{\circ}\text{C}$  is presumed to solve Equation 6-10 to get the time to boilover.

Group	Initial $T_{bp}$ (K)	Constant					
		$a_0$	$a_1$	$a_2$	$a_3$	$a_4$	$a_5$
Low-boiling Naphtha	283.15	14275.23	-39093.71	30313.9	-19093.5	5713.55	20522.3
High-boiling Naphtha	310.93	23873.55	-65672.82	50898.4	-32208.59	9634.06	34291.8
Jet Naphtha	389.82	2936.27	-7364.53	6174.37	-4551.89	1612.38	3886.81
Kerosene	398.71	6372.93	-16789.44	13343.9	-8622.18	2638.58	8820.57
Fuel Oil	455.37	12317.2	-32786.53	25335.8	-16093.8	4917.36	17248.8
Gas Oil	488.71	5409.57	-13616.02	10697.1	-6889.45	2114.95	7198.81

**Table 6-2: Constants for Equation 5-17 (Riazi & Daubert, 1987)**

Consequently, once the time to boilover is obtained, the fraction of fuel vaporised,  $x_V$  can be estimated using Equation 6-33. The result obtained is then used to determine a new value for the temperature  $T_{hz}$ . The process is repeated until the difference between the newly obtained  $T_{hz}$  and the previous value for  $T_{hz}$  is  $< 1$  unit temperature (e.g.  $1^\circ\text{C}$ ) giving the predicted hot zone temperature.

### 6.3.6 Analysis of the Predictive Parameter

Equation 6-10 which is used to predict the time to boilover contains a number of estimated parameters. It is important to weigh the influence of these parameters on the predicted time to boilover in order to determine their significance. By knowing the influence of each of the parameters, determines the importance that must be placed on ensuring the accuracy of estimating their value prior to the predicting the time to boilover.

#### 6.3.6.1 Influence of Radiation Heat Flux on Boilover Onset

The energy for the hot zone formation comes directly from radiation of heat from the flame. Based on relevant studies, about five per cent of the total heat release energy from flames was found to be transferred to the fuel, and consequently a small amount of energy was used for the hot zone formation (Koseki, 1994). In another study (Garo *et al.*, 1999), it was shown that only a

small fraction of the heat released by the flame is retained by the fuel and water layers (of the order of 1%). On that note, the analysis on the time required for boilover to occur by varying the flame heat flux feedback to the fuel-water interface was carried out.

The heat flux feedback to the fuel-water interface is determined by the multiplication of the total heat release of the fuel by combustion and a constant that represents the fraction of radiative heat feedback to fuel surface as shown in Equation 6-25. The variation of the heat feedback in the prediction analysis is achieved by fitting values of 1.65, 1.7 and 1.75% as the fraction of the total heat release to the fuel surface. The results of the effect of changing the heat flux to the fuel surface on time to boilover are shown in Figure 6-11. The fraction of 1.7% of the total heat release returned to the fuel-water interface provides prediction results that agreed well with the experimental values for the field scale tests involving crude oil in a tank of 1.2 m diameter (i.e. FS Test 2, 3, 4, 5, 6, 9, 10, 11, 12, 13 and 14).

Figure 6-11 shows boilover occurs faster when the radiation heat flux returned to the fuel surface is higher. The findings indicate that the dependence of the time to boilover on the fraction of the heat transferred from the flame into the fuel is strong. An increase of the heat feedback fraction from 1.7% to 1.75% (about 3% increase) will change (i.e. reduce) the time to boilover by about 10%. The prediction of the time to boilover is hence significantly depends on the heat radiation from the flame transferred into the fuel.



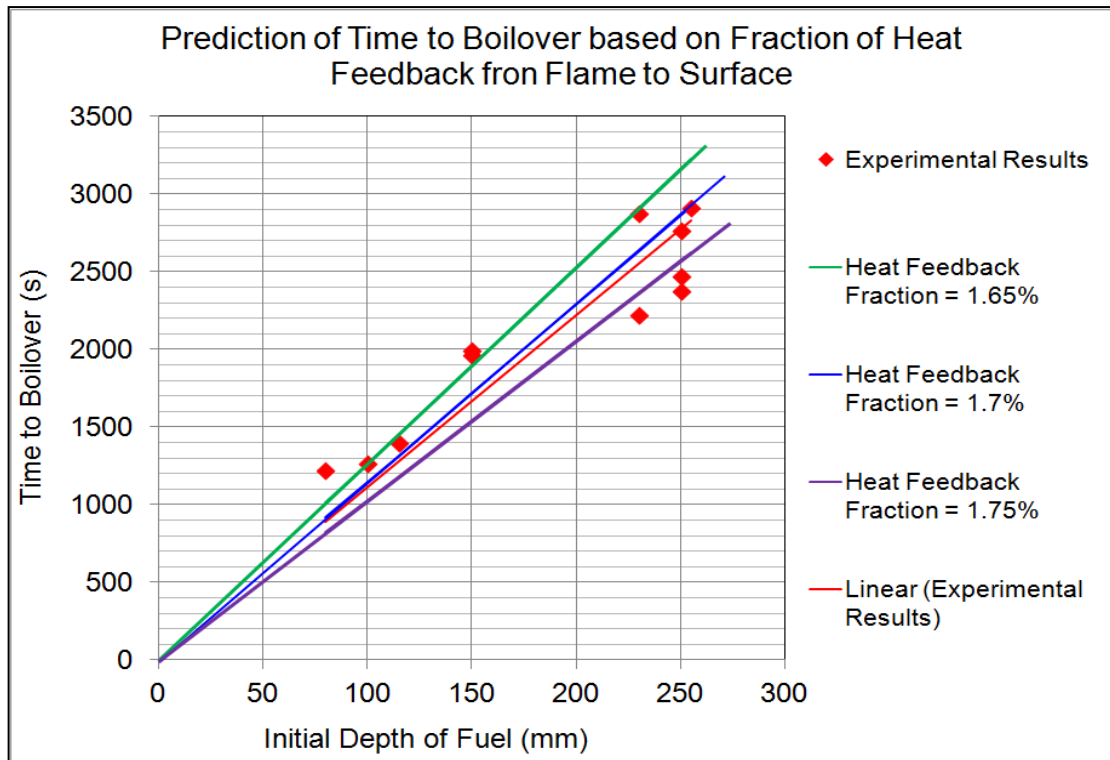


**Figure 6-11: Time required to boilover based on the different fraction of radiation heat flux returned to fuel. The experimental results are from the field scale tests in 1.2 m diameter tank involving crude oil**

### 6.3.6.2 Influence of Fuel Storage Temperature

Due to the extensive development of the oil industry throughout the world, there is concern in different geographical areas that high (or low) ambient (storage) temperature could affect the boilover occurrence and hence contribute to serious safety issues concerning fuel storage facilities. Hence, another parameter considered in the heat balance to predict the boilover onset is the fuel storage temperature. The time to boilover was predicted for a range of storage temperature to determine the extent to which this parameter influenced the boilover onset time.

Figure 6-12 shows the influence of the storage temperature on the time to boilover.

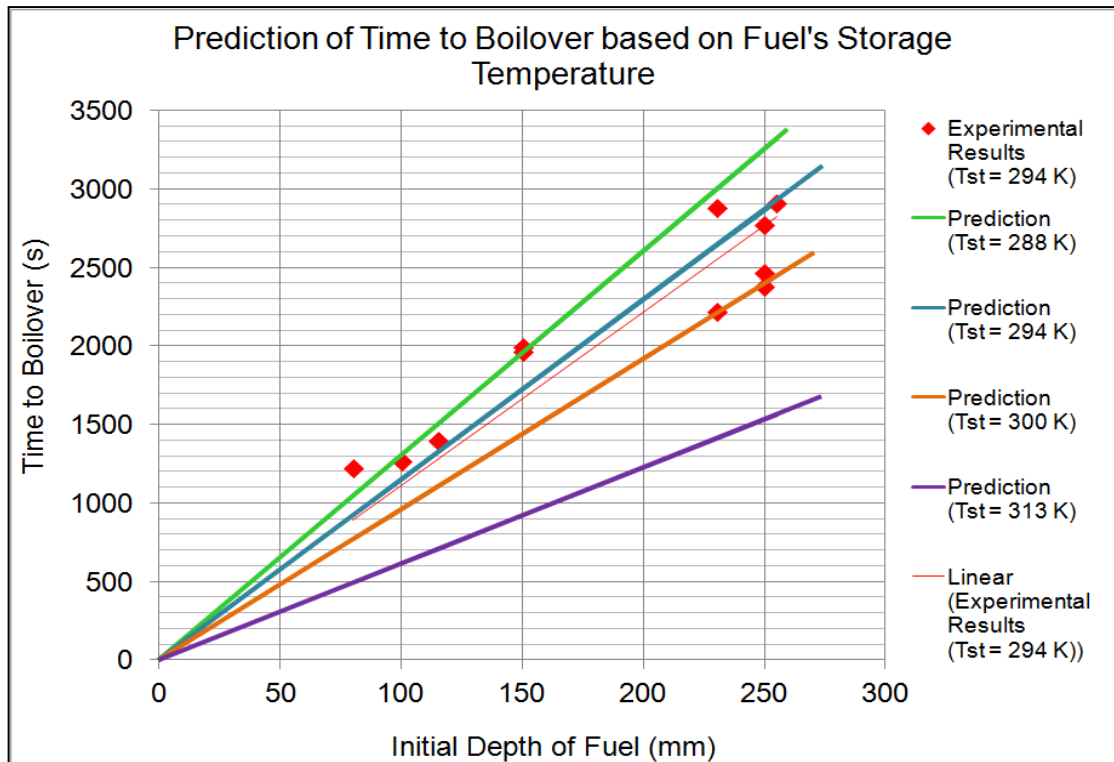


**Figure 6-12: Influence of initial storage temperature on the time to boilover. The experimental results are from the field scale tests in 1.2 m diameter tank involving crude oil**

The figure shows that an increase of the fuel's initial storage temperature from 294 K to 300 K (about a 2% increase) resulted in about a 16% reduction in the boilover time (from 915 s reduced to 767 s for initial fuel depth of 80 mm). This observation indicates that the initial fuel temperature will significantly influence the prediction of the time to boilover; in which a higher initial fuel temperature will contribute to a shorter onset time.

### 6.3.6.3 Impact of Fuel Density and Effect of Fuel Boiling Points

The time to boilover as proposed by Equation 6-10 requires estimates of the fuel's physical properties (density and boiling point). Generally, in the oil industry, there is a wide range of liquid hydrocarbon being handled that may have the potential to boilover (fuels with wide range of boiling points and with high viscosity). Such a wide range of liquid hydrocarbons possess different properties e.g. density and boiling point. Crude oil, for example, has densities ranging from about  $800 \text{ kg m}^{-3}$  (45.3 API) for light crude oil to over  $1000 \text{ kg m}^{-3}$

(less than 10 API) for heavy crude oil and bitumen (Speight, 1999). The boiling point ranges from approximately  $-1^{\circ}\text{C}$  to over  $720^{\circ}\text{C}$  ( $30^{\circ}\text{F}$  to over  $1328^{\circ}\text{F}$ ).

Hence analysis on the impact of the fuel's properties, i.e. the density and boiling point on the predictions of the time to boilover, were carried out. The time required for the fuel to boilover based on different values of density was evaluated and are shown in Figure 6-13.

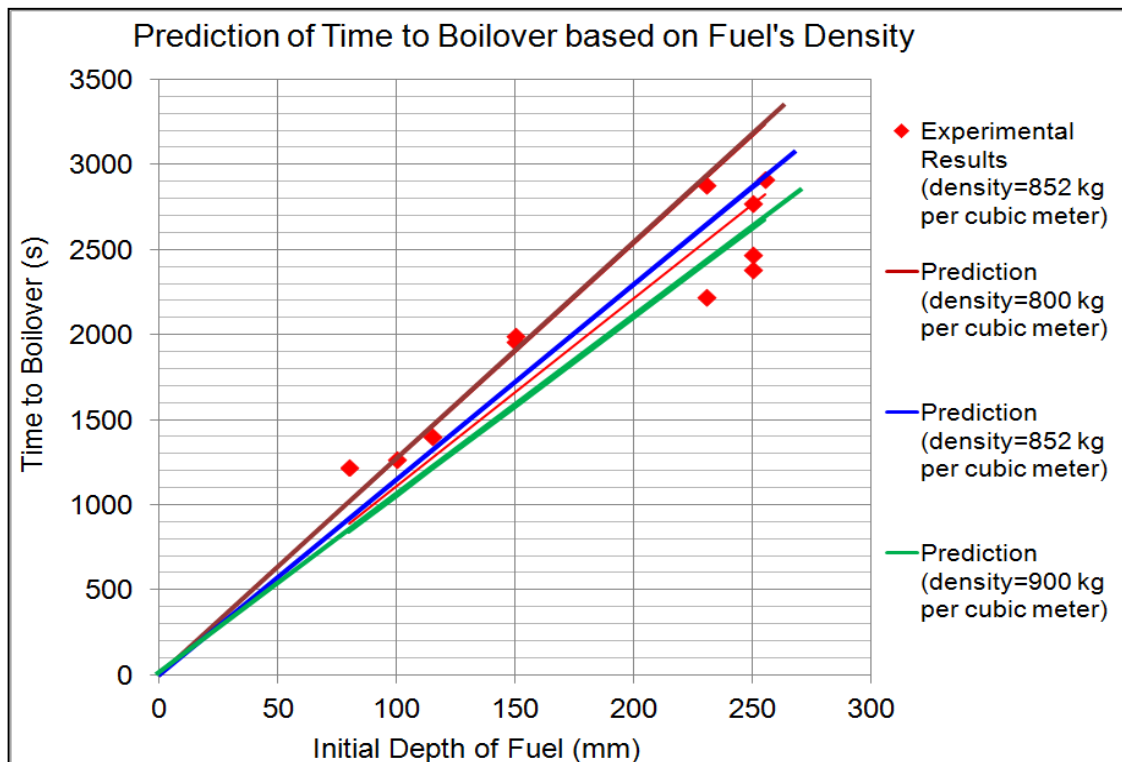


**Figure 6-13: Prediction of time to boilover based on the different fuel's densities. The experimental results are from the field scale tests in 1.2 m diameter tank involving crude oil**

Based on Equation 6-13, the times to boilover are close to one another for each of the density values for which predictions were performed. The figure shows that an increase of the fuel's density from  $852\text{ kg m}^{-3}$  to  $900\text{ kg m}^{-3}$  (about a 6% increase) resulted in about a 8% reduction in the boilover time (from 915 s reduced to 838 s for initial fuel depth of 80 mm). Based on this observation, it was deduced that results from one fuel density can be used for fuels with different densities.

The time required for the fuel to boilover based on the average boiling point of the fuel is as shown in Figure 6-14. The fuel's average boiling point is the main parameter to estimate the fuel's surface regression rate (Equation 6-29), which will be used, with strong importance, in the prediction of time to boilover.

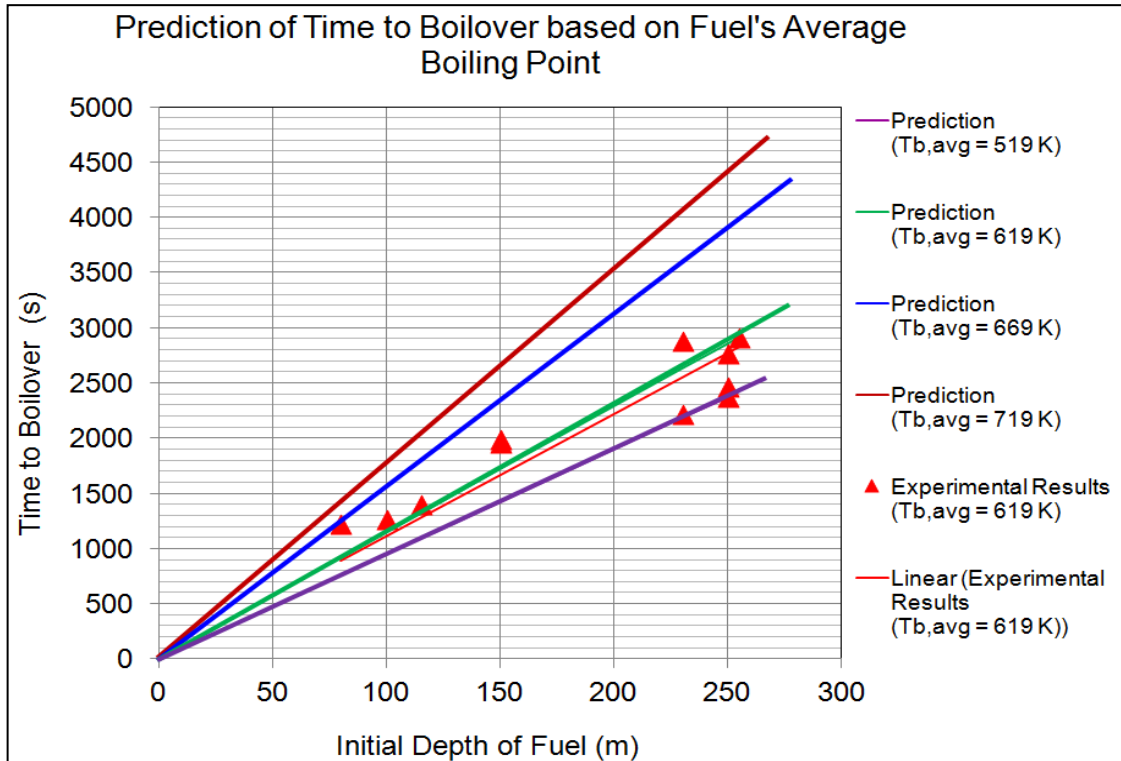


**Figure 6-14: Prediction of time to boilover based on the fuel's average boiling point. The experimental results are from the field scale tests in 1.2 m diameter tank involving crude oil**

Based on the figure, the model calculations show that increases in the fuel's average boiling point will significantly affect the time to boilover. An increase of the fuel's average boiling point from 619 K to 719 K (about a 17% increase) will show about a 30% increase in the boilover time.

The analysis of the parameters shows that the prediction of time to boilover is influenced significantly by the magnitude of the heat feedback from the flame into the fuel, the average boiling point of the fuel and the storage temperature of the fuel. However, changes in the fuel density do not have any significant effect on the time to boilover.

## 6.4 CONSEQUENCES OF BOILOVER PHENOMENON

A boilover results in the generation of a fireball-like flame. A boilover also results in the ejection of burning liquid over a wide area. The severity of the consequences depends upon the amount of fuel vapour consumed in the fireball and the quantity of liquid fuel ejected out of the tank and forming a pool fire surrounding the tank. These quantities of fuel vapour and fuel liquid depend on the amount of fuel consumed throughout the steady burning phase prior to the boilover occurrence and hence, on the amount of fuel remained in the tank immediately prior to boilover.

### 6.4.1 Mass of Liquid Fuel Remaining Prior to Boilover

Following the start of the full surface burning of the fuel, most of the lighter components are vaporized and consumed in the flame prior to boilover. The remaining liquid fuel will consist of the heavier components at a high temperature. The mass of the remaining fuel,  $m_{liq}$  (kg) could be estimated through the following correlation:

$$m_{liq} = \left( \frac{\pi D^2}{4} \right) (z_f - v_a t_{bo}) \rho_L \quad \text{Equation 6-35}$$

It is important to estimate the mass of fuel within the tank prior to boilover in order to estimate the consequences of the boilover phenomenon. The mass remained will affect the characteristics of the fireball-like flame resulting from the boilover and the area affected due to the expulsion of the burning fuel from the tank. From this remaining mass of fuel, the fraction that vaporises during boilover can be determined giving the amount of fuel consumed in the fireball.

### 6.4.2 Consumption of Vaporised Fuel in a Fireball-Like Flame during Boilover

When boilover starts, a column of a very rich concentration of fuel is lifted up rapidly into the atmosphere up to an elevation where sufficient air is available to

permit violent burning. The lifting is due to the action of a piston effect (due to expansion of water to steam) expelling the fuel content outside the tank. The lifting is possible since the pressure from the steam expansion is larger than the pressure generated by the liquid column,  $P^*$  (Pa).

$$P^* = [P_{atm} + (\rho_L z_{f,tbo} g)] \quad \text{Equation 6-36}$$

where  $z_{f,tbo}$  is the height of remaining liquid fuel column in the tank immediately prior to boilover (m),  $P_{atm}$  is the atmospheric pressure (Pa) and  $g$  is the gravitational acceleration ( $\text{m s}^{-2}$ ).

During the expulsion, a fraction of the liquid fuel is vaporised and expands thus feeding the pool fire to produce a fireball-like flame. The vaporisation is assumed to occur due to temperature increase during the boilover. The temperature during the vaporisation process is estimated via:

$$T_{vap,bo} = T_{hz} + T^* \quad \text{Equation 6-37}$$

The temperature increase,  $T^*$  (K) at which a fraction of the remaining liquid fuel vaporises at the instance of boilover is determined via the vapour pressure curve equation and the vaporisation pressure,  $P^*$ , as follows:

$$T^* = \exp \left[ \frac{(\ln P^* - \beta)}{\alpha} \right] - T_{bp,tbo} \quad \text{Equation 6-38}$$

where

$T_{bp,tbo}$  is the boiling point (K) of liquid at boilover time,  $t_{bo}$   
 $\alpha, \beta$  are the constants for (assumed) straight line of vapour pressure curve equation between two points of initial conditions,  $P_{atm}$  &  $T_{bp,tbo}$  and critical conditions,  $T_{cr}$  &  $P_{cr}$ .

As the fuel composition changes due to the vaporisation of the lighter ends, the average boiling temperature of the remaining fuel also changes. The boiling

point of the liquid fuel at boilover time  $T_{bp, tbo}$  is taken as an average between the hot zone temperature immediately prior to boilover,  $T_{hz}$  and the maximum boiling point of fuel. The constants  $\alpha$  and  $\beta$  are determined through the following correlations:

$$\alpha = \left[ \ln \left( \frac{P_{cr}}{P_{atm}} \right) \right] / \left[ \ln \left( \frac{T_{cr}}{T_{bp, tbo}} \right) \right]$$

$$\beta = \ln P_{atm} - \alpha \ln T_{bp, tbo}$$

Once the vaporisation temperature,  $T_{vap,bo}$  is obtained (by solving Equation 6-37), the fraction of the fuel that vaporised and is consumed in the fireball during boilover,  $x_{vap}$  can be estimated using Equation 6-34. For this case,  $T$  in Equation 6-34 (which is taken to be  $T_{vap,bo}$ ) is the temperature at which liquid fuel is vaporised and feeds the fireball-like flame during boilover ( $^{\circ}\text{F}$ ) and  $x$  (which is taken to be the fraction of fuel vaporised during boilover,  $x_{vap}$ ) is the volume fraction of fuel that have been vaporised during the boilover and consumed in the fireball. The value of  $x_{vap}$  is estimated in order to obtain a temperature concurrent with (as close as) the value obtained for  $T_{vap, bo}$ .

The mass of fuel consumed in the fireball-like flame,  $m_{vap}$  (kg) can then be determined.

$$m_{vap} = x_{vap} m_{liq}$$

**Equation 6-39**

The mass of fuel consumed in the fireball,  $m_{vap}$  is used to characterise the diameter, duration and elevation of the fireball-like flame formed during the boilover. In addition, the balance of the liquid fuel,  $m_{fin}$  that would be ejected out during boilover can also be estimated via the following correlation:

$$m_{fin} = m_{liq} - m_{vap}$$

**Equation 6-40**

Determination of the amount of liquid fuel ejected out of the tank during boilover enables an estimation to be made of the area affected by the spread of fuel over the ground around the tank. The affected area may extend to a diameter several times that of the tank.

### **6.4.3 Thermal Effects of Fireball**

Boilover is considered as an eruption of hot fuel giving rise to a release of burning vapour which results in the generation of a fireball.

During boilover, a column of steam and fuel with a very rich concentration of fuel is lifted up from the tank due to the piston effect resulted from the conversion of water to steam. The lifting is possible since the generation of pressure from the sudden vaporisation of water is considerably larger than the atmospheric pressure plus the pressure generated by the remaining liquid fuel column in the tank prior to the boilover. Because of this pressure disparity, much of the liquid fuel is quickly ejected into the atmosphere and in response to this, a rapid drop in pressure occur and hence a portion of the fuel flashes to vapour and fuel droplets are vaporised by the existing tank fire. This vapour expands rapidly, shattering some of the remaining larger liquid droplets into smaller drops which are also readily vaporised, thereby creating an unstable cloud consisting of vapour, liquid drops and air. Since the tank fire ignites this cloud and creates a fireball that grows rapidly until it reaches a maximum size. The fireball rises as a result of the momentum of the release and buoyancy. As it rises, the limited fuel supply is consumed and the fireball breaks up and self extinguished.

The fireball emits a large amount of radiant energy and is capable of causing injuries and damage over a wide area several times greater than the size of the fireball. The radiant energy relates to the emissive power of the fireball which gives the power radiated per unit surface area of the fireball. The surface emissive power controls the intensity of thermal radiation received by an object



at a distance from the fireball. In order to estimate the surface emissive power, an estimation of the diameter and duration of the resulting fireball is necessary.

#### 6.4.3.1 Fireball Diameter, Duration and Elevation

The basics model reported in the literature by various authors for fireball diameter,  $D_{fb}$  (m) and duration,  $t_{fb}$  (seconds) are provided as a function of the fuel mass consumed (kg) in the fireball through equations of the form:

$$D_{fb} = a m_{vap}^b \quad \text{Equation 6-41}$$

$$t_{fb} = c m_{vap}^d \quad \text{Equation 6-42}$$

where  $a$ ,  $b$ ,  $c$  and  $d$  are constants. The constants are not precisely known and vary in each of the basic models available in the literature. The data for the parameters are given in Table 6-3.

References	$a$	$b$	$c$	$d$
<i>Data values</i>				
CCPS (2000)	5.80	0.333	0.450	0.333
Engelhard (2005)	6.48	0.325	0.852	0.260
Fay and Lewis (1977)	6.28	0.333	2.530	0.167
Hardee and Lee (1973)	6.24	0.333	1.100	0.167
Hasegawa and Sato (1978)	5.25	0.314	1.070	0.181
Moorhouse and Pritchard (1982)	5.33	0.327	1.089	0.327
Prugh (1994)	6.48	0.325	0.825	0.260
Roberts (1982)	5.80	0.333	0.450	0.333
<i>Statistics</i>				
Mean	5.95	0.328	1.040	0.253
Standard Deviation	0.49	0.01	0.62	0.07

**Table 6-3: Data for constant parameters  $a$ ,  $b$ ,  $c$ , and  $d$  of the empirical relationships for fireball diameter and duration from literature**

The values of  $a$ ,  $b$ ,  $c$ , and  $d$  used in this work are the mean values. Hence:

$$D_{fb} = 5.95 m_{vap}^{0.328} \quad \text{Equation 6-43}$$

$$t_{fb} = 1.04 m_{vap}^{0.253} \quad \text{Equation 6-44}$$

Table 6-4 below shows a comparison between the experimental data taken from Roberts *et al.* (2000) and the predictions of Equation 6-43 and Equation 6-44. The expressions suggested give good agreement with the experimental data.

Propane released (kg)	Predicted Diameter (m)	Measured Diameter		Predicted Duration (s)	Measured Duration	
		Crosswind (m)	Up/Downwind (m)		Crosswind (s)	Up/Downwind (s)
279	38	45	41	4.3	3	3.8
710	51	45	43	5.5	5	4.6
1272	62	75	74	6.3	6.5	5.9
1708	68	85	71	6.8	7	6.6

**Table 6-4: Measured and predicted fireball diameter and duration - Comparison based on data from Roberts *et al.* (2000)**

Equation 6-43 estimates the maximum diameter of the fireball. Generally, once formed, the fireball will start to lift off due to buoyancy and air entrainment. As the fireball starts to rise, the diameter stays constant until the fireball reaches its maximum elevation and starts to dissipate. The fireball duration expressed by Equation 6-44 represents the overall duration which includes the time from the start of the fireball to its dissipation. The maximum elevation,  $z_{fb}$  at which most fireballs emit the majority of their energy, can be estimated via the correlation suggested by CCPS (2000):

$$z_{fb} = 0.75 D_{fb}$$

**Equation 6-45**

Equation 6-45 represents the maximum height of the centre of the fireball above the ground. This is achieved half way through the duration of the fireball, and the maximum diameter is attained at the same time.

It is important to highlight that the correlations for a fireball given above are used in this work in the form of a static model. The fireball's maximum diameter and maximum height are assumed to have been reached instantaneously and remain constant over the full duration of the event. Such an approach is used, though simplified, since the expressions can provide sufficient, quick and conservative estimations for responders during emergency situations.

### 6.4.3.2 Surface Emissive Power

The diameter and height above ground level are important parameters for determining the thermal effects of a fireball. The radiant energy of a fireball will depend, among other important factors, on the flame temperature as indicated by the Stefan-Boltzman equation. However, all of the factors, including the flame temperature are difficult to quantify.

In this work, the thermal radiation is calculated using the radiant flux emitted from the surface of the fireball, otherwise known as the surface emissive power,  $E$  (energy per unit area per unit time, kW m<sup>-2</sup>). CCPS (2000), Engelhard (2005) and Prugh (1994) provide the equation to estimate the surface emissive power based on the radiative fraction of the total heat release during combustion. The frequently-used equation assumes that a fraction of the heat of combustion is emitted as radiation to the surroundings from the surface of the fireball. It is further assumed that heat is radiated at a constant rate during the fireball

development. The relationship proposed is  $E = \frac{f_R m_{vap} \Delta h_c}{\pi D_{fb}^2 t_{fb}}$ ; and using the

relationships between the fuel mass vaporized and consumed in the fireball,  $m_{vap}$ , the fireball diameter,  $D_{fb}$ , and duration,  $t_{fb}$ , the correlation reduces to:

$$E = 0.0086 f_R m_{vap}^{0.091} \Delta h_c$$

**Equation 6-46**

The term  $f_R$  represents the radiative fraction of the total heat release by combustion of the fuel involved. Prugh (1994) suggests a range of values from 0.25 to 0.40 for the radiative fraction which is quite similar to the range of values 0.3 to 0.4 suggested by CCPS (2000).

Given a radiation source and a receptor, not all points on the radiating surface can radiate towards to the receptor. Therefore not all the power emitted by the source is received by the receptor.

The power flux received,  $E_R$ , can be estimated from the relationship proposed by Prugh (1994) and CCPS (2000):

$$E_R = E F \delta \tau \quad \text{Equation 6-47}$$

where

$F$  is the view factor

$\delta$  is the absorptivity of the receptor

$\tau$  is the atmospheric transmissivity.

The view factor,  $F$  is the solid angle subtended by the emitting surface from the location and orientation of the receptor. The view factor for a spherical emitting surface from an infinitely small plane receptor located at a distance  $L$  from the centre of the sphere and oriented such that the normal to the plane surface of the receptor is directed towards the centre of the sphere is govern by (Lees, 2005 & Engelhard, 2005):

For the relative locations and orientations of the sphere and receptor shown in Equation 6-15:

$$F = \frac{D_{fb}^2}{4L^2} \cos \theta \quad \text{Equation 6-48}$$

The term  $L$  can be expressed as  $(X^2 + z_{fb}^2)^{0.5}$  where  $X$  is the ground distance measured from the projected centre of the fireball to the receptor as shown Figure 6-15.

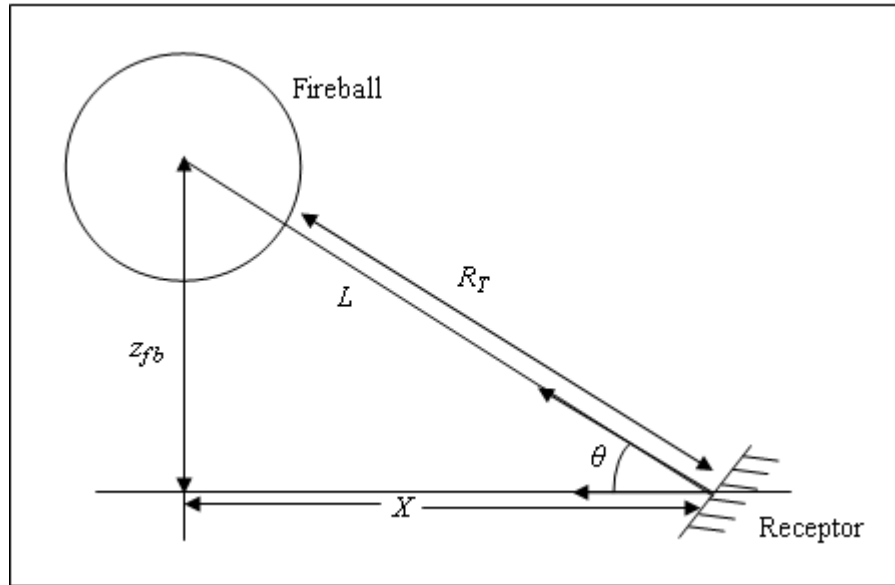


Figure 6-15: Position of fireball and target

The absorptivity is generally defined as the proportion of the incident radiation on a reception that is absorbed by the receptor's surface. In this work,  $\delta$  is assumed to be between 0.9 and 1.0.

The atmospheric transmissivity,  $\tau$  represents the ratio of the radiant energy that would be incident upon a receptor in the absence of an intervening atmosphere between the emitting surface and the receptor to that actually incident upon the receptor. The reduction in the incident radiation is a result of absorption and scattering by the atmosphere. The absorption of thermal radiation results mostly from water vapour in the atmosphere. A useful relationship between the fractional atmospheric transmissivity,  $\tau$ , the partial pressure of water,  $p_w$  (in Pascal) and distance  $R_T$  (in meters), and is given by the model of Engelhard (2005) and CCPS (2000):

$$\tau = \frac{2.02}{(p_w R_T)^{0.09}}$$

Equation 6-49

The partial pressure of water,  $p_w$  is determined by means of a correlation involving the relative humidity,  $RH$ , %, and ambient temperature,  $T_{atm}$ , K, (CCPS, 2000) as follows:

$$p_w = 1013.25 RH \exp\left(14.4114 - \frac{5328}{T_{atm}}\right) \quad \text{Equation 6-50}$$

The distance,  $R_T$  represents the distance between the surface of the fireball and the receptor and is given by:

$$R_T = (X^2 + z_{fb}^2)^{0.5} - 0.5 D_{fb} = L - 0.5 D_{fb} \quad \text{Equation 6-51}$$

Equation 6-47 hence gives an estimation of the incident radiation received per cubic meter of a receptor's surface. It is important to point out that  $R_T$  is not a single value. It is different for each point over the spherical surface. However, in this work, a single value  $R_T$  is used to obtain conservative estimates in the prediction.

#### 6.4.4 Area Affected by the Spread of Burning Fuel

During boilover, due to the production of steam as the hot zone reached the fuel-water interface at the tank bottom, a column of fuel-steam mixture is lifted into the atmosphere. The height of this fuel-rich column,  $z_{mix}$  is expected to be larger than the height of the storage tank,  $z_T$ . The difference between the two heights gives the estimated volume of hot fuel being spread outside the tank and hence the area affected due to the ejected fuel during the boilover.

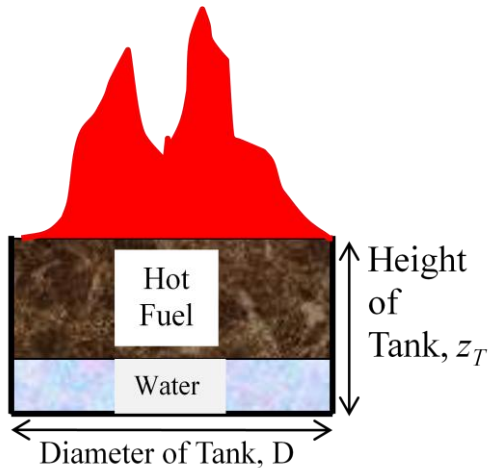


Figure 6-16: (a) Base of hot zone reached the fuel-water interface

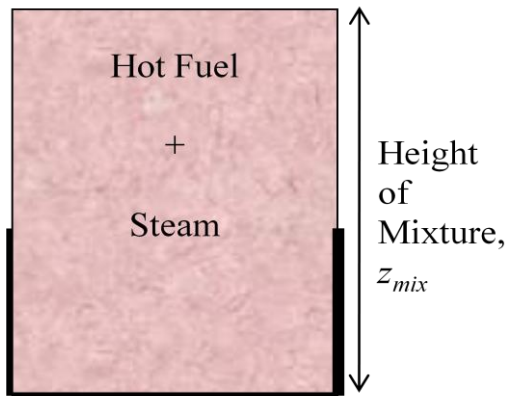


Figure 6-16: (b) a column of fuel-steam mixture is lifted into the atmosphere during boilover

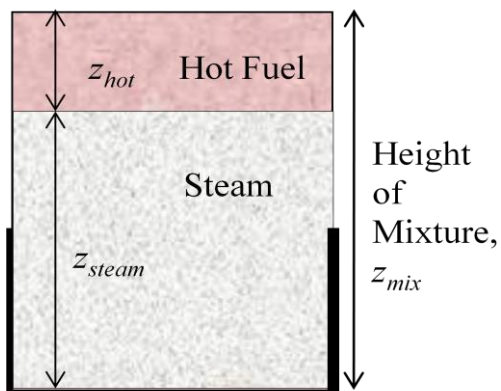


Figure 6-16: (c) Simple basis to determine height of the fuel-steam mixture

As the burning progresses, the base of the hot zone (hot fuel) moves downward at a pseudo constant rate towards the fuel-water interface. The hot zone heats the fuel-water interface and hence a boilover occurs (see Figure 6-16(a)).

During boilover, due to the production of steam, a column of fuel-steam mixture is lifted into the atmosphere (see Figure 6-16(b)). Ideally the height of the mixture is given by:

$$z_{mix} = \frac{m_{steam} + m_{fin}}{\frac{\pi D^2}{4} \rho_{mix}} \quad \text{Equation 6-52}$$

where  $m_{steam}$  is the mass of steam,  $m_{fin}$  is the balance of the liquid fuel during boilover after subtracting the fraction that was consumed in the fireball (see Equation 6-40) and  $\rho_{mix}$  is the density of the fuel-steam mixture.

The density of the fuel-steam mixture however is difficult to be assessed.

Hence the height of the fuel-steam mixture is determined by following the basis shown in Figure 6-16(c):

$$z_{mix} = z_{steam} + z_{hot} \quad \text{Equation 6-53}$$

where

$z_{steam}$  is the height of column of steam produced, m  
 $z_{hot}$  is the height of column of the hot liquid fuel, m

The height of the column of the hot liquid fuel is calculated based on the balance of the liquid fuel,  $m_{fin}$  that would be ejected out during boilover, the fuel density at storage temperature,  $\rho_L$  and the tank cross-sectional area,  $A$ .

$$z_{hot} = \frac{m_{fin}}{\rho_L A} \quad \text{Equation 6-54}$$

The height of the steam column can be approximated if the volume of steam produced is known. The volume of steam produced relates to the volume of water vaporised during boilover. The volume of water is estimated by assuming certain thickness of the water at the base of the tank vaporised as boilover occurred (approximately 1-3 mm of water vaporised as observed in the laboratory scale tests). The volume of steam is then quantified using the following relation:

$$V_{steam} = \frac{\rho_w}{\rho_{steam}} V_{water} \quad \text{Equation 6-55}$$

where  $\rho_w$  is the density of water at  $T_{atm}$  ( $\text{kg m}^{-3}$ ) and  $\rho_{steam}$  is the density of steam at  $T_{vap,bo}$  ( $\text{kg m}^{-3}$ ). The density of steam at  $T_{vap,bo}$  is determined via:

$$\rho_{steam} (\text{at } T_{vap,bo}) = \rho_{steam} (\text{at } T_{atm}) \left( \frac{T_{atm}}{T_{vap,bo}} \right) \quad \text{Equation 6-56}$$



The amount of fuel ejected out due to the occurrence of boilover then is estimated via the following:

$$V_E = \pi \frac{D^2}{4} (z_{mix} - z_T) \quad \text{Equation 6-57}$$

where  $V_E$  is the volume of hot fuel mixture being expelled out from the storage tank ( $\text{m}^3$ ) and  $z_T$  is the height of the wall of the tank (m). Two empirical correlations for the spillage affected area are obtained from the literature and given in Table 6-5. Both of them are provided as a function of the volume of hot fuel mixture being expelled out from the tank through an equation of the form:

$$A_E = a (V_E)^b \quad \text{Equation 6-58}$$

where

$A_E$  is the area affected by the spillage of hot fuel during boilover,  $\text{m}^2$

References	$a$	$b$
<i>Data values</i>		
Grimaz, S., Allen, S., Stewart, J.R. and Dolcetti, G. (2008)	153.3	0.8
Mackay, D. and Mohtadi, M. (1975)	53.5	0.89
<i>Statistics</i>		
Mean	103.4	0.825
Standard Deviation	70.6	0.04

**Table 6-5: Empirical relationships for spillage affected area and data for parameters in the relationship  $a$  and  $b$**

Mackay and Mohtadi (1975) and Grimaz *et al.* (2008) presented correlations for the area of fuel spilled onto flat ground due to accidents which resulted in the catastrophic rupture of a container and an instantaneous release of fuel. The estimation by Grimaz *et al.* (2008) takes into consideration the intrinsic permeability of soil and the relative permeability of fuel. The value used for the permeability of soil is  $1 \times 10^{-9} \text{ m}^2$  (for common types of soil e.g. silt and clean sand) and the permeability of fuel is 0.9 (at which the soil condition is typically slightly wet).

The following equation is used to predict the spillage affected area,  $A_E$  for the work carried out in this thesis:

$$A_E = 103.4 (V_E)^{0.825} \qquad \text{Equation 6-59}$$

## 6.5 CONCLUSIONS

The proposed predictive tool assumes that the thermal transfer is carried out by mass transfer in which the lighter components of fuel are vaporised, rise to the fuel surface and feed the fire. This upward movement results in the downward movement of hot heavier components. The net effect is the establishment of vigorous convective currents within a layer known as the hot zone. This assumption allows the use of simple equations based on physical and thermodynamic laws to predict the development of the hot zone, its temperature and the time at which the boilover occurs. The regression rate of the fuel surface enables the amount of fuel available to be ejected during boilover to be determined.

Revising at the results of the field and laboratory scale tests, it was summarised that at any point during a storage tank fire (in which a boilover is a possibility), an exponential temperature profile is observed just beneath the fuel surface. Below the exponential profile, a vertical temperature profile representing an isothermal layer is established. This is the stage when the hot zone is forming and growing. Below the vertical profile is another exponential temperature profile which represents the base of the hot zone. This base of the hot zone moves downward at a pseudo constant rate towards the fuel-water interface. Finally there is the last stage in which the base of the hot zone has reached the interface but does not immediately boil the water. The hot zone heats further the fuel-water interface and hence a boilover occurs. In this last third stage, there appears to be a delay between the hot zone arriving in the vicinity of the interface and boilover occurring.

Ideally, the development of a predictive tool for the boilover onset should consider the three stages that constitute the time to boilover. However, in order to aid the development of a predictive tool on boilover onset, the heating mechanism is simplified by considering that the heat involved in the process is only used for vaporising the component in the hot zone and for raising the temperature of the unheated fuel to the hot zone temperature. The tool is based on the stage in which the base of the hot zone moves downward towards the fuel-water interface.

An analysis of the parameters shows that the prediction of the time to boilover is influenced significantly by the:

- i. the magnitude of the heat feedback from the flame into the fuel
- ii. the average boiling point of the fuel
- iii. the storage temperature of the fuel

However, differences in the fuel density do not have any significant effect on the time to boilover. It was deduced that predictions obtained from one fuel density can be used for similar fuels with slightly different densities.

The boilover phenomenon results in the generation of a fireball-like flame and also a catastrophic ejection of burning liquid hydrocarbon over a wide area. The fireball-like flame emits a large amount of radiant energy and hence can cause injuries and damage over a wide area. The fireball's surface emissive power,  $E$  (energy per unit area per unit time, kW m<sup>-2</sup>) was estimated based on the radiative fraction of the total heat release during combustion. The catastrophic ejection of burning liquid fuel would lead to ground spillage in the surrounding area. No specific study relating to the spillage of burning liquid fuel on the ground following boilover was identified. Hence the predictive calculations were based on studies to estimate area of fuel spilled on flat ground due to accidents in which a catastrophic rupture of container and an instantaneous release of none burning fuel occurred.

## **7 COMPARISON OF PREDICTIVE TOOL AND EXPERIMENTAL DATA**

In order to evaluate the performance of the predictive tool on the time to boilover and the consequences outlined in Sections 6.3 and 6.4, experimental measurements were compared against the predictions made by the empirical correlations (Chapter 3) and the predictive tool (Chapter 6) tool, using the experimental parameters as input.

One of the objectives of this research is to produce predictive tools capable of predicting the important parameters associated with a boilover event i.e. the time to boilover, the amount of fuel remaining in the tank prior to boilover and hence the quantity of fuel that would be ejected during boilover and the consequences of a boilover i.e. fire enlargement, fireball effects and the ground area affected by the expulsion of oil during a boilover event.

The main criterion of the predictive tools is that they should produce readily accessible results to guide a wide range of emergency response personnel on handling the boilover phenomenon. In order for the predictive tools to be useful during crisis, they should be easy to use, capable of modelling the situation at hand and produce a conservative, easy to understand representation of the incident in a very short period of time.

### **7.1 REQUIRED INPUT FOR PREDICTIVE TOOL**

This section explains the data used to validate the correlations of the predictive tool as a whole. The input data mainly consists of two types:

- i. Initial Input Parameters – these are the data which are taken directly from the physical parameters of the fuel storage (or in the context of this section, the data from the experimental set-up). The data includes the tank dimension, storage temperature and the fuel properties.

- ii. Interim Parameters – these are the calculated data required to solve the correlations proposed in Section 6.3 and 6.4. These data are able to be estimated by using the initial input data.

### **7.1.1 Initial Direct Input Parameters**

The initial input parameters are the data obtained from the fuel's properties and the physical storage system. The initial input data required for the correlations used in the predictive tools are as follows:

- i. Storage tank diameter and height (m)
- ii. Storage temperature (K)
- iii. Height of fuel in storage tank (m)
- iv. Fuel properties: normal boiling temperature (K), density ( $\text{kg m}^{-3}$ ) and specific gravity of liquid hydrocarbon - 60°F/60°F

As noted in Section 6.3.6, these parameters weighed significantly in the predictive calculations on the time to boilover and hence the accuracy of such parameters should be emphasized.

### **7.1.2 Interim Parameters for Boilover Onset**

These interim parameters consist of the thermal properties of the fuels. These properties mainly vary with temperatures and hence the availability of these parameters in the literature is limited and/or varies with the condition of the materials, in accordance with the study objectives.

Empirical models are used to calculate the parameters directly, such as the latent heat of vaporization, the heat of combustion and the radiant heat flux received for hot zone formation: they are not used to describe the combustion process. The empirical models are preferred for use, due to their reliability and speed. In addition, as described in Section 6.3, less correlated empirical

equations are the main preferences. One main point to highlight is that empirical correlations should only be used within their range of applicability: this is the range over which the experiments were based on or carried out.

These are the interim parameters that would be estimated and used to solve for the prediction of the time to boilover:

- i. Specific heat ( $\text{J kg}^{-1} \text{ }^\circ\text{C}^{-1}$ ) for liquid hydrocarbon at temperature  $T$  ( $^\circ\text{C}$ )
- ii. Latent heat of vaporisation of component vaporising in the hot zone ( $\text{J kg}^{-1}$ )
- iii. Constant rate of vaporisation of component vaporising in the hot zone or mass burning rate ( $\text{kg s}^{-1}$ )
- iv. Constant rate of heat flux radiant to fuel surface ( $\text{W m}^{-2}$ )

#### **7.1.2.1 Specific Heat**

Specific heat,  $C_p$  is defined as the quantity of heat required to raise a unit mass of material through one degree of temperature. The specific heat is often required in estimating the net heat fluxes necessary to heat (or cool) a material prior to vaporisation. The specific heat is estimated by the correlation proposed by Speight (2001) as in Equation 6-15.

#### **7.1.2.2 Latent Heat of Vaporisation**

The heat of vaporization of the liquid hydrocarbon fuel is related to the heat capacity of the fuel. The heat of vaporization,  $\Delta h_{lh}$  represents the heat required to vaporise a given mass or volume of liquid into vapour. Equation 6-22 is used in the estimation of fuel's latent heat of vaporization which would provide good estimation results for hydrocarbons with an average error of 2.0% (Poling *et al.*, 2000; Riazi & Daubert, 1987). The fuel density and average boiling point are required in determining the heat of vaporization of the fuel involved.

### 7.1.2.3 Mass Burning Rate

The constant rate of vaporisation of fuel component vaporising in the hot zone or simply mass burning rate of fuel is the mass of the liquid fuel consumed by the flame per unit time. The mass burning rate is controlled by several factors, such as fuel composition, the burning surface area and the heat supplied to evaporate the fuel. The time to boilover is influenced by the speed of the base of the hot zone within burning fuel which is linked to the mass burning rate of the fuel. For both pure and multi-component liquid fuels, the mass burning rate of fuel could be determined via the calculating the rate of liquid fuel surface progresses downward. In the absence of experimental data, the surface regression rate is estimated by Equation 6-29. Once the surface regression rate,  $v_a$  ( $\text{m s}^{-1}$ ) is estimated, the mass burning rate of fuel,  $\dot{m}_V$  ( $\text{kg s}^{-1}$ ) is deduced via Equation 6-6.

### 7.1.2.4 Heat Flux Radiant to Fuel Surface

In the case of storage tank fires, heat from the flame returns to fuel and heats and vaporises the more volatile components of the fuel. At the same time, the heat also increases the temperature of the less volatile components up to the temperature of the hot zone. Hence the energy for the hot zone formation comes directly from radiant heat from the flame, but only a small amount of energy of the total heat release energy is transferred to the liquid fuel and used for the hot zone formation. For this reason, it is realised that the heat flux reaching the surface of the burning fuel represents a small fraction of the total heat release rate of the pool fire (Koseki, 1994 and Garo *et al.* 1999). This is aligned with the point source thermal radiation model which stated that the energy radiated from the flame is a specified fraction of energy released during combustion. The heat flux radiated from the flame to the fuel surface is estimated by Equation 6-24. However, the solution for the heat flux radiated to the fuel surface requires the quantification of the fuel mass burning rate per unit area,  $\dot{m}_V''$  ( $\text{kg m}^{-2} \text{s}^{-1}$ ) and heat of combustion,  $\Delta h_c$  ( $\text{J kg}^{-1}$ ). The mass burning rate per unit area is estimated by Equation 6-25 which involved the mass burning rate of fuel and the cross sectional area of the storage tank. The heat of

combustion of the fuel is determined via less correlated Equation 6-30 which only depends on the fuel specific gravity.

## 7.2 CALCULATION PROCEDURE OF PREDICTIVE TOOL

A boilover can occur several hours after the fuel in a storage tank caught fire. Modelling of such dangerous phenomenon would allow the determination of important characteristics features of the relevant scenario. The important parameter to be determined is the time to boilover upon full surface ignition. The procedural predictive calculation of the time to boilover, in the context of this work, is carried out using the Microsoft Excel platform.

### 7.2.1 Input for Predictive Tool

The following Table 7-1 illustrates the main inputs of the tool. It summarises the tank specifications and the properties of the liquid fuels used in the field scale boilover tests FS Test 5 and 6.

<b>PREDICTING ONSET OF BOILOVER UPON IGNITION OF ATMOSPHERIC STORAGE TANK OF FUEL</b>			
<b><u>Input Parameters</u></b>			
<b><u>General</u></b>			
Tank Diameter:		1.2	m
Storage Temperature:		294	K
		21	°C
Ambient Temperature:		294	K
Relative Humidity:		72	%
Density of Water at Reference Temperature	20°C	998.1	kg m <sup>-3</sup>
<b><u>Fuel properties: Crude Oil</u></b>			
Initial Depth inside Tank:		0.15	m
Normal Boiling Temperature:	Initial	266.5	K
	Final	971.5	K
	Average	619.0	K
Density at Reference (Storage) Temperature:		852.0	kg m <sup>-3</sup>
Specific Gravity (60°F/60°F):		0.854	-

**Table 7-1: Input Data for Predictive Tool for FS Test 5 and 6**



## 7.2.2 Interim Parameters Estimated

The following are the interim parameters that have been estimated based on the inputs from Table 7-1 and used to solve for the prediction of the time to boilover.

<b>PREDICTING ONSET OF BOILOVER UPON IGNITION OF ATMOSPHERIC STORAGE TANK OF FUEL</b>		
<b><u>Interim Parameter</u></b>		
Specific Heat of Fuel:	2710.2	J kg <sup>-1</sup> K <sup>-1</sup>
Latent Heat of Vaporisation of Fuel:	141726.6	J kg <sup>-1</sup>
Rate of Vaporisation of Fuel (Mass Burning Rate of Fuel):	0.051	kg s <sup>-1</sup>
Surface Regression Rate of Fuel	5.31 x 10 <sup>-5</sup>	m s <sup>-1</sup>
Mass Burning Rate of Fuel per unit Area (Mass Burning Flux of Fuel):	0.045	kg m <sup>-2</sup> s <sup>-1</sup>
Heat of Combustion of Fuel:	4.27 x 10 <sup>7</sup>	J kg <sup>-1</sup>
Heat Flux Radiant to Fuel Surface:	32833.3	W m <sup>-2</sup>

**Table 7-2: Interim Parameters estimated for the prediction of time to boilover for FS Test 5 and 6**

The heat flux from the flame to the surface and into the fuel is very significant in determining the time to boilover as shown in Section 6.3.6. It is important to highlight that the heat flux reaching the surface of the burning fuel and contribute to the formation of hot zone represents a small fraction of the total heat release rate of the pool fire. However, the fraction of heat radiated that contributes to the hot zone formation is difficult to be determined. The fraction of the heat radiated from the flame surface to the surrounding is typically calculated based on the heat release rate of the fire and the actual radiant heat flux measured at a particular location away from the fire. In the scope of this work, the fraction of the heat radiated back to the fuel would be presumed in order to get the best fit between the predicted values and the actual experimental results on the time for boilover. For FS Test 5 and 6, the fraction of heat radiated that contributes to the hot zone formation was presumed to be 0.0165 (1.65% of the total heat release rate). The presumed fraction would give a heat flux feedback to the surface and into the fuel of about 32000 W m<sup>-2</sup>. It is

important to highlight that the predicted results are significantly dependent on the heat flux returning into the fuel and the necessity to better manage this parameter.

### 7.2.3 Calculation of the Time to Boilover, Fraction of Fuel Vaporised and Temperature of Hot Zone

The time to boilover relates with the time taken for the lower boundary of hot zone to reach the fuel-water interface and boil the water. When the lower boundary of the hot zone reached the fuel-water interface and boils the water at instant, the time for this to happen is taken as the time to boilover and determined via Equation 6-10. This predictive calculation on the time to boilover, as stated in Section 6.1.3, is based only on the stage at which the base of the hot zone is moving downwards towards the fuel-water interface at a pseudo constant rate at a temperature of  $T_{hz}$ . Hence the prediction of the time to boilover starts with the determination of the temperature  $T_{hz}$  (Equation 6-33) and the fraction of fuel vaporized prior to boilover (Equation 6-32). The following Table 7-3 illustrates the predicted time to boilover, the fraction of fuel that had vaporised and the hot zone temperature prior to boilover for FS Test 5 and 6.

Iteration	$t_{bo}$ (s)	$x_v$	$T_{hz}$ (°F)	$T_{hz}$ (K)
Initial	1430.6			403.15
1	1524.9	0.506	278.95	410.34
2	1592.1	0.539	288.18	415.47
3	1639.1	0.563	294.64	419.06
4	1671.2	0.580	299.04	421.51
5	1692.8	0.591	302.00	423.15
6	1707.0	0.599	303.96	424.24
7	1716.4	0.604	305.25	424.95
8	1722.5	0.607	306.08	425.42

**Table 7-3: The predicted time to boilover, the fraction of fuel that vaporised and hot zone temperature prior to boilover for FS Test 5 and 6.**

The final hot zone temperature at the instant when boilover occurred is determined by the successive iterations until the difference of the newly calculated  $T_{hz,i}$  is less than one unit temperature when compared to the previous

calculated temperature  $T_{hz,i-1}$  i.e.  $(T_i - T_{i-1} < 1.0$  unit temperature). Based on Table 7-3, the predicted time to boilover is 1828 s after the establishment of full surface fire and the temperature  $T_{hz}$  at the instant of the occurrence of boilover is 432.3 K (159.1°C). The observed times to boilover for FS Test 5 and 6 are 1962 s and 1992 s, respectively.

#### **7.2.4 Calculation of Mass of Liquid Fuel Remaining Prior to Boilover**

The other important aspect to be determined when dealing with boilover is estimating the mass of the remaining fuel prior to boilover in order to estimate the consequences of the phenomenon. The mass remained will affect the characteristics of the fireball-like flame resulted from the boilover and the area affected due to the expulsion of the burning fuel from the tank. Since the start of the full surface burning of the fuel, most of the lighter components have been vaporized and consumed in the flame. The liquid fuel then will consist of the heavier components with its temperature increasing as the base of the hot zone formed regressed towards the base of the tank. The mass of the liquid fuel remaining prior to boilover (shown in Table 7-4) represents these high temperature heavy components and could be estimated through Equation 6-34.

#### **7.2.5 Consumption of Vaporised Fuel in Fireball-Like Flame during Boilover**

As the base of the hot zone reached the fuel-water interface, it would heat up and boil the water. This indicates the start of the boilover. When boilover starts, the mass of the remaining liquid fuel (Section 7.2.4) is lifted up rapidly into the atmosphere up to an elevation where sufficient air is available to permit violent burning. The lifting is due to the expansion of water to steam that pushed the fuel content outside the tank and is possible since the pressure from the steam expansion is larger than the pressure generated by the mass of the remaining liquid fuel prior to boilover. During the expulsion occurred throughout the boilover, fraction of the remaining liquid fuel will further vaporised and

expanded; feeding the burning surface to produce a fireball-like vigorous flame. The vaporisation is assumed to occur due to temperature increase during the boilover. Taking into consideration the fraction vaporised during the boilover, the mass of fuel vaporized and consumed in the vigorous fireball-like flame (shown in Table 7-4) would be determined using Equation 6-38. The mass of fuel consumed in the fireball then could be used to characterise the diameter, duration and elevation of the fireball-like flame formed during the boilover. In addition, the balance of the liquid fuel inside the tank (from the difference between the remaining liquid fuel prior to boilover and that vaporised in the fireball) that will be ejected out during the boilover phenomenon (shown in Table 7-6) can be determined through Equation 6-39.

Table 7-4 provides the results of the calculations on the characterisation of the fireball-like flame formed during the boilover.

<b>PREDICTING CONSEQUENCES OF BOILOVER UPON IGNITION OF ATMOSPHERIC STORAGE TANK OF FUEL</b>		
<b><u>Fireball-like Flame Characteristics</u></b>		
Mass of Liquid Fuel Remaining Prior to Boilover:	56.8	kg
Mass of Fuel Consumed in Fireball due to Boilover:	34.6	kg
Maximum Diameter of the Fireball:	19.0	m
Overall Fireball Duration:	2.5	s
Maximum Height of the Centre of the Fireball above the Ground:	14.3	m

**Table 7-4: Predictions on the mass of liquid remaining in tank prior to boilover and the mass that consumed in fireball and the calculations on the diameter, duration and elevation of the fireball-like flame formed during the boilover**



**Figure 7-1: Photographs taken during progression of steady burning (left) and the boilover occurrence (right) of FS Test 5. Take note on the difference of the size (height) of the fireball-like flame during the occurrence of the boilover.**

## **7.2.6 Thermal Effects of Fireball**

The fireball's diameter, duration and lifting height above ground level are important in determining the thermal effects or radiant energy of a fireball during the boilover phenomenon. The radiant energy from the fireball is taken as a fraction of the combustion heat emitted to the surroundings in all directions from the outer surface of the fireball. The energy is estimated via Equation 6-45. However, for a given radiation source and a receptor, not all the points of the radiating surface can radiate straight to the receptor and not all the power emitted by the source would be received by the receptor. The power flux received by the receptor from the exposure to the fireball can be estimated from the correlation given in Equation 6-46.

**PREDICTING CONSEQUENCES OF BOILOVER UPON IGNITION OF  
ATMOSPHERIC STORAGE TANK OF FUEL**

**Thermal Effects of the Fireball-like Flame**

Fireball Radiation View Factor:	0.05	
Atmospheric Transmissivity (0.9 – 1.0):	0.9	
Absorptivity of Receptor/Target:	0.752	
Ground Distance Measured from the Projected Centre of Fireball to Receptor:	42.5	m
Partial Pressure of Water:	1783.9	Pa
Distance between Surface of Fireball and Receptor:	33.0	m
Surface Emitted Flux or Surface Emissive Power:	202.9	kW m <sup>-2</sup>
Power Flux Received by Receptor:	6.9	kW m <sup>-2</sup>

**Table 7-5: Estimations on the power flux received by a target/receptor at a distance away from the fireball in FS Test 5 and 6**

The quantification of the power flux received by the receptor at a distance away from the fireball requires the information on atmospheric transmissivity, absorptivity of receptor and radiation view factor. For FS Test 5 and 6, the atmospheric transmissivity is determined at 80% relative humidity and at ambient temperature of 21°C. The absorptivity is generally defined as the amount of radiation absorbed by a surface compared to that absorbed by a black body. In this example, the absorptivity is taken to be 0.9 (i.e. the absorptivity for dark or rubberized surface).

The power flux received by the receptor is also linked to the fireball surface emissive power. The determination of the surface emissive power depends on the fraction of heat radiated. Prugh (1994) suggests the values of 0.25 to 0.40 for the fraction of the heat radiated from the fireball which are quite similar to those suggested by CCPS (2000); that is of 0.30 to 0.40. In this example, the fraction of 0.40 is used. The distance of the target or receptor from the surface of the fireball is assumed to be 40 m in order to estimate the power flux reached the target. The amount of heat received would determine the harmful effects towards the object/target.

### 7.2.7 Determination of the Area Affected by the Spread of Burning Fuel

A boilover associated with fires in large storage tank have resulted in high loss of life and significant property damage due to the consequences of the expulsion of hot burning oil. The expulsion of the hot burning oil could cover a wide area surrounding the affected storage tank. Equation 6-53 is used to predict the spillage affected area for the work carried out in this thesis.

<b>PREDICTING CONSEQUENCES OF BOILOVER UPON IGNITION OF ATMOSPHERIC STORAGE TANK OF FUEL</b>		
<b><u>Affected Area due to Expulsion of Burning Fuel</u></b>		
Mass of Liquid Fuel Ejected due to Boilover:	22.2	kg
Height of Hot Fuel-rich Column Lifted by Steam Expansion:	1.3	m
Volume of Hot Fuel Expelled Out from Tank:	1.27	m
Area Affected by Spillage of Hot Fuel during Boilover:	126.1	m <sup>2</sup>
Radius of Affected Area	6.3	m

**Table 7-6: Determination of the area affected due to the expulsion of hot burning fuel due to boilover occurrence for FS Test 5 and 6**

Based on Table 7-6, the area affected due to the expulsion of the hot burning fuel due to boilover is estimated to be about 6 m from the centre of the tank.

Figure 7-2 displays the area affected due to the expulsion of hot burning fuel based on the experimental observations and based on the estimation by the predictive tool proposed.

Looking at the estimated results from Table 7-3 and Table 7-6, the predictive calculations are able to produce conservative estimates and could reasonably predict the time to boilover and the area affected/fire spread due to fuel expulsion.

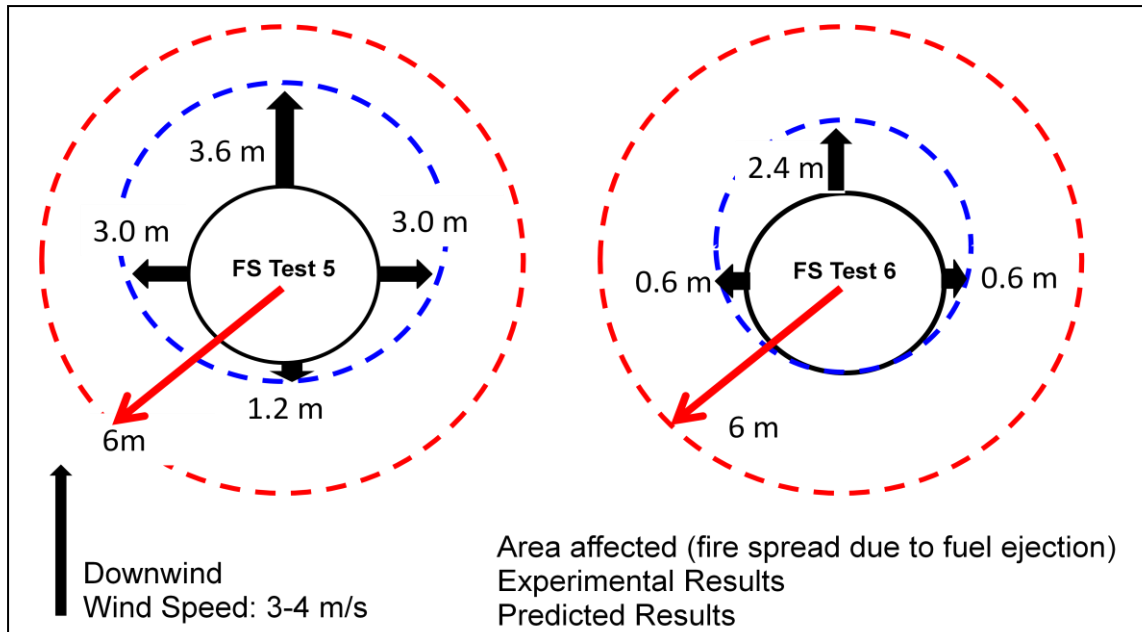


**Figure 7-2 : Comparison of area affected due to spillage of hot burning fuel due to boilover between the experimental results and predictive calculation.**

### 7.3 COMPARISON OF EMPIRICAL MODEL AND PREDICTIVE TOOL: FIELD AND LABORATORY SCALE TESTS

The detailed analysis conducted on results of the field scale tests in Chapter 3 has produced two empirical models that linked the time to boilover with the initial depth of the fuel. The first empirical model (Empirical Model 1) is deduced from the linear trend line for the plot of the observed time to boilover versus the initial depth of the fuel of the field scale tests. The Empirical Model 1 is given in Equation 3-1. This empirical model of time to boilover developed however is based on the observed experiments involving crude oil. Consequently, Empirical Model 1 could only be considered to be applicable to events involving crude oil.

The second model (Empirical Model 2) is obtained by determining the speed of the base of the hot zone using the thermocouple profiles as shown through Table 3-10 and Figure 3-14 in Section 3.3.2. The speed of the base of the hot zone is determined for the specific type of fuel. The average speed of the base of the hot zone for crude oil was determined to be  $0.203 \text{ mm s}^{-1}$ . The average



speed for the diesel and gasoline mixture was  $0.232 \text{ mm s}^{-1}$ . The initial depth of the fuel is then divided with this speed to give the time to boilover.

The observed time to boilover from the field and laboratory scale tests are compared with the prediction by the empirical models and predictive tool proposed in Chapter 6. The fraction that contributes to the hot zone formation used in the predictive tool estimation was 0.017.

### 7.3.1 Field Scale Tests

#### 7.3.1.1 Crude Oil

Table 7-7 shows the time to boilover for the field scale tests involving crude oil predicted by the empirical models and the predictive tool.

Test No.	Fuel Depth (mm)	Observed Time to Boilover (s)	Predicted Time to Boilover		
			Empirical Model 1 (s)	Empirical Model 2 (s)	Predictive Tool (s)
FS Test 2	80	1222	689	394	915
FS Test 3	100	1268	861	493	1144
FS Test 4	115	1401	991	567	1316
FS Test 5	150	1962	1292	739	1716
FS Test 6	150	1992	1292	739	1716
FS Test 9	230	2220	1981	1133	2632
FS Test 10	230	2880	1981	1133	2632
FS Test 11	250	2770	2154	1232	2861
FS Test 12	250	2470	2154	1232	2861
FS Test 13	250	2380	2154	1232	2861
FS Test 14	255	2910	2197	1256	2918
FS Test 15	270	1881	2326	1330	1801
FS Test 16	270	1679	2326	1330	1801
FS Test 17	290	2973	2498	1429	1935
FS Test 18	380	2760	3273	1872	2535
FS Test 19	440	2824	3790	2167	2936
FS Test 20	475	2940	4092	2340	3169
FS Test 22	485	4282	4178	2389	3236
FS Test 23	500	4530	4307	2463	3336
FS Test 24	500	4494	4307	2463	3336

**Table 7-7: Predictive results on the time to boilover for field scale tests involving crude oil by the empirical models and predictive tool proposed**

Table 7-8 shows the examples of the calculation to predict the time to boilover using the empirical models from Chapter 3.

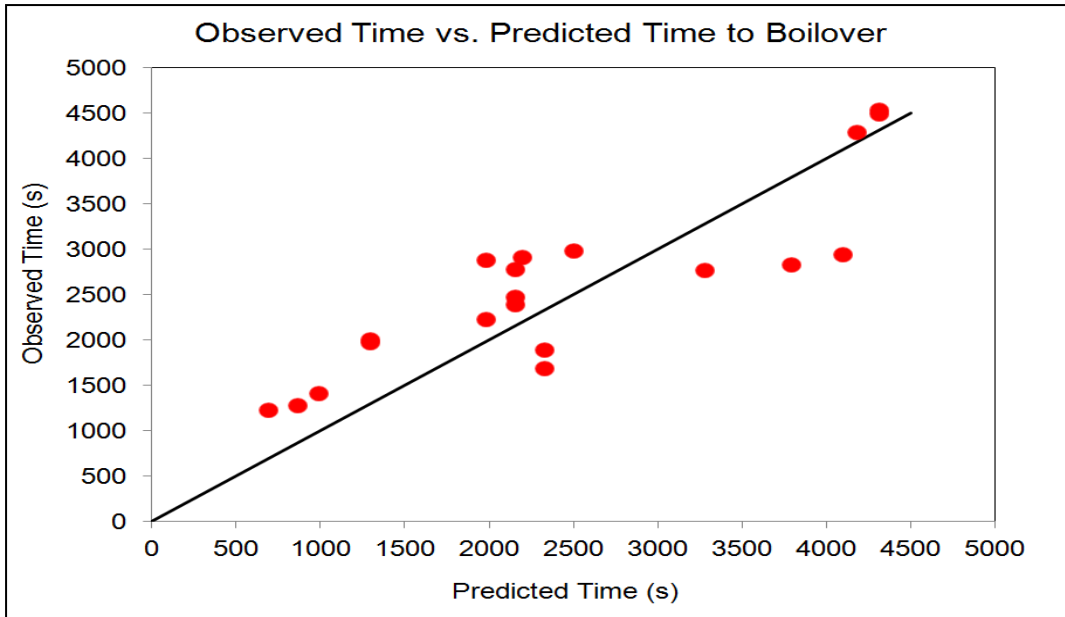
<u>Details:</u>	
FS Test 22	
Initial Depth of Fuel:	485 mm
Observed Time to Boilover:	4282 s
<u>Empirical Model 1</u>	
Predicted Time to Boilover:	$t_{bo} = 8.614 h_0$ $= 8.614 \text{ s mm}^{-1} (485 \text{ mm})$ $= 4178 \text{ s}$
<u>Empirical Model 2</u>	
Predicted Time to Boilover:	$t_{bo} = \frac{\text{Initial depth of fuel}}{\text{Speed of base of hot zone}}$ $= \frac{485 \text{ mm}}{0.203 \text{ mm s}^{-1}}$ $= 2389 \text{ min}$

**Table 7-8: Prediction on time to boilover using the empirical models deduced from Chapter 3**

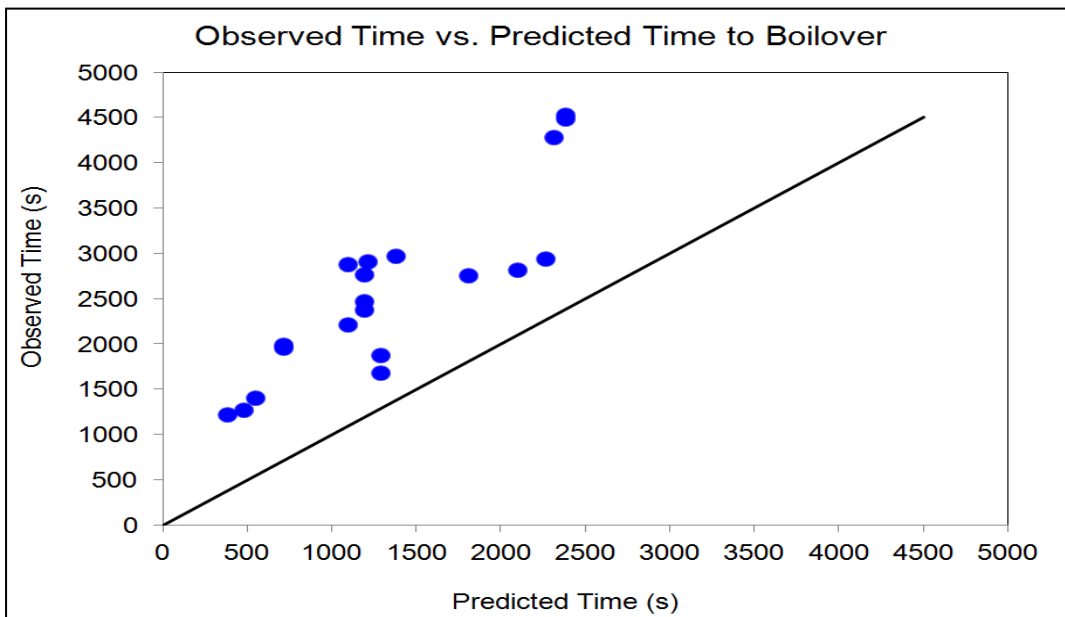
The prediction by the proposed predictive tool is conducted similar to the steps explained in Section 7.2.1, 7.2.2 and 7.2.3.

Figure 7-3 shows the comparison between the experimental results and the predicted time to boilover by the Empirical Model 1 for field scale tests involving crude oil. The figure shows agreement with between the observed and predicted time to boilover.

Figure 7-4 shows the comparison between the time to boilover observed in the field scale tests and the predicted time to boilover by the Empirical Model 2. The figure shows that the model provides faster time to boilover compared to the observed time.



**Figure 7-3: Experimental results versus predicted time to boilover by Empirical Model 1 for field scale tests involving crude oil**



**Figure 7-4: Observed time to boilover against predicted time to boilover by Empirical Model 2 for field scale tests involving crude oil**

Figure 7-5 compares the time to boilover observed in the field scale tests with the estimates of the predictive tool proposed in Chapter 6. The fraction that contributes to the hot zone formation used in the predictive tool estimation was 0.017. The figure shows the best agreement between the observed and predicted times to boilover in which more plots congregate together near the equality line.

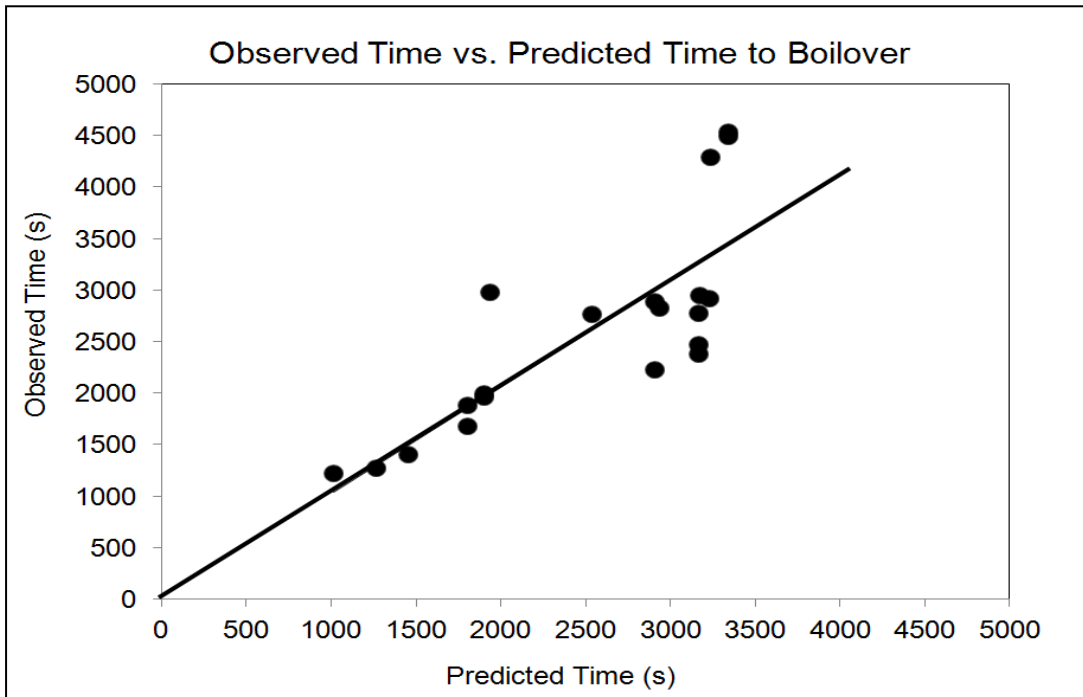


Figure 7-5: Observed time to boilover against predicted time to boilover by Predictive Tool for field scale tests involving crude oil

**7.3.1.2 Fire Spread due to Boilover**

Figure 7-6 shows the comparison between the observed affected area due to the fire spread during boilover in the field scale tests with the predicted results obtained using the predictive tool proposed in Chapter 6.

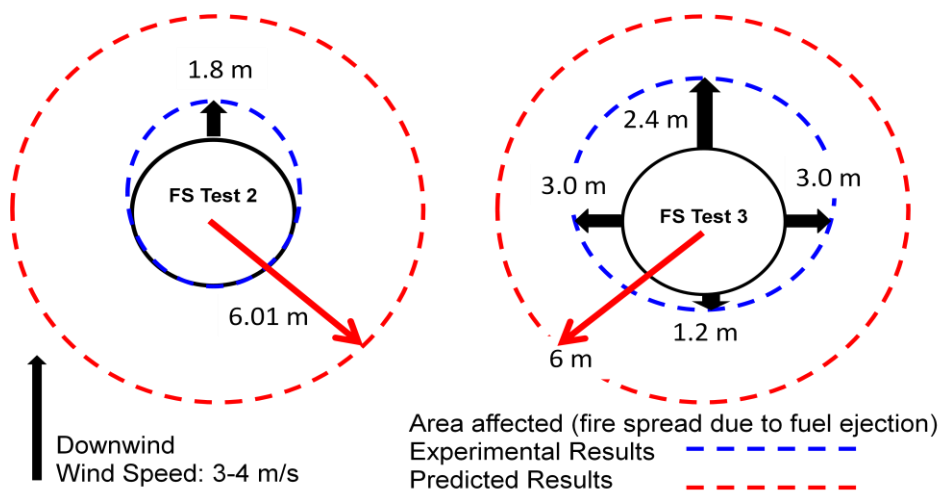
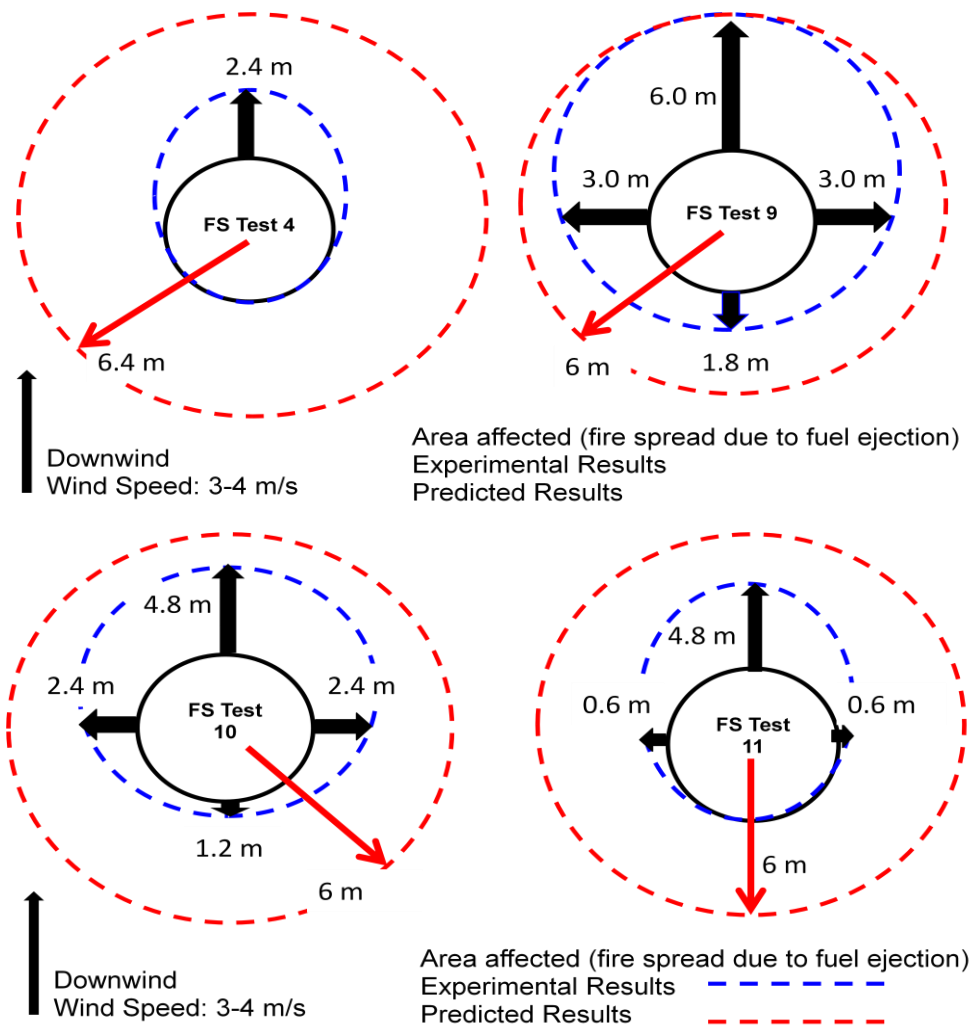


Figure 7-6: Observed versus predicted area affected due to fire spread during boilover for test FS Test 2, 3 , 4, 9, 10 and 11

Figure 7-6 (continued)



### 7.3.1.3 Diesel and Gasoline Mixture

Table 7-9 shows the time to boilover for the field scale tests involving mixture of diesel and gasoline predicted by the Empirical Model 2 and the predictive tool. Both predictive results concur with the observed time to boilover. The data available is limited but the predictions by the predictive tool give better agreement with the observed time to boilover.

Test No.	Fuel Depth (mm)	Observed Time to Boilover (s)	Predicted Time to Boilover	
			Empirical Model 2 (s)	Predictive Tool (s)
FS Test 42	2.44	2188	2241	2721
FS Test 46	1.2	1252	862	1564
FS Test 47	1.2	2400	1034	1877

**Table 7-9: Predictive results on the time to boilover for field scale tests involving mixture of diesel and gasoline by the empirical model and predictive tool proposed**

### 7.3.2 Comparison with Laboratory Field Test

The observed times to boilover from the laboratory scale tests are compared with the predicted time obtained from the predictive tool. The laboratory boilover rig was fabricated and used primarily to determine whether or not a fuel will boilover. Though temperature measurements were conducted and the profiles were similar to the field scale tests but the observation for the speed of the base of the hot zone would not be accurate. This is because the fuel was heated using electrical heaters and not by back radiation from the fire. Consequently, the determination of the speed of the base of the hot zone or the regression rate of the fuel is not possible. The prediction of the time to boilover for the purpose of comparison with the observed time from the laboratory scale tests therefore will only be done via the predictive tool developed for this thesis.

The prediction by the proposed predictive tool is conducted similar to the steps explained in Section 7.2.1, 7.2.2 and 7.2.3.

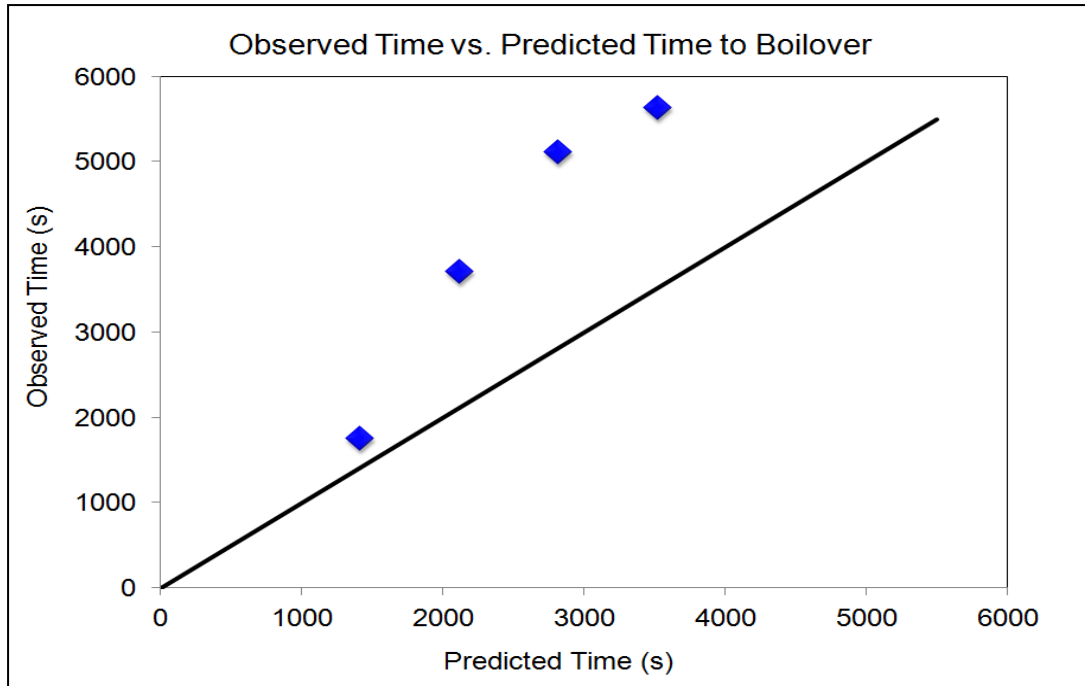
#### 7.3.2.1 Crude Oil

Table 7-10 shows the time to boilover for the laboratory scale tests involving crude oil predicted by the predictive tool.

Test No.	Fuel Thickness (mm)	Initial Storage Temp. (Avg. °C)	Observed Time to Boilover (s)	Predicted Time to Boilover (s)
LS Test 21	80	19	1746	1407
LS Test 22	120	19	3706	2112
LS Test 23	160	18	5106	2815
LS Test 24	200	18	5627	3519

**Table 7-10: Predictive results on the time to boilover for laboratory scale tests involving crude oil by the predictive tool proposed**

Figure 7-7 compares the time to boilover observed with the estimates of the predictive tool. The figure shows that the model provides faster time to boilover compared to the observed time. The fraction of heat radiated that contributes to the hot zone formation used in the predictive tool calculation was presumed to be 0.016.



**Figure 7-7: Observed time to boilover against predicted time to boilover by Predictive Tool for laboratory scale tests involving crude oil**

### 7.3.2.2 Diesel and Gasoline Mixture

Table 7-11 shows the time to boilover for the laboratory scale tests involving mixture of diesel and gasoline predicted by the predictive tool.

Test No.	Fuel Thickness (mm)	Initial Storage Temp. Avg. (°C)	Observed Time to Boilover (s)	Predicted Time to Boilover (s)
LS Test 7	80	16	1605	1082
LS Test 8	80	18	1999	1082
LS Test 9	80	46	1184	580
LS Test 10	80	19	2284	1082
LS Test 11	150	5	4366	2029
LS Test 12	200	19	5569	2705

**Table 7-11: Predictive results on the time to boilover for laboratory scale tests involving mixture of diesel and gasoline by the predictive tool proposed**

Figure 7-8 compares the time to boilover observed with the estimates of the predictive tool. The fraction of heat radiated that contributes to the hot zone formation used in the predictive tool calculation was presumed to be 0.016. The figure shows that the model provides faster time to boilover compared to the observed time.

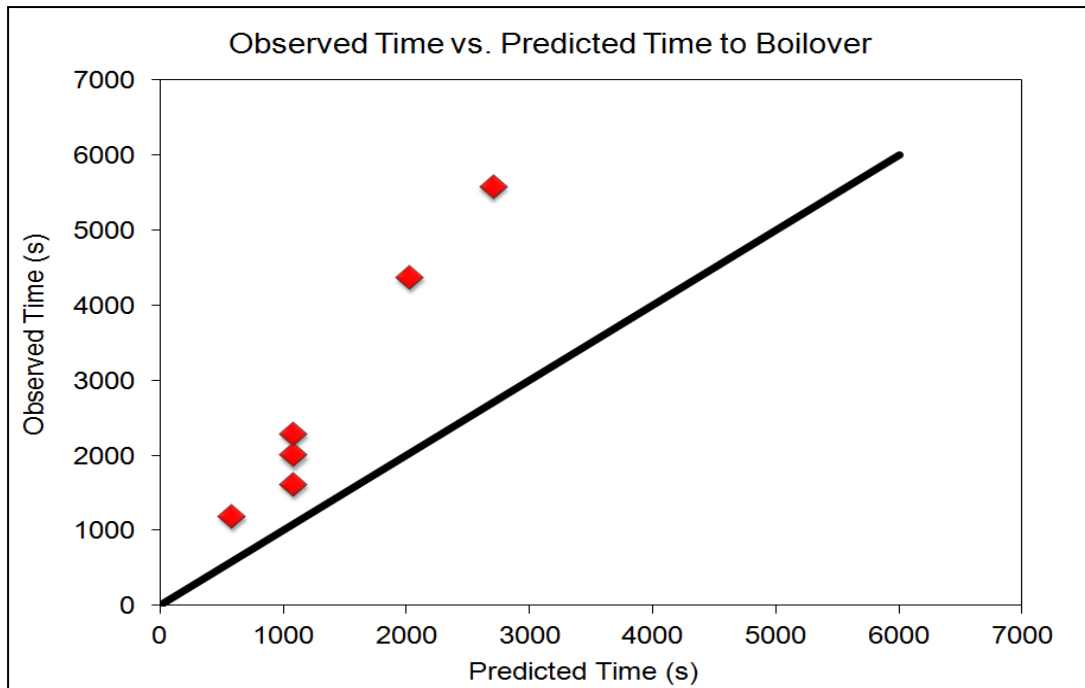


Figure 7-8: Observed time to boilover against predicted time to boilover by Predictive Tool for laboratory scale tests involving mixture of diesel and gasoline

## 7.4 COMPARISON OF EMPIRICAL MODEL AND PREDICTIVE TOOL: BOILOVER STUDIES

In order to test further the validity of the empirical models and the predictive tool with larger range of experiments, the prediction on the time to boilover were compared with the time of trials carried out in the experimental works available in the literature.

### 7.4.1 Experimental Study of Boilover in Crude Oil Fires (Koseki, Kokkala and Mulholland, 1991)

Koseki *et al.* conducted experimental study of boilover phenomena using crude oil to analyse effect of the initial fuel layer thickness on boilover. The study was carried out using circular steel pans of diameter 0.3, 0.6, 1 and 2 m. Comparisons were made between the observed time to boilover with the time predicted by the empirical models and the predictive tool established for this thesis purpose. The fuel specifications are not provided in detailed for the tests conducted, and hence the specifications of the LASTFIRE Phase 2 light crude



oil are used to carry out the prediction. Table 7-12 below shows a summary of the key results for selected pan diameter obtained from the study, the time to boilover observed and the predicted time to boilover based on the works proposed in this thesis.

Pan diameter (m)	Fuel Thickness (mm)	Observed Time to Boilover (min)	Predicted Time to Boilover (min)		
			Empirical Model 1	Empirical Model 2	Predictive Tool
0.6	69	15.7	9.9	5.5	14.6
1	60	21.8	8.6	4.8	12.7
	100	32.1	14.3	7.9	21.2

**Table 7-12: Summary of selected test details, the results on the time to boilover observed in the test and the predicted time to boilover**

The times to boilover predicted by the empirical models and the predictive tools are shorter than the observed time in the experiment. Though very conservative, the predictive tool provides better predictions as it is able to predict to the similar order of magnitude of the time to boilover. The fraction that contributes to the hot zone formation used in the predictive tool calculation was 0.016.

#### **7.4.2 Large-scale Boilover Experiments using Crude Oil (Koseki *et al.*, 2006)**

Knowing that it is necessary to know the hazardous aspects of large-scale tank fires for loss prevention, the National Research Institute of Fire and Disaster of Japan, the University of Tokyo and the Tomakomai-Tobu Oil Storage Company organized a campaign of experiments on boilover. Two runs of test were carried out using a crude oil mixtures equivalent to Arabian Light crude oil, which was supplied by Idemitsu Kosan Co. Experiments were conducted in a stainless steel pan of 5 m diameter with fuel pools at 450 mm in depth and the water layer thickness was 100 mm. The tank specifications are given in Figure 7-9. The tank was fitted with thermocouples which number and set-up are presented in Figure 7-10.

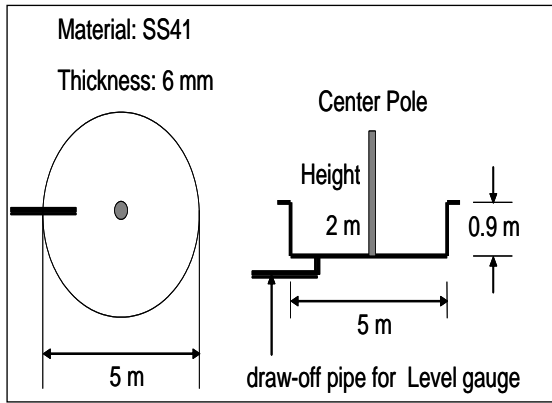


**Figure 7-9: Tank specification for experiment**

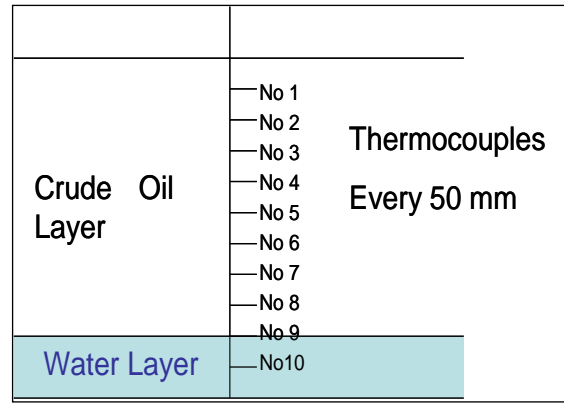


**Figure 7-10: Position of thermocouples along with the pan axis**

In the experiment, the researchers measured the fuel level regression, irradiance level at certain distance around the burning pan and the temperature profiles within the burning liquid and the flame. The summary of the results and measurements of the tests are presented in Table 7-13.

Details	Run I	Run II
Crude Oil Layer	0.45 m (9.0 Kiloliters: KL)	0.45 m (9.0 KL)
Water Layer	0.10 m (0.2 KL)	0.10 m (0.2 KL)
Wind direction and speed	West-northwest 8.5 m/sec	North 3.2 m/sec
Amount of Burn up	2.4 KL, 119 mm	2.5 KL, 122 mm
Time to boilover	<b>78.8 min.</b>	<b>66.4 min.</b>
Heat wave descending rate	5.7 mm/min.	6.7 mm/min.

**Table 7-13: Summary of Koseki *et al.* (2006) Experimental Results**

The time to boilover is predicted using the empirical models obtained from Chapter 3 and the results are shown in Table 7-14 below. The crude oil used in the Japanese tests had similar specification with the one used in the LASTFIRE Phase 2 and 3 field scale tests. Hence, the prediction by the proposed predictive tool is conducted using similar condition and fuel properties. The prediction by the proposed predictive tool is conducted similar to the steps explained in Section 7.2.1, 7.2.2 and 7.2.3. The fraction that contributes to the hot zone formation used in the calculation was 0.016. The simulation by the predictive tool gave a predicted time to boilover of 62.7 min.

<u>Empirical Model 1</u>	
Predicted Time to Boilover:	$t_{bo} = 8.614 h_0$ $= 8.614 \text{ s mm}^{-1} (450 \text{ mm})$ $= 3876.3 \text{ s}$ $= 64.6 \text{ min}$
<u>Empirical Model 2</u>	
Predicted Time to Boilover:	$t_{bo} = \frac{\text{Initial depth of fuel}}{\text{Speed of base of hot zone}}$ $t_{bo} = \frac{450 \text{ mm}}{0.203 \text{ mm s}^{-1}} = 2216.7 \text{ s}$ $= 36.9 \text{ min}$

**Table 7-14: Predicted time to boilover determined using the empirical models for the Japanese large-scale boilover experiments using crude oil**

The times to boilover predicted by the empirical models and the predictive tools are shorter than the observed time in the experiment.

## 7.5 COMPARISON OF EMPIRICAL MODEL AND PREDICTIVE TOOL: BOILOVER INCIDENTS

A number of boilovers associated with fires in large storage tank have also being reported that occurred in the last century (Persson & Lonnermark, 2004). Some of these accidents resulted in high loss of life and significant property damage due to the consequences of the expulsion of hot burning oil. The following summaries of three of the accidents illustrate the severity of a boilover event. The observed time to boilover for these boilover incidents are compared with the predicted time to boilover estimated by the empirical models of Chapter 3 and the predictive tool of Chapter 6.

### 7.5.1 Czechowice-Dziedzice Refinery, Poland

In 1971, lightning hit a 33 m diameter tank at Czechowice-Dziedzice Refinery, Poland that contained crude oil, causing its cone roof to collapse and causing a full surface fire (Persson & Lonnermark, 2004). In total there were four identical crude oil tanks nearby each other. Once the refinery fire brigade arrived to the scene, the fire was attacked with foam. Surrounding tanks were cooled with

water and foam monitors. Five hours after the fire started, a rapid boilover occurred, throwing burning oil in all directions up to 250 m away. It was reported that 33 people died as a consequence of the boilover. Table 7-15 shows the key information related to the boilover incident.

<b>Key information</b>	
System:	Cone roof tank of 12 000 m <sup>3</sup> capacity
Product	Crude oil
Tank data	$D = 33$ m and $z_T = 14.7$ m
Storage temperature	$T_{st} = 300$ K
Ambient temperature	$T_{atm} = 298$ K
Initial fuel height	$z_f = 11.7$ m
Time to boilover:	<b>17 hour 30 minutes</b>
Oil Spread	More than 300 m away
Cause:	Ignition of the tank contents due to lightning
Casualties:	33 people dead

**Table 7-15: Key information on the tank specifications, time to boilover and post boilover effects for Czechowice-Dziedzice boilover incident**

Table 7-16 show the input data and the interim data results calculated for the boilover incident.

<b>PREDICTING ONSET OF BOILOVER UPON IGNITION OF ATMOSPHERIC STORAGE TANK OF FUEL</b>			
<b><u>Input Parameters</u></b>			
<b><u>General</u></b>			
Tank Diameter:		33	m
Tank Height:		14.7	m
Storage Temperature:		303	K
Ambient Temperature:		25	°C
Ambient Temperature:		298	K
Relative Humidity:		72	%
Density of Water at Reference Temperature	20°C	998.1	kg m <sup>-3</sup>
<b><u>Fuel properties: Crude Oil</u></b>			
Initial Depth inside Tank:		11.7	m
Normal Boiling Temperature:	Initial	390	K
	Final	900	K
	Average	625.7	K
Density at Reference (Storage) Temperature:		800.0	kg m <sup>-3</sup>
Specific Gravity (60°F/60°F):		0.727	-

<b>PREDICTING ONSET OF BOILOVER UPON IGNITION OF ATMOSPHERIC STORAGE TANK OF FUEL</b>		
<b><u>Interim Parameter</u></b>		
Specific Heat of Fuel:	3189.0	J kg <sup>-1</sup> K <sup>-1</sup>
Latent Heat of Vaporisation of Fuel:	163430.1	J kg <sup>-1</sup>
Rate of Vaporisation of Fuel (Mass Burning Rate of Fuel):	34.644	kg s <sup>-1</sup>
Surface Regression Rate of Fuel	5.06 x 10 <sup>-5</sup>	m s <sup>-1</sup>
Mass Burning Rate of Fuel per unit Area (Mass Burning Flux of Fuel):	0.041	kg m <sup>-2</sup> s <sup>-1</sup>
Heat of Combustion of Fuel:	4.33 x 10 <sup>7</sup>	J kg <sup>-1</sup>
Heat Flux Radiant to Fuel Surface and form Hot Zone:	78951.7	W m <sup>-2</sup>

**Table 7-16: Input parameters for predictive calculation for boilover incident at Czechowice-Dziedzice, Poland**

Table 7-17 shows the predicted time to boilover for the Czechowice-Dziedzice boilover incident. The time to boilover is predicted to be 16.8 hours (60551 s). The table also indicates that prior to the boilover; about 26% of the fuel were consumed in the fire. The temperature of the hot fuel i.e. the hot zone was predicted to be about 449.7 K (176.6°).

<b>PREDICTING ONSET OF BOILOVER UPON IGNITION OF ATMOSPHERIC STORAGE TANK OF FUEL</b>			
<b>Iteration</b>	<b><math>t_{bo}</math> (s)</b>	<b><math>x_v</math></b>	<b><math>T_{hz}</math> (K)</b>
Initial	41328		403.15
1	56838	0.179	440.74
2	59865	0.246	448.07
3	60440	0.259	449.47
4	60551	0.262	449.73
5	60571	0.262	449.78

**Table 7-17: Results of predictive tool calculation on boilover onset time.**

Figure 7-11 below shows the comparison between the observed time to boilover and the predicted time to boilover for the incident at the Czechowice-Dziedzice Refinery.

The prediction by Empirical Model 1 provides longer time to boilover compared to the observed time. The time results by Empirical Model 2 and the predictive

tool give better agreement to the observed time to boilover. The time results from the predictive tool highlight the great dependence on the heat flux feedback to the surface and into the fuel. The heat flux is determined by fraction of heat radiated that contributes to the hot zone formation. The predictive tool provides the best estimated time to boilover if a value of 0.045 is used as the fraction of heat radiated that contributes to the hot zone formation.

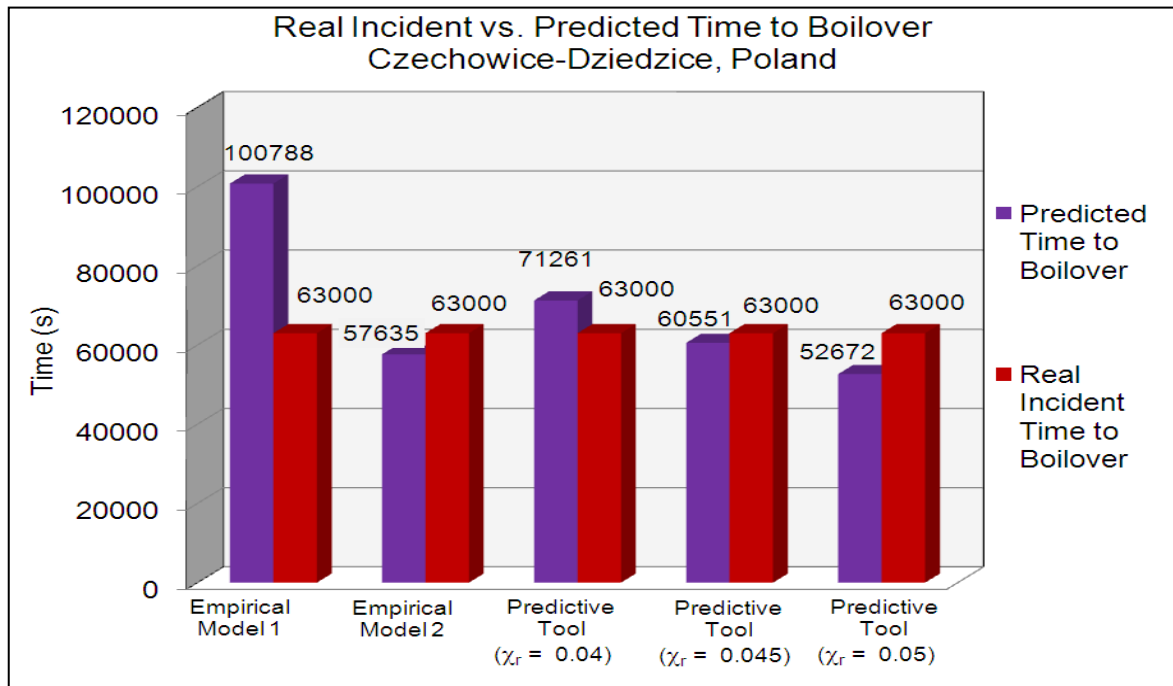


**Figure 7-11: Comparison between real incident time to boilover with the predicted values from the empirical models and the predictive tool developed for Czechowice-Dziedzice incident**

Table 7-18 shows the predicted results on the consequences of the boilover phenomenon for Czechowic-Dziedzice boilover incident. Based on the fraction of fuel that vaporized prior to the boilover i.e. 26% of the initial fuel (as shown in Table 7-17), the mass of liquid fuel remaining in the tank at the moment when the boilover occurred was determined to be about  $5.9 \times 10^6$  kg. Some of this fuel was further vaporized and consumed in the fireball during the occurrence of the boilover. And the remaining fuel which was about  $5.7 \times 10^6$  kg was expelled to the surrounding area adjacent to the tank, as shown in Table 7-18.

Table 7-18 also displays the surface emissive power of the fireball-like flame and the heat flux received by a receptor located at 40 m away from the centre of

the tank. The value of 40 m was just an example used to carry out the prediction calculations. The surface emissive power is predicted to be about 453.8 kW m<sup>-2</sup> by using a radiative fraction of 0.40 of the total heat released by the fuel combustion. The fraction value is the maximum proposed by Prugh (1994).

### **PREDICTING CONSEQUENCES OF BOILOVER UPON IGNITION OF ATMOSPHERIC STORAGE TANK OF FUEL**

#### **Fireball-like Flame Characteristics**

Mass of Liquid Fuel Remaining Prior to Boilover:	5.9 x 10 <sup>6</sup>	kg
Mass of Fuel Consumed in Fireball due to Boilover:	2.1 x 10 <sup>5</sup>	kg
Maximum Diameter of the Fireball:	330	m
Overall Fireball Duration:	23	s
Maximum Height of the Centre of the Fireball above the Ground:	247	m

#### **Thermal Effects of the Fireball-like Flame**

Fireball Radiation View Factor:	0.277	
Atmospheric Transmissivity:	0.651	
Absorptivity of Receptor/Target (0.9 – 1.0):	Presumed value	0.9
Ground Distance Measured from the Projected Centre of Fireball to Receptor:	40	m
Partial Pressure of Water:	3395.4	Pa
Distance between Surface of Fireball and Receptor:	85.6	m
Surface Emitted Flux or Surface Emissive Power: (taking the radiative fraction of total heat released by combustion as 0.4)	453.8	kW m <sup>-2</sup>
Power Flux Received by Receptor:	115.18	kW m <sup>-2</sup>

#### **Affected Area due to Expulsion of Burning Fuel**

Mass of Liquid Fuel Ejected due to Boilover:	5.7 x 10 <sup>6</sup>	kg
Height of Hot Fuel-rich Column Lifted by Steam Expansion:	27.5	m
Volume of Hot Fuel Expelled Out from Tank:	10978.9	m <sup>3</sup>
Area Affected by Spillage of Hot Fuel during Boilover:	222834	m <sup>2</sup>
Radius of Affected Area	266	m

**Table 7-18: Results of predictive tool calculation on boilover onset time and area affected for Czechowice-Dziedzice incident.**

## 7.5.2 Tocoa Power Plant, Venezuela

Another case of a similar nature was reported in 19<sup>th</sup> December 1982 at a thermal power plant in Tocoa, Venezuela. A three-person crew went to measure the amount of fuel in a tank which contained No. 6 fuel oil. Moments later, a huge explosion ripped off the tank roof (Garrison, 1984). By the time the fire brigade had arrived, a fire involving the contents of the tank was well established. About 8 hours after the fire had started, there was a violent boilover. The oil expulsion and resulting fireball killed over 150 people before the ejected burning liquid raced down the hillside toward the plant and local population. Table 7-19 shows the key information related to the boilover incident at Tocoa, Venezuela.

<b>Key information</b>	
System:	Cone roof tank of 40 000 m <sup>3</sup> capacity storing fuel oil No. 6
Product	Fuel oil No. 6 (mixed with 5 to 20% of heavy naphta - power company fuel specification allowance)
Tank data	$D_t = 55$ m and $H_t = 17$ m
Storage temperature	$T_{st} = 333$ K
Ambient temperature	$T_{atm} = 298$ K
Initial fuel height	$h_0 = 6.1$ m
Time to boilover:	<b>6 hour 15 minutes</b>
Fireball dimensions	Height - about 330 m
Oil Spread	More than 300 m away Burning oil was thrown about 8 tank diameters downwind
Cause:	Ignition of the tank contents due to explosion of a mix of vapour and aerosol of fuel oil No. 6 overheated above its flash point during a gauging operation.
Casualties:	More than 150 people dead and 500 injured

**Table 7-19: Key information on the tank specifications, time to boilover and post boilover effects for Tocoa boilover incident**

Table 7-20 show the input data provided and the interim data calculated for the prediction of the time to boilover for the incident at Tocoa, Venezuela.



**PREDICTING ONSET OF BOILOVER UPON IGNITION OF  
ATMOSPHERIC STORAGE TANK OF FUEL**

**Input Parameters**

Tank Diameter:		55	m
Tank Height:		17	m
Storage Temperature:		333	K
Ambient Temperature:		25	°C
Ambient Temperature:		298	K
Relative Humidity:		75	%
Density of Water at Reference Temperature	20°C	998.1	kg m <sup>-3</sup>

**Fuel properties: Crude Oil**

Initial Depth inside Tank:		6.1	m
Normal Boiling Temperature:	Initial	453	K
	Final	853	K
	Average	621.6	K
Density at Reference (Storage) Temperature:		890.0	kg m <sup>-3</sup>
Specific Gravity (60°F/60°F):		0.892	-

**Interim Parameter**

Specific Heat of Fuel:		4262.4	J kg <sup>-1</sup> K <sup>-1</sup>
Latent Heat of Vaporisation of Fuel:		134568.1	J kg <sup>-1</sup>
Rate of Vaporisation of Fuel (Mass Burning Rate of Fuel):		83.1	kg s <sup>-1</sup>
Surface Regression Rate of Fuel		3.93 x 10 <sup>-5</sup>	m s <sup>-1</sup>
Mass Burning Rate of Fuel per unit Area (Mass Burning Flux of Fuel):		0.035	kg m <sup>-2</sup> s <sup>-1</sup>
Heat of Combustion of Fuel:		4.23 x 10 <sup>7</sup>	J kg <sup>-1</sup>
Heat Flux Radiant to Fuel Surface and form Hot Zone::		207054.3	W m <sup>-2</sup>

**Table 7-20: Input parameters and interim parameters calculated for predictive calculation of boilover incident at Tocoa, Venezuela**

The interim parameters in Table 7-20 were used to estimate the time to boilover for the TACOA boilover incident. Consequently, the time to boilover is predicted to be about 6.0 hours (21664 s) after the burning started, as shown in Table 7-21.

<b>PREDICTING ONSET OF BOILOVER UPON IGNITION OF ATMOSPHERIC STORAGE TANK OF FUEL</b>			
<b>Iteration</b>	<b><math>t_{bo}</math> (s)</b>	<b><math>x_v</math></b>	<b><math>T_{hw}</math> (K)</b>
Initial	7964		403.15
1	18220	0.051	493.49
2	21094	0.117	518.80
3	21588	0.136	523.15
4	21664	0.139	523.81
5	21674	0.140	523.91

**Table 7-21: Results of predictive tool calculation on boilover onset time for Tocoa boilover incident.**

Table 7-21 also indicates that prior to the boilover, about 14% of the fuel were vaporised and burnt in the fire. The temperature of the hot fuel at the instant of boilover occurrence i.e. the hot zone was predicted to be about 523.8 K (250.7°C).

The observed time to boilover from the incident is compared with the prediction by the empirical models deduced from the field scale tests and the predictive tool proposed in Chapter 6. Figure 7-12 below shows the comparison between the real incident time and the predicted time to boilover.

The empirical models over predict the time of the boilover occurrence. The time results from the predictive tool again highlight the great dependence on the heat flux feedback to the surface and into the fuel. The heat flux is determined by fraction of heat radiated that contributes to the hot zone formation. A fraction with a value of 0.14 provides the best prediction of the time to boilover for Tocoa incident.

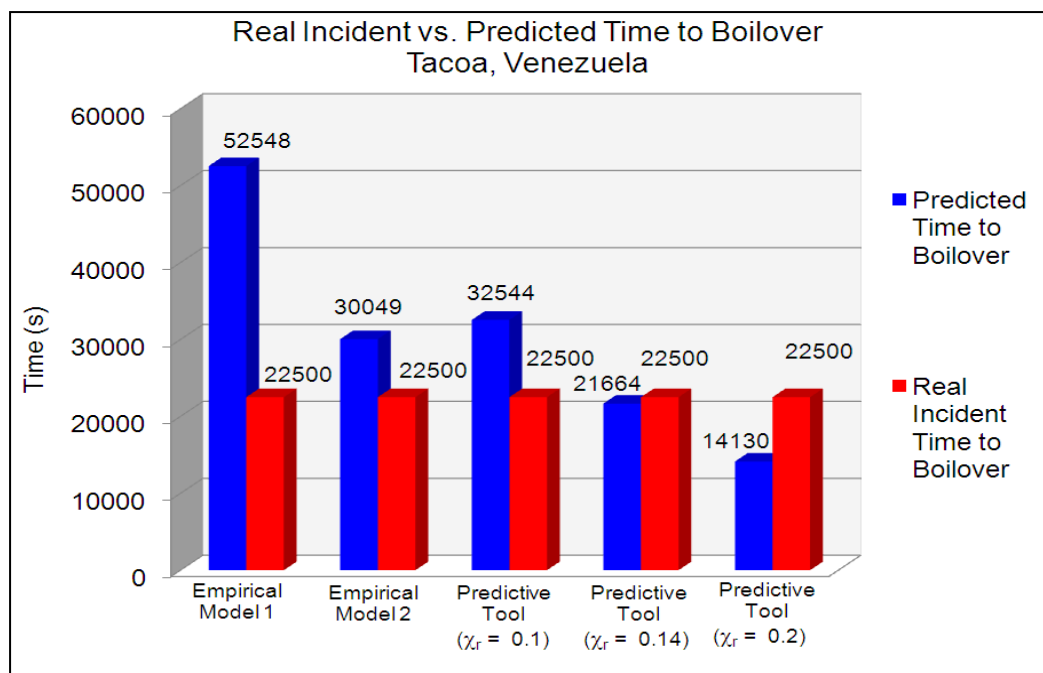


**Figure 7-12: Comparison between real incident time to boilover with the predicted values from the empirical models and the predictive tool developed for Tacoma incident**

Table 7-22 shows the predicted results on the consequences of the boilover. Based on the fraction of fuel that vaporized prior to the boilover (as shown in Table 7-21), the mass of liquid fuel remaining in the tank at the moment when the boilover occurred was determined to be about  $1.1 \times 10^7$  kg. Some of this fuel was further vaporized and consumed in the fireball during the occurrence of the boilover. And the remaining fuel which was about  $7.9 \times 10^6$  kg was expelled to the surrounding area adjacent to the tank, as shown in Table 7-22.

#### PREDICTING CONSEQUENCES OF BOILOVER UPON IGNITION OF ATMOSPHERIC STORAGE TANK OF FUEL

##### Fireball-like Flame Characteristics

Mass of Liquid Fuel Remaining Prior to Boilover:	$1.1 \times 10^7$	kg
Mass of Fuel Consumed in Fireball due to Boilover:	$3.2 \times 10^6$	kg
Maximum Diameter of the Fireball:	811	m
Overall Fireball Duration:	46	s
Maximum Height of the Centre of the Fireball above the Ground:	608.2	m

**Table 7-22: Results of predictive tool calculation on boilover onset time and area affected for Tacoma boilover incident.**

Table 7-22 (continued)

PREDICTING CONSEQUENCES OF BOILOVER UPON IGNITION OF ATMOSPHERIC STORAGE TANK OF FUEL			
<b><u>Thermal Effects of the Fireball-like Flame</u></b>			
Fireball Radiation View Factor:		0.116	
Atmospheric Transmissivity :		0.522	
Absorptivity of Receptor/Target (0.9 – 1.0):		0.9	
Ground Distance Measured from the Projected Centre of Fireball to Receptor:	Presumed value	40	m
Partial Pressure of Water:		16553.4	Pa
Distance between Surface of Fireball and Receptor:		204.1	m
Surface Emitted Flux or Surface Emissive Power: (taking the radiative fraction of total heat released by combustion as 0.4)		568.4	kW m <sup>-2</sup>
Power Flux Received by Receptor:		118.19	kW m <sup>-2</sup>
<b><u>Affected Area due to Expulsion of Burning Fuel</u></b>			
Mass of Liquid Fuel Ejected due to Boilover:		7.9 x 10 <sup>6</sup>	kg
Height of Hot Fuel-rich Column Lifted by Steam Expansion:		23.3	m
Volume of Hot Fuel Expelled Out from Tank:		15005.2	m <sup>3</sup>
Area Affected by Spillage of Hot Fuel during Boilover:		288350	m <sup>2</sup>
Radius of Affected Area		303	m

Table 7-22 also shows the surface emissive power of the fireball-like flame and the heat flux received by a receptor, let's say, located at 40 m away from the centre of the tank. The surface emissive power is predicted to be about 568.4 kW m<sup>-2</sup>. The radiative fraction of the total heat released by the fuel combustion is 0.40.

### 7.5.3 Amoco Refinery, Milford Haven, United Kingdom

In 1983, another boilover occurred at the Amoco Refinery tank farm in Milford Haven, United Kingdom. On the 30th August 1983, a fire started in a crude oil storage tank TO11, which had a volume capacity of 94000 m<sup>3</sup>. At that time, it was reported that the tank was half filled with about 47000 m<sup>3</sup> of the crude. The storage tank had a floating roof installed and was the biggest tank of the site. The tank was 78 m in diameter and stood 20 m high. It was set up in a

16222 m<sup>2</sup> containment dike by itself. Unfortunately, hours later, the floating roof lost its structural integrity and sank. After a short period of time, loud crackling noises with increasing flame intensity forced the fire service to evacuate the scene. The rare phenomenon of multiple boilovers occurred in this incident. During each boilover, steam pushed out the oil out of the tank to a height of almost 900 m (3000 ft). Although the incident did not jeopardize life or production, the estimated loss of crude oil was £4 million (1983 prices) (Robertson, 2000 and Persson & Lonnermark, 2004). Table 7-23 shows the key information related to the boilover

<b>Key information</b>	
System:	Floating roof tank of 94,000 m <sup>3</sup> capacity of light crude oil
Product:	Light Crude Oil
Tank data	$D = 78$ m and $z_T = 20$ m
Cause:	Ignition by burning particles from the near flare stack of vapour from crude oil seeping onto the roof as a result of stress fatigue cracks due to the constant high winds
Time to boilover:	First: <b>13 hours 10 minutes</b> ; Second: <b>15 hours 25 minutes</b>
Time to disaster end:	60 hours
Casualties:	No serious injuries
Damages:	Two tanks severely damaged, one tank externally damaged

**Table 7-23: Key information on the tank specifications, time to boilover and post boilover effects for Milford Haven boilover incident**

Table 7-24 shows the input data and the calculated interim parameter for the prediction of the time to boilover for the incident at Amoco Refinery, Milford Haven. The interim parameters in Table 7-24 were used to estimate the time to boilover for the Milford Haven boilover incident. Consequently, the time to boilover is predicted to be 12.6 hours (45252 s) as shown in Table 7-25. The table also indicates that the fraction of fuel vaporised and consumed in the fire prior to the boilover is 27%. The temperature of the hot fuel i.e. the hot zone was predicted to be about 450.2 K (177.1°C).

**PREDICTING ONSET OF BOILOVER UPON IGNITION OF  
ATMOSPHERIC STORAGE TANK OF FUEL**

**Input Parameters**

**General**

Tank Diameter:	78.0	m
Tank Height:	20.0	m
Storage Temperature:	303	K
Ambient Temperature:	20	°C
Ambient Temperature:	293	K
Relative Humidity:	88	%
Density of Water at Reference Temperature	20°C	kg m <sup>-3</sup>

**Fuel properties: Crude Oil**

Initial Depth inside Tank:		m
Normal Boiling Temperature:	Initial	320.0 K
	Final	900.0 K
	Average	536.7 K
Density at Reference (Storage) Temperature:	802	kg m <sup>-3</sup>
Specific Gravity (60°F/60°F):	0.801	-

**Interim Parameter**

Molecular Weight	300.2	g mol <sup>-1</sup>
Specific Heat of Fuel:	3185.0	J kg <sup>-1</sup> K <sup>-1</sup>
Latent Heat of Vaporisation of Fuel:	189210.5	J kg <sup>-1</sup>
Rate of Vaporisation of Fuel (Mass Burning Rate of Fuel):	225.7	kg s <sup>-1</sup>
Surface Regression Rate of Fuel	5.89 x 10 <sup>-5</sup>	m s <sup>-1</sup>
Mass Burning Rate of Fuel per unit Area (Mass Burning Flux of Fuel):	0.047	kg m <sup>-2</sup> s <sup>-1</sup>
Heat of Combustion of Fuel:	4.33 x 10 <sup>7</sup>	J kg <sup>-1</sup>
Heat Flux Radiant to Fuel Surface and form Hot Zone:	92036.5	W m <sup>-2</sup>

**Table 7-24: Input parameters and interim parameters calculated for predictive calculation of boilover incident at Milford Haven, United Kingdom**

<b>PREDICTING ONSET OF BOILOVER UPON IGNITION OF ATMOSPHERIC STORAGE TANK OF FUEL</b>			
<b>Iteration</b>	<b><math>t_{bo}</math> (s)</b>	<b><math>x_v</math></b>	<b><math>T_{hz}</math> (K)</b>
Initial	30785		403.15
1	42427	0.181	441.03
2	44722	0.250	448.49
3	45165	0.263	449.93
4	45252	0.266	450.21
5	45268	0.267	450.27

**Table 7-25: Results of predictive tool calculation on boilover onset time for Milford Haven incident.**

The observed time to boilover from the incident is compared with the prediction by the empirical models deduced from the field scale tests and the predictive tool. Figure 7-13 below shows the comparison between the real incident time and the predicted time to boilover for the boilover incident at Milford Haven.

The empirical models over predict the time of the boilover occurrence. The time results from the predictive tool again highlight the great dependence on the heat flux feedback to the surface and into the fuel. The heat flux is determined by fraction of heat radiated that contributes to the hot zone formation. A fraction with a value of 0.045 provides the best prediction of the time to boilover.

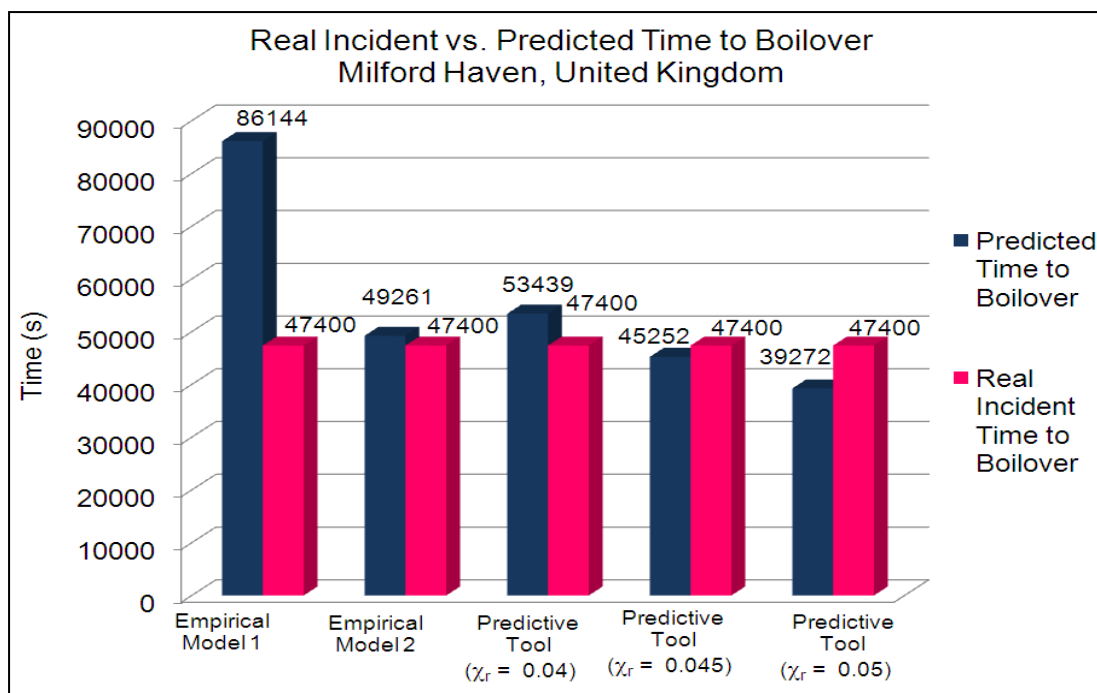


**Figure 7-13: Comparison between real incident time to boilover with the predicted values from the empirical models and the predictive tool developed for Milford Haven incident**

Table 7-26 shows the predicted results on the consequences of the boilover phenomenon. The mass of liquid fuel remaining in the tank at the moment when the boilover occurred was predicted to be about  $2.8 \times 10^7$  kg. Some of this fuel i.e.  $8.4 \times 10^5$  kg, was further vaporized and consumed in the fireball during the occurrence of the boilover, as displayed in Table 7-26. The table also shows the remaining amount fuel that was expelled to the surrounding area adjacent to the tank which was about  $2.7 \times 10^7$  kg.

Table 7-26 also shows the surface emissive power of the fireball-like flame and the heat flux received by a receptor, let's say, located at 40 m away from the centre of the tank. The surface emissive power is predicted to be about  $515.5 \text{ kW m}^{-2}$ . The radiative fraction of the total heat released by the fuel combustion is 0.40. The receptor was estimated to receive about  $51.4 \text{ kW m}^{-2}$  of mean heat flux during the occurrence of the boilover.



**PREDICTING CONSEQUENCES OF BOILOVER UPON IGNITION OF  
ATMOSPHERIC STORAGE TANK OF FUEL**

**Fireball-like Flame Characteristics**

Mass of Liquid Fuel Remaining Prior to Boilover:	2.8 x 10 <sup>7</sup>	kg
Mass of Fuel Consumed in Fireball due to Boilover:	8.4 x 10 <sup>5</sup>	kg
Maximum Diameter of the Fireball:	523	m
Overall Fireball Duration:	33	s
Maximum Height of the Centre of the Fireball above the Ground:	392	m

**Thermal Effects of the Fireball-like Flame**

Fireball Radiation View Factor:	0.179	
Atmospheric Transmissivity :	0.621	
Absorptivity of Receptor/Target (0.9 – 1.0):	Presumed value	0.9
Ground Distance Measured from the Projected Centre of Fireball to Receptor:	40	m
Partial Pressure of Water:	3735.0	Pa
Distance between Surface of Fireball and Receptor:	132.7	m
Surface Emitted Flux or Surface Emissive Power: (taking the radiative fraction of total heat released by combustion as 0.4)	515.5	kW m <sup>-2</sup>
Power Flux Received by Receptor:	126.63	kW m <sup>-2</sup>

**Affected Area due to Expulsion of Burning Fuel**

Mass of Liquid Fuel Ejected due to Boilover:	2.7 x 10 <sup>7</sup>	kg
Height of Hot Fuel-rich Column Lifted by Steam Expansion:	26.3	m
Volume of Hot Fuel Expelled Out from Tank:	30225.8	m <sup>3</sup>
Area Affected by Spillage of Hot Fuel during Boilover:	513845	m <sup>2</sup>
Radius of Affected Area	404	m

**Table 7-26: Results of predictive tool calculation on boilover onset time and area affected for Milford Haven incident.**

## 7.6 CHARACTERISTICS OF PREDICTIVE TOOL

Section 7.3, 7.4 and 7.5 show that the predictive tool is capable of providing good estimates of the onset time and the consequences of the boilover. The predictive results are conservatives but yet show good agreement with the observed time to boilover.

The time results from the predictive tool highlight the great dependence on the heat flux feedback to the surface and into the fuel. The heat flux is determined by fraction of heat radiated that contributes to the hot zone formation. Table 7-27 shows the fraction of heat radiated to the fuel that contributes to the hot zone formation used in the predictions for the boilover tests and incidents for the conduct of the comparison study in Section 7.3, 7.4 and 7.5.

Tests for Comparison Study	Type of Fuel	Tank Diameter (m)	Fraction of Heat Radiated used in the Prediction
FS Test	Crude oil	1.2	0.017
	Diesel and Gasoline		0.017
LS Test	Crude oil	0.298	0.016
	Diesel and Gasoline		0.016
Koseki, Kokkala and Mulholland (1991)	Crude oil	0.6	0.016
	Crude oil	1	0.016
Koseki <i>et al.</i> (2006)	Crude oil	5	0.016
Czechowice-Dziedzice Refinery, Poland	Crude oil	33	0.045
Tacoa Power Plant, Venezuela	Fuel oil no. 6	55	0.140
Amoco Refinery, Milford Haven, United Kingdom	Crude oil	78	0.045

**Table 7-27: Fraction of heat radiated to the fuel that contributes to the hot zone formation used in the comparison study**

Based on Table 7-27, the fraction of heat radiated to the fuel that contributed to the hot zone formation increases with tank diameter for the crude oil. The possible explanation on this observation is that for larger surface area, more energy is required to heat and vaporise the fuel to the hot zone temperature.

As for the fuel oil no. 6, the large fraction of heat radiated required in the predictive calculation is due to its high initial boiling point. In this scenario, more heat is required to bring the fuel to its boiling point.

It is important to highlight that there are some important considerations required in assessing and managing the results of the predictive tools. Section 7.6.1 discusses the limitation of the predictive tools.

### 7.6.1 Limitation of Predictive Tool

1. The predictive tool does not include meteorological parameters to calculate the time to boilover. The modelled combustion parameters e.g. mass burning rate of fuel, fuel surface regression rate and mass burning flux of fuel do not depend on the wind speed, but on the fuel specification only. This limit of the model could be overcome by the use of a wind speed integrating correlation to calculate the rate of combustion or burning.
2. The time results from the predictive tool did not taken into account occurrence of slop over or froth over before the boilover occurrence and any emergency strategies to minimise fuel in tank e.g. tank being emptied during fire fighting activities. The predictive tool can only predict single boilover occurrence (e.g. as in the case of Milford haven boilover incident)
3. As discussed at the beginning of Section 7.6, the time results from the predictive tool highlight the great dependence on the heat flux feedback to the surface and into the fuel. The heat flux is determined by fraction of heat radiated that contributes to the hot zone formation. A better method to determine or to estimate the fraction of heat radiated that contributes to the hot zone formation will ensure valid and reliable prediction.
4. The correlations for characterizing a fireball used in this work are in the form of a static model. The fireball's maximum diameter and maximum height are assumed to have been reached instantaneously and remain constant over the full duration of the event. The usage of dynamic mode that model the time-varying behaviour of fireball can provide more accurate prediction of the thermal radiation consequences of actual fireballs.

5. The prediction on the affected area (if not contained through bund or dike system) was carried out with the basis that the spill was considered as due to a catastrophic rupture of tank. The entire contents (in the case of this thesis, it is the balance of the liquid fuel inside the tank will be ejected out during boilover) are instantaneously released onto the surrounding ground. The spread of the spillage was considered to happen on a flat and solid ground (i.e. non-absorbance ground). In addition, the effects of meteorological factors (e.g. wind) were not considered during the expulsion of the fuel.

## **7.6.2 Application of Predictive Tool**

### **7.6.2.1 Safer and More Effective Fire Fighting Strategies**

Findings from Section 7.5 have shown that the empirical models and the predictive tool developed in the scope of this thesis managed to provide conservative but yet reasonable predictive results on the boilover onset time and its consequences.

Such predictive results are important and will be significant inputs to the development of safer and more effective fire fighting strategies in handling fire scenario with a potential of boilover occurrence by assessing the following points:

- i. Boilover time prediction
- ii. Affected area due fire spread estimation
- iii. Effect of tank size, fuel quantity and fuel storage temperature on both boilover time and consequences

The early and reliable determination of the time to boilover and the affected area due to fuel ejection and fire spread will allow sufficient time for emergency procedures to be implemented and for people to be evacuated from areas threatened by the incident.

### 7.6.2.2 Safety Distances

One parameter of concern in the occurrence of a boilover is the heat fluxes from the flame surface to the environment. The mean heat fluxes from the flame surface will increase tremendously during the boilover as a fireball-like flame was produced. This radiant energy is capable of causing injuries and damage over a wide area several times greater than the size of the fireball. Based on the threshold of injury and damage due to exposure to the radiant energy, a safe distance is necessary to be determined in order to minimise the effects of exposure.

Broeckmann and Schecker (1995) calculated the mean heat fluxes from the flame surface to the environment during the normal course of the fire and obtained a value of about  $45 \text{ kW m}^{-2}$ . The calculations were carried out based on the temperature distribution for the test conducted in a 2 m tank. Due to the temperature rise during boilover, this mean heat flux value has increased by a factor of nearly 3 i.e. the mean heat flux of  $120 \text{ kW m}^{-2}$ . Combined with the increased flame dimensions (length and diameter), Broeckmann and Schecker recommended that the safety spacing was to be increased by a factor of 6 for preventing severe burns and damage to equipment.

Ferrero *et al.*, (2006) have quantified the increase in mean heat flux from the flame surface at the time of onset of thin layer boilovers, and the impacts on the safety distances for different tank diameters. The results showed that at a given point (e.g. at a distance of 3 to 5 times the tank diameter), at the time of onset of the phenomenon, the mean heat flux measured is about 1.2 to 2 times greater than during the tank fire. It was recommended that during the occurrence of the boilover, the safety distances must be increased in relation to the stationary phase (tank fire), with or without wind. This increase must be greater than 65% for small diameters (1.5m) and between 25 and 30% in relation to the stationary state for tanks of over 6 metres in diameter.

Based on the predictive calculations in Section 7.5, the surface emissive power and the power flux received by the receptor from the fireball-like flame during

boilover can be estimated. These values can be used to determine an increase factor which characterizes the increase in the mean heat flux due to the flame enlargement during the boilover occurrence when compared to the heat flux from the stationary fire. The increase factor is important in determining the safety distance as shown in the studies by Broeckmann and Schecker (1995) and Ferrero *et al.*, (2006).

## 7.7 CONCLUSION

Two empirical models were deduced from the results of field scale tests in Chapter 3. The first empirical model (Empirical Model 1) is deduced from the linear trend line for the plot of the observed time to boilover versus the initial depth of the fuel of the field scale tests. Multiplying an initial depth of fuel by the slope of the trend line gives the time to boilover. The second model (Empirical Model 2) allows the prediction of the time to boilover,  $t_{bo}$  by dividing the initial depth of fuel by the speed of the base of the hot zone determined using the thermocouple profiles.

Empirical Model 1 produces good predictions on the time to boilover when compared with the observed time to boilover in the field scale tests and with the time to boilover recorded in Koseki *et al.* (2006). The model under predict the time to boilover in the comparison with the time to boilover observed in Koseki, Kokkala and Mulholland (1991). However, Empirical Model 1 predicts longer time to boilover in the comparison study for all the real boilover incidents.

Empirical Model 2 provides faster time to boilover compared to the observed time in the field scale tests, the boilover studies and for the Czechowice-Dziedzice boilover incident. The model predicts longer time to boilover in the Tocoa Power Plant and Amoco Refinery boilover incidents.

These empirical models of time to boilover developed were based on the observed experiments. It should also be noted that the experiments were undertaken at a small scale compared with full-size storage tanks. Hence, the

predicted time to boilover using these empirical models may not be accurate when compared to the time to boilover in full-size events.

The predictive tool proposed in Chapter 6 was developed in order to provide predictions on the important parameters associated with a boilover event i.e. the time to boilover, the amount of fuel remaining in the tank prior to boilover and hence the quantity of fuel that would be ejected during boilover and the consequences of a boilover i.e. fire enlargement, fireball effects and the ground area affected by the expulsion of oil during a boilover event. Section 7.3, 7.4 and 7.5 has shown that the predictive tool is capable of providing good estimates of the onset time and the consequences of the boilover. The predictive results are conservatives but yet show good agreement with the observed time to boilover.

Certain considerations in the development of safer and more effective fire fighting strategies in handling fire scenario with a potential of boilover occurrence, can be assessed using the predictive tool developed. The early and reliable determination of the time to boilover and the affected area due to fuel ejection and fire spread will allow sufficient time for emergency procedures to be implemented and for people to be evacuated from areas threatened by the incident.

## **8 HIGHLIGHTS OF WORK AND CONCLUSION**

### **8.1 Highlights of Work**

Boilover is a very dangerous accidental phenomenon, which can lead to serious injuries especially to emergency responders. The boilover can occur several hours after the fuel in a storage tank caught fire. The delayed boilover occurrence is an unknown strong parameter when managing the emergency response operations especially those involved with potential boilover occurrence. Modelling and simulation of the boilover phenomenon will allow the prediction of the important characteristics features of such an event and enable corresponding safety measures to be prepared. Of particular importance when managing the emergency response operations in tank farms in which fuels are stored that have the potential for boilover to occur, is the time from ignition to the occurrence of boilover.

A condition necessary for boilover is the formation of a hot zone within the burning fuel. The thickness of the hot zone increases with time after ignition, due to vaporisation of the light components of the fuel by the heat received from the flame at the burning surface. It is known that when the base of the hot zone reaches a water layer at the tank bottom, boilover might occur. In order to establish a tool for the prediction of the boilover events, it is necessary to understand what happens within the fuel during a fire. Such understanding is important in order to recognize and determine the mechanisms for the hot zone formation and growth which are essentials, especially for predicting the onset time of boilover.

In order to further clarify these processes, boilover experiments and tests were planned and carried out at field scale by the Large Atmospheric Storage Tank FIRE (LASTFIRE) project. The main aims of the field scale tests were to evaluate the nature and consequences of a boilover, and to establish a common mechanism that would explain the boilover occurrence.



Field scale preliminary tests were carried out and the results were used to establish a test methodology and measurement parameters for future tests. Basic analysis of the preliminary tests illustrated the complexity of the boilover mechanisms. Following the preliminary tests of the boilover study, three further series of boilover tests were performed using larger tanks of 1.2 and 2.44 m diameter. The aims were to carry out boilover tests with different fuels, different fuels amounts and different water levels and to consider the escalation probability and consequences of crude fires prior to, and during boilover. The tanks were fitted with thermocouples at different levels, enabling knowledge of exactly how the temperature gradient inside the tank was progressing. The analysis on the temperature evolution in certain fuels showed that hot zone was formed. Another important observation was that there are three stages observed in the mechanism of boilover incidence. At the start of the fire there is a stage when the hot zone is formed. This is followed by a period when the bottom of the hot zone moves downwards at a pseudo constant rate in which the distillation process (vaporisation of the fuel's lighter ends) is taking place. The final stage is involved the heating up of the lowest fuel layer consisting of components with very high boiling points and occurrence of boilover. In the field scale tests, enlargement of flames during the study were observed in many cases. The flames were observed to be approximately 5 to 20 times the diameter of the tank and hot burning fuel was thrown out from the tank which landed several tank diameters away.

Undertaking field scale experiments, however, is difficult to carry out so often due to high costs and high safety concerns. In order to allow well defined and repeatable experiments to be performed and to obtain more detailed measurements and visual records of the behaviour of the liquids in the pool, a novel laboratory scale rig has been designed, built and commissioned. The rig allowed the conduct of a study of boilover in a cost effective, safe and carefully controlled manner. The rig is used to determine whether or not a fuel will boilover. The laboratory scale rig was also instrumented with a network of thermocouples, in order to monitor the temperature evolution throughout the

liquid and its variation with time. A study of the temperature distribution inside the fuel enabled the hot zone formation to be observed in several of the tests conducted.

A number of small and larger scale experiments had been completed in the field and laboratory scale tests which produced a wide spectrum of results, evaluating the effect of tank diameters, fuel depth, and water depth on the rate and extent of the boilover. The analysis of the results had elucidated further the processes of the hot zone formation and its growth, and hence mechanisms involved in the boilover occurrence.

Based on the observations of the mechanisms involved in the boilover occurrence from the field and laboratory scale tests, predictive calculations were developed which focus on the provision of an estimate on the time to boilover upon the establishment of a full surface fire and an estimate of the amount of fuel remaining in the tank prior to the occurrence of the boilover. A determination of the remnants of the fuel is essential in estimating the consequences of the event. In order to aid the development of a predictive tool for boilover onset, the heating mechanism is simplified by considering that the heat involved in the process is only used for vaporising the component in the hot zone and for raising the temperature of the unheated fuel to the hot zone temperature (instead of considering the three stages observed in the mechanism of boilover incidence as discussed in Section 3.2.3 and early section of Chapter 6). The proposed predictive tool assumes that the thermal transfer is carried out by mass transfer in which the lighter components of fuel are vaporised and feed the fire. This upward movement results in the downward movement of hot heavier components. The net effect is the establishment of vigorous convective currents within the hot zone. This assumption allows the use of simple equations based on physical and thermodynamic laws to predict the development of the hot zone, its temperature and the time at which the boilover occurs. When comparisons were made, the predicted time to boilover shows acceptable agreement with the observed time to boilover of the tests results. However, it is important to highlight that there are some limitations on

the conduct of the predictive calculation and careful considerations are necessary while assessing and managing the results of the predictive tools.

## 8.2 Conclusion

The conclusions from the results of the field scale tests were:

1. All of the tests involving crude oil resulted in boilover as did the tests involving mixtures of diesel and gasoline.
2. Hence, for boilover to occur it is necessary to have a fuel with wide boiling range and for the boiling points of the heavier components to be significantly greater than the boiling point of water.
3. The onset time of boilover showed a linear increase as the initial depth of the fuel increased.
4. The burning of the refined fuels such as the aviation fuel (AVTUR), diesel, gasoline and light fuel oil (LFO) did not result in boilover.
5. The analysis on the temperature evolution in the fuel showed that hot zone was formed. The analysis also indicated that the minimum fuel-water interface temperature required for a boilover is approximately 110°C.
6. A closer look at the temperature distribution inside the fuel was carried out. By observing the temperature variation as a function of time, the fundamental stages of the evolution of hot zone and hence the mechanism of boilover can be detected. Based on the discussion of the Section 3.2.3, it could be deduced that there are three stages observed in the mechanism of boilover incidence. At the start of the fire there is a stage when the hot zone is formed. This is followed by a period when the bottom of the hot zone moves downwards at a pseudo constant rate in which the distillation process (vaporisation of the fuel's lighter ends) is taking place. The final stage is when the hot zone reaches the fuel-water interface and is heating up further the lowest fuel layer consisting of components with very high boiling points which must be heated to a temperature sufficiently above that of the boiling point of water so that

the water is superheated and rapid vaporization of the water occurs. Consequently, a boilover was observed.

7. The average surface regression rates for the crude oils that were used in the field scale tests were determined to be within the range of 0.025 - 0.070 mm s<sup>-1</sup>. The average surface regression rates for the tests involving the mixture of diesel and gasoline were within the range of 0.057 to 0.135 mm s<sup>-1</sup>. The average surface regression rate for diesel was within the range of 0.050 to 0.054 mm s<sup>-1</sup>. The surface regression rate for gasoline fire test was 0.084 mm s<sup>-1</sup>,
8. The average speed of the base of the hot zone for the crude oils that were used in the field scale tests were within the range of 0.12 to 0.317 mm s<sup>-1</sup>. The average speed of the base of the hot zone for the tests involving the mixture of diesel and gasoline were within the range of 0.183 to 0.320 mm s<sup>-1</sup>. The average speed of the base of the hot zone for diesel was within the range of 0.048 to 0.052 mm s<sup>-1</sup>. The average speed of the base of the hot zone for gasoline fire test was about 0.073 mm s<sup>-1</sup>.
9. Comparing the average surface regression rate (point 7) and average speed of the base of the hot zone (point 8), it is observed that the latter provides higher values for those tests in which boilover was observed. This observation indicates that the thermal front moved faster than the regress of the fuel surface and hence a hot zone layer was formed.
10. Two empirical correlations for predicting time to boilover were deduced from the results of field scale tests:
  - a. The first empirical model (Empirical Model 1) is deduced from the linear trend line for the plot of the observed time to boilover versus the initial depth of the fuel of the field scale tests (see Equation 3.1). Multiplying an initial depth of fuel by the slope of the trend line gives the time to boilover.
  - b. The second model (Empirical Model 2) allows the prediction of the time to boilover,  $t_{bo}$  by dividing an initial depth of fuel by the speed of the base of the hot zone determined using the thermocouple profiles (see Equation 3-2).

11. Effect of surface heat flux on time to boilover was examined by applying layers of non conducting material on the surface of a burning fuel. It is assumed that by applying layers of non conducting materials on the surface, the heat transferred from the flame to the fuel would be reduced. The significance of the result obtained is that by limiting the heat absorbed by the fuel from the fire, the time to boilover could be prolonged and even to the extent of eliminating the phenomenon.

The conclusion of the laboratory scale boilover tests are:

1. Data obtained from the laboratory scale tests and its subsequent analysis has demonstrated that the laboratory scale boilover rig has enabled the study of the boilover to be conducted in a controlled and safe manner and that repeatability of the experimental results are acceptable.
2. In the tests that produced boilover, the thermocouple measurement within the fuel showed that, for the characteristics of the experiments performed for this thesis, a hot zone was created.
3. When the isothermal region through the heater was discounted, the thermocouple measurements also showed the lack of creation of a hot zone for those fuels that did not boilover
4. Boilover was observed for fuels in which a hot zone was established with a temperature significantly above the boiling point of water
5. Fuel surface regression rates for the experiments were obtained from the analysis of the thermocouple results. For the mixture of mineral oil and n-butyl acetate, the surface regression rates were in the range of 0.002 - 0.009 mm s<sup>-1</sup>. The fuel surface regression rates for the mixture of diesel + gasoline were observed to be within the range of 0.008 - 0.017 mm s<sup>-1</sup>. The regression rates for crude oil were in the range of 0.008 - 0.010 mm s<sup>-1</sup>. Table 5-3 shows the average fuel surface regression rate determined for each of the laboratory scale boilover tests.

6. Speed of the base of the hot zone can be estimated through detailed analysis of the temperature profiles in the fuel layer. The temperature profiles within the fuel were determined from time histories of the temperatures at fixed points. The average speed of the base of the hot zone for crude oil was found to be within the range of 0.135 to 0.224 mm s<sup>-1</sup>, diesel was between 0.044 to 0.058 mm s<sup>-1</sup>, gasoline was 0.035 mm s<sup>-1</sup> and for the mixture of diesel + gasoline was in the range of 0.056 to 0.152 mm s<sup>-1</sup>. Table 5-5 shows that the average speed of the base of the hot zone for each of the laboratory scale boilover tests.
7. A significant observation from all the laboratory scale experiments on crude oil was that the average temperature measured at the fuel-water interface during the boilover period was about 110°C.
8. The laboratory scale test results, though limited, indicate that in the case of storage tank fires with a possibility of boilover occurrence, a higher initial fuel temperature will contribute to a shorter onset time.
9. By reducing the heating temperature i.e. by limiting the heat absorbed by the fuel from the fire, the time to boilover could be prolonged and even to the extent of eliminating the phenomenon.

The conclusions from the works of developing the predictive tool for boilover incident were:

1. A predictive tool proposed was developed in order to provide predictions on the important parameters associated with a boilover event i.e. the time to boilover, the amount of fuel remaining in the tank prior to boilover and hence the quantity of fuel that would be ejected during boilover and the consequences of a boilover i.e. fire enlargement, fireball effects and the ground area affected by the expulsion of oil during a boilover event.
2. The predictive tool developed is capable of providing good estimates of onset time to boilover and predicts consequences of the boilover. The predictive results are conservatives but yet show good agreement with observed time to boilover in real boilover incidents.

3. An analysis of the parameters involved in the prediction of the time to boilover indicates that the predicted results are influenced significantly by the:
  - a. the magnitude of the heat feedback from the flame into the fuel
  - b. the average boiling point of the fuel
  - c. the storage temperature of the fuel
4. However, differences in the fuel density do not have any significant effect on the time to boilover. It was deduced that predictions obtained from one fuel density can be used for similar fuels with slightly different densities.
5. The time results from the predictive tool highlight the great dependence on the heat flux feedback to the surface and into the fuel. The heat flux is determined by fraction of heat radiated from the flame to the fuel that contributes to the hot zone formation.
6. Apart from the time to boilover, the predictive calculation is able to provide estimate of amounts of fuel remained in the tank at the instance of boilover occurrence. Consequently, the tool is capable of predicting the amount of burning fuel being ejected and hence the area affected by the extensive ground fire surrounding the tank.
7. Surface emissive power and the power flux received by the receptor from the fireball-like flame during boilover can be estimated. These values can be used to determine an increase factor which characterizes the increase in the mean heat flux due to the flame enlargement during the boilover occurrence when compared to the heat flux from the stationary fire. The increase factor is important in determining the safety distance when handling fire scenario with a potential of boilover occurrence.
8. Certain considerations in the development of safer and more effective fire fighting strategies in handling fire scenario with a potential of boilover occurrence, can be assessed using the predictive tool developed. The early and reliable determination of the time to boilover and the affected area due to fuel ejection and fire spread will allow sufficient time for emergency procedures to be implemented and for people to be evacuated from areas threatened by the incident.

9. There are some limitations on the conduct of the predictive calculation and hence careful considerations are necessary while assessing and managing the results of the predictive tools.

### **8.3 Future Recommendations**

As noted at the end of Chapter 7, the predictive tool developed has certain limitations and hence the some of the items recommended for future work shall focus on overcoming the limitations discussed.

1. The field scale test aimed to cover different types of fuels and weather conditions. It would be useful to broaden the scope of the experimental work to test the potential for a fuel to boilover, its burning characteristics, boilover consequences etc. on an individual basis. There are several factors that need to be taken into account and the best way to determine boilover characteristics would be to base guidance on the results of empirical tests. For example, crude from one site may have different boilover probability and consequences than another and the best way of qualifying this would be to test fuels that are actually handled on site.
2. The results from the limited tests conducted in the field and laboratory scale tests on the effect of surface heat flux on time to boilover showed promising results in which by limiting the heat absorbed by the fuel from the fire, the time to boilover could be prolonged and even to the extent of eliminating the phenomenon. A study on the effects of additive in fuel towards the time to boilover would be of interest. The introduction of the additives may affect the thermo-physical properties of the fuel (e.g. thermal conductivity) and hence influence the rate of the heat penetrated within the fuel.
3. It is useful to modify the predictive tool to consider the meteorological parameters to calculate the time to boilover. The predictive tool could consider the use of a wind speed integrating correlation to calculate the



combustion parameters e.g. mass burning rate of fuel, fuel surface regression rate and mass burning flux of fuel.

4. As discussed at the beginning of Section 7.6, the time results from the predictive tool highlight the great dependence on the heat flux feedback to the surface and into the fuel. The heat flux is determined by fraction of heat radiated that contributes to the hot zone formation. A better method to determine or to estimate the fraction of heat radiated that contributes to the hot zone formation will ensure valid and reliable prediction. An experimental study where measurements of the heat flux within the burning fuel (or heated fuel in the context of laboratory scale tests) can be carried out.
5. An experimental program to obtain data on the spread of burning fuel or affected area due to the spillage during boilover for reliable predictive model development and validation would also be of interest.
6. The correlations for characterizing a fireball used in this work are in the form of a static model. The usage of dynamic mode that model the time-varying behaviour of fireball can provide more accurate prediction of the thermal radiation consequences of actual fireballs.
7. The laboratory scale experiments provide visualizations of the physical behaviour within the hot liquid fuel which allow better understanding on the formation of the hot zone, its growth and the boiling of the water at the fuel-water interface. The knowledge will be useful, through the contribution to the literature, especially for personnel involved with tank fire hazard management. In addition to that, the capability of the predictive tool to predict the amounts of burning fuel ejected from a tank due to boilover and hence the surrounding affected area would also be of interest.

---

## REFERENCES

- API-2021 (2001) "Management of Atmospheric Storage Tank Fires", *API Recommended Practice 2021*, American Petroleum Institute, API Publishing Services, Washington D.C.
- Arai, M., Saito, K. and Altenkirch, R.A. (1990) "A Study of Boilover in Liquid Pool Fires Supported on Water Part I: Effects of a Water Sub-layer on Pool Fires", *Combustion Science and Technology* 71, pg. 25-40.
- Babraukas, V. (1983) "Estimating Large Pool Fire Burning Rates", *Fire Technology* 19, No. 4, pp. 251-261.
- Babraukas, V. (1986) "Free Burning Fires", *Fire Safety Journal* 11, pp. 33-51.
- Blinov, V.I. and Khudyakov, G.N. (1961) "Diffusive Burning of Liquids", *Academic of Science Moscow* (English translation by US Army Engineering Research and Development Laboratories), pp. 157-163.
- Broeckmann, B. and Schecker, H-G. (1995) "Heat Transfer Mechanisms and Boilover in Burning Oil-water System", *Journal of Loss Prevention in the Process Industries* 8, No. 3, pp. 137-147.
- Broeckmann, B. and Schecker, H-G. (1992) "Boilover Effects in Burning Oil-Tanks", *7<sup>th</sup> International Symposium on Loss Prevention and Safety Promotion in the Process Industries Sicily, Italy*, 4<sup>th</sup> - 8<sup>th</sup> May.
- Brownell, L.E. and Young, E.H. (1977) "Process Equipment Design", John Wiley & Sons Inc, New York, pp. 98-119.
- Bugai, V.T., Oreshenkov, A.V. and Burmistrov, O.A. (1998) "Determination of Heat of Combustion of Fuels by Calculation", *Chemistry and Technology of Fuels and Oils* 34, No.5, pp. 272-274.
- Burgess, D., Strasser, A. and Grumer, J. (1961) "Diffusive Burning of Liquid Fuels in Open Trays".[Online] Division of Fuel Chemistry, American Chemical Society, Washington DC.[Viewed on 14/06/2011]. Available from: <http://www.anl.gov/PCS/acsfuel/preprint%20archive/Files/Volumes/Vol05-2.pdf>.
- Burgoyne, J. and Katan, L. (1947) "Fires in Open Tanks of Petroleum Products: Some Fundamental Aspects", *Journal of the Institute of Petroleum* 33, No. 1, pp. 158-191.
- Casal, J. (2008) "Boilover", *Evaluation of the Effects and Consequences of Major Accidents in Industrial Plants Vol. 8, Industrial Safety Series*, Elsevier, pp. 100-117.

- CCPS (2000) "Chapter 2: Consequence Analysis" in *Guidelines for Chemical Process Quantitative Risk Analysis, Second Edition*, Centre of Chemical Process Safety, American Institute of Chemical Engineers, New York, pp.204-216.
- Chang, J.I and Lin, C-C. (2006) "A Study of Storage Tank Accidents", *Journal of Loss Prevention in the Process Industries* 19, pp. 51-59.
- Chatris, J.M., Quintela, J., Folch, J., Planas, E., Arnaldos, J. and Casal, J. (2001) "Experimental Study of Burning Rate in Hydrocarbon Pool Fires", *Combustion and Flame* 126, pp. 1373-1383.
- Chow, W.K. and Han, S.S. (2011) "Heat Release Rate Calculation in Oxygen Consumption Calorimetry", *Applied Thermal Engineering* 31, No. 2-3, pp. 304-310.
- Chulkov, P. V. (1968) "Numerical and Graphical Methods of Determining the Heat of Combustion of Oil Products", *Chemistry and Technology of Fuels and Oils* 4, No. 1, pp. 68-70.
- Cornwell, J.B. (1999) "Real-Time Modelling During Emergency Situations – Is This A Good Idea?", *Mary Kay O'Conner Process Safety Centre Annual Symposium – Beyond Regulatory Compliance, Making Safety Second Nature*, College Station, Texas.
- Daubert, T. E. and Danner, R. P. (1997) "API Technical Data Book – Petroleum Refining 6th Edition", *American Petroleum Institute: Washington D. C.*, pp. 7-181 – 7-182.
- Drysdale, D. (1987) "Steady Burning of Liquids and Solid Fuels" in *An Introduction to Fire Dynamics*, John Wiley and Sons, New York, pp. 152-160.
- Drysdale, D. (1999) "An Introduction to Fire Dynamics - Second Edition", John Wiley and Sons, West Sussex.
- Engelhard, W.F.J.M. (2005) "Chapter 6: Heat Flux from Fires", in van den Bosch, C.J.H. and Weterings, R.A.P.M. (Eds.), "Methods for the Calculation of Physical Effects Due to Releases of Hazardous Materials (Liquid and Gases)", *TNO Yellow Book 3<sup>rd</sup> Edition*, Committee for the Prevention of Disasters, The Hague, The Netherlands, pp. 6-1-6-127.
- Evans, D., Walton, W., Baum, H., Mulholland, G., Lawson, J., Koseki, H. and Ghoniem, A. (1991) "Smoke Emission from Burning Crude Oil", *Technical Seminar Arctic and Marine Oilspill Program, Environment Canada*, pp. 421-449.
- Fan, W.C., Hua, J.S. and Liao, G.X. (1995) "Experimental Study on the Premonitory Phenomena of Boilover in Liquid Pool Fires Supported on Water", *Journal of Loss Prevention in Process Industries* 8, No. 4, pp. 221-227.

- Fay, J.A. (2006) "Model of Large Pool Fires", *Journal of Hazardous Materials* 136, No. 2, pp.219-232.
- Garo, J.P. and Vantelon, J.P. (1999) "Thin Layer Boilover of Pure or Multicomponent Fuels", In: Zarko, V.E., Weiser, V., Eisenreich, N. and Vasil'ev, A.A. (Eds), *Prevention of Hazardous Fires and Explosions, The Transfer to Civil Applications of Military Experiences, NATO Sciences Series, Series 1, Disarmament Technology* Vol. 26, Kluwer Academic, Dordrecht, pp. 167-182.
- Garo, J.P., Gillard, P., Vantelon, J.P. and Fernandez-Pello, A.C. (1999a) "Combustion of Liquid Fuels Spilled on Water - Prediction of Time to Start of Boilover", *Combustion Science and Technology* 147, No. 1, pp. 39-59.
- Garo, J.P., Vantelon, J.P., Gillard, P. and Fernandez-Pello, A.C. (1999b) "Combustion of Liquid Fuels Spilled on Water. Prediction of Time to Start of Boilover", *Combustion Science and Technology* 147, No. 1, pp. 39-59.
- Garo, J.P., Vantelon, J.P. and Koseki, H. (2006) "Thin-layer Boilover: Prediction of its onset and intensity", *Combustion Science and Technology*, 178 (7), pp. 1217–1235.
- Garo, J.P., Vantelon, J.P. and Fernandez-Pello, A.C. (1994) "Boilover Burning of Oil Spilled on Water", *Twenty-Fifth Symposium (International) on Combustion, The Combustion Institute*, pp. 1481-1488.
- Garo, J.P., Vantelon, J.P., Gandhi, S. and Torero, J.L. (1999) "Determination of the Thermal Efficiency of Pre-boilover Burning of a Slick of Oil on Water", *Spill Science & Technology Bulletin* 5, No. 2, pp. 141-151.
- Garrison, W.W. (1984) "Fire & Boilover at Power Plant at Tocoa, near Caracas, Venezuela, 1982", *Loss Prevention Bulletin* 57, pp. 26-27.
- Gottuk, D.T. and White, D.A. (2002) "Chapter 15: Liquid Fuel Fires", in Section 2: Fire Dynamics, *SFPE Handbook of Fire Protection Engineering 3<sup>rd</sup> Edition*, NFPA Inc., Massachusetts, pp. 2-297 - 2-315.
- Grimaz, S., Allen, S., Stewart, J.R. and Dolcetti, G. (2008) "Fast Prediction of the Evolution of Oil Penetration into the Soil Immediately After an Accidental Spillage for Rapid-Response Purposes", *AIDIC-CISAP3: 3<sup>rd</sup> International Conference on Safety & Environment in Process Industry 2008*, Italian Association of Chemical Engineering.
- Grumer, J., Strasser, A., Kubala, T.A. and Burgess, D. (1961) "Uncontrolled Diffusive Burning of Some New Liquid Propellant", [Online] Division of Fuel Chemistry, American Chemical Society, Washington DC.[Viewed on 14/06/2011]. Available from:<http://www.anl.gov/PCS/acsfuel/preprint%20archive/Files/Volumes/Vol05-2.pdf>.

---

Hall, H. (1925) "Oil Tank Fire Boilovers", *Mechanical Engineering* 47, No. 7, pp. 540-544.

Hamins, A., Kashiwagi, T. and Burch, R.R. (1996) "Characteristics of Pool Fire Burning", In: Totten, G.E. and Reichel, J. (Eds.), *Fire Resistance of Industrial Fluids, ASTM STP 1284*, American Society for Testing and Materials, Philadelphia, pp. 15-41.

Hamins, A., Klassen, M., Gore, J. And Kashiwagi, T. (1991) "Estimate of Flame Radiance via a Single Location Measurement in Liquid Pool Fires", *Combustion and Flame* 86, pp. 223-228.

Hamins, A., Yang, J.C. and Kashiwagi, T. (1999) "A Global Model for Predicting the Burning Rates of Liquid Pool Fires", *National Institute of Standards and Technology Interagency Reports (NISTIR) 6381*, Building and Fire Research Laboratory, NIST.

Hasegawa, K. (1989) "Experimental Study on the Mechanism of Hot Zone Formation in Open Tank Fires", *Fire Safety Science 2 - Proceedings of the Second International Symposium*, pp. 221-230.

Hattwig, M. and Steen, H. (2004) "Handbook of Explosion Prevention and Protection", Wiley-VCH, pp. 488.

Hristov, J., Planas-Cuchi, E., Arnaldo, J. And Casal, J. (2004) "Accidental Burning of a Fuel Layer on a Waterbed: A Scale Analysis of the Models Predicting the Pre-Boilover Time and tests to Published Data", *International Journal of Thermal Sciences* 43, pp. 221-239.

Hua, J.S., Fan, W.C. and Liao, G.X. (1998) "Study and Prediction of Boilover in Liquid Pool Fires with a Water Sub-layer using Micro-explosion Noise Phenomena", *Fire Safety Journal* 30, pp. 269-291.

Inamura, T., Saito, K. and Tagavi, K.A. (1992) "A Study of Boilover in Liquid Pool Fires Supported on Water Part II: Effects of In-depth Radiation Absorption", *Combustion Science and Technology* 86, pp. 105-119.

Koseki, H. (1989) "Combustion Properties of Large Liquid Pool Fires", *Fire Technology* 25, no. 3, pp. 241-255.

Koseki, H. (1994) "Boilover and Crude Oil Fire", *Journal of Applied Fire Science* 3, No. 3, pp. 243-272.

Koseki, H. (1999) "Large Scale Pool Fires: Results of Recent Experiments", *Proceedings of the 6<sup>th</sup> International Symposium, Fire Safety Science* 6, pp. 115-132.

Koseki, H. and Iwata, Y. (2000) "Tomakomai Large Scale Crude Oil Fire Experiments", *Fire Technology* 36, No. 1, pp. 24-38.

- Koseki, H., Kokkala, M. and Mulholland, G.W. (1991a) "Experimental Study of Boilover in Crude Oil Fires", *Fire Safety Science – Proceedings of the 3<sup>rd</sup> International Symposium*, pp. 865-874.
- Koseki, H. and Mulholland, G.W. (1991b) "The Effect of Diameter on the Burning of Crude Oil Pool Fires", *Fire Technology* 27, No. 1, pp. 54-65.
- Koseki, H., Natsume, Y., Iwata, Y., Takahashi, T. and Hirano, T. (2003) "A Study on Large-scale Boilover using Crude Oil Containing Emulsified Water", *Fire Safety Journal* 38, pp. 665-677.
- Koseki, H., Natsume, Y., Iwata, Y., Takahashi, T. and Hirano, T. (2006) "Large scale Boilover Experiments using Crude Oil", *Fire Safety Journal* 41, pp. 529-535.
- Lee, B.I. and Kesler, M.G. (1975) "A generalized thermodynamic correlation based on three-parameter corresponding states", *AIChE Journal* 21(3), pp. 510–527.
- Lees, F.P. (2005) "Chapter 16: Fireballs" in Mannan, S. (Ed), *Lee's Loss Prevention in the Process Industries Vol. 1, 3rd Edition*, pp. 16/176-16/190.
- Mackay, D. and Mohtadi, M. (1975) "The Area Affected by oil Spills on Land", *The Canadian Journal of Chemical Engineering* 53, No. 1, pp. 140-143.
- Martinsen, W.E. and Marx, J.D. (1999) "An Improved Model for the Prediction of Radiant Heat from Fireballs" *International Conference and Workshop on Modelling Consequences of Accidental Releases of Hazardous Materials September 1999*.
- Michaëlis, P. (2008) "Boilover Theory and Means to Anticipate Potential Consequences – Part 3", *Internal Report for LASTFIRE Group*, TOTAL France Refining Division, pp.197-221.
- Michaëlis, P., Dumas, J-L. and Gautier, L. (2005) "LASTFIRE II – Validation of Boilover TOTAL Model Prediction", *Internal Group Report, LASTFIRE II Update Meeting April 2005 Kuala Lumpur*.
- Mudan, K.S. (1984) "Thermal Radiation Hazards from Hydrocarbon Pool Fires", *Progress in Energy and Combustion Science* 10, pp. 59-80.
- Perry, R. H., and D. W. Green, Eds., (1997) "Section 2: Solid and Liquid Heat Capacity", in "*Perry's Chemical Engineers' Handbook*" 6<sup>th</sup> Edition, McGraw-Hill, New York, pp. 2 -351.
- Persson, H. and Lönnermark, A. (2004) "Tank Fires - Review of Fire Incidents 1951–2003", *SP Fire Technology Report 14, BRANDFORSK Project 513-021, SP Swedish National Testing and Research Institute*.

- Petty, S.E. (1983) "Combustion of Crude Oil on Water", *Fire Safety Journal* 5, pp. 123-134.
- Planas–Cuchi, E., Montiel, H., and Casal, J. (1997) "A Survey of the Origin, Type and Consequences of Fire Accidents in Process Plants and in the Transportation of Hazardous Materials", *Process Safety and Environmental Protection* 75, pp. 3-8.
- Poling, B.E., Prausnitz, J.M. and O'Connell, J.P. (2000) "*Properties of Gases and Liquids*" 5<sup>th</sup> Ed., McGraw-Hill, New York.
- Prugh, R.W. (1994) "Quantitative Evaluation of Fireball Hazards", *Process Safety Progress* 13, No. 2, pp. 83-91.
- Resource Protection International (RPI), *Boilover Study PHASE 1 – Preliminary Test Series*, Report for LASTFIRE Update Group, April 2004.
- Resource Protection International (RPI), *Boilover Study PHASE 2 – Instrumented Test Series*, Report for LASTFIRE Update Group, September 2004.
- Resource Protection International (RPI), *Boilover Study PHASE 3 – Continuation Tests Series*, Report for LASTFIRE Update Group, August 2005.
- Resource Protection International (RPI), *Boilover Study PHASE 4*, Report for LASTFIRE Update Group, June 2006.
- Resource Protection International (RPI), [Online] *LASTFIRE – Large Atmospheric Tank FIRE*, 2007, [Viewed on May 2008] Available online: <http://www.resprotint.co.uk/lastfire.htm>.
- Riazi, M.R. and Daubert, T.E. (1987) "Characterization Parameters for Petroleum Fractions", *Industrial and Engineering Chemistry Research* 26, No. 4, pp. 755–759.
- Roberts, T., Gosse, A. and Hawksworth, S. (2000) "Thermal Radiation from Fireballs on Failure of Liquefied Petroleum Gas Storage Vessels", *Proceedings of the Institute of Chemical Engineers (IChemE) Symposium Series* 147, pp. 105-120.
- Robertson, J. (2000), [Online] "Explosive Phenomena: Boilovers", [Viewed on 16 June 2008] Available online: <http://www.chemeng.ed.ac.uk/~jskillin/teaching/safety4/jroberts/milford.htm>.
- Růžička V, Jr., and Domalski, E.S. (1993) "Estimation of the Heat Capacities of Organic Liquids as a Function of Temperature using Group Additivity, I. Hydrocarbon Compound", *Journal of Physical and Chemical Reference Data* 22, No. 3, pp. 597-618.

- Shaluf, I. M., Abdullah, S. A. (2011) "Floating Roof Storage Tank Boilover", *Journal of Loss Prevention in the Process Industries* 24, pp. 1-7.
- Speight, J. (2001) "*Chapter 5 Handbook of Petroleum Analysis*", Wiley-Interscience, New York, pp. 127-163.
- Speight, J.G. (1999) "Chapter 8: Properties and Evaluation", *The Chemistry and Technology of Petroleum Third Edition*, Marcel Dekker Inc. New York, pp. 306.
- TNO Yellow Book (2005) "Methods for the Calculation of the Physical Effects Resulting from Releases of Hazardous Materials (Liquids and Gases)", *Report CPR 14E Third Edition*, Committee for the Prevention of Disasters, TNO, Chapter 6.
- Torero, J.L., Olenick, S.M., Garo, J.P. and Vantelon, J.P. (2003) "Determination of the Burning Characteristics of a Slick of Oil on Water", *Spill Science & Technology Bulletin* 8, No. 4, pp. 379–390.
- Walters, R.N. (2001) "Molar Group Contributions to the Heat of Combustion", *Technical Report, National Technical Information Service (NTIS)*.
- Wisniak, J. (2001) "Frederick Thomas Troutun: The Man, the Rule, and the Ratio", *The Chemical Educator* 6, No. 1, pp.55-61
- Zabetakis, M.G. and Burgess, D.S. (1961) "Research on the Hazards Associated with the Production and Handling of Liquid Hydrogen", *Report of Investigations 5707, U.S. Bureau of Mines*, pp. 27-35.
- Zalosh, R.G. (2003) "Appendix A: Flame Radiation Review", in "Industrial Fire Protection Engineering", John Wiley and Sons